PUCRS

PONTIFÍCIA UNIVERSIDADE CATÓLICA DO RIO GRANDE DO SUL
ESCOLA DE CIÊNCIAS DA SAÚDE E DA VIDA
PROGRAMA DE PÓS-GRADUAÇÃO EM ECOLOGIA E EVOLUÇÃO DA
BIODIVERSIDADE

MIGUEL MACHADO DA SILVA

PHYLOGENETIC RELATIONSHIPS IN STEPHANOPINAE: SYSTEMATICS OF *STEPHANOPIS* AND *SIDYMELLA* BASED ON MORPHOLOGICAL CHARACTERS (ARANEAE: THOMISIDAE)

Porto Alegre
2020

PÓS-GRADUAÇÃO - *STRICTO SENSU*

Pontifícia Universidade Católica
do Rio Grande do Sul

PONTIFÍCIA UNIVERSIDADE CATÓLICA DO RIO GRANDE DO SUL

ESCOLA DE CIÊNCIAS DA SAÚDE E DA VIDA

PROGRAMA DE PÓS-GRADUAÇÃO EM ECOLOGIA E EVOLUÇÃO DA BIODIVERSIDADE

PHYLOGENETIC RELATIONSHIPS IN STEPHANOPINAE: SYSTEMATICS OF *STEPHANOPIS* AND *SIDYMELLA* BASED ON MORPHOLOGICAL CHARACTERS (ARANEAE: THOMISIDAE)

Miguel Machado da Silva

TESE DE DOUTORADO

PONTIFÍCIA UNIVERSIDADE CATÓLICA DO RIO GRANDE DO SUL

Av. Ipiranga 6681 - Caixa Postal 1429

Fone: (051) 320-3500

CEP 90619-900 Porto Alegre - RS

Brasil

2020

PONTIFÍCIA UNIVERSIDADE CATÓLICA DO RIO GRANDE DO SUL

ESCOLA DE CIÊNCIAS DA SAÚDE E DA VIDA

PROGRAMA DE PÓS-GRADUAÇÃO EM ECOLOGIA E EVOLUÇÃO DA BIODIVERSIDADE

PHYLOGENETIC RELATIONSHIPS IN STEPHANOPINAE: SYSTEMATICS OF *STEPHANOPIS* AND *SIDYMELLA* BASED ON MORPHOLOGICAL CHARACTERS (ARANEAE: THOMISIDAE)

Miguel Machado da Silva
Orientador: Renato A. Teixeira

TESE DE DOUTORADO
PORTO ALEGRE –RS –BRASIL
2020

"Nobody exists on purpose. Nobody belongs anywhere. We're all going to die. Come watch TV."

Morty Smith

Dedico os frutos do presente estudo à minha mãe, Gilce Elenar Leite Machado, e ao meu pai, Paulo Roberto da Silva. Vocês sempre serão meus "coautores", de coração, em todos artigos publicados. Obrigado por todo o incentivo e apoio. Amo muito vocês!

SUMÁRIO

AGRADECIMENTOS

RESUMO

Dentre as subfamílias atualmente aceitas em Thomisidae, Stephanopinae destaca-se pelo grande número de espécies e gêneros que ainda carecem de estudos taxonômicos e filogenéticos que contribuam para a maior compreensão quanto a suas relações evolutivas e diversidade. A recuperação do polifiletismo para Stephanopinae é citada frequentemente, indicando a necessidade de uma investigação mais profunda sobre a composição do grupo e testes de monofilia para seus gêneros componentes. Desta forma, o trabalho a seguir objetivou revisitar e redefinir os limites morfológicos de *Sidymella* e *Stephanopis* por meio de revisões taxonômicas, bem como testar a monofilia de ambos os gêneros e discutir suas relações filogenéticas. Para tanto, foi construída uma matriz de dados baseada em 117 caracteres morfológicos codificados para 77 táxons terminais, a qual foi submetida a análises de máxima parcimônia (com pesagem igual dos caracteres e pesagem implícita) e inferência bayesiana. Os suportes de ramos foram calculados através do índice relativo de Bremer e por meio de reamostragens simétricas, enquanto a estabilidade nodal foi representada por "tapetes Navajo" em um teste de sensitividade. Os resultados obtidos indicam o polifiletismo tanto de *Sidymella* quanto de *Stephanopis*, sendo as espécies componentes deste último divididas em cinco grupos distintos: o "clado *cambridgei*", o qual tem suas espécies componentes combinadas à com *Isala*, o "clado *championi*", no qual justifica-se a revalidação o gênero *Paratobias*; o "clado *ditissima*", cujas espécies são transferidas para *Coenypha*; o "clado *pentacantha*", que abriga as espécies de distribuição sul-americana do gênero *Stephanopis*, e finalmente o "clado *altifrons*", tratado como *Stephanopis* (*stricto sensu*) por compreender a espécie-tipo *S. altifrons* e outras quinze espécies Australianas. *Sidymella* apresenta espécies emergindo também em distintas linhagens, sendo atribuído ao "clado *lucida*" o status de *Sidymella* (*stricto sensu*) uma vez que é composto pela espécie-tipo do gênero e demais representantes de distribuição Neotropical. Espécies Australianas até então atribuídas a *Sidymella* são por hora tratados como clados dissidentes ("clado *trapezia*, "clado *hirsuta*" e "clado *angulata*"), ainda que apresentem evidências morfológicas suficientes que justifiquem suas proposições como gêneros novos.

A revisão taxonômica das espécies Neotropicais de *Sidymella* permitiu a redescrição de *S. furcillata*, *S. longispina*, *S. lucida* e *S. kolpogaster*, enquanto duas novas espécies foram descritas (*S. excavata* e *S. marmorata*). Atos taxonômicos adicionais foram realizados: *S. nigripes* é considerada *species inquirenda* enquanto *S. obscura*, *S. parallela* e *S. spinifera* são colocadas em *nomina dubia*. Novos registros de distribuição para *Sidymella* na região Neotropical são apresentados, assim como as diagnoses e descrições são atualizadas. A composição do gênero, anteriormente de 21 espécies, diminui para 20. De forma similar, é apresentada a revisão taxonômica de *Stephanopis*, no entanto, restringindo-se às espécies do gênero que possuem distribuição Australiana. Neste estudo é apresentada uma chave dicotômica para machos e fêmeas, de modo a facilitar o reconhecimento e identificação das espécies do grupo que ocorrem na Austrália, Papua Nova Guiné, Indonésia e Fiji. A espécie-tipo *S. altifrons* é redescrita e as espécies *S. aspera*, *S. depressa*, *S. monticola*, *S. elongata* e *S. scabra* são consideradas seus sinônimos júnior. Os machos de *S. altifrons*, *S. angulata*, *S. nigra*, *S. armata*, S. *fissifrons* e *S. longimana* são descritos pela primeira vez. Neótipos são propostos para as espécies *S. nigra* e *S. barbipes*, sendo a fêmea desta última descrita de forma inédita. Sete novas espécies são descritas (*S. arenata*, *S. squalida*, *S. flagellata*, *S. nana*, *S. spiralis*, *S. similis*, *S. carcinoides*) e nove são consideradas *nomina dubia* (*S. bradleyi*, *S. clavata*, *S. cristipes*, *S. malacostracea*, *S. minuta*, *S. ornata*, *S. secata* e *S. vilosa*). A espécie *S. thomisoides* é considerada *species inquirenda* e *S. cheesmanae* é combinada à *Phrynarachne*. Novos dados de distribuição são providos e comentários à cerca da validade do gênero e de sua relação com espécies de *Sidymella* e outros Stephanopinae da região Australiana embasam a proposição feita pelos autores para a possível existência de grupos distintos dentro de *Stephanopis*, os quais são discutidos na análise filogenética.

Palavras-chave: Sistemática, taxonomia, aranha-caranguejo, espécie nova, Neotropical.

RESUMO

The subfamily Stephanopinae stands out among other groups in Thomisidae by its significative number of species and genera that are still in need of taxonomic reviews and phylogenetic studies, which would help us to better comprehend their diversity and evolutive relationships. The polyphyletism of Stephanopinae has been frequently recovered in recent phylogenetic works, indicating the necessity to perform monophyly tests for its component genera and proper investigations on the composition of the group. Therefore, the present study aimed the redefinition of the morphological boundaries of *Stephanopis* and *Sidymella* through taxonomic reviews, as well as test the monophyly of both genera discussing their phylogenetic relationships. To do so, a data matrix with 117 morphological characters, coded for 77 terminal taxa, was assembled. This matrix was submitted to parsimony analysis (under equal weights and an implied weighting scheme) and bayesian inference. Branch supports were estimated through relative Bremer support index and symmetric resampling, while nodal stability was represented by "Navajo rugs" of a sensitivity test. The obtained results indicate that both *Sidymella* and *Stephanopis* are polyphyletic, with the component species of this latter emerging in five distinct groups: the "*cambridgei* clade", which has all its species transferred to *Isala*; the "*championi* clade", proposed here as *Paratobias* **gen. rev.**; the "*ditissima* clade", whose comprised species are combinated to *Coenypha*; the "*pentacantha* clade", comprising all South-American species of *Stephanopis*, and finally the "*altifrons* clade", considered here as *Stephanopis* (*stricto sensu*) for comprehend the type-species *S. altifrons* and other 15 species with Australian distribution. *Sidymella* also presented species emerging in distinct lineages, being attributed to the "*lucida* clade" the status of *Sidymella* (*stricto sensu*), since it is composed by the type species of the genus *S. lucida* and other Neotropical representatives. Australian species hitherto attributed to *Sidymella* are for now treated as dissident clades ("*trapezia* clade", "*hirsuta* clade" and "*angulata* clade"), even presenting strong evidences that suggest their possible validity as new independent genera.

The taxonomic review of Neotropical *Sidymella* species allowed the redescription of *S. furcillata*, *S. longispina*, *S. lucida* and *S. kolpogaster* and two new species to be

described (*S. excavata* and *S. marmorata*). Additional taxonomic acts were also proposed: *S. nigripes* is considered *species inquirenda* while *S. obscura*, *S. parallela* e *S. spinifera* are put in *nomina dubia*. New distribution records for *Sidymella* in the Neotropics are presented as well as diagnoses and descriptions are updated. Thereby, the genus previously composed by 21 species, now comprises 20. Similarly, we presente a taxonomic review of *Stephanopis*, but in this case, focusing on the Australian representatives of the genus. In this study an identification key for males and females is provided. The type-species *S. altifrons* is redescribed while *S. aspera*, *S. depressa*, *S. monticola*, *S. elongata* e *S. scabra* are considered its junior synonyms. Males of *S. altifrons*, *S. angulata*, *S. nigra*, *S. armata*, S. *fissifrons* e *S. longimana* are described for the first time. Neotypes are proposed for *S. nigra* and *S. barbipes*, being the female of this latter originally described in this same work. Seven new species are proposed (*S. arenata*, *S. squalida*, *S. flagellata*, *S. nana*, *S. spiralis*, *S. similis* and *S. carcinoides*) and nine are considered *nomina dubia* (*S. bradleyi*, *S. clavata*, *S. cristipes*, *S. malacostracea*, *S. minuta*, *S. ornata*, *S. secata* and *S. vilosa*). The species *S. thomisoides* is considered *species inquirenda* and *S. cheesmanae* is transferred to *Phrynarachne*. New distribution records are provided and a brief comment section regarding the validity of the genus and its relationship with *Sidymella* and other stephanopines is presented, supporting the proposition for the possible existence of distinct groups of species in *Stephanopis*, which would come to be posteriorly discussed in the phylogenetic analysis.

Keywords: Systematics, taxonomy, crab-spider, new species, Neotropical.

APRESENTAÇÃO GERAL

O presente trabalho de tese traz os resultados de quatro anos de estudo sobre a taxonomia e sistemática de *Stephanopis* e *Sidymella*. Ambos os gêneros são considerados polifiléticos e as topologias obtidas sugerem não somente atos taxonômicos dentro destes grupos como também propõem mudanças significativas na composição de outros gêneros da subfamília Stephanopinae. O capítulo um portanto é a sessão mais abrangente do presente estudo, tido como principal e portanto é o primeiro a ser apresentado. No entanto, em ordem cronológica, os capítulos quatro e cinco o antecedem. O capítulo quatro visa a revisão taxonômica das espécies de *Sidymella* que ocorrem na Região Neotropical, enquanto o capítulo cinco foca na taxonomia das espécies Australianas do gênero *Stephanopis*. Ambos os capítulos estão publicados e tiveram por objetivo realizar uma "limpeza taxonômica" e reconhecer os limites morfológicos dos gêneros através da atualização de diagnoses e descrições de suas espécies componentes. Ademais, o significativo número de sinonímias realizadas nestes trabalhos evitou a codificação múltipla das mesmas espécies na matriz de dados da análise filogenética.

O capítulo 2 consiste na proposição de um gênero novo para acomodar as espécies Neotropicais de *Stephanopis* pertencentes ao "clado *pentacantha*", como sugerido no capítulo 1. Este capítulo traz uma revisão taxonômica do grupo, com novos registros de distribuição, descrição de novas espécies, sinonímias e novas combinações. O capítulo 3, por sua vez, apresenta algo semelhante ao propor a transferência e redescrição das espécies de distribuição Andino-patagônica anteriormente atribuídas a Stephanopis, ou "clado *ditissima*", como tratado no capítulo 1, para *Coenypha*. Este capítulo também traz novos registros de distribuição, sinonímias e descrições inéditas de espécies.

INTRODUÇÃO GERAL

Thomisidae Sundevall, 1833 é atualmente a sétima maior família de aranhas, com 2.145 espécies descritas em 170 gêneros (World Spider Catalog, 2020). Desde sua proposição original, autores subsequentes têm concentrado esforços para discutir aspectos relativos à sua taxonomia e sistemática de forma ampla (Simon, 1895; Roewer, 1954; Ono, 1988, Benjamin *et al*., 2008; Benjamin, 2011, Teixeira *et al*., 2014; Ramirez, 2014). Simon (1895) produziu um dos mais relevantes trabalhos taxonômicos clássicos sobre aranhas, e foi pioneiro ao compilar dados precedentes e sugerir uma classificação de grupos dentro da família Thomisidae, ordenando-as nas subfamílias Aphanthochilinae, Strophiinae, Stiphropodinae, 'Stephanopsinae' (*lapsus calami* de Stephanopinae), Misumeninae e Philodrominae. Este autor foi além ao inferir a existência de subdivisões dentro das subfamílias de Thomisidae, as quais podem ser entendidas como prováveis tribos. Dentro de 'Stephanopsinae' Simon (1895) menciona os grupos Hedaneae, Stephanopoideae, Phrynarachneae e Stephanopseae. O grupo Stephanopseae (*sensu* Simon, 1895), por exemplo, é caracterizado pelos: enditos convergentes; lábio curto e truncado; pelos dois pares anteriores de pernas notavelmente maiores que os demais; e a presença de macrocerdas bem desenvolvidas na região ventral das tíbias e metatarsos das pernas anteriores. Este grupo inclui os atuais gêneros *Borboropactus* Simon, 1884, *Synalus* Simon, 1895, *Isala* Koch, 1876, *Epicadinus* Simon, 1895, *Onocolus* Simon, 1895, *Epicadus* Simon, 1895, *Tobias* Simon, 1895, *Stephanopis* O. Pickard-Cambridge, 1869, *Sidymella* Strand, 1942 e *Coenypha* Simon, 1895. Após os trabalhos de Simon (1895; 1903), diversos estudos discutiram a relação e validade das subfamílias de Thomisidae (Petrunkevich, 1928; Mello-Leitão, 1929; Roewer, 1954; Homman, 1975). A revisão da sistemática clássica e discussões subsequentes foi feita por Ono (1988), que além de incluir informações sobre olhos, pernas, enditos e quelíceras na caracterização destas subfamílias, propõe um dendrograma com sua hipótese sobre o relacionamento delas (Fig. 1).
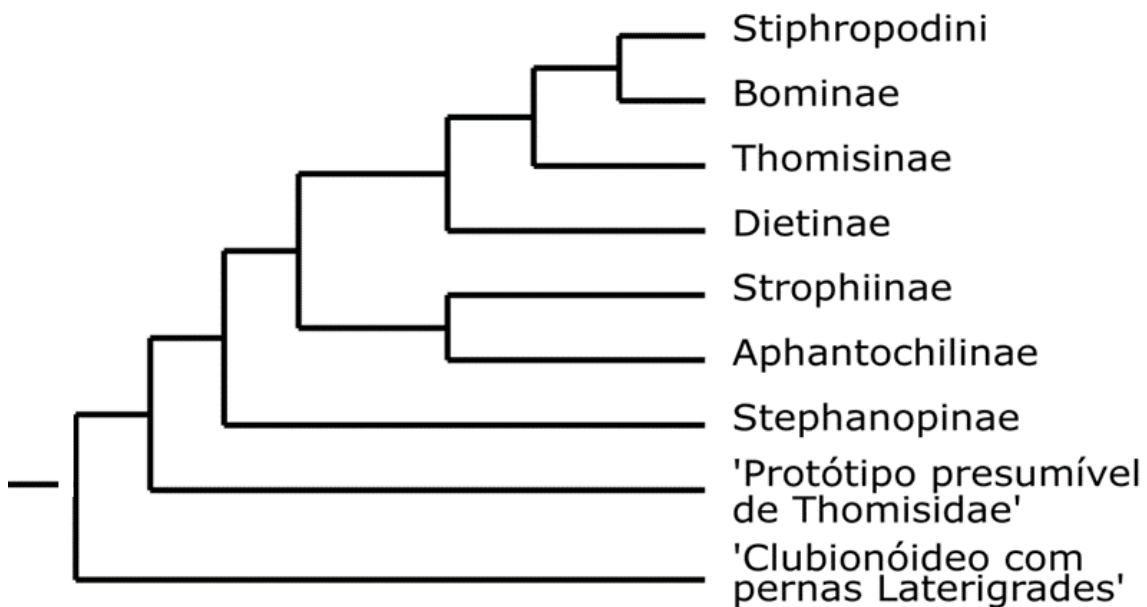
Figura 1. Dendrograma representando as relações entre as subfamílias de Thomisidae (Modificado de Ono, 1988).

Ono (1988) considera Stephanopinae como a subfamília basal de Thomisidae e a caracteriza por seus componentes possuírem enditos dispostos paralelamente, lábio curto e truncado, pernas anteriores robustas e armadas com macrocerdas ventrais nas tíbias e metatarsos, e pelos olhos medianos posteriores bem desenvolvidos, geralmente maiores do que os olhos laterais posteriores. Ono (1988) também ressalta que a presença de dentes nas quelíceras seria a possível característica diagnóstica para Stephanopinae e além disso, reitera os comentários de Simon (1895) ao relacionar a subfamília a um ancestral hipotético de Thomisidae que seria possivelmente correlato a um "clubionóide de pernas laterígradas" (Fig. 1).

Estudos filogenéticos mais recentes que testaram a monofilia de Thomisidae (Benjamin *et al.*, 2008; Benjamin, 2011), também corroboram em parte o que foi proposto por Simon (1895). Embora a monofilia de Stephanopinae não seja recuperada, os resultados de Benjamin *et al*. (2008) e Benjamin (2011) apontam uma estreita relação entre alguns dos gêneros integrantes de Stephanopseae (*sensu* Simon, 1895) (*Onocolus* Simon, 1895, *Sidymella* Strand, 1942 e *Stephanopis* O. Pickard-Cambridge, 1869). Tais gêneros são chamados por Benjamin (2011) de "clado *Stephanopis*", e são relacionados pela presença da região ocular projetada anteriormente. Tal característica já havia sido

2

utilizada por Pickard-Cambridge (1869) como diagnose de *Stephanopis*, gênero descrito a partir de uma fêmea de *S. altifrons* Cambridge, 1869 coletada no sul da Austrália.

Atualmente, *Stephanopis* é formado por 47 espécies válidas distribuídas ao longo da Zona de Transição Sul-americana (*sensu* Morrone, 2006), da Região Neotropical e da Região Australiana (World Spider Catalog, 2020). Suas espécies são caracterizadas também por apresentarem a fila anterior de olhos fortemente recurva, olhos medianos anteriores maiores que os demais e alocados sobre a protuberância cefálica anteriormente mencionada (Pickard-Cambridge, 1869). O prosoma dos indivíduos é levemente achatado, largo na parte posterior e afilado na porção anterior, usualmente coberto por muitos tubérculos setíferos; região ocular além de elevada, bilobada (Simon, 1895); o opistosoma usualmente é ovalado, rugoso na porção posterior e densamente coberto por cerdas (Pickard-Cambridge, 1869, Simon, 1895). Apesar dos caracteres diagnósticos supostamente notáveis, Simon (1895) menciona que *Stephanopis* é um gênero pouco homogêneo, apontando disparidades marcantes entre as espécies australianas (i.e. *S. altifrons*; *S. scabra*; *S. cambridgei*) e as sul-americanas (i.e. *S. ditissima*); principalmente com relação ao comprimento e altura do prosoma, ao formato do abdômen, e as proeminências que esta região pode apresentar. Segundo Simon (1895), *Stephanopis* poderia ser subdividido em quatro subgrupos, representado pelas espécies *S. altifrons*, *S. ditissima*, *S. bicornis* e *S. rubrosignata*, ou quiçá nem possuir valor genérico. Ademais, ele comenta brevemente à respeito da similaridade entre *Stephanopis* e *Sidymella*, baseando-se no compartilhamento do formato bilobado do opistossoma de alguns indivíduos e por seus prossomas alongados e com área ocular proeminente.

A suposta proximidade entre *Stephanopis* e *Sidymella* foi recentemente corroborada na análise cladística realizada por Benjamin (2011), onde ambos gêneros, juntamente com *Onocolus*, emergiram como integrantes do que este autor propôs como "clado *Stephanopis*" (Fig. 2). Posteriormente, ao considerar variáveis biogegráficas e realizar uma análise filogenética para verificar as relações entre os Thomisidae da fauna neozelandesa, Sirvid *et al.* (2013) corroborou a relação próxima destes gêneros ao recuperar *Stephanopis* nr. *corticalis* dentro do clado *Sidymella* (Fig. 4).
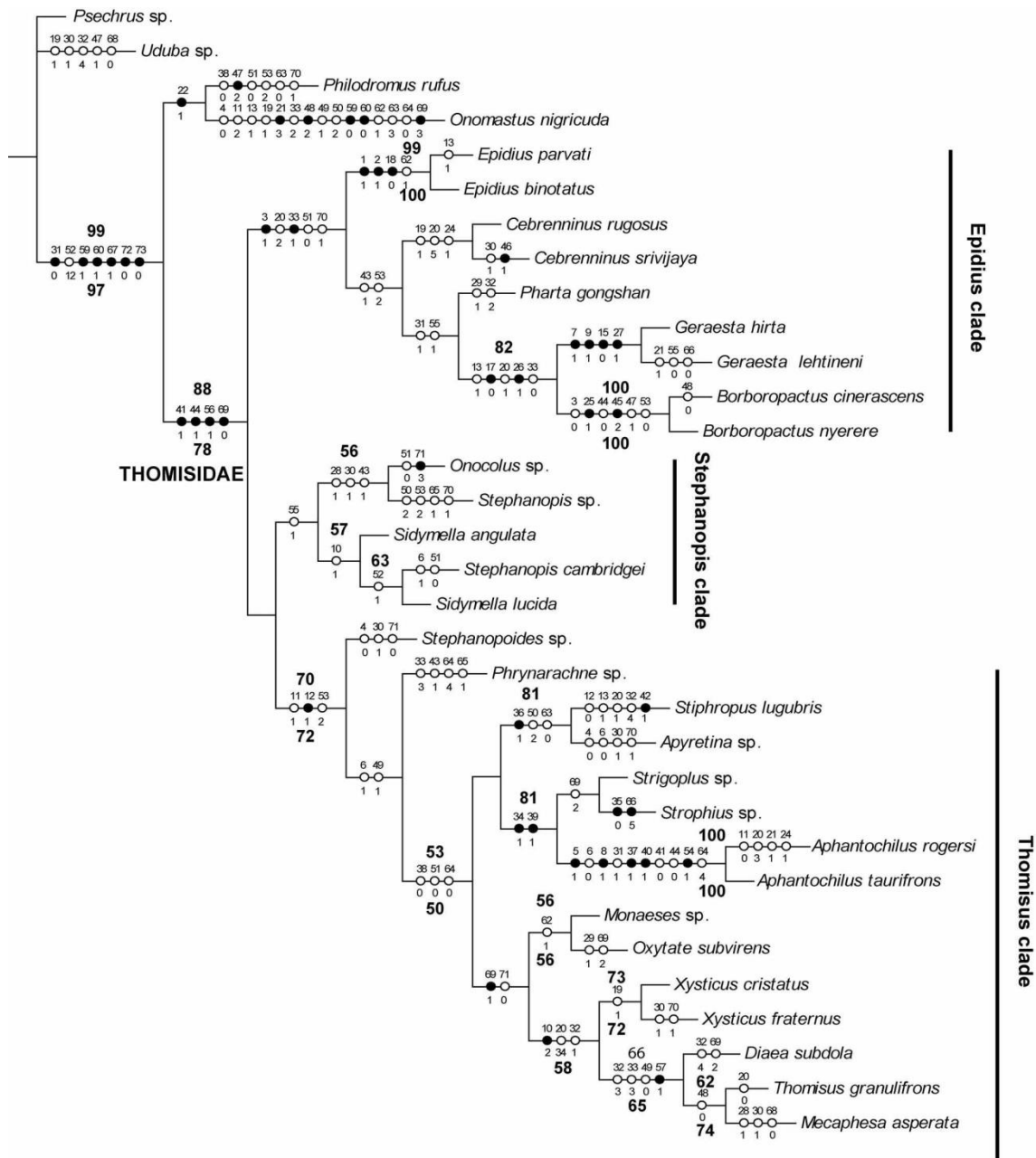
Figura 2. Hipótese filogenética para as relações em Thomisidae obtidas por análise de pesagem implícita (comprimento = 222, C.I. = 0.74, R.I. = 0.83). Números acima dos ramos representam os valores de Bootstrap e abaixo os de Jacknife, ambos acima de 50% (Retirado de Benjamin, 2011).

4
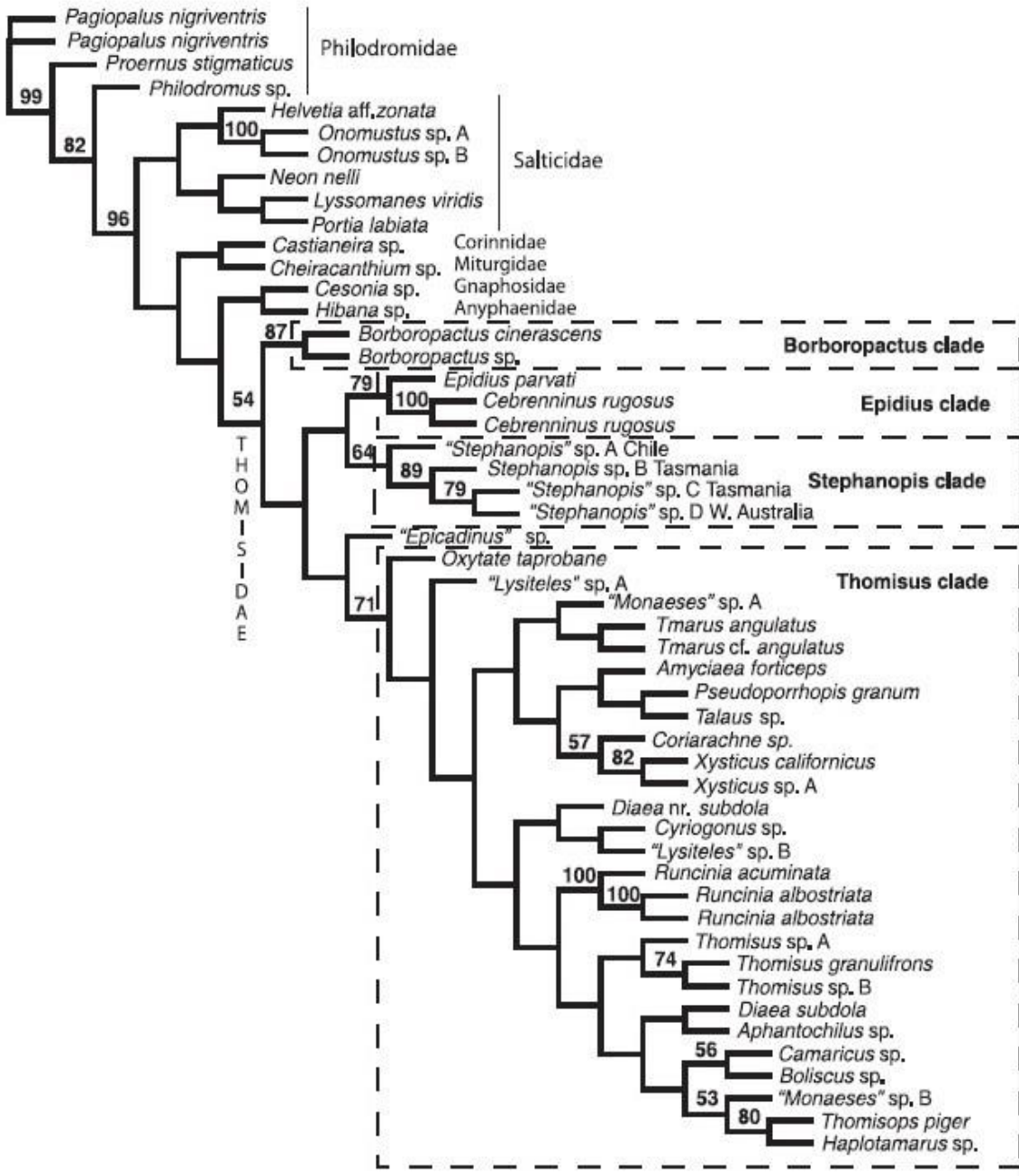
Figura 3. Uma das duas árvores mais parcimoniosas (L ¼ 3377) encontrada sob otimização direta. Relação abertura de gap/ custo de extensão de gap = 2/1. Valores de Jacknife maiores que 60 são mostrados acima dos ramos (Retirado de Benjamin, 2008).

5
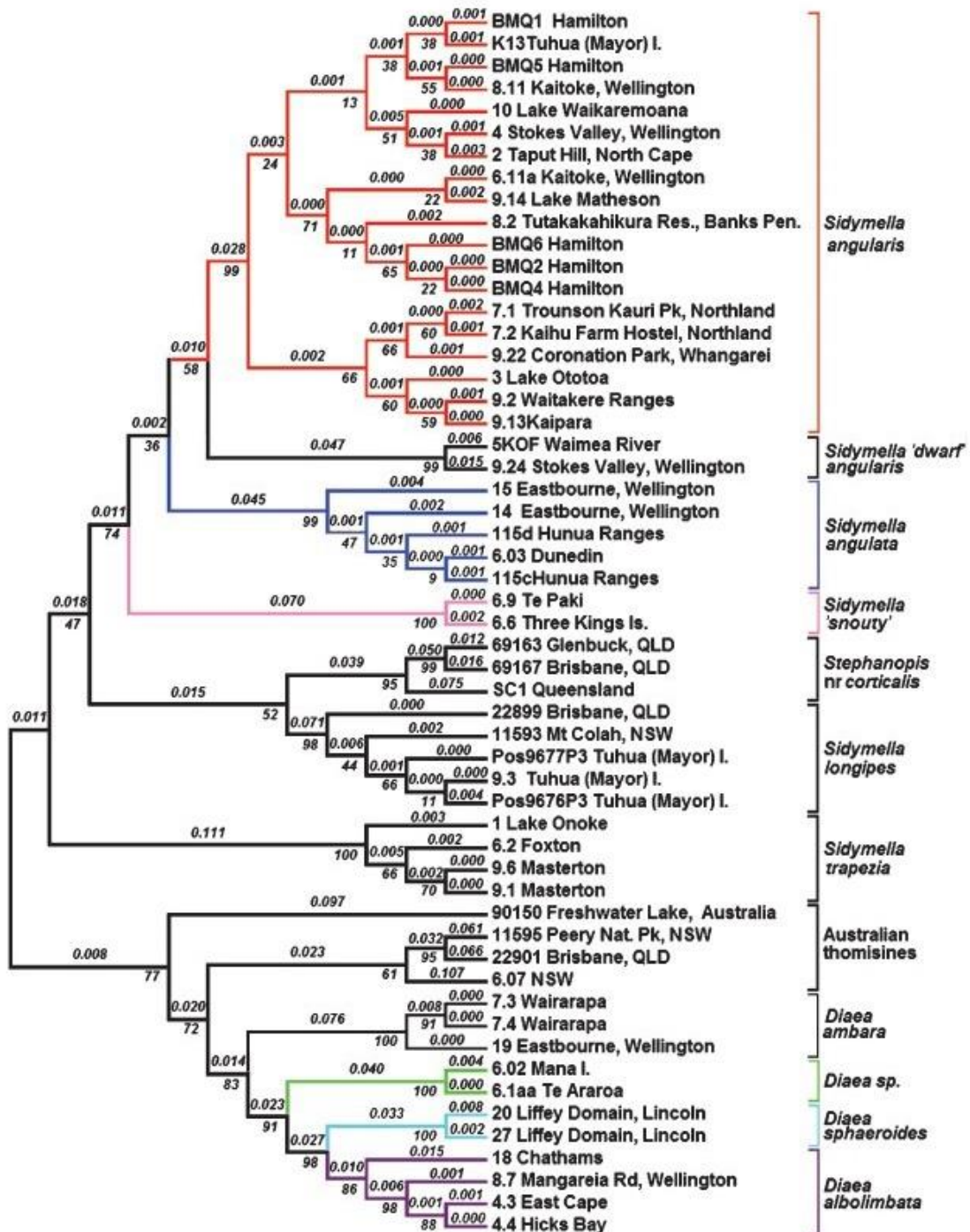
Figura 4. Árvore topológica de máxima verossimilhança baseada nos dados de sequenciamento do COI. Valor de comprimento dos ramos estão acima dos mesmos e valores de Bootstrap, abaixo. Ramos representando espécies não endêmicas da fauna da Nova Zelândia estão em preto (Retirado de Sirvid *et al*., 2013).

6

Apesar dos comentários feitos por Simon (1895), apontando disparidades observadas entre espécies australianas e chilenas de *Stephanopis*, ao propor o "clado *Stephanopis*", Benjamin *et al.* (2008) resgatam um monofiletismo entre estes organismos (Fig. 3). Recentemente, Machado & Teixeira (Chapter 1) evidenciaram as semelhanças morfológicas somáticas e das genitálias de *Stephanopis ditissima* Nicolet, 1849 e *Coenypha edwardsi* (Nicolet, 1849), sugerindo que as espécies de *Stephanopis* da fauna chilena descritas por Nicolet (1849) possam estar estreitamente relacionadas a *Coenypha*, ou que ambas sejam sinônimas. O gênero *Coenypha* compreende atualmente apenas quatro espécies, todas endêmicas do Chile (World Spider Catalog, 2020), e foi proposto por Simon (1895) para incluir inicialmente *Stephanopis edwardsi*. As espécies integrantes de *Coenypha* são caracterizadas pelo prossoma plano e mais largo do que longo, olhos anteriores dispostos em fileira fortemente recurva, pernas anteriores maiores e mais robustas que as posteriores e com fêmures dilatados, e pelo opistossoma tão largo quanto longo, com porção anterior truncada e posterior com projeções proeminentes (Simon, 1895).

Evidências baseadas em estudos taxonômicos como os de Simon (1895) e em análises filogenéticas recentes como as de Benjamin (2011) e Wheeler *et al*., (2017), sugerem a necessidade de uma maior investigação quanto às relações inter e intragenéricas em *Sidymella* e *Stephanopis*. Isso permitiria a delimitação destes grupos, sua diagnose e identificação de suas espécies componentes. Segundo Benjamin (2011), há muitos gêneros e espécies de Stephanopinae pouco estudadas, especialmente nas regiões Australianas e Neotropicais, e o aprimoramento do conhecimento sobre eles poderia trazer novas hipóteses de classificação para Thomisidae.

Revisões taxonômicas e descrições a respeito da composição das diversas famílias de aranhas, encontram-se fragmentadas no tempo (Platnick & Raven, 2013). Em razão de diversos motivos históricos, biogeográficos e pela própria riqueza de aranha no neotrópico, o conhecimento taxonômico do táxon nesta região, ainda é considerada incipiente (Platnick, 1991). Sobre Thomisidae neotropicais, talvez o trabalho mais inclusivo tenha sido o de Mello-Leitão (1929), onde este autor descreve diversas espécies pertencentes às subfamílias Aphantochilinae e Stephanopinae. Desde então, alguns trabalhos de revisão taxonômica e descrições de novas espécies em Stephanopinae foram realizados por Lise (1973), Lise (1981), Bonaldo & Lise (2001) Lise (2005) e Benjamin (2013).

Embora Lise (1973) tenha redescrito espécies de *Sidymella*, este autor focou seu estudo apenas em indivíduos de distribuição Neotropical, negligenciando a fauna australiana, a qual historicamente possui relação taxonômica a *Stephanopis* (e.i. nove das atuais 21 espécies de *Sidymella* foram descritas originalmente em *Stephanopis*, e ambos os gêneros possuem a mesma distribuição geográfica). De modo similar, *Coenypha* é formado por quatro espécies com distribuição restrita ao Chile e representa um gênero proposto com base em uma espécie que anteriormente era parte integrante de *Stephanopis*. A grande maioria das espécies de *Stephanopis* apresenta apenas descrições originais, as quais são pouco informativas e carecem de representações detalhadas de caracteres diagnósticos.

Tal histórico taxonômico sobreposto dos gêneros supracitados, tem sido constantemente corroborado em trabalhos filogenéticos recentes (Benjamin *et al*., 2008; Benjamin, 2011; Sirvid, 2013, Machado *et al*., 2017). Sirvid *et al*. (2013), por exemplo, recuperam *Stephanopis corticalis* no mesmo clado de *Sidymella longipes*. Ao testar a monofilia de Thomisidae Benjamin (2011) traz espécies de *Stephanopis* e *Sidymella* como parte integrante do clado *Stephanopis*; e Benjamin *et al*. (2008) apresenta espécies australianas de *Stephanopis* relacionadas a uma espécie da fauna chilena deste mesmo gênero. Em contrapartida, Machado *et al*. (2017) recuperam uma espécie Andina de *Stephanopis* relacionada a *Coenypha*, mas em clado distinto das demais espécies de *Stephanopis*, sugerindo a necessidade de possíveis transferências ou até sinonímias entre os dois gêneros. O estudo da taxonomia e das relações filogenéticas entre *Stephanopis* e *Sidymella* contribuiria para o reconhecimento da composição de espécies destes gêneros e representaria avanços no conhecimento da filogenia de Stephanopinae.

OBJETIVOS

Objetivo geral

Verificar Testar a monofilia de *Stephanopis* e *Sidymella*, avaliando suas relações filogenéticas dentro da subfamília Stephaopinae.

Objetivos específicos

a. Propor revisões taxonômicas dos gêneros *Stephanopis* e *Sidymella*, descrevendo possíveis novas espécies e elaborando chaves dicotômicas que contribuam para o fácil reconhecimento de seus táxons componentes.

b. Descrever possíveis novos gêneros após a análise filogenética.

REFERÊNCIAS

Benjamin, S.P. 2011. Phylogenetics and comparative morphology of crab spiders (Araneae: Dionycha, Thomisidae). Zootaxa, 3080: 1–108.

Benjamin, S.P. 2013. On the crab spider genus *Angaeus* Thorell, 1881 and its junior synonym *Paraborboropactus* Tang and Li, 2009 (Araneae: Thomisidae). Zootaxa, 3635: 71–80.

Benjamin, S.P., Dmitrov, D., Gillespie, R.G. & Hormiga, G. 2008. Family ties: molecular phylogeny of crab spiders (Araneae: Thomisidae). Cladistics, 24: 708–722.

Bonaldo, A.B., Lise, A.A. 2001. A review of the neotropical spider genus Stephanopoides (Araneae, Thomisidae, Stephanopinae). Biociências, 9(1): 63–80.

Bond, J.E. & Beamer, D. 2006. A morphometric analysis of mygalomorph spider carapace shape and its efficacy as a phylogenetic character (Araneae). Invertebrate Systematics, 20: 1–8.

Bremer, K. 1994. Branch support and tree stability. Cladistics, 10: 295–304.

Bryant, H.N. 1995. Why autapomorphies should be removed: a reply to Yeates. Cladistics, 11: 381–384.

Goloboff, P.A., Farris, J.S. & Nixon, K.C. 2008. TNT: Tree Analysis Using New Technology. Disponível em: www.zmuc.dk/public/philgeny.

Homann, H. 1975. Die Stellung der Thomisidae und der Philodromidae im System der Araneae (Chelicerata, Arachnida). Morphologie und Ökologie der Tiere, Zeitschrift für, 80: 181–202.

Lise, A.A. 1973. Contribuição ao conhecimento do gênero *Sidyma* no Brasil, com descrição de uma nova espécie (Araneae, Thomisidae). Iheringia - Série Zoologia, Porto Alegre, 43: 3–47.

Lise, A.A. 1981. Tomisideos Neotropicais V: Revisão do gênero *Onocolus* Simon, 1895 (Araneae, Thomisidae, Stephanopsinae). Iheringia - Serie Zoologia, Porto Alegre, 57: 3–97.

Lise, A.A. 2005. *Rejanellus*, a new genus of Thomisidae (Araneae, Stephanopinae). Iheringia. Série Zoologia, 95(2): 151–164.

Machado, M., Teixeira, R.A., & Lise, A.A. 2015. Taxonomic notes on the crab spider genus *Tobias* Simon, 1895 (Araneae, Thomisidae, Stephanopinae). Zootaxa, 4034(3): 565–576.

Machado, M.S., Teixeira, R. A., & Lise, A. A. 2017. Cladistic analysis supports the monophyly of the Neotropical crab spider genus *Epicadus* and its senior synonymy over *Tobias* (Araneae: Thomisidae). Invertebrate Systematics, 31: 442–455.

Maddison, W.P. & Maddison, D.R. 2011. Mesquite: a modular system for evolutionary analysis. Version 2.75.Disponível em: http://mesquiteproject.org

Mello-Leitão, C. F. 1929. Aphantochilidas e Thomisidas do Brasil. Archivos do Museu Nacional do Rio de Janeiro, Rio de Janeiro, 31: 9–359.

Morrone, J. 2006. Biogeographic Areas and Transition Zones of Latin America and the Caribbean Islands Based on Panbiogeographic and Cladistic Analyses of the Entomofauna. Annual Review of Entomology, 51: 467–494.

Nicolet, A.C. 1849. Aracnidos. In: Gay, C. (ed.) Historia física y política de Chile. Zoología 3: 319–543.

Nixon, K.C. 1999 – 2004. Winclada (BETA) ver. ASADO 1.89. Published by the author, Ithaca, NY.

Ono, H. 1988. A revisional study of the spider family Thomisidae (Arachnida, Araneae) of Japan. Tokyo: National Science Museum, 1–252 pp.

Petrunkevitch, A. 1928. Systema Aranearum. Transactions of the Connecticut Academy of Arts and Sciences, 29: 1–270.

Pickard-Cambridge, O. 1869. Descriptions and sketches of some new species of Araneida, with characters of a new genus. Annals and Magazine of Natural History 4(3): 52–74.

Platnick, N.I. 1991. Patterns of biodiversity: tropical vs temperate. Journal of Natural History, 25(5): 1083-1088.

Platnick, N.I. & Raven, R.J. 2013. Spider Systematics: Past and Future. Zootaxa, 3683 (5): 595–600.

Ramírez, M.J. 2014. The morphology and phylogeny of Dionychan spiders (Araneae: Araneomophae). Bulletin of the American Museum of Natural History, 390: 1–374.

Roewer, C.F. 1954. Katalog der Araneae von 1758-1940. Institut Royal des Sciences Naturelles de Belgique, Bruxelles, 1–1751 pp.

Silva-Moreira, T.D., & Machado, M. 2016. Taxonomic revision of the crab spider genus *Epicadus* Simon, 1895 (Arachnida: Araneae: Thomisidae) with notes on related genera of Stephanopinae Simon, 1895. Zootaxa, 4147(3): 281–310.

Simon, E. 1895. Histoire naturelle des araignées. Paris, 761–1084 pp.

Simon, E. 1903. Arachnides de la Guinée espagnole. Memorias de la Real Sociedad Española de Historia, 1: 65–124.

Sirvid, P.J., Moore, N.E., Chambers, G.K., & Prendergast, K. 2013. A preliminary molecular analysis of phylogenetic and biogeographic relationships of New Zealand Thomisidae (Araneae) using a multi-locus approach. Invertebrate systematics, 27(6): 655–672.

Stevens, P.F. 1991. Character states, morphological variation, and phylogenetic analysis: a review. Systematic Botany, 16: 553–583.

Sundevall, J.C. 1833. Conspectus Arachnidum. Londiini Gothorum, 1–39 pp.

Teixeira, R.A., Campos, L.A. & Lise, A.A. 2013. Philogeny of Aphantochilinae and Strophinae sensu Simon (Araneae ; Thomisidae). Zoologica Scripta, 43(1): 65–78.

World Spider Catalog (2020) World Spider Catalog, version 21.0. Natural History Museum Bern. Disponível em: http:// wsc.nmbe.ch (acessado em 09 Abril de 2020)

Chapter 1: Phylogenetic relationships in Stephanopinae: systematics of *Stephanopis* and *Sidymella* based on morphological characters (Araneae: Thomisidae)

Miguel Machado* and Renato Augusto Teixeira

Laboratório de Aracnologia, Escola de Ciências, Pontifícia Universidade Católica do Rio Grande do Sul (PUCRS), Porto Alegre, Rio Grande do Sul, Brazil

Abstract

A matrix of 117 morphological characters scored for 77 terminal taxa was subjected to parsimony analysis under equal and implied weighting schemes and to Bayesian inference in order to test the relationships in and between *Stephanopis* and *Sidymella* species, as well as its implications for the systematics of the subfamily Stephanopinae. A sensitivity test was performed to evaluate nodal stability and assess the best corroborated hypothesis. Our results indicate the polyphyletism of both genera and the topologies obtained allowed the proposition of the following taxonomic acts: The "*altifrons* clade" is the only group considered as *Stephanopis* (*stricto sensu*), with species restricted to the Australian Region; most species from the Neotropical Region, hitherto attributed to this genus, formed the well-supported "*pentacantha* clade", while two of them, restricted to Central America, were recovered as the "*championi* clade". The latter shows significative evidences for the revalidation of *Paratobias* **gen. rev**.; the "*cambridgei* clade" emerged with *I. punctata* nested within, having all its component species transferred to *Isala*. None of the *Sidymella* species with Australian distribution seem to be part of this genus, which occurs in fact only in the Neotropical Region and is closely related to *Coenypha*. This latter has an increment of three species transferred from *Stephanopis*. Aside from the "*lucida* clade", which is considered here as *Sidymella* (*stricto sensu*), three other groups and a single species emerged apart from this genus: the "*hirsuta* clade", "*trapezia* clade", "*angularis* clade" and *S. rubrosignata*. Morphological evidences seem to justify the proposition of all these groups as new genera.

Keywords: Australian; Cladistic; Neotropical; spider; systematics

Introduction

The subfamily Stephanopinae has been the focus of recent revisional works (Benjamin, 2013; Benjamin, 2015; Machado *et al*., 2015; Benjamin, 2016; Silva-Moreira and Machado, 2016; Benjamin, 2017; Machado *et al*., 2017; Machado *et al*., 2018; Prado *et al.*, 2018; Machado *et al*., 2019a, Machado *et al*., 2019b). Even so, most of its component genera are still poorly known and diagnosed, which is reflected in the lack of resolution and constant recovery of its polyphyletic relations (Benjamin *et al*., 2008; Benjamin, 2011; Wheeler *et al*., 2017). The genus that gives name to the subfamily had its Australian species recently revised by Machado *et al*. (2019b), but despite the recent efforts to better understand the morphology of *Stephanopis* O. Pickard-Cambridge, 1869, our knowledge regarding the Neotropical and Andean species of the genus rely only on original descriptions. A similar scenario is observed for *Sidymella* Strand, 1942, which also had its diagnosis and description updated by Machado *et al*. (2019a). However, in this case only the Neotropical species were considered in the taxonomic work while the Australian ones remain in need of revision.

The distribution regions of both *Stephanopis* and *Sidymella* overlap, occurring along the Neotropical and Australian Regions (World Spider Catalog, 2020). Some species present striking morphological similarities and crossed taxonomic backgrounds. Descriptions of wrongly assigned species also highlight their blurred taxonomic limits. Simon (1895) already mentioned that *Stephanopis* was barely homogenous, pointing out some notable differences between its Australian (*i.e.*, *S. altifrons* O. Pickard-Cambridge, 1869*; S. scabra* L. Koch, 1874*; S. cambridgei* Thorell, 1870) and South American species (*i.e.*, *S. ditissima* Nicolet, 1874), especially regarding the length and height of their prosoma as well as the shape of their abdominal projections. According to this author, there were four distinguishable groups within *Stephanopis* (represented by *S. altifrons* O. Pickard-Cambridge, 1869, *S. ditissima* (Nicolet, 1849), *S. bicornis* L. Koch, 1874 and *Sidymella rubrosignata* (L. Koch, 1874) – the latter previously assigned to *Stephanopis*), which made him question the validity of the genus. While Simon (1895) considered Australian and Neotropical representatives of *Stephanopis* to make this statement, Machado *et al*. (2019b), based on comparisons of both somatic and sexual traits, inferred existence of three different groups within a group of species with distribution ranges restricted to Australia, Indonesia, Papua New Guinea and Fiji, called them '*cambridgei* group', '*lata* group' and '*altifrons* group'.

The genus *Stephanopis* currently comprises 47 species, being originally proposed based on a female of *S. altifrons* and is characterized by their high clypeus, cephalic prominence, dorsoventrally depressed prosoma, robust legs with dorsal acute projections and remarkable setiferous tubercles along their patellae and tibiae (Machado *et al.*, 2019b). Despite the recent taxonomic review and updated diagnosis, the validity of the genus remains uncertain. Unlike what is presented in current morphological studies on spiders, genitalic features were not always considered in classic taxonomic works. The most common characteristics considered by earlier naturalists to assign a given species to *Stephanopis* were general somatic features related to the cryptic habitus of the spiders (e.g., Nicolet, 1849; O. Pickard-Cambridge, 1869; Bradley, 1871; Koch, 1874; Mello-Leitão, 1929). Both the Australian and Neotropical species of *Stephanopis* indeed share characteristics of a typical bark-dwelling stephanopine, as pointed by Machado *et al.* (2017), such as rugose tegument and predominantly dark body coloration. Additionally, many species bear soil particles attached to their tegument or present some association with lichens and/or fungi (Machado *et al.*, 2019b). Nevertheless, it is still unknown if this set of features is the result of an evolutionary convergence related to hunt/camouflage adaptations or if *Stephanopis* is indeed monophyletic. The same question deserves a proper study in regard to the bifid opisthosoma of *Sidymella* species, a trait that was still recently considered by Machado et al. (2019a) as one of the main traits to diagnose the genus.

The genus *Sidymella*, described based on the type-species *Sidymella lucida* (Keyserling, 1880), is currently recognized by males having a long, thin and curled embolus, well-developed pars pendulum and retrolateral tibial apophysis with a short basal branch (Machado *et al.*, 2019a). Females present a median septum on the epignyal plate, long and coiled copulatory ducts and compartmentalized spermathecae with accessory glands (Machado *et al.*, 2019a). Despite sharing the presence of the posterior pair of lateral projections on the opisthosoma, other somatic characteristics observed in Australian representatives of the genus on the other hand, are not comprehended by the diagnosis and descriptions provided by Machado *et al.* (2019b). Moreover, the genital features mentioned above differs from what Koch (1874) described for *S. bicuspidata* (L. Koch, 1874), *S. hirsuta* (L. Koch, 1874), *S. lobata* (L. Koch, 1874), *S. longipes* (L. Koch, 1874), *S. rubrosignata* (L. Koch, 1874) and *S. trapezia* (L. Koch, 1874). Therefore, a broader study must be carried out to check such incongruences.

Considering these previous observations and insights, in the current study we perform a phylogenetic analysis based on an extensive morphological dataset that aims to test the monophyly and relationships in between *Stephanopis* and *Sidymella*.

Materials and methods

Cladistic analysis

The character matrix (Supplementary Material data 1) was assembled in Mesquite 3.51 (Maddison and Maddison, 2018) starting from preliminary results published by Machado *et al*. (2017), from where most of the characters were adapted or originally interpreted. We also incorporated propositions made by Benjamin (2011) and Ramírez (2014) into our dataset. Aiming to explore different perspectives of reconstruction of the evolutionary relationships, two optimality criteria were chosen: Bayesian inference (BI) and maximum parsimony (MP). In spite of recent discussions regarding which would be the best method to infer phylogenies based on morphological characters (Goloboff *et al*., 2008b; O'Reilly *et al*., 2018; Goloboff *et al*., 2018a, 2018b; Puttick *et al*., 2019), some authors such as Smith (2019) show that both approaches are likely to be equally informative. In compliance with the proposition made by this author, we chose to perform analyses using both methods, comparing the results to find the most congruent and supported clades. Poorly resolved topologies (e.g., EW parsimony) were submitted to search routines where taxa with variable placement in the topology (wild cards) were pruned from the tree [pcrprune]. Pruning was applied only when the absence of a clade or taxon provided more gains in resolution (resolved nodes) than removed terminals.

The Bayesian inference was performed in MrBayes 3.2.0 (Ronquist *et al*., 2012). The parameters were the same as those considered by Ronquist *et al*. (2012) as appropriate to the kind of data these authors called "standard", i.e.*,* matrices varying from zero to nine. The routines used were as follows: (1) set the JC model [lset nst=1 rates=equal]; (2) set MCMC generation parameter [mcmcp ngen=5000000 relburnin=no printfreq=1000 samplefreq=1000 nchains=4 savebrlens=yes]; (3) run the analysis [mcmc]. After that, the stationary distribution of the chains was recovered with Tracer v.1.6.0 (Rambaut *et al*., 2014) and used to burn-in the first 10% of the

generations. The remaining generations were used to estimate the posterior probability in a majority consensus tree.

Heuristic searches for most-parsimonious trees were made in TNT 1.1 (Goloboff et al., 2008a). Under maximum parsimony, the dataset was submitted to two different analysis: (1) equal weighting (EW) and (2) implied weighting (IW). For the latter, we followed the methodology described by Mirande (2009), which attributes several K values to a symmetric variation of the mean fit that each extra step represents in relation to a transformation. The values for concavity indices were calculated in a way that each extra step represent X% of the value of the previous transformation. Thus, we assigned 16 distortion values to "X" ranging from 50% to 90% of fitting. The parameters used in this weighting regime were the same as those by Machado et al. (2017). Seeking to create a simplified batch of search routines, we followed the tutorial provided by Weiler et al. (2016) to calculate the parameters manually (Supplementary Material data 2 — 'stephanopisroutine.run'). The following commands were set for analyses of MP (commands in TNT are shown in brackets): (1) memory was set to keep up to 500,000 trees [hold500000]; (2) search started from a random tree [rseed*]; (3) ratchet was set to perturb up to 5% of the characters, both down and up and to do 10 cycles of auto-constrains [rat:equal upfac5 downfac5 autoconst10]; (4) rearrangements were performed by random addition sequence (RAS) using tree bisection and reconnection (TBR) in cycles of sectorial searches (including default parameters of consensus-based and random rearrangement), 100 iterations of ratchet and 2 of tree fusing (Nixon, 1999; Goloboff, 1999) [xmult:ras css rss rat100 fuse2]; (5) rearrangement cycles were repeated 10 times until the most parsimonious result was obtained twice [xmult: hit2 rep10]; (6) finally, the obtained results were submitted to a new TBR turn with branch-swap [bb]. The strict consensus was saved and posteriorly edited in WinClada-Asado ver. 1.89 (Nixon, 1999–2004), where the characters were optimized. Branch supports were estimated through relative Bremer support (Goloboff and Farris, 2001) and symmetric resampling (Goloboff et al., 2003) in a similar manner to that of the abovementioned routine (Supplementary Material data 3 — 'stephanopisSUP.run').

Although all resulting trees should be seen as plausible results to be considered as the main hypothetical topology, the "best" tree must represent the major taxonomic stability on the highest supported trees. Thus, we compared pairs of trees counting how many SPR movements (pruning a subtree and rearranging it by its root to the

edge of the resulting tree) were required to make both topologies identical, converting such movements into a similarity index (Teixeira *et al*., 2014). The best phylogenetic reconstruction was the one whose tree had the greatest sum of similarities, being considered the most congruent. The consensus of all trees, including BI and both EW and IW for MP, were summarized on the "best/most congruent" tree in a sensitivity analysis performed in the software Ybyrá (Machado, 2015).

Choice of terminal taxa and examined species

Recent studies suggest that Stephanopinae is not monophyletic once none of its proposed diagnostic features had been recovered as reliable morphological synapomorphies. Consequentially, most of its component genera behave unpredictably in phylogenies, presenting poorly supported and unclear relationships. In light of this issue and seeking to avoid problems regarding character polarization, we included as many Stephanopinae genera as possible in our data matrix. Two species of *Tmarus* were also scored to verify the placement of the "*Thomisus* clade" (*sensu* Benjamin *et al*., 2008). The tree was rooted in *B. nyerere* once *Borboropactus* is considered to be sister to all other Thomisidae genera.

The ingroup includes 31 of the 47 valid species of *Stephanopis*, 13 of the 20 species currently assigned as *Sidymella*. Species known only by their type material or examined through photographs were not scored, as handling the specimens or SEM preparations and detailed observation of microstructures were not possible. All Australian representatives of *Stephanopis* were included in the matrix, while the Neotropical diversity of the genus was partially sampled. This was deliberately done because the taxonomic review of Australian species was recently published (Machado *et al*., 2019b), while the Neotropical species remain in need of revision. Nevertheless, as we are currently working on the morphological delimitation of the Neotropical species, we refrained to score species that are undoubtedly synonyms of those already shown here. Similarly, the recently revised *Sidymella* species from the Neotropical Region (Machado *et al*., 2019a) were all included, whereas Australian species that were identified as junior synonyms or *nomina dubia* (Chapter 2) were not scored. Three undescribed species were also added to test their placement in the phylogeny.

For the sake of objectivity, during the discussion we followed Morrone (2014) and Morrone (2015) in considering the regionalization of the Neotropical ecozone and

Andean Region, respectively. In this way, we refer to distinct clades of the ingroup according their geographic distribution. (e.g., "Australian *Stephanopis*", "Neotropical *Stephanopis*", "Australian *Sidymella*" and "Neotropical *Sidymella*"). Despite a considerable part of the Andes Mountain Range is outside of the Andean Region, the term "Andean *Stephanopis*" is used to objectively refers to the group of species of this genus which are recorded along the Subantartic and Patagonian regions (*sensu* Morrone (1994).

The specimens examined (Appendix 1) are deposited in the following institutions (acronyms and curators in parentheses): Australian Museum, Sydney, Australia (AMS, Graham Milledge), California Academy of Sciences, San Francisco, United States of America (CAS, Lauren Esposito), Instituto Butantan, São Paulo, Brazil (IBSP, Antonio D. Brescovit), Instituto Nacional de Pesquisas da Amazônia, Manaus, Brazil (INPA, L. R. França), Museo Nacional de Historia Natural, Santiago, Chile (MNNC, Andrea Martínez), Museu de Ciências e Tecnologia da Pontifícia Universidade Católica do Rio Grande do Sul, Porto Alegre, Brazil (MCTP, Renato A. Teixeira), Museu de Ciências Naturais da Fundação Zoobotânica do Rio Grande do Sul, Brazil (MCN, Ricardo Ott), Museu Nacional do Rio de Janeiro, Brazil (MNRJ, Adriano B. Kury), Museu Paraense Emílio Goeldi, Belém, Brazil (MPEG, Alexandre B. Bonaldo), Museum für Naturkunde der Humboldt-Universität, Berlin, Germany (ZMB, Jason Dunlop), Museum National d'Histoire Naturelle, Paris, France (MNHN, Christine Rollard), Museum of Comparative Zoology of Harvard, Cambridge, United States of America (MCZ, Gonzalo Giribet and Laura Liebensperger), Oxford University Museum of Natural History, Oxford, United Kingdom (OUMNH, Zoë M. Simmons), Queensland Museum, Brisbane, Australia (QM, Robert Raven) and Universidade Federal de Minas Gerais, Belo Horizonte, Brazil (UFMG, Adalberto J. Santos).

Laboratory procedures and specimen preparation

The terminology used to name both somatic and copulatory structures follows that of Machado *et al*. (2018). The female genitalia were detached and submerged in pancreatin solution in a double boiler for a few minutes. The slight and gradual increase in temperature provided total digestion of the soft tissues without risking the integrity of the delicate diagnostic structures. Males had their left palpus removed and

represented in ventral and retrolateral views. Palpi were not submerged in KOH because in Thomisidae the compact tegulum allows the observation of all structures (e.g., apophysis, embolus, tegular ridge, etc.) in the ventral view without the need for expansion processes. The material was observed under a stereomicroscope model Zeizz®Stemi SV6. Photographs of the dorsal habitus, front and both male and female genitalia were taken on a Multipurpose Zoom Microscope Leica M205A with a digital camera, and scanning electron microscopy was conducted with a Philips XL 30 from the Centro de Microscopia e Microanálises (CEMM) of the Pontifícia Universidade Católica do Rio Grande do Sul (PUCRS).

The anatomical abbreviations used in this study are as follows: AH, anterior hood; ALE, anterior lateral eyes; AME, anterior median eyes; CD, copulatory duct; CO, copulatory opening; EpT, epyginal teeth; S, spermathecae; MSept, median septum; MS, median spire; PLE, posterior lateral eyes; PME, posterior median eyes; RTA, retrolateral tibial apophysis; RTAvbr, retrolateral tibial apophysis' ventral branch; VTA, ventral tibial apophysis; Em, embolus; CP, cymbial process; T, tegulum; PrsP, pars pendulum; C, conductor; MA, median apophysis; TR, tegular ridge.

Results

The 117 morphological characters (Appendix 2) of our final dataset were scored for both sexes in 58 of the 77 terminal taxa. Six species were represented only by males and 13 only by females. Seventy percent of the entries were composed of somatic features while male genitalia represented 20.5% of the analysed data and the epigyna represented 9.5% of the characters (Supplementary Material Data 1).

Equal weight analysis found 288 most parsimonious trees with 734 steps, consistency index (CI) = 20 and retention index (RI) = 70. The strict consensus shows a lack of resolution among the outgroup species and for basal branches in general; however, terminal clades were better resolved (Fig. 1). Implied weight analysis of 16 distortion groups subjected to similarity comparisons (sprdiff command) showed three most-congruent trees with identical topologies. The most parsimonious tree obtained under K= 17.89 (fit=23.209) is used as a hypothetical reconstruction to discuss character transformations and the relationships in the ingroup (Fig. 2). The topology obtained through Bayesian inference had 95% similarity (three spr moves) when compared to equal weight parsimony (Fig. 1). Regardless of how homoplasies were

treated (equal or implied weight), most deep relationships were weakly supported, and both *Stephanopis* and *Sidymella* were shown to be polyphyletic under any optimality criteria (Figs 1 and 2).

The polyphyletic relations in *Stephanopis* showed species emerging in five distinct clades (Fig. 3 – taxa typed in red). The genus *Coenypha* was nested within the "Andean *Stephanopis*", being this clade recovered as sister group to "Neotropical *Sidymella*". The "Australian *Stephanopis*", on the other hand, emerged in two major clades: one is composed of the '*altifrons* group' + '*lata* group' [*sensu* Machado *et al*. (2019b)], and the other is formed by all species of the '*cambridgei* group' [*sensu* Machado *et al*. (2019b)] with *Isala punctacta* nested within. Most "Neotropical *Stephanopis*" emerged as sister to *Rejanellus*, integrating the '*Epicadus* group' [*sensu* Silva-Moreira and Machado (2016)]. While this clade is composed by species recorded for the Amazon Rainforest, Atlantic Forest and Cerrado biomes, the species with distribution restricted to Central America *S. championi* and *Stephanopis* sp.1 were recovered in a dichotomy with species of the '*cambridgei* group' [*sensu* Machado et al. (2019b)].
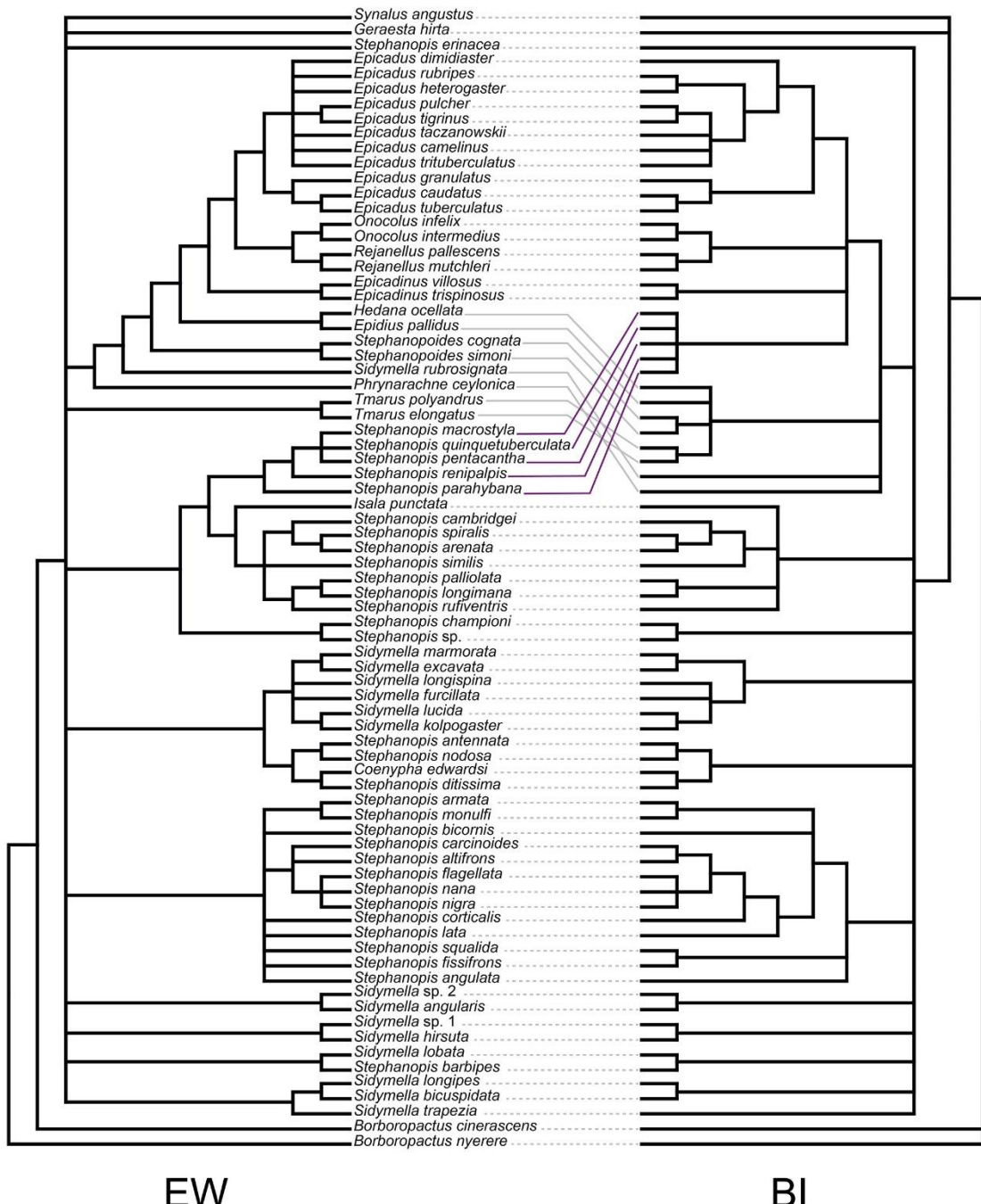
Figure 1. Topologic comparison between consensuses trees obtained under equal weighting parsimony (EW) and Bayesian inference (BI).
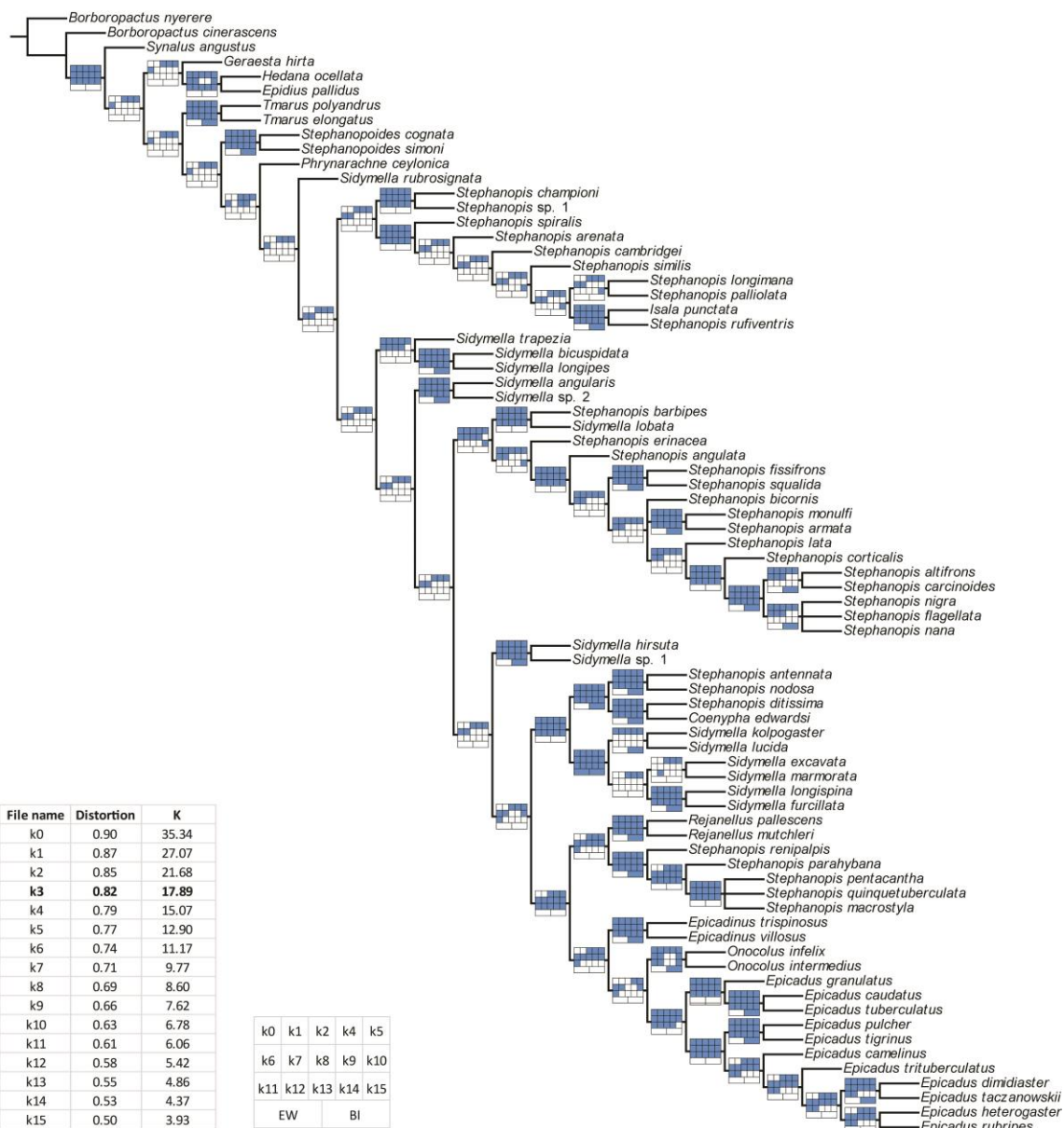
Figure 2. Hypothetical reconstruction of the relationships of *Stephanopis* and *Sidymella* based on the strict consensus of the most congruent tree (K= 17.89) obtained after implied weighted analysis. Nodal stability is represented by the "Navajo rugs" along the branches (analysis recovering the clades as shown in the discussed topology are represented by blue squares while alternative resolutions are those in white). EW = Equal weight; BI = Bayesian inference.

The species of *Sidymella* emerged as polyphyletic, arranged in five distinct clades (Fig. 3 – taxa typed in blue). All "Neotropical *Sidymella*" emerged in a single clade related to *Coenypha* + "Andean *Stephanopis*". The Australian representatives of the genus, on the other hand, were split into four distinct groups, which were relatively

well-supported by resampling analysis and Bremer support values, except the "*trapezia* clade".
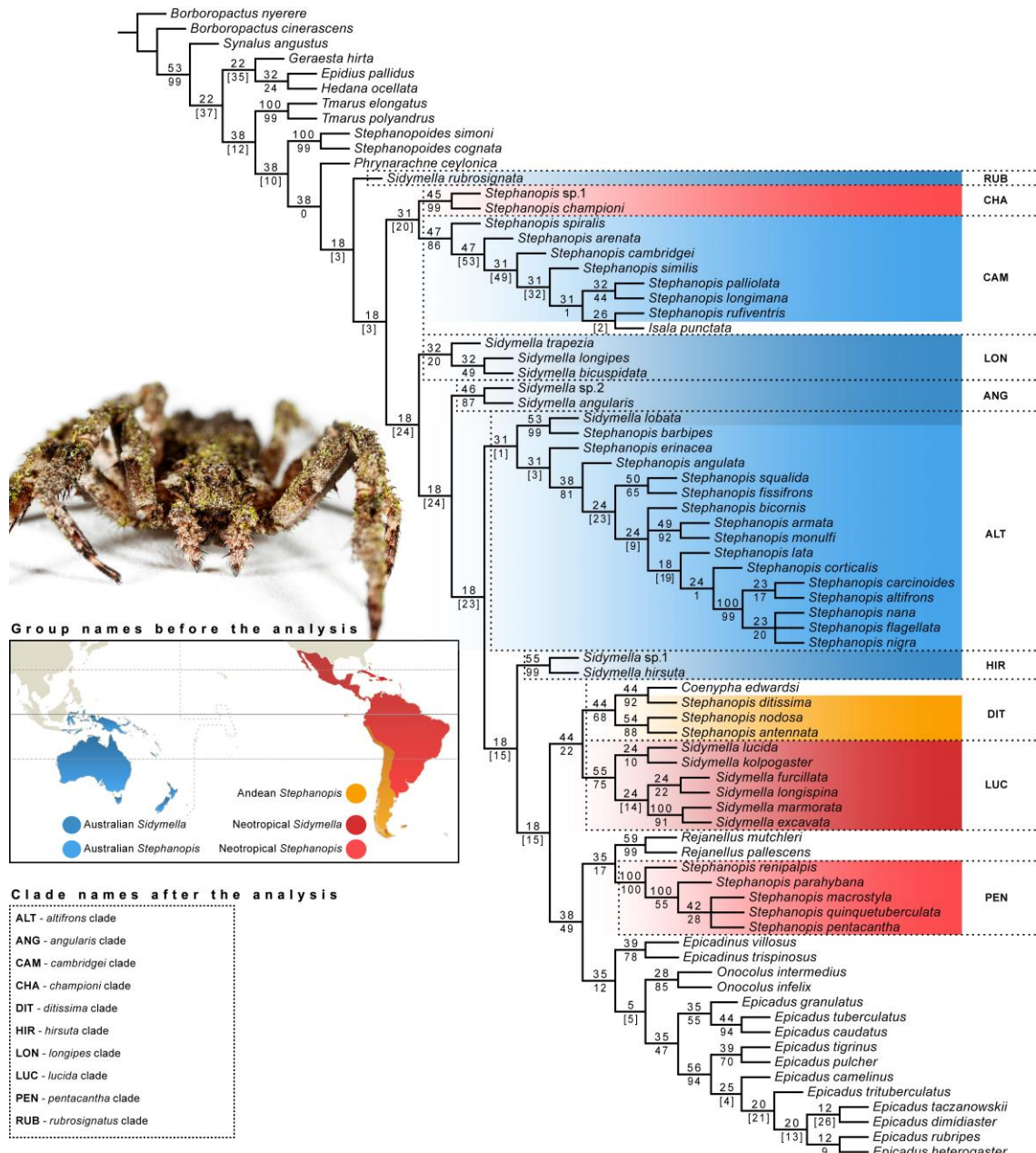
Figure 3. Clade supports obtained by relative Bremer index (above the branches) and symmetric resampling analysis (below the branches). A color scheme is applied to represent the geographical distribution of the clades represented on the working phylogenetic hypothesis.

Discussion

Recent phylogenetic works on spiders have been frequently showing weakly supported and unstable relationships among stephanopines (Benjamin, 2011; Ramírez, 2014; Wheeler *et al.*, 2017). As noted by Benjamin *et al.* (2008), most genera in this subfamily, especially from the Australian and Neotropical regions, are not monophyletic. Benjamin (2011) highlights that, in these regions, there is a considerable number of species yet to be described and that most genera are in need of taxonomic revisions. This author states that these might be good reasons that can explain the instability and lack of support for these thomisid groups in phylogenetic works, which seems to be applicable to both genera studied here.

The presence of rugose tegument (char. 1, state 1; see Fig. S1A), considered by Simon (1895) as a diagnostic feature of *Stephanopis*, was also found in *Epicadinus*, *Onocolus*, *Phrynarachne*, *Rejanellus*, *Isala*, *Epicadus*, *Coenypha*, *S. bicuspidata*, *S. angularis*, *Geraesta*. The cryptic behaviour through adhesion of lichen or soil particles (char. 3, state 1; see Fig. S1F), another diagnostic feature of the genus, was coded as present for *Borboropactus*, *Synalus*, *Isala*, *Epicadus* (in part), *Epicadinus*, the '*cambridgei* group' [*sensu* Machado et al. (2019b)] and for all Neotropical species of *Stephanopis* except (*S. championi* + *Stephanopis* sp. 1). The square-ended/bifid abdomen, defined here by the presence of dorsolateral projections on the opisthosoma in the absence of both median and ventrolateral ones, was thought to be a diagnostic character for *Sidymella* (Machado et al. 2019a), however, this feature appeared in 11 other distinct clades.

Although highly diverse in regard to their somatic characteristics, it is accepted that the genital morphology in Thomisidae is quite conservative (Benjamin, 2011). However, our findings point to a significant number of both sexual and somatic traits behaving as homoplasies along the tree (Figs. 4 – 7). The topology discussed here is for the most part concordant with what was observed by the authors mentioned above. The relatively weak branch supports seem to be related to repeated state reversals and to a high number of homoplastic characters (Figs 4–7). The increase in the data input, however, allowed a new interpretation regarding the composition of both *Stephanopis* and *Sidymella* as well as the relationships between these genera.

Stephanopis

"*altifrons* clade"

In the taxonomic work provided by Machado *et al*. (2019b), the authors suggested the possible existence of three distinct groups of species in the genus ('*cambridgei* group', '*altifrons* group' and '*lata* group'). This latter was not independently recovered by non-ambiguous synapomorphic characters as alpha-taxonomy insights previously suggested. Instead, all its component species emerged in a single and weakly-supported clade with species assigned to the '*altifrons* group' [*sensu* Machado et al. (2019b)]. Moreover, a dichotomy between this major clade with *S. barbipes* + *S. lobata* **comb. nov.** was recovered based on three homoplastic features. Despite its considerable heterogeneity, hereinafter we call this group as the "*altifrons* clade".

Among the species that comprise *Stephanopis*, *S. erinacea* stands out as the only insular taxon, occurring far from the Australian territory, being recorded in the Fiji Islands. The restricted distribution and specific selective pressures possibly suffered by this species may have contributed to the evolution of a highly apomorphic organism that, although retaining some important similarities with its congeners, had developed distinct somatic features that are not observed in any other *Stephanopis* species. Besides that, the male of *S. erinacea* is unknown, thus, a significant session of the matrix related to male genital features were not scored for this taxon (what may have contributed for poor resolutions and the instability of the clade). The unpredictable behaviour of this terminal taxon in the EW analyses led us to perform another method for topology test. As a result, the removal of this wild card through pruning in equal weights analysis resulted in gaining six additional nodes in the outgroup resolution while the topology of the "*altifrons* clade" remained stable (Appendix 3). One way or another, the group presented in the main hypothetical reconstruction was recovered based on three homoplasies (Fig. 4): the absence of dorsolateral projections on the opisthosoma and absence of both macrosetae on the ocular quadrangle (char. 43, state 0; see Fig. S3G) and clypeus margin (char. 19, state 0; see Fig. S3G). All males of the '*lata* group' [*sensu* Machado et al. (2019b)] (e.g. *S. lata*, *S. armata*, *S. monulfi*, *S. bicornis*, *S. angulata*, *S. corticalis*. *S. fissifrons* and *S. squalida*) present a diagnostic structure on the dorsal portion of their cymbium: a group of arrow-shaped setae arranged close together that looks similar to a small brush (char. 117, state 1; see Fig.

S14H). However, this structure was interpreted as ambiguous in our analyses because the male of *S. erinacea* is unknown, and palpal characters are missing for this terminal taxon. Thus, this feature was not represented along the tree branches. According to Dr. Martín Ramírez (pers. Comm), this setae-cluster probably have a chemosensory function, even though high magnification SEM images of the tip of these structures were not taken. Further investigations should be carried out to verify this assumption. Males of the '*lata* group' [*sensu* Machado et al. (2019b)] also have a truncated branch on the ventral portion of the RTA (char. 106, state 0; see Fig. S7A) while neither females nor males in this group have the remarkable cephalic prominence observed in the '*altifrons* group' [*sensu* Machado et al. (2019b)]. This latter emerged as a derivate group with its putative synapomorphies being the high cephalic portion (char. 22, state 2; see Fig. S5D) bearing a pair of lateral tubercles (char. 20, state 1; see Fig. S3G) (Fig. 4). Comparative studies with morphometric and ecological approaches must be encouraged to test if the flattened habitus of species of the '*altifrons* group' [*sensu* Machado et al. (2019b)] could be related to a specific niche specialization (hunt on trunks and under tree barks), such as Dias & Brescovit (2003) suggested for *Pachistopelma rufonigrum* Pocock, 1901, a theraphosid spider that lives between bromeliads.

Recovered by five homoplastic characters and presenting significant nodal stability and branch supports, the clade (*Stephanopis barbipes* + *Sidymella lobata*) is clearly the most controversy clade in *Stephanopis* (Figs 1 and 2). A series of leg characteristics sets these two species apart from the rest of the main clade in a dichotomy; however, although questionable, maintaining *S. barbipes* in the genus seems to be the most reasonable decision for now (Fig. 4). Their distinct trichobothria disposition (char. 46, state 0; see Fig. S6F) morphology of tarsal claws (char. 69, state 1; see Fig. S8E) and density of its setae tuft, as well as the size proportion between their metatarsal macrosetae (char. 71, state 1; see Fig. S7A), might explain the divergence from other species of the genus. However, genital features such as the presence of pars pendulum on male palp (char. 115, state 1; see Fig. S8A, D and G) and membranous chambee-like copulatory ducts in female genitalia (char. 88, state 1; see Machado *et al*. (2019b), Fig. 37D) pull them together as the sister clade of the "*lata* + *altifrons*" group. The recovery of *S. lobata* **comb. nov.** as a sister species to *S. barbipes* was strongly supported, and for that reason, the most parsimonious decision was to keep this latter in *Stephanopis* and propose the transference of a species that

clearly does not fit in *Sidymella* instead of erecting a new genus to accommodate both. Even though, we highlight that the placement of *S. barbipes* and *S. lobata* **comb. nov.** is highly questionable and deserves future investigations.
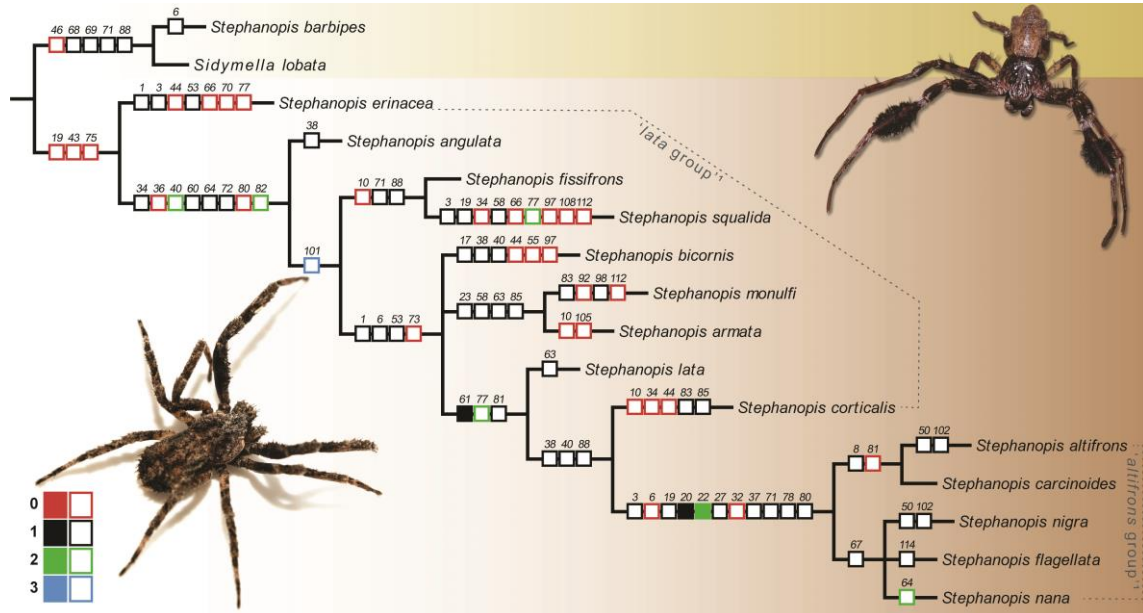
Figure 4. Character transformations in the "*altifrons* clade" based on the topology of the most congruent tree (K= 17.89). Filled squares represent synapomorphies and those in white are homoplastic characters. Character states: red (0); black (1); green (2); blue (3). 1 — '*lata* group' and '*altifrons* group' (*sensu* Machado *et al*. 2019b)

"*cambridgei* clade"

Species previously assigned to the '*cambridgei* group' by Machado *et al*. (2019b) were recovered as a stable clade with *I. punctata* nested within (Fig. 5). The similarities with *Isala* include the longitudinal dual band on the prosoma (char. 13, state 1; see Fig. S2H), the flattened cephalic area, five ventral macrosetae on tibiae I and II (char. 13, state 1; see Fig. S2H) in females, and the presence of modified setae on these same leg segments for males (char. 62, state 1; see Fig. S8C). This latter character was mentioned by Machado *et al*. (2019b), who described it as a set of long, thin and filiform barbs. All parsimony analysis using implied weighting schemes recovered this clade (Fig. 2) with relatively high support (Fig. 3), with its component species presenting the granular surfaced opisthosoma (char. 78, state 2; see Fig. S8F) as the only unambiguous synapomorphy. This group was also recovered by the presence of barbed clavate setae on their opisthosoma (Fig. S10b), which according to

Gawryszewski (2014) are positively related to the effectiveness of becoming camouflaged through debris retention. This author found three different types of setae in *S. altifrons* and *S. cambridgei* that seem to be specialized for retaining organic particles. While *S. altifrons* present all three types of elongated and branched setae (generalized here as "needle-shaped"), *S. cambridgei* have just one, which we coded as "clavate" while Gawryszewski (2014) describes it as cuneiform, barbed and dorsally striated. We are in agreement with Gawryszewski (2014) that this variation in setae morphology could be related to selection for retaining different types of debris, which might indicate niche partitioning. The paraphyletic relationship between these clades can also be observed through differences in sexual traits. While males of *S. altifrons* have a RTAvbr and females present a shallow epignyal plate with exposed copulatory openings (char. 91, state 0; see Machado *et al*. (2019b), Fig. 3C and E), the '*cambridgei* group' gathers males without RTAvbr and females with well-developed folds delimiting the atrium and covering the copulatory openings (see Machado *et al*., 2019b, Fig. S10C). Therefore, the morphological distinctions listed above are seen as evidence indicating that the entire "*cambridge*i clade" belongs to a genus other than *Stephanopis*. As the taxonomy of the entire clade was recently revised by Machado et al. (2019b), we suggest here the transference of all species of the '*cambridgei* group' to *Isala*.
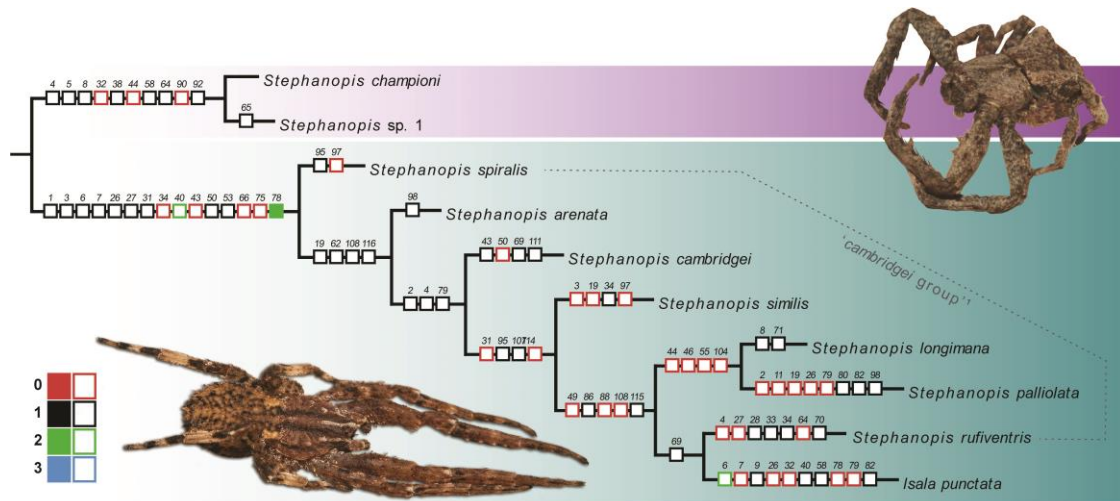
Figure 5. Character transformations and detail of the dichotomy between the "*cambridgei* clade" (petrol) and the "*championi* clade" (purple) based on the topology of the most congruent tree (K= 17.89). Filled squares represent synapomorphies and

those in white are homoplastic characters. Character states: red (0); black (1); green (2); blue (3). 1 — '*cambridgei* group' [*sensu* Machado *et al*. (2019b)].

Benjamin (2011) recovered *S. cambridgei* nested in *Sidymella*, having a close relationship with *S. lucida*, the type species of this genus. In our results, on the other hand, *S. cambridgei* and other Australian species belonging to the "*cambridgei* clade" have emerged as sister of a small clade of *Stephanopis* species with distribution restricted to Central America (Fig. 5). This dichotomy, though, was weakly supported as it was recovered by only five weighting schemes in our sensitivity analysis; thus, it is probably spurious (Fig. 2). Three of the five homoplasies that recover the dichotomy between these clades are based on setae morphology and its microstructures (Fig. 5); however, their component species are noticeably distinct with regard to their copulatory structures (such as the absence of RTA for *Stephanopis* sp. 1) and most of its somatic characters. Moreover, under 10 implied weighting schemes, the *S. championi* + *Stephanopis* sp. 1 clade emerged independently or somehow unrelated to the "*cambridgei* clade" (Fig. 2).

"championi clade*"*

Simon (1903) synonymized *Paratobias* with *Stephanopis* arguing that the disposition and curvature of the eye rows were highly variable among the species of this group. Not only was this decision misled, as this author did not present any major comparison among these genera, there are other somatic unconformities that never seem to have been considered, such as the different number of tibial macrosetae (Char. 64), femoral tubercles (Char. 50), presence or absence of the thoracic median spire (Char. 23) and the shape of the opisthosoma (Chars. 74, 75 and 76). The paraphyletic relationship with other species of *Stephanopis*, low branch support values and weak nodal stability are indicative that "*championi* clade" should be considered as a distinct genus. Not only somatic but also genitalic features of *S. championi* such as the absence of RTA on male palp, did not match those observed in the "*cambridgei* clade" neither the "*altifrons* clade". Thus, in order to assume the most parsimonious taxonomic decision, we propose that the *S. championi* should be restored to its original genus, *Paratobias* (see taxonomic section).

"*pentacantha* clade"

While two species of Stephanopis from Central America emerged close to the "*cambridgei* clade", the remaining Neotropical species were placed inside the "*Epicadus* group" (Fig. 6), a potential clade suggested by Silva-Moreira and Machado (2016) and partially recovered by Machado *et al*. (2017). A similar topology was recovered by Wheeler *et al*. (2017) with considerable support. Machado *et al*. (2017) recovered *S. altifrons* as closely related to the Neotropical species; however, the less inclusive approach on Australian representatives of the genus prevented these authors from considering genital features that come to be crucial for elucidating the relationships in *Stephanopis*. In addition to the presence of a median spire on the thoracic portion of the prosoma (Char. 23, state 1; see Fig. S2F) and the opisthosoma bearing five conical projections, this clade also diverges from *Stephanopis* by a series of sexual traits: male palp having a dorsally curved (Char. 101, state 2) and single-tipped RTA, absence of tegular ridge and tegulum smooth surface (Char. 108, state 0; Char. 110, state 0; see Fig. S12B). Differing from *S. altifrons* and its correlated terminal taxa, this clade is composed of species where males lack the PrsP (Char. 115, state 0) and the CP (Char. 116, state 0). The female genitalia has a single pair of elliptical and smooth spermathecae, whereas females of *Stephanopis* have coiled spermathecae (Char. 89) with glandular heads (Char. 90) that are preceded by chamber-like copulatory ducts (Char. 86).

Alongside with *Rejanellus*, these are now the only known representatives in the "*Epicadus* group" with females having short CD and males lacking the RTAvbr on their palpi. Although sharing these features, the "*pentacantha* clade" present other characteristics (e.g. five conical projections on the opisthosoma; leaf-shaped setae; presence of MS) that set them apart from its sister genus. Its component species were grouped with strong branch supports (Fig. 3) and recovered by two synapomorphic characters: presence of ventral macrosetae on patellae I and II (Char. 54, state 1; see Fig. S8B) and male palp bearing pear-shaped tegulum (Char. 95, state 2; see Fig. S12B). Despite the dichotomy with *Rejanellus*, the evidences listed above are interpreted as sufficient to justify the proposition of the "*pentacantha* clade" as a new genus. Although well-supported, the internal topology of the group is poorly resolved. This occurs due to the conservative morphology of its component species, which can only be distinguished from each other by details of their genitalia, such as the

curvature, size and shape of the RTA and embolus, or the presence/absence of the median septum on the epigynal plate. A study focusing on their taxonomy is essential to explore these morphological aspects, updating descriptions and diagnostic structures.

"*ditissima* clade"

The relationship between *Stephanopis* species from the Andean region and *Coenypha* was well supported by molecular evidence (Wheeler *et al*., 2017) and corroborated by morphologic studies (Machado *et al*., 2017). Although preliminary, the insights and results obtained by Machado *et al*. (2017) regarding the topology of the clade remained consistent in comparison to what we found in the present work (Fig. 2). According to Machado *et al*. (2017), the coincident geographical distribution and several similarities regarding the morphology of copulatory structures of these species could indicate possible synonymies or new combinations between the two genera. The inclusion of two more species of *Stephanopis* from the Andean region in our data matrix aimed to test if those previous hypotheses could be corroborated through broader morphological comparisons. The disposition and shape of copulatory structures in *Coenypha,* such as the intromittent median septum, exposed copulatory ducts, acute RTA, laminar embolus and abdominal projections laterally disposed, are remarkably similar to what is observed in *S. ditissima*, *S. nodosa* and *S. antennata*. The node gathering these "Andean *Stephanopis*" in a clade with *Coenypha* is shown to be stable, being recovered under all weighting schemes and Bayesian analysis (Fig. 2), and here called "*ditissima* clade". The group with four species presented significant branch supports (Fig. 3), being recovered by five homoplastic characters (Fig. 6) and corroborating previous evidences based on morphological (Machado *et al*., 2017) and molecular data (Wheeler *et al*., 2017). Therefore, we point out that the *Stephanopis* species belonging to the "*ditissima* clade" should be transferred to *Coenypha* (Fig. 6).
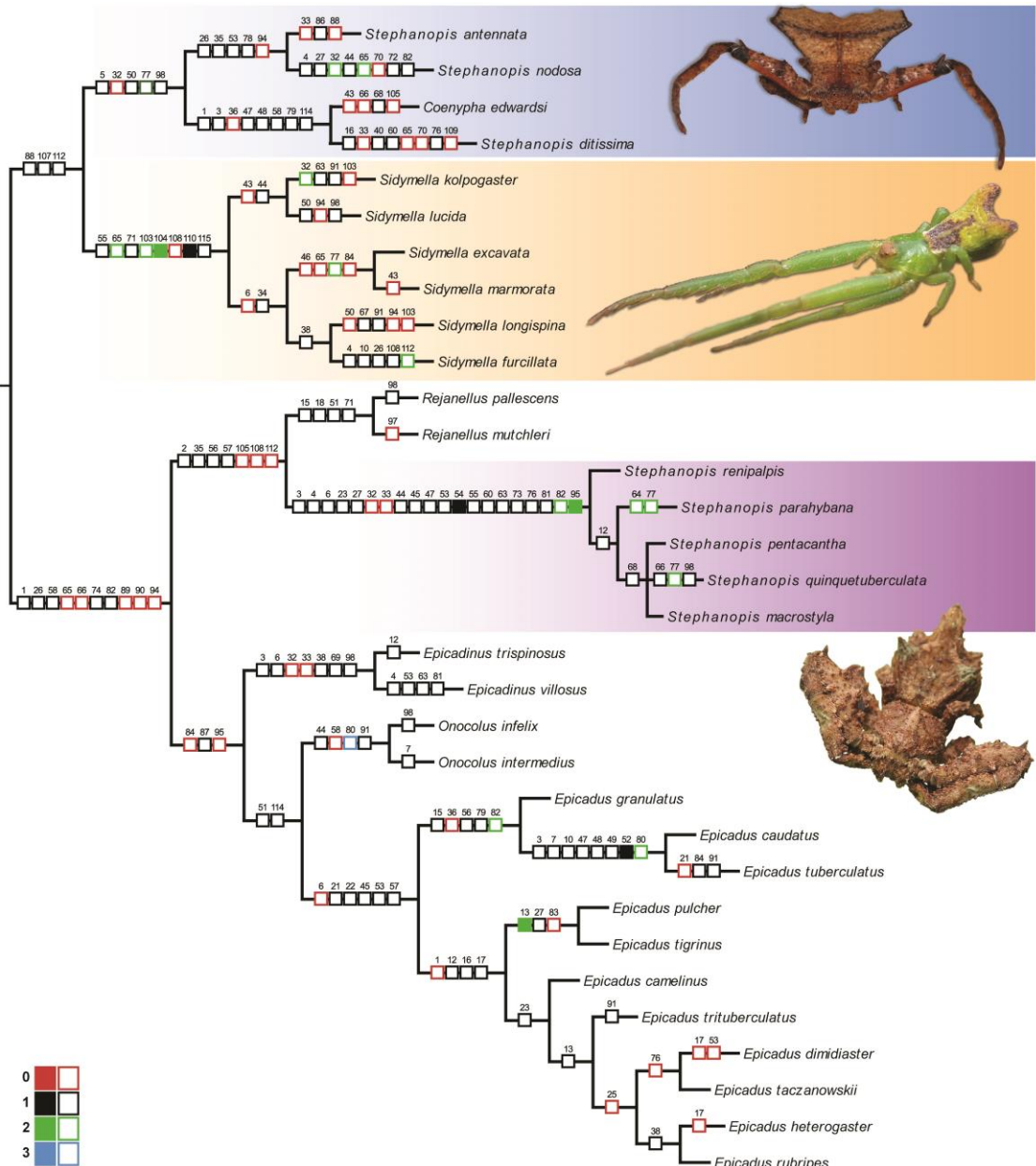
Figure 6. Character transformations, detailed topology of the relationships between "*ditissima* clade" (blue) and "*lucida* clade" (orange); emergence of the "*pentacantha* clade" (purple) as part of the '*Epicadus* group' based on the topology of the most congruent tree (K= 17.89). Filled squares represent synapomorphies and those in white are homoplastic characters. Character states: red (0); black (1); green (2); blue (3).

The close relationship between *Coenypha* and the "Neotropical *Sidymella*" was similarly observed in Wheeler *et al*. (2017). Additionally, our findings show these two sister clades being related to the entire "*Epicadus* group". The *Coenypha* + "Neotropical *Sidymella*" relationship was recovered not only by the presence of membranous and hyaline copulatory ducts of the female genitalia (Char. 88, state 1)

but also by males bearing a flattened and laminar embolus (Char. 107, state 1; see Fig. S13F) resting on tegulum (Char. 112, state 1).

Sidymella

According to the diagnosis provided by Machado *et al*. (2019a), *Sidymella* is similar to *Coenypha* due to a series of characteristics related to the epigynum and the male palp. These authors are not wrong in their statement if only the Neotropical species of *Sidymella* are being considered in such a comparison. The Australian representatives of the genus, although presenting some somatic features common to the Neotropical species, such as the presence of spiniform macrosetae on the mesial surface of femora I (interpreted here as dorsolateral setiferous tubercles) (Char. 49, state 1; see Fig. S7A and B) and epigynum with accessory glandular heads (Char. 90, state 1; see Fig. S10G), emerged in four different clades (Fig. 2). The evidence obtained through our data also suggest that the bifid opisthosoma, a character that was still being recently considered by Machado *et al*. (2019a) as valid way to recognize and distinguish *Sidymella* from other stephanopines, in fact appeared in 11 different groups. Thus, contrary to what previous taxonomic works had been showing (Lise, 1973; Machado *et al*. 2019a), the presence of dorsolateral humps on the abdomen of these spiders seems to be insufficient to undoubtedly characterize the genus. Moreover, the composition of *Sidymella* as a natural group is implausible if we consider that this and other somatic characters shared between Neotropical and Australian species of *Sidymella* come to result from an adaptive convergence to the same hunting behaviour. These spiders are commonly found on tree branches and plant stems with their forelegs close together and directed frontwards, camouflaging themselves as twigs (pers. obs.). The polyphyletic emergence of *Sidymella*, as currently circumscribed, is corroborated by molecular evidence presented by Wheeler *et al*. (2017). Similar to our results, the findings presented by these authors recover the Neotropical species of *Sidymella* as sister group to *Coenypha* (Fig. 6) while Australian species are related to *Stephanopis* (here, represented by the emergence of *S. barbipes* + *S. lobata* **comb. nov.**) (Fig. 7). Although visibly distinct regarding their somatic features, the palpal architecture of *Sidymella* species from the Australian region is similar to those of *Stephanopis* by presenting CP (Char. 116, state 1; see Fig. S13A),

filiform embolus (Char. 107, state 0; see Figs 18G and 20E) and the RTA acute (Char. 103, state 1; see Fig. S12H) with grooved surface (Char. 104, state 1).

The group composed by *S. lucida* and five other species of *Sidymella* recorded in the Neotropical Region (World Spider Catalog, 2020) was recovered with good stability (Fig. 2). The clade also presented significant branch supports (Fig. 3), being sustained by two synapomorphies that set them apart from Australian species: RTA with nodose texture (Char. 104, state 2; see Fig. S13B) and tegulum with scaled surface (Char. 110, state 1; see Fig. S14D). Thereby, although we call this group the "lucida clade" throughout the discussion, we anticipate that this is the only clade that should truly be considered as Sidymella (stricto sensu). Australian species currently attributed to this genus are hereinafter treated as "dissident" clades, which should be proposed as new genera in future taxonomic works. (Fig. 7).

"*angularis* clade"

The maximum likelihood analyses performed by Sirvid *et al*. (2013) for 28S and H3 sequences and combining COI, 28S, H3 and ND1 data are consistent with the morphological evidence presented here in showing the close relationship between (*S. trapezia* + *S. longipes*) and *S. angularis* (Fig. 2). According to Sirvid *et al*. (2010) and Sirvid *et al*. (2013), the recent establishment of *S. longipes* and *S. trapezia* in New Zealand suggests a capacity of long-range dispersal over water, contrary to the vicariant hypotheses usually considered to explain the distribution of stephanopines in the Australian Region. Although Sirvid *et al*. (2013) had found molecular evidence supporting separate New Zealand lineages within the Australasian stephanopines, the hypothetical reconstruction discussed here suggests a proximity between *S. angularis*, a common species that is widely spread in New Zealand, and *Sidymella* sp. 2, recorded along the east coast of Australia (Fig. 3). The node grouping the two species was recovered by all optimality criteria except equal weights (Fig. 2) and showed significant branch supports (Fig. 3). The clade presented one synapomorphy: the presence of dual median spire on the thoracic portion of the prosoma (Char. 24, state 1; see Fig. S4B), a feature that was mentioned by Bryant (1933) and Sirvid *et al*. (2013) as a putative character to suggest a new generic assignment to *S. angularis*. There is a significant number of undescribed species in Australian collections that present similar characteristics observed in *S. angularis* and *Sidymella* sp. 2 (pers. obs.).

An analysis with a broader sampling, molecular data and a biogeographical approach would help to elucidate the phylogenetic relationships and dispersal mechanisms used by these crab spiders along the Australian Region.
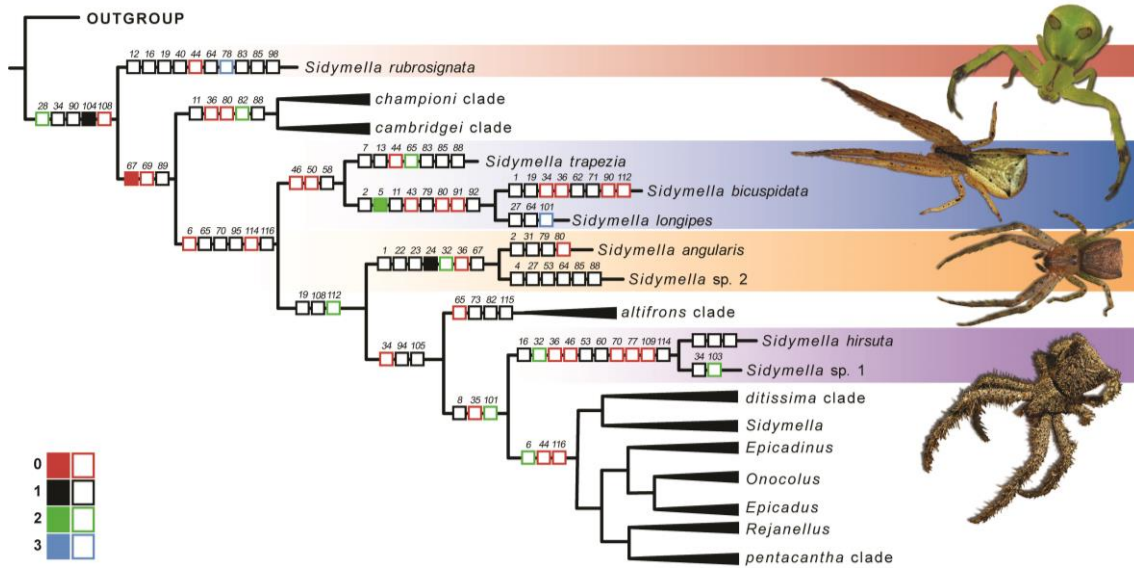
Figure 7. Section of the working phylogenetic hypothesis detailing the character transformations and relationships between the "*angularis* clade" (orange), *S. rubrosginata* (red), "*trapezia* clade" (blue) and "*hirsuta* clade" (purple). Filled squares represent synapomorphies and those in white are homoplastic characters. Character states: red (0); black (1); green (2); blue (3).

"*hirsuta* clade"

The clade "*hirsuta* clade" is formed by spiders that resemble *Epicadinus* by their "spiny" habitus, with long and needle-shaped setae covering their entire prosoma (Char. 11, state 0 and 2), opisthosoma (Char. 80, state 1; see Fig. S9H) and legs. The group was supported by 10 homoplastic characters and one synapomorphy: RTAvbr spoon-shaped (Char. 106, state 3; see Fig. S13E). Because of how the characters were treated in our analyses, this ambiguous feature was not shown along the branch on the working phylogenetic hypothesis. Nevertheless, the emergence of the genus by itself is held by strong branch supports (Fig. 3) and good nodal stability (Fig. 2). As observed in *Stephanopis*, the male palp architecture of species of the "*hirsuta* clade" is characterized by the presence of a RTAvbr, well-developed CP, oval-shaped tegulum and filiform embolus meandering at its distal portion (whip-like). The arrangement and shape of copulatory structures of females, although slightly different from those of

Stephanopis, also show some degree of resemblance to what is observed in the latter. Females of the "*hirsuta* clade" have flattened, narrowed and tubular copulatory ducts (Char. 86, state 0; Fig. S10E and G) and spermathecae significantly longer than those of *Stephanopis*. Despite having opisthosoma with a pair of "protruding corners" (dorsolateral projections), a feature considered by Koch (1874) to justify the original description of *S. hirsuta* in *Sidymella*, other somatic characters (e.g., number and arrangement of tibial and metatarsal macrosetae; disposition of teeth of the tarsal claws) wildly differ from those of the species type of this genus. The relationship of the "*hirsuta* clade" with the clade composed by of the "*Epicadus* group" and (*Coenypha* + *Sidymella*) was based on three highly homoplastic characters, each presenting numerous state reversals. Moreover, both Bremer indexes and symmetric resampling analyses presented low support values for this more inclusive clade (Fig. 3) as well as sensitivity analyses showing weak nodal stability in this section of the topology (Fig. 2). Such results, along with the unpredictable behaviour of the clade, suggest that the placement of the "*hirsuta* clade" is particularly arguable. Similarities and shared characters between this group and *Stephanopis*, in addition to their coincident geographical distribution, must also be considered as evidence that the placement of the "*hirsuta* clade" with most Neotropical stephanopine genera sampled in this study is questionable and most likely to be spurious.

"*trapezia* clade"

The close relationship between *S. trapezia* and *S. corticalis*, found by Sirvid *et al.* (2013) through maximum likelihood analyses of COI sequence data, was not recovered by morphological evidence, let alone the placement of *S. longipes* in *Stephanopis*. Both of these *Sidymella* species were grouped in the same clade with *S. bicuspidata* by three homoplasies related to leg characteristics (Fig. 7). However, the topology of the group was inconsistent and weakly supported, sometimes with *S. trapezia* behaving as a wildcard and occasionally (*S. bicuspidata* + *S. longipes*) emerging separately. Every so often, parsimony with implied weights recovered only *S. trapezia* as a sister group of to the "*cambridgei* clade" and occasionally in a clade with *S. bicuspidata* + *S. longipes* as a sister to the "*cambridgei* clade", being this latter in a dichotomy with *Stephanopis*. As observed for the "*angularis* clade" and "*hirsuta* clade", the "*trapezia* clade" also share with the "*altifrons* clade" and the "*cambridgei*

clade" the presence of CP close to the RTA of the male palp. Such structure seems to be constant in these groups of Australian stephanopines and might contribute to their weakly resolved relationship in the face of their remarkable somatic disparities.

The "*trapezia* clade" is formed by taxa that clearly do not fit with the recently updated diagnosis of *Sidymella* and the taxonomic background presented by Machado *et al*. (2019a) was corroborated by the emergence of the Neotropical species far apart from those hitherto called "Australian *Sidymella*". Therefore, we believe that although significantly heterogeneous and lacking good nodal stability, the "*trapezia* clade" must be proposed as a new genus in a future taxonomic work. Only then, the most parsimonious decision will be taken, avoiding the maintenance of a paraphyletic status for *Sidymella*, erection of a monospecific genus to accommodate only *S. trapezia* or the proposition of the three species as *incertae sedis*.

The species *S. rubrosignata* behaved unpredictably, presenting even weaker supports and being more unstable than the "*trapezia* clade". Alternative resolutions represented this species emerging within the "*Epicadus* group" due to the presence of characters such as the disk-shaped tegulum on male palp (Char. 95, state 0) and the median longitudinal band (Char. 12, state 1) with a guanine white spot on the thoracic portion (Char. 16, state 1), or independently (as shown in the discussed tree), but always as sister to the remaining taxa of the ingroup (Fig. 2). Considering all analysis and morphological evidence presented here, once again, justifying the description of a stephanopine species in *Sidymella* based merely on the presence of a pair of lateral projections on the opisthosoma has proven to be insufficiently grounded and inaccurate. None of the diagnostic features regarding the male palp architecture or copulatory duct disposal of species of *Sidymella* are observed in *S. rubrosignata*. The independent emergence of this taxon is recovered by 10 homoplastic characters and supports Simon's (1895) insights considering it as a group apart from *Stephanopis* as well (Fig. 7). Thus, we believe that *S. rubrosignata* deserves a new generic assignment in a near future, even initially proposing a monospecific genus in order to retain the validity of the name rather than consider the species as *incertae sedis*.

Conclusions

The hypothetical reconstruction presented in this study is based on the most comprehensive morphological data matrix focusing on Stephanopinae to date. Our results corroborate classic taxonomic insights recovering the four groups mentioned by Simon (1895) as doubtful, as distinct clades. Recent phylogenetic analyses based on morphological (Benjamin, 2011; Ramírez, 2014) and molecular (Benjamin *et al.* 2008; Wheeler *et al.*, 2017) data were shown to be congruent with the present findings, suggesting that both *Stephanopis* and *Sidymella* are polyphyletic, as currently circumscribed. Different approaches and methodologies were applied to estimate nodal stability and branch supports, seeking to base desired taxonomic changes with plausibility and consistency.

Despite certain morphological heterogeneity between its representatives and low branch supports, *Stephanopis* (*stricto sensu*) is recognized by the authors as a group formed only by species of the "*altifrons* clade", gathering all Australasian representatives that Machado *et al.* (2019b) attributed to the '*lata* group' and '*altifrons* group', in their taxonomic revision. The genus also includes the clade *S. barbipes* + *S. lobata* **comb. nov.** in dichotomy with all its remaining congeneric species. On the other hand, *Sidymella* (*stricto sensu*) should be treated as a genus comprised solely by species of the "*lucida* clade".

The outgroup relationships are partially concordant with those obtained by Benjamin (2011), Ramírez (2014) and Machado *et al.* (2017). Divergences were expected once we focused on sampling the ingroup extensively, while the high diversity of the outgroup genera remained poorly represented. These specimens were scored to polarize the characters, so their weakly supported relationships, as shown in the hypothetical reconstruction, are preliminary and insufficiently accurate to bring forth grounded discussions. The lack of resolution as well as the weak supports obtained by resampling analysis and relative Bremer indexes for deep branches is a result of a highly homoplastic matrix with many missing data and state reversals. Notwithstanding, the significant amount of either homoplastic or synapomorphic characters showed that terminal clades are in general recovered with good nodal stability regardless of how the data are analysed. This constancy obtained with a phylogenetic approach, along with extensive studies on the morphology of the group,

provided a more thorough understanding of its relationships, compiling evidence to ensure stable taxonomic decisions in the future.

Taxonomy

Thomisidae Sundevall, 1833
Stephanopinae O. Pickard-Cambridge, 1871
Stephanopis **O. Pickard-Cambridge, 1869**
Stephanopis altifrons **O. Pickard-Cambridge, 1869**

Diagnosis

The genus *Stephanopis* (*stricto sensu*) is composed of bark-dwelling spiders with a dorsoventrally compressed, flattened habitus. They have high cephalic prominence, well-developed clypeus and opisthosoma rounded at the rear or ending abruptly (pentagonal). The genus can also be distinguished by males having palpi with retrolateral CP, pars pendulum, embolus rigid at its proximal portion, becoming gradually flexible, filiform and meandering at its distal half; the RTA is wide, obtuse and single-tipped in all species of the '*lata* group' [*sensu* Machado et al. (2019b)]. However, males of derivate species belonging to the '*altifrons* group' [*sensu* Machado et al. (2019b)] (and *S. barbipes*) present acute and bifid RTA (well-developed RTAvbr). Female genitalia is characterized by the epigynal plate with shallow, flattened atrium, slit-shaped CO and wide, chamber-like dopulatory ducts preceding a pair of asymmetric cylindrical spermathecae.

Composition

The genus *Stephanopis* (*stricto sensu*) is composed by 16 valid species distributed along Australia and Southeast Asia: *Stephanopis altifrons* O. Pickard-Cambridge, 1869; *Stephanopis angulata* Rainbow, 1899; *Stephanopis armata* L. Koch, 1874; *Stephanopis barbipes* Keyserling, 1980; *Stephanopis bicornis* L. Koch, 1874; *Stephanopis carcinoides* Machado, 2019; *Stephanopis corticalis* L. Koch, 1876; *Stephanopis erinacea* Karsch, 1878; *Stephanopis fissifrons* Rainbow, 1920; *Stephanopis flagellata* Machado, 2019; *Stephanopis lata* O. Pickard-Cambridge, 1869; *Stephanopis lobata* (L. Koch, 1874) **comb. nov.**; *Stephanopis monulfi* Chrysanthus,

1964; *Stephanopis nana* Machado, 2019; *Stephanopis nigra* O. Pickard-Cambridge, 1869 and *Stephanopis squalida* Machado, 2019.

Note

Other valid species that are currently described in Stephanopis that were not listed above, will be properly addressed in future taxonomic works where new genera will be officially proposed.

Thomisidae Sundevall, 1833
Stephanopinae O. Pickard-Cambridge, 1871
Sidymella **Strand, 1942**
Sidymella lucida **(Keyserling, 1880)**

Diagnosis

The component species of *Sidymella* (*stricto sensu*) can be distinguished from other thomisids by the presence of stout spines on the mesial surface of femora I and macrosetae above their ALE. Males are diagnosed by their long and laminar embolus with well-developed pars pendulum curving at their terminal portion. Unlike other stephanopines, which have smooth-surfaced RTAs or with parallel creases on it, males of *Sidymella* present a rounded RTA with nodose texture and truncated short RTAvbr; a prominent trichobotrium can be observed on the dorsum of the palpal tibia. Females differ from those of other genera by their coiled copulatory ducts leading to a pair of walnut-shaped spermathecae internally compartmentalized in small chambers.

Composition

The genus *Sidymella* (*stricto sensu*) is composed by six valid species with distribution range restricted to the Neotropical Region: *Sidymella lucida* (Keyserling, 1880); *Sidymella excavata* Machado & Guzati, 2019; *Sidymella furcillata* (Keyserling, 1880); *Sidymella longispina* (Mello-Leitão, 1943); *Sidymella marmorata* Machado & Guzati, 2019 and *Sidymella kolpogaster* (Lise, 1973).

Note

Other valid species that are currently described in *Sidymella* that were not listed above, will be properly addressed in future taxonomic works where new genera will be officially proposed.

Thomisidae Sundevall, 1833

Stephanopinae O. Pickard-Cambridge, 1871

Coenypha **Simon, 1895**

Coenypha edwardsi **(Nicolet, 1849)**

Diagnosis

Species of *Coenypha* are similar to those of *Sidymella* due to the presence of a retrolateral trichobothria on the male palp and the disposition of the coiled and membranous copulatory ducts of the female genitalia. However, species of *Coenypha* can be easily recognized by their flattened habitus, wide opisthosoma, enlarged femora I and slightly curved anterior tibiae. The epigynal plate of females have exposed openings separated by a robust median septum, and their copulatory ducts are wider than those of *Sidymella*, leading to a pair of walnut-shaped spermathecae (with several constrictions and internal subdivisions). The male palp bears a long and laminar embolus, such as in *Sidymella*. However, in *Coenypha*, the tegulum is smooth surfaced and the RTA has grooves instead of nodes.

Composition

The genus Coenypha (*stricto sensu*) is composed, after the taxonomic acts proposed here, by seven valid species recorded for the Andean and Patagonian Regions: *Coenypha edwardsi* (Nicolet, 1849); *Coenypha antennata* (Tullgren, 1902) **comb. nov.**; *Coenypha ditissima* (Nicolet, 1849) **comb. nov.**; *Coenypha fasciata* Mello-Leitão, 1926; *Coenypha fuliginosa* (Nicolet, 1849); *Coenypha lucasi* (Nicolet, 1849) and *Coenypha nodosa* (Nicolet, 1849) **comb. nov.**

Thomisidae Sundevall, 1833

Stephanopinae O. Pickard-Cambridge, 1871

Isala **L. Koch, 1876**

Isala punctata **L. Koch, 1876**

Diagnosis

Species of *Isala* resembles those of *Borboropactus* by the cryptic behavior, with individuals frequently presenting lichen, sand and other soil particles attached to their tegument, and by the elongated body shape: prosoma and opisthosoma longer than wide, and anterior legs (I and II) aligning parallel to each other and directing frontwards. However, males of Isala can be recognized and distinguished by their well-developed palpi with cymbial projection, long and curved RTA and filiform embolus, lacking the median apophysis and the conductor, observed for *Borboropactus*. Females of this latter have acute lateral projections on the epigynal plate, known as "epigynal teeth", while females of *Isala* present a flattened atrium and folds of the epigynal plate strongly sclerotized, forming almost like "pockets" that protect and hide the copulatory ducts (in ventral view). Moreover, the ocular arrangement in *Isala* is characterized by the ALE noticeably bigger than the AME and the anterior eye row strongly recurved, while in *Borboropactus* the anterior eyes are all similar in size and arranged in a straight row.

Composition

After the taxonomic acts listed hereinafter, we recognize *Isala* as a genus with Australian distribution, composed by eight valid species: *Isala punctata* L. Koch, 1876; *Isala arenata* (Machado, 2019) **comb. nov.**; *Isala cambridgei* (Thorell, 1870) **comb. nov.**; *Isala longimana* (Thorell, 1881) **comb. nov.**; *Isala palliolata* (Simon, 1908) **comb. nov.**; *Isala rufiventris* (Bradley, 1871) **comb. nov.**; *Isala similis* (Machado, 2019) **comb. nov.** and *Isala spiralis* (Machado, 2019) **comb. nov.**

Thomisidae Sundevall, 1833

Stephanopinae O. Pickard-Cambridge, 1871

Paratobias **(F. O. Pickard-Cambridge, 1900) gen. rev.**

Paratobias championi **(F. O. Pickard-Cambridge, 1900) sp. rev.**

Diagnosis

The genus *Paratobias* resembles *Coenypha* by the cryptic bark-dwelling habitus with dorsoventrally depressed prosoma. However, *Paratobias* can be distinguished by the presence of acute ocular projections, trapezoid opisthosoma and reduced AME (1/3 the size of the ALE). The female genitalia is characterized by a shallow and wide median field with copulatory openings positioned laterally, covered by the limits of the epigynal plate folds (Fig. S11C).

Composition

The genus *Paratobias* is currently represented by a single species: *Paratobias championi* (F. O. Pickard-Cambridge, 1900) **sp. rev.**

Taxonomic acts

Stephanopis arenata Machado, 2019: Holotype female from Scotia Sanctuary, New South Wales, Australia, 33°07'36"S 141°10' 40"E, (AMS KS.128001, examined). Transferred to *Isala — Isala arenata* (Machado, 2019) **comb. nov.**

Stephanopis cambridgei Thorell, 1870: Holotype female from Australia, (NHRS 1163, examined). Transferred to *Isala — Isala cambridgei* (Thorell, 1870) **comb. nov.**

Stephanopis longimana Thorell, 1881: Holotype female from Cape York, Queensland, Australia, 10°42'S 142°31'E, (MCSNG, examined). Transferred to *Isala — Isala longimana* (Thorell, 1881) **comb. nov.**

Stephanopis palliolata Simon, 1908: Syntype male from Wooroloo, Western Australia, Australia, (ZMB 20726, examined). Transferred to *Isala — Isala palliolata* (Simon, 1908) **comb. nov.**

Stephanopis rufiventris Bradley, 1871: Holotype female from, Tia (40 km east of Walcha), New South Wales, Australia, 31°12'S 151°48'E, (OUMNH 618, examined). Transferred to *Isala — Isala rufiventris* (Bradley, 1871) **comb. nov.**

Stephanopis similis Machado, 2019: Holotype female from Kanangra Boyd National Park (Boyd plateau near to Jenolan Caves), New South Wales, Australia, 34°03'S 150°05'E, (AMS KS.30026, examined). Transferred to *Isala — Isala similis* (Machado, 2019) **comb. nov.**

Stephanopis spiralis Machado, 2019: Holotype female from Koorawatha National Reserve, New South Wales, Australia, 34°01'55"S 148°35'59"E, (AMS KS.114827, examined). Transferred to *Isala — Isala spiralis* (Machado, 2019) **comb. nov.**

Stephanopis antennata Tullgren, 1902: Holotype female from Aysén, Chile (NHRS, examined). Transferred to *Coenypha — Coenypha antennata* (Tullgren, 1902) **comb. nov.**

Stephanopis ditissima (Nicolet, 1849): Holotype female from Chile, (MNHN 4176, examined). Transferred to *Coenypha — Coenypha ditissima* (Nicolet, 1849) **comb. nov.**

Stephanopis nodosa (Nicolet, 1849): Holotype female from Valdivida, Chile, (MNHN 4194, examined). Transferred to *Coenypha — Coenypha nodosa* (Nicolet, 1849) **comb. nov.**

Sidymella lobata (L. Koch, 1874): Syntype female from Sydney, Australia (ZMB 3414, examined). Transferred to *Stephanopis — Stephanopis lobata* (L. Koch, 1874) **comb. nov.**

Acknowledgements

References

Benjamin, S. P., Dimitrov, D, Gillespie, R. G., Hormiga, G. 2008. Family ties: molecular phylogeny of crab spiders (Araneae: Thomisidae). Cladistics 24, 708–722.

Benjamin, S. P. 2011. Phylogenetics and comparative morphology of crab spiders (Araneae: Dionycha, Thomisidae). Zootaxa 3080, 1–108.

Benjamin, S. P. 2013. On the crab spider genus *Angaeus* Thorell, 1881 and its junior synonym *Paraborboropactus* Tang and Li, 2009 (Araneae: Thomisidae). Zootaxa 3636, 71–80.

Benjamin, S. P. 2015. On the African crab spider genus *Geraesta* Simon, 1889 (Araneae: Thomisidae). Afr Invertebr 56, 309–318.

Benjamin, S. P. 2016. Revision of *Cebrenninus* Simon, 1887 with description of one new genus and six new species (Araneae: Thomisidae). Rev Suisse Zool 123, 179–200.

Benjamin, S. P. 2017. A new species of *Angaeus* from Malaysia with possible affinity to related genera within Stephanopinae (Araneae: Thomisidae). Zootaxa 4337, 297–300.

Bradley, H. B. 1871. Descriptions of eight new species of *Stephanopis* (Cambridge). Transactions of the Entomological Society of New South Wales 2, 233–238.

Dias, S. C., Brescovit, A. D. 2003. Notes on the behavior of Pachistopelma rufonigrum Pocock (Araneae, Theraphosidae, Aviculariinae). Rev Bras Zool 20, 13–17.

Gawryszewski, F. M. 2014. Evidence suggests that modified setae of the crab spiders *Stephanopis* spp. fasten debris from the background. Zoomorphology 133, 205–215.

Goloboff, P. 1999. Analyzing large data sets in reasonable times: Solutions for composite optima. Cladistics 15, 415–428.

Goloboff, P., Farris, J. 2001. Methods for quick consensus estimation. Cladistics 17, S26–S34.

Goloboff, P. A., Farris, J. S., Källersjö, M., Oxelman, B., Ramírez, M., Szumik, C. A. 2003. Improvements to resampling measures of group support. Cladistics 19, 324–332.

Goloboff, P. A., Farris, J. S., Nixon, K. C. 2008a. TNT, a free program for phylogenetic analysis. Cladistics 24, 774–786.

Goloboff, P. A., Carpenter, J. M., Arias, J. S., Miranda-Esquivel, D. R. 2008b. Weighting against homoplasy improves phylogenetic analysis of morphological data sets. Cladistics 24, 758–773.

Goloboff, P. A., Galvis, A. T., Arias, J. S. 2018a. Parsimony and model-based phylogenetic methods for morphological data: comments on O'Reilly et al. Palaeontology 61, 625–630.

Goloboff, P. A., Torres, A., Arias, S. 2018b. Weighted parsimony outperforms other methods of phylogenetic inference under models appropriate for morphology. Cladistics 34, 407–437.

Koch, L. 1874. Die Arachniden Australiens. Verlag von Bauer & Raspe, Nürnberg, DE.

Machado, D. J. 2015. YBYRÁ facilitates comparison of large phylogenetic trees. Version 3.0, Available at: https://www.ib.usp.br/grant/anfibios/researchSoftware.html (accessed on 14 October 2019)

Machado, M., Teixeira R. A., Lise A. A. 2015. Taxonomic notes on the crab spider genus *Tobias* Simon, 1895 (Araneae, Thomisidae, Stephanopinae). Zootaxa 4034, 565–576.

Machado, M., Teixeira R. A., Lise A. A. 2017. Cladistic analysis supports the monophyly of the Neotropical crab spider genus *Epicadus* and its senior synonymy over *Tobias* (Araneae: Thomisidae). Invertebr. Syst. 31, 442–455.

Machado, M., Teixeira R. A., Lise A. A. 2018. There and back again: More on the taxonomy of the crab spider genus *Epicadus* (Thomisidae: Stephanopinae). Zootaxa 4382, 501–530.

Machado, M., Guzati, C., Viecelli, R., Molina-Gómez, D., Teixeira R. A. 2019a. A taxonomic review of the crab spider genus Sidymella (Araneae, Thomisidae) in the Neotropics. Zoosyst. Evol. 95, 319–344.

Machado, M., Teixeira, R. A., Milledge, G. A. 2019b. On the Australian bark crab spiders genus Stephanopis: Taxonomic review and description of seven new species (Araneae: Thomisidae: Stephanopinae). Rec Aust Mus 71, 217–276.

Maddison, W.P., Maddison, D.R. 2019. Mesquite: a modular system for evolutionary analysis. Version 3.6, Available at: http://mesquiteproject.org (accessed on 18 November 2019).

Mello-Leitão, C.F. 1929. Aphantochilidas e Thomisidas do Brasil. Archivos do Museu Nacional, Rio de Janeiro, BR.

Mirande, J. M. 2009. Weighted parsimony phylogeny of the family Characidae (Teleostei: Characiformes). Cladistics 25, 574–613.

Morrone, J. J. 1994. Distributional patterns of Rhytirrhinini (Coleoptera: Curculionidae) and the historical relationships of the Andean provinces. Global Ecology and Biogeography Letters 4, 188–194.

Morrone, J. J. 2014. Biogeographical regionalisation of the Neotropical region. Zootaxa 3782, 1–110.

Morrone, J. J. 2015. Biogeographical regionalisation of the Andean region. Zootaxa 3936, 207–236.

Nicolet, H. 1849. Aracnidos. In: Gay, C. (ed.), Historia física y política de Chile. Museo de Historia Natural de Santiago, Santiago, pp. 319-543.

Nixon, K. C. 1999. The Parsimony Ratchet, a new method for rapid parsimony analysis. Cladistics 15, 407–414.

Nixon, K. C. 1999–2004. Winclada (BETA) ver. Asado 1.89. Published by the author, Ithaca, New York. Avaible at: http://www.cladistics.com/about_winc.htm (accessed 20 March 2014).

O'Reilly, J., Puttick, M. N., Pisani, D., Donoghue, P. C. J. 2018. Probabilistic methods surpass parsimony when assessing clade support in phylogenetic analyses of discrete morphological data. Paleaontology 61, 105–118.

Pickard-Cambridge, O. 1869. Descriptions and sketches of some new species of Araneida, with characters of a new genus. Ann Mag Nat Hist 3, 52–74.

Prado, A.W., Baptista, R. L. C., Machado, M. 2018. Taxonomic review of *Epicadinus* Simon, 1895 (Araneae: Thomisidae). Zootaxa 4459, 201–234.

Puttick, M. N., O'Reilly, J. E., Pisani, D., Donoghue, P. C. J. 2019. Probabilistic methods outperform parsimony in the phylogenetic analysis of data simulated without a probabilistic model. Palaeontology 62, 1–17.

Rambaut, A., Drummond, A. J., Xie, D., Baele, G., Suchard, M. A. 2018. Posterior summarisation in Bayesian phylogenetics using Tracer 1.7. Syst. Biol. 5, 901–904.

Ramírez, M. J. 2014. The morphology and phylogeny of dionychan spiders (Araneae: Araneomorphae). B Am Mus Nat Hist 390, 1–374.

Ronquist, F., Teslenko, M., Van Der Mark, P., Ayres, D. L., Darling, A., Höhna, S., Larget, B., Liu, L., Suchard, M. A., Huelsenbeck, J. P., 2012. Mrbayes 3.2: efficient bayesian phylogenetic inference and model choice across a large model space. Syst. Biol. 61, 539–542.

Smith, M. R. 2019. Bayesian and parsimony approaches reconstruct informative trees from simulated morphological datasets. Biol. Lett. 15, 20180632.

Simon, E. 1895. Histoire naturelle des araignées. Librairie Encyclopédique de Roret, Paris, FR.

Simon, E. 1903. Histoire naturelle des araignées. Librairie Encyclopédique de Roret, Paris, FR.

Silva-Moreira, T., Machado, M. 2016. Taxonomic revision of the crab spider genus *Epicadus* Simon, 1895 (Arachnida: Araneae: Thomisidae) with notes on related genera of Stephanopinae Simon, 1895. Zootaxa 4147, 281–310.

Sirvid, P. J., Moore, N. E., Chambers, G. K., Prendergast, K. 2013. A preliminary molecular analysis of phylogenetic and biogeographic relationships of New Zealand Thomisidae (Araneae) using a multi-locus approach. Invertebr. Syst. 27, 655–672.

Teixeira, R. A., Campos, L. A., Lise, A. A. 2014. Philogeny of Aphantochilinae and Strophinae sensu Simon (Araneae; Thomisidae). Zool. Scr. 43, 65–78.

Weiler, L., Ferrari, A., Grazia, J. 2016. Phylogeny and biogeography of the South American subgenus *Euschistus* (*Lycipta*) Stål (Heteroptera: Pentatomidae: Carpocorini). Insect Syst Evol, 47, 313–346.

Wheeler, W. C., Coddington, J. A., Crowley, L. M., Dimitrov, D., Goloboff, P. A., Griswold, C. E., Hormiga, G., Prendini, L., Ramírez, M. J., Sierwald, P., Almeida-Silva, L., Álvarez-Padilla, F., Arnedo, M. A., Benavides Silva L. R., Bnejamin, S. P., Bond, J. E., Grismado, C. J., Hasan, E., Hedin, M., Izquierdo, M. A., Labarque, F. M., Ledford, J., Lopardo L., Maddison, W. P., Miller, J. A., Piacentini, L. N.,

Platnick, N. I., Polotow, D., Silva-Dávila, D., Scharff, N., Szuts, T., Ubick, D., Vink, C. J., Wood, H. M., Zhang, J. 2017. The spider tree of life: phylogeny of Araneae based on target-gene analyses from an extensive taxon sampling. Cladistics 33, 574–616.

World Spider Catalog, 2020. World Spider Catalog. Natural History Museum Bern, available online at http://wsc.nmbe.ch, version 21.0, accessed on 24 January 2020.

Appendix and supplementary material

Appendix 1 — List of examined species

Outgroup

1. *Borboropactus cinerascens* **(Doleschall, 1859)** – Papua New Guinea: Madang Province: 1♀, 22.IV.1989, Papua New Guinea expedition 1989 leg. (CAS 9051720); Papua New Guinea: Madang Province: 1♂, 04.IV.1989, Papua New Guinea expedition 1989 leg. (CAS 9051721).

2. *Borboropactus nyerere* **Benjamin, 2011** – Tanzania: Usambara Mountains (Mazumbai Forest – 4°45'0.00"S, 38°30'0.00"E): 1♂ and 3♀, 12–20.XI.1995, C. Griswold, N. Scharff and D. Ubick leg. (CAS 9046658).

3. *Coenypha edwardsi* **(Nicolet, 1849)** – Chile: Talca (35°25'23.68"S, 71°38'54.53"W): 1♂, 19.VI.1981, Ross and Michelbacher leg. (CAS 9046659); Chile: Algol (33°27'39.31"S, 70°45'10.75"W): 1♀, 20.V.1986, H. Levi leg. (CAS9046660).

4. *Epicadinus villosus* **(Blackwall, 1862)** – Brazil: Rio Grande do Sul: Machadinho: 1♂, 01.IX.1988, Projeto Ita-Machadinho leg. (MCTP 0537); Brazil: Rio Grande do Sul: Santa Maria: 1♀, 11.II.1999, C. B. Kotzian and L. Indrusiak leg. (MCTP 41354).

5. *Epicadinus trispinosus* **(Taczanowski, 1872)** – Panama: Arraiján (8°58'41.17"N, 79°40'21.59"W): 1♂ and 1♀, 07.VI.1950, A. M. Chickering leg. (MCZ).

6. *Epicadus camelinus* **Simon, 1895** – Brazil: Acre (Senador Guiomard): 1♀, XI.2010, A. J. Santos leg. (UFMG 11007).

7. *Epicadus caudatus* **Mello-Leitão, 1929** – Brazil: Santa Catarina (Florianópolis): 1♀, 06.X.1995, A. A. Lise leg. (MCTP 7593).

8. *Epicadus dimidiaster* **Machado, Teixeira & Lise, 2018** – Brazil: Pará (Floresta Nacional de Caxiuanã – 1°45'12"S, 51°31'14"W): ♀ holotype, J. M. C. Cordeiro leg. (MPEG 30605); Brazil: Pará (Melgaço): ♂ paratype, 03.X.2005, C. A. Lopes leg., 1°43'43"S, 51°29'00"W (MPEG 30603).

9. *Epicadus heterogaster* (Guérin, 1829) – Brazil: Roraima (Reserva Biológica Ilha de Maracá): 1♂, 14.II.1992, A. B. Bonaldo leg. (MCTP 1772); Brazil: Paraná (Morretes): 1♀, 09–20.I.1995, Arachnology laboratory staff leg. (MCTP 7101).

10. *Epicadus granulatus* Banks, 1909 – Brazil: Amazonas (Novo Progresso): 1♀, (MNHN 3403); Brazil: Pará (Campo de Provas Brigadeiro Velloso): 1♂, 15.IX.2003, D. R. Santos-Souza leg. (MPEG 005373).

11. *Epicadus pulcher* Mello-Leitão, 1929 – Brazil: Amazonas (São Paulo de Olivença): ♀ holotype (MNHN 137).

12. *Epicadus rubripes* (Mello-Leitão, 1924) – Brazil: Rio Grande do Sul: Guaíba (Fazenda Matzenbacker): 2♂, 26.VIII.1994, A. A. Lise et al. leg. (MCTP 5432); Brazil, Rio Grande d Sul: Viamão: 1♀, 20.XII.2000, P. P. Júnior leg. (MCTP 21868).

13. *Epicadus tigrinus* Machado, Teixeira & Lise, 2018 – Panama: Panama City (Summit Municipal – 9°3'54.80"N, 79°38'43.07"W): ♀ holotype, A. M. Chickering leg. (MCZ 14839); Panama: Reserva Florestal Fortuna (8°35'5.63"N, 82°23'18.88"W), ♂ paratype, 22.I.2006, R. J. Miranda leg. (MCTP 39867).

14. *Epicadus tuberculatus* Mello-Leitão, 1929 – Brazil: São Paulo (Iporanga): 1♀, X.2001, E. H. Wienkoski leg. (MNRJ 11520); Brazil: Roraima (Caracaraí): 1♂, 28.V.2006, A. Tourinho leg. (INPA 1825).

15. *Epicadus taczanowskii* Roewer, 1951 – Brazil: Mato Grosso (Barra do Tapirape): 1♀, 1–23.XII.1961, B. Malkin leg. (AMNH); Brazil: Mato Grosso (Canarana): 1♂, 16.VI.2006, N. Lo-Man-Hung leg. (MPEG 022628).

16. *Epicadus trituberculatus* (Taczanowski, 1872) – Brazil: Amazonas (Coari): 1♀, 26.IX.2004, A. B. Bonaldo leg. (MPEG 022672); Brazil: Amapá (Ilha de Maracá): 1♂,1–14.II.1992, A. A. Lise leg. (MCTP 1943).

17. *Epidius pallidus* (Thorell, 1890) – Indonesia: Sumatra: 1♀, holotype, T. Thorell leg. (OUMNH 1233).

18. *Geraesta hirta* Simon, 1889 – Madagascar: Antsiranana (Amber Mountain National Park –12°35'47.00"S, 49°09'.34"E): 5♀ and 3♂, 02-07.II.2001, C. Griswold leg. (CAS 9006884).

19. *Isala punctata* **L. Koch, 1876** – Australia: Tasmania: Trevallyn (41°25'60.00"S, 147°70'.00"E): 1♂ and 2 j, 11.VII.1939, V. V. Hickman leg. (AMS KS31520).

20. *Hedana ocellata* **Thorell, 1890** – Sri Lanka: 1♀, 20.XI.1960, R. Sherriffs leg. (ZMUC298).

21. *Onocolus infelix* **Mello-Leitão, 1941** – Brazil: Rio Grande do Sul (Viamão): 1♂ and 1♀, 17.X.1995, A. A. Lise et al. leg. (MCTP 8098).

22. *Onocolus intermedius* **(Mello-Leitão, 1929)** – Brazil: Rio Grande do Sul (Viamão): 2♂ and 1♀, 7.X.1994, A. A. Lise et al. leg. (MCTP 5628).

23. *Phrynarachne ceylonica* **(O. Pickard-Cambridge, 1884)** – Sri Lanka: 1♂ and 1♀, 01.XI.1912, O. Pickard-Cambridge leg. (OUMNH 1268).

24. *Rejanellus mutchleri* **(Petrunkevich, 1930)** – Puerto Rico: Adjuntas (Jayua Road): ♂ holotype and ♀ paratype, 02.VI.1915, A. J. Mutchler leg. (AMNH 49681).

25. *Rejanellus pallescens* **(Bryant, 1940)** – Cuba: Pico Turquino: ♀ holotype, VI.1936, P. J. Darlington leg. (MCZ). Haiti: Port-au-Prince: ♂ alotype, 02.X.1934, P. J. Darlington leg. (MCZ).

26. *Stephanopoides cognata* **O. Pickard-Cambridge, 1892** – Brazil: Amazonas (Japurá): 1♀, 06.II.2017, P. I. Simões leg. (MCTP 41153). Panama: Barro Colorado Island (9°09'17.00"N, 79°50'53.00"W): 1♂, A. M. Chickering leg. (MCZ 133895).

27. *Stephanopoides simoni* **Keyserling, 1880** – Brazil: Pará (Melgaço, Floresta Nacional de Caxiuanã – 1°57'29.79"S, 51°40'36.40"W): 1♂ and 1♀, 11.VIII.1996, A. A. Lise et al. leg. (MCTP 9506).

28. *Synalus angustus* **(L. Koch, 1876)** – Australia: Sydney (Royal National Park – 34°7'13.88"S, 151°2'7.75"E): 1♀, 19.XI.1996, B. Speechley and R. Mascord leg. (AMS KS108747).

29. *Tmarus elongatus* **Mello-Leitão, 1929** – Brazil: Rio Grande do Sul (Porto Alegre): 1♀, 29.IX.2018, J. Massim leg. (MCTP 43391); Brazil: Rio Grande do Sul (Itaara): 1♂, 05.I.2006, L. Indrusiak and G. Deprá leg. (MCTP 21687).

30. *Tmarus polyandrus* **Mello-Leitão, 1929** – Brazil: Rio Grande do Sul (Nova Santa Rita): 1♂, II.2009, A. Oliveira et al. leg. (MCTP36455); Brazil Rio Grande do Sul: (Novo Cabrais): 1♀, 25.X.2007, R. G. Buss leg. (MCTP 28419).

Ingroup

1. *Sidymella angularis* (Urquhart, 1885) – New Zealand: Mercury Islands (Korapuki Island): 1♀ and 1♂, 02.III.1998, B. M. Fitzgerald leg. (MCTP 11043).

2. *Sidymella bicuspidata* (L. Koch, 1874) – Australia: New South Wales (Barren Grounds – 34°40'35"S, 150°42'42"E): 1♀, 19.IX.2012, G. Milledge and H. Smith leg. (AMS KS119143); Australia: New South Wales (Bulls Ground State Forest 31°35'S, 152°41'E): 1♂, 1999, A. York leg. (AMS KS77832).

3. *Sidymella excavata* Machado & Guzati, 2019 – Colombia: Cundinamarca (Mosquera – 4°41'0.06"N, 74°15'0.25"W): ♀ paratype, 20.X.2000, E. Florez and J. Pinzon leg. (ICN 3404). Ecuador: Pichincha (0°15'00.0"S, 78°35'00.0"W): ♂ paratype, 19.IV.1988, W. Maddison leg. (MCZ 133397).

4. *Sidymella furcillata* (Keyserling, 1880) – Brazil: Rio Grande do Sul (Porto Alegre): 2♂ and 1♀, 18.I.1992, A. D. Brescovit leg. (MCN 21958).

5. *Sidymella hirsuta* (L. Koch, 1874) – Australia: New South Wales (Hornsby Heights – 33°40'0.00"S, 151° 5'60.00"E): 1♂ and 4♀, 24.IV.1971, R. E. Mascord leg. (AMS KS118364).

6. *Sidymella kolpogaster* (Lise, 1973) – Brazil: Santa Catarina (Rancho Queimado – 27°40'22"S, 49°01'19"W): 1♂, 09–13.X.1995, A. Braul and M. Silveira leg. (MCTP 7009). Brazil: Rio Grande do Sul (Estrela Velha – 29°15'19"S, 53°13'36"W): 1♀, 21.X.1998, A.B. Bonaldo leg. (MCN 30791).

7. *Sidymella lobata* (L. Koch, 1874) – Australia: Queensland (Kuranda Range – 16°50'14.08"S, 145°40'20.05"E): 1♀, 02.II.1975, R. E. Mascord leg. (AMS KS108582).

8. *Sidymella longipes* (L. Koch, 1874) – Australia: New South Wales (Sydney – 33°56'59.67"S, 151°11'59.29"E): 1♂ and 1♀, 10.VII.1966, R. E. Mascord leg. (AMS KS108575).

9. *Sidymella longispina* (Mello-Leitão, 1943) – Brazil: Rio Grande do Sul (Pantano Grande – 30°11'27"S, 52°22'26"W): 1♀, 05.IV.2008, G. Deprá leg. (MCTP 40084); Brazil: Rio Grande do Sul (Santa Maria – 27°53'39"S, 55°21'20"W): 3♂, 1952, C. Viana leg. (MCTP 3537).

10. *Sidymella lucida* **(Keyserling, 1880)** – Brazil: Rio Grande do Sul (São Martinho da Serra – 29°32'16"S, 53°51'18"W): 1♀, 19.X.1993, L. Indrusiak and R. A. Boelter leg. (MCTP 40116); Brazil: Rio Grande do Sul (Santa Maria – 29°40'59"S, 53°48'00"W): 1♂, 28.VII.1995, C. B. Kotzian and L. Indrusiak leg. (MCTP 40100).

11. *Sidymella marmorata* **Machado & Guzati, 2019** – Ecuador: Quito (0°19'3.83"S, °59'19.95"W): ♀ paratype, 24.II.1965, L. Pena leg. (MCTP 42654).

12. *Sidymella rubrosignata* **(L. Koch, 1874)** – Australia: New South Wales (Royal National Park – 34°4'30.28"S, 151° 3'23.97"E): 1♀, 15.XII.1966, R. E. Mascord leg. (AMS KS108606). Australia: New South Wales (Currawong – 33°35'42.72"S, 151°17'52.75"E): 1♂, 03.X.1965, R. E. Mascord leg. (AMS KS108603).

13. *Sidymella trapezia* **(L. Koch, 1874)** – Australia: Southern Territory (Adelaide – 35°06"S, 138°28"E): 1♀, 01.XI.1967, H. Cooper leg. (SAM NN23202).

14. *Sidymella* **sp. 1** – Australia: New South Wales (Wangi Point Reserve – 33°4'52"S, 151°36'34"E): 1♀, 23.III.2012, G. Milledge & H. Smith leg. (AMS KS118352). Australia: New South Wales (Lane Cove – 33°48'57"S, 151°10'E): 1♂, 07.XI.1965, R.E. Mascord leg. (AMS KS108597).

15. *Sidymella* **sp. 2** – Australia: Tasmania (Launceston – 41°26'60"S, 147°10'0.00"E): 1♀, IV.1930, V.V. Hickman leg. (AMS KS31539). Australia: Tasmania (Tarraleah – 42°18'6.49"S, 146°26'57.88"E): 1♂, 01.I.1954, V.V. Hickman leg. (AMS KS31366).

16. *Stephanopis altifrons* **O. Pickard-Cambridge, 1869** – Australia: New South Wales (Hunters Hill – 33°50'S, 151°08'E): 1♀, 10.XI.1965, R.E. Mascord leg. (AMS KS108663). Australia: New South Wales (Berry – 34°47'S, 150°42'E): 1♂, 28.VIII.1966, R.E. Mascord leg. (AMS KS108647).

17. *Stephanopis angulata* **Rainbow, 1899** – Papua New Guinea: Morobe (Wau – 7°20'13.69"S, 146°42'57.37"E): 1♀, 07.IX.1971, N. C. Coleman leg. (QM S104672). Papua New Guinea: East New Britain (Gazelle Peninsula – 4°38'23.00"S, 151°59'5.00"E): 1♂, 18.V.1980, S. Smith leg. (MCZ 134019).

18. *Stephanopis antennata* **Tullgren, 1902** – Chile: Chiloé (Isla Quinchao – 42°28'9.00"S, 73°30'53.00"W): 1♀, 19.II.1997, T. Cekalovic leg. (MNHN). Chile: Chiloé (42°27'22.52"S, 73°52'47.37"W): 1♂, 27.XII.1981, L. Peña leg. (MNHN).

19. *Stephanopis arenata* **Machado, 2019** – Australia: New South Wales (Scotia Sanctuary – 33°07'36"S 141°10' 40"E): 1♀, II.2009, H. Gibb leg. (AMS KS128001). Australia: New South Wales (Lower Murray – 33°51'16"S 141°07'06"E): 1♂, 12–16.X.1998, M. Lebreton leg. (AMS KS66762).

20. *Stephanopis armata* **L. Koch, 1874** – Australia: Queensland (Burnleigh Heads – 28° 6'14.40"S, 153°26'9.60"E): 1♀, 01–07.X.1976, M. Bishop leg. (QM S110118). Australia: Queensland (Buholt Creek Reserve – 27°35'27"S, 153°10'19"E): 1♂, 17.II.2008, H. Smith and G. Anderson leg. (AMS KS103218).

21. *Stephanopis barbipes* **Keyserling, 1890** – Australia: Queensland (Tallebudgera Valley – 28°11'2.00"S, 153°22'1.00"E): ♂ neotype, 01.I.1986, D. J. Cook leg. (AMS KS110112). Australia: Tasmania (Punch Bowl – 41°27'S, 147° 10'E): 1♀, 17.V.1928, V. V. Hickman leg. (AMS KS31359).

22. *Stephanopis bicornis* **L. Koch, 1874** – Australia: New South Wales (Mount Colah – 33°39'45"S, 151°07'12" E): 1♂, 15.IV.2013, H. M. Smith leg. (AMS KS122205). Australia: New South Wales (Livingstone – 35°22'S, 147°22'E): 1♀, 19.IX.2001, C. Car leg. (AMS KS101228).

23. *Stephanopis cambridgei* **Thorell, 1870** – Australia: Southern Territory (Mylor – 35°03'S, 138° 46'E): 1♀, 08.V.1980, A. D. Austin leg. (AMS KS10530). Australia: Queensland (Reechmont – 28°09'42.4"S, 153°11'47.9"E): 1♂, III.2017, A. Grabolle leg. (AMS KS128377).

24. *Stephanopis carcinoides* **Machado, 2019** – Australia: Queensland (Bunya Mountains – 26°52'50.31"S 151°35'50.58"E): 1♀ and 1♂, 17.III.1976, Queensland Museum staff leg. (QM S104677).

25. *Stephanopis championi* **(F. O. Pickard-Cambridge, 1900)** – Honduras: Cortés (Parque Nacional Cusuco – 15°32′31″ N, 88°15′49″ W): 1♀, 14.VII.2013, D. R. Williams, S. J. Longhorn and K. O. Sagastume leg. (OUMNH).

26. *Stephanopis corticalis* **L. Koch, 1876** – Australia: New South Wales (Dubbo – 32°15'49.27"S, 148°27'18.53"E): 1♀, 29.I.1957, H. Levi leg. (AMS KS108671).

27. *Stephanopis ditissima* **(Nicolet, 1849)** – Chile: Santiago (Cordoba Coast – 33°26'56.00"S, 70°40'9.35"W): 1♀, 15-20.II.1979, L. Peña leg. (MNHN). Chile: Correntoso (Llanquihue – 41°15'38.27"S, 73° 0'28.23"W): 1♂, I.1969, L. Peña leg. (MCZ).

28. *Stephanopis erinacea* Karsch, 1878 – Fiji (17°42'48.14"S, 178° 3'54.12"E): ♀ holotype (ZMB 1878).

29. *Stephanopis fissifrons* Rainbow, 1920 – Australia: New South Wales (Lord Howe Island – 31°33'15"S, 159°04'50"E): 1♀, 20.II.2001, J. Tarnawski leg. (AMS KS84026). Australia: Lord Howe Island (31°32'05"S, 159°04'23"E): 1♂, 26.X.1978, T. Kingston and B. Miller leg. (AMS KS86885).

30. *Stephanopis flagellata* Machado 2019 – Australia: New South Wales (Scotia Sanctuary – 33°09'23"S, 141°07'46"E): ♂ paratype, 01.II.2011, C. Silvey leg. (AMS KS120712).

31. *Stephanopis lata* O. Pickard-Cambridge, 1869 – Australia: Tasmania (Hobart – 42°52'S, 147°19'E): 1♂ and 1♀, IX.1958, V. V. Hickman leg. (AMS KS31449).

32. *Stephanopis longimana* Thorell, 1881 – Australia: Queensland (Yandin Natural Reserve – 26°34'55.87"S, 152°58'46.03"E): 1♀, 09.VII.2006, D. Harms leg. (ZMB 48561). Australia: Queensland (Beerwah Forestry Reserve – 26°51'S, 152°57'E): 1♂, 10.X.1990, M. Glover leg. (QM S19432).

33. *Stephanopis macrostyla* Mello-Leitão, 1929 – Brazil: Rio de Janeiro (Teresópolis): ♂ holotype (MNHN 11467).

34. *Stephanopis monulfi* Chrysanthus, 1964 – Australia: Queensland (Cairns 16°55'S, 145°46'E): 1♂ and 1♀, 13.VIII.1969, N. C. Coleaman leg. (AMS KS108716).

35. *Stephanopis nana* Machado, 2019 – Australia: Queensland (Moolayember Creek National Park – 25°14.5'S, 148°37.4'E): ♀ paratype, 10.III.2006, C. Burwell leg. (QM S80820).

36. *Stephanopis nigra* O. Pickard-Cambridge, 1869 – Australia: Queensland (Wide Bay-Burnett): 1♀, 25.IV.2001, E. Ford leg. (QM S55042). Australia: New South Wales (Irishman State – 30°33'43"S, 152°42'12"E): 1♂, 25.XI.1999, G. Milledge and H. Smith leg. (AMS KS65781).

37. *Stephanopis nodosa* (Nicolet, 1849) – Chile: Concepción: 1♀, 14.I.1977, T. Cekalovic leg. (MCZ 133404). Chile: Concepción (Huálpen): 1♀, 11.I.1989, M. Ramírez leg. (MCN-Ar 18703).

38. *Stephanopis palliolata* Simon, 1908 – Australia: Queensland (Yandina – 26°33'52.84"S, 152°57'26.42"E): 1♂, 09.VII.2006, D. Harms leg. (ZMB 48561).

39. *Stephanopis parahybana* **Mello-Leitão, 1929** – Brazil: Rio Grande do Sul (Montenegro – 29°41'20"S, 51°27'39"W): 3♂ and 2♀, 03.XI.1977, A. A. Lise leg. (MCN 8075).

40. *Stephanopis pentacantha* **Mello-Leitão, 1929** – Brazil: Rio Grande do Sul (Santa Maria – 29°40'31"S, 53°43'10"W): 1♀, 15.I.1998, L. Indrusiak & M. Monteiro leg. (MCTP 38671). Brazil: Rio Grande do Sul (São Francisco de Paula – 29°28'51"S, 50°10'28"W): 1♂, VIII.2001, L.A. Bertoncello leg. (MCTP 25762).

41. *Stephanopis quinquetuberculata* (Taczanowski, 1872) – Brazil: Bahia (Reserva Biológica de Una – 15°10'42"S, 39°06'13"W): 1♂, 15–28.XI.2000, A. D. Brescovit et al. leg. (IBSP 46740).

42. *Stephanopis renipalpis* **Mello-Leitão, 1929** – Brazil: Rio de Janeiro (Angra dos Reis –23°08'30"S, 44°08'26"W): 1♂, 02–12.II.2012, M. Ramírez leg. (MCTP 42730).

43. *Stephanopis rufiventris* **Bradley, 1871** – Brazil: Queensland (Kenilworth State Forest – 26°42'21"S, 152°31'41"E): 1♀, 07.V.1998, G. Milledge leg. (AMS KS53360).

44. *Stephanopis similis* **Machado, 2019** – Australia: Western territory (34°57'S, 116°16'E): 1♂, 15.II.1979, M. Gray leg. (AMS KS15423). Australia: New South Wales (Barrington Tops National Park – 32°03'43"S, 151°34'39"E): 1♀, 13.XI-19.XII.2007, G. Milledge and H. Smith leg. (AMS KS102991).

45. *Stephanopis spiralis* **Machado, 2019** – Australia: New South Wales (Coolah Tops National Park – 31°44'00"S, 150°00'30"E): 1♀, 07.XI.2001, M. Gray, G. Milledge and H. Smith leg. (AMS KS75074). Australia: New South Wales (Yathong Nature Reserve – 32°50'56"S, 146°10'58"E): 1♂, III.2001, D. Eldridge leg. (AMS KS78947).

46. *Stephanopis squalida* **Machado, 2019** – Australia: Queensland (Mount Finnigan – 15°48'13.25"S, 145°18'22.07"E): 1♀, 19–22.IV.1982, Monteith, Yeastes and Cook leg. (QM S110120). Australia: Queensland (Cape Tribulation – 16°5'16.04"S, 145°27'17.20"E): 1♂, 27.IX–07X.1982, Monteith, Yeates and Thompson leg. (QM S111092).

47. *Stephanopis* **sp. 1** – Mexico: Veracruz (Estação de Biologia Tropical "Los Tuxtlas" – 18°36'N, 95°07'W): 1♀, 29.VI–01.VII.1983, W. Maddison & R.S. Anderson leg. (MCZ 134014).

Appendix 2 — List of characters

Prosoma

1. Carapace, surface, texture: 0 = smooth (Fig. S1b); 1 = granular (Fig. S1a) (from Benjamin, 2011 – character 63).

2. Carapace, setae sockets, shape: 0 = conical (Fig. S1d); 1 = spherical (Fig. S1c); 2 = flat (Fig. S1e).

3. Carapace, crypsis through detritus adhesion: 0 = absent; 1 = present (Fig. S1f) (from Ramírez (2014) – character 389).

4. Sternum, coloration: 0 = uniform (Fig. S1e); 1 = stained/bicolor (Fig. S1f) (from Machado et al. (2017) – character 4).

5. Sternum, setae, general shape: 0 = pointed (Fig. S1g); 1 = clavate (Fig. S1h); 2 = baciliform (Fig. S2a) (from Machado et al. (2017) – character 5).

6. Sternum, setae, scales, shape: 0 = smooth (Fig. S1g); 1 = plumose (Fig. S2b); 2 = serrated (Figs S1h, S2c) (from Machado et al. (2017) – character 6).

7. Sternum, surface: 0 = smooth (Fig. S2b); 1 = granular (Fig. S2c) (from Benjamin (2011) – character 63).

8. Sternum, anterior curvature: 0 = straight (Fig. S2e); 1 = concave (Fig. S2f) (from Machado et al., 2017 – character 8).

9. Sternum, posterior border, emargination between coxae IV: 0 = absent; 1 = present (from Machado et al., 2017 – character 9).

10. Carapace, setae, type: 0 = one type of setae; 1 = two different types of setae (Fig. S2d – Black arrow indicates a pointed setae and the white arrow points to a filamentous setae).

11. **Carapace, setae, general shape:** 0 = pointed (Fig. S1d); 1 = clavate; 2 = filamentous (Fig. S2d); 3 = foliaceous (Fig. S1c) (from Machado et al., 2017 – character 10).

12. **Carapace, dorsal view, median longitudinal band:** 0 = absent; 1 = present (Fig. S2g) (from Machado et al., 2017 – character 13).

13. **Carapace, dorsal view, median longitudinal band, type:** 0 = single (Fig. S2g); 1 = dual (Fig. S2H).

14. **Carapace, dorsal view, median longitudinal band, color in relation to the rest of the carapace:** 0 = darker (Fig. S2h); 1 = lighter (Fig. S2g) (from Machado et al., 2017 – character 14).

15. **Male carapace, dorsal view, median area, granules:** 0 = absent (Fig. S3d); 1 = present (Fig. S3a) (from Machado et al., 2017 – character 15).

16. **Carapace, dorsal view, thoracic portion, guanine white spot:** 0 = absent; 1 = present (Fig. S3b) (from Machado et al., 2017 – character 16).

17. **Carapace, frontal view, clypeus, black stripes:** 0 = absent; 1 = present (Figs S3c, S3h) (from Machado et al., 2017 – character 17).

18. **Carapace, lateral view, clypeus slope:** 0 = vertical (Fig. S3f); 1 = proclive (Fig. S3e) (from Machado et al., 2017 – character 18).

19. **Carapace, frontal view, clypeus, median pair of macrosetae:** 0 = absent; 1 = present (Fig. S3d) (from Machado et al., 2017 – character 20).

20. **Carapace, cephalic portion, frontal view, lateral tubercles:** 0 = absent; 1 = present (Fig. S3g – black arrows).

21. **Carapace, clypeus, lateral margin profile:** 0 = not projected (Fig. S3g – white arrows); 1 = projected (Fig. S3h – white arrows) (from Machado et al., 2017 – character 21).

22. **Carapace, thoracic portion, height in relation to cephalic portion:** 0 = same height (Figs S3e, S4c); 1 = higher (Fig. S3f); 2 = lower (Fig. S5d) (from Machado et al., 2017 – character 22).

23. **Carapace, thoracic portion, lateral view, median spire:** 0 = absent (Fig. S3e); 1 = present (Figs S3f, S4a, S4c) (from Machado et al., 2017 – character 23).

24. **Carapace, thoracic portion, median spire, type:** 0 = single (Fig. S4a); 1 = double (Fig. S4b).

25. **Carapace, thoracic portion, lateral view, median spire, orientation:** 0 = vertical (Fig. S3f); 1 = tilted (Fig. S4c) (from Machado et al., 2017 – character 24).

26. **Chelicerae, frontal view, papules:** 0 = absent; 1 = present (Fig. S4e) (from Machado et al., 2017 – character 25).

27. **Chelicerae, coloration:** 0 = uniform (Fig. S4b); 1 = stained/bicolor (Fig. S4d) (from Machado et al., 2017 – character 26).

28. **Chelicerae, promarginal teeth line, teeth number:** 0 = zero; 1 = two (Fig. S4g); 2 = three (Fig. S4h) (from Machado et al., 2017 – character 27).

29. **Chelicerae, retromarginal teeth line, teeth number:** 0 = zero; 1 = one (Fig. S4g); 2 = two (Fig. S4h) (from Machado et al., 2017 – character 28).

30. **Chelicerae, teeth, size proportion:** 0 = subequal (Figs S4g, S4h); 1 = heterodont (Fig. S4f) (from Machado et al., 2017 – character 29).

31. **Labium, apex, macrosetae:** 0 = absent (Fig. S5b); 1 = present (Fig. S5a) (from Machado et al., 2017 – character 30).

32. Labium, general shape: 0 = rectangular (Fig. S5a); 1 = trapezoidal; 2 = rounded (Fig. S5b) (from Machado et al., 2017 – character 31).

33. Endite, general shape: 0 = truncated; 1 = rounded (from Machado et al., 2017 – character 32).

34. Chelicerae, frontal view, macrosetae: 0 = absent (Fig. S5f); 1 = present (Fig. S5e).

35. Eyes, relative size between ALE and AME: 0 = subequal (Fig. S5f); 1 = ALE 2x the diameter of AME or more (Fig. S5h) (from Machado et al., 2017 – character 33).

36. Eyes, ALE black cup: 0 = reduced (Fig. S5e); 1 = well developed (Fig. S5g) (from Ramírez, 2014 – character 16).

37. Ocular area, cephalic prominence: 0 = absent (Figs S3e, S5e, S5f); 1 = present (Figs S3g, S5d).

38. Eyes, ocular projections above ALE: 0 = absent (Figs S3e, S4c); 1 = present (Figs S3f, S3g, S3h).

39. Eyes, anterior row, curvature: 0 = straight (Fig. S5F); 1 = recurve (Fig. S5h) (from Machado et al., 2017 – character 36).

40. Eyes, posterior row, curvature: 0 = recurve (Fig. S6d); 1 = procurve (Fig. S6a); 2 = straight (Fig. S6c) (adapted from Machado et al., 2017 – character 37).

41. Eyes, tapetum, type: 0 = grate-shaped (Fig. S6d); 1 = canoe-shaped (Fig. S6e).

42. Eyes, guanine mask: 0 = absent (Figs S4b, S5e—S5h); 1 = present (Fig. S5c).

43. Eyes, median ocular quadrangle, macrosetae: 0 = absent; 1 = present (Fig. S6d).

44. Carapace, dorsal view, radial furrows: 0 = absent; 1 = present (Figs S6a, S6c).

45. Carapace, dorsal view, posterior slope, pair of circular taints: 0 = absent; 1 = present (Figs S2g, S6a).

Legs

46. Tibiae, trichobothria, disposition: 0 = in line (Fig. S6f); 1 = clustered (Fig. S6g).

47. Femora I and II, apical region, mesial apophysis: 0 = absent; 1 = present (Fig. S6h) (from Machado et al., 2017 – character 39).

48. Femora I and II, apical region, ectal apophysis: 0 = absent; 1 = present (Fig. S6h) (from Machado et al., 2017 – character 40).

49. Femora I, dorsolateral setiferous tubercles: 0 = absent (Fig. S6h); 1 = present (Figs S7a, S7b, S7c, S7g, S7h) (from Machado et al., 2017 – character 41).

50. Femora I, dorsolateral setiferous tubercles, number: 0 = one (Fig. S7b); 1 = two; 2 = three or more (Fig. S7a).

51. Femora I and II, ventral setiferous tubercles: 0 = absent; 1 = present (Figs S7e, S7f) (from Machado et al., 2017 – character 42).

52. Femora I and II, ventral setiferous tubercles, socket type: 0 = conical (Fig. S7e); 1 = blister-shaped (Fig. S7f) (from Machado et al., 2017 – character 43).

53. Femora I and II, coloration: 0 = uniform (Fig. S7g); 1 = stained (Fig. S7h) (from Machado et al., 2017 – character 44).

54. Patellae I and II, ventral macrosetae: 0 = absent; 1 = present (Fig. S8b) (from Machado et al., 2017 – character 45).

55. Patellae, median keel: 0 = absent; 1 = present (Fig. S8a) (from Machado et al., 2017 – character 46).

56. Patellae shape on transversal section: 0 = circular; 1 = rectangular (from Machado et al., 2017 – character 47; see Fig. S7c).

57. Tibiae and metatarsi, duster-shaped setae: 0 = absent; 1 = present (Fig. S8d).

58. Tibiae I and II, lateral view tibial depression: 0 = absent; 1 = present (Fig. S8g) (adapted from Machado et al., 2017 – character 48).

59. Tibiae I and II, lateral view, tibial depression, length: 0 = short (Fig. S7c, S7h); 1 = long (Fig. S8g) (from Machado et al., 2017 – character 49).

60. Tibiae I and II, dorsal setiferous tubercles: 0 = absent (Figs S7a, S7b); 1 = present (Figs S7c, S7d, S7h).

61. Tibiae I and II, dorsal setiferous tubercles, number: 0 = two (Figs S7c, S7h); 1 = three (Fig. S7d).

62. Male tibiae and metatarsi I and II, brushes: 0 = absent; 1 = present (Fig. S8c).

63. Tibiae, lateral view, shape: 0 = straight (Figs S7b, S7g); 1 = curved (Fig. S7a) (from Machado et al., 2017 – character 50).

64. Tibiae I and II, ventral macrosetae, number: 0 = three pairs; 1 = four pairs (Fig. S7h); 2 = five pairs (Fig. S7b); 3 = six pairs (from Machado et al., 2017 – character 52).

65. Metatarsi I and II, ventral macrosetae, number: 0 = three pairs (Fig. S7h); 1 = four pairs; 2 = five pairs (Fig. S7a) (from Machado et al., 2017 – character 53).

66. Metatarsi I and II, lateral view, mesial macrosetae: 0 = absent; 1 = present (Fig. S7c).

67. Metatarsi I and II, lateral view, mesial macrosetae, number: 0 = one (Fig. S7c); 1 = two; 2 = three (Fig. S7g).

68. Tarsi, claw tuft density: 0 = under the claws (Fig. S8f); 1 = covering the claws (Fig. S8e) (from Machado et al., 2017 – character 54).

69. Tarsi, tarsal claws, teeth disposition: 0 = restricted to the proximal portion of the claw (Fig. S8f); 1 = distributed along the entire claw (Fig. S8e) (from Machado et al., 2017 – character 55).

70. Tarsi, tarsal claws, teeth, arrangement: 0 = symmetric (both claws have approximately the same number of equal-sized teeth) (Fig. S8e); 1 = asymmetric claws noticeably different, with mesial claw having at least twice the number of teeth of the ectal one; mesial teeth are thin and acute while ectal teeth are stouter (Fig. S8f) (from Machado et al., 2017 – character 56).

71. Metatarsi I and II, ventral macrosetae, proportion: 0 = subequal (Fig. S7c); 1 = distal pair smaller than others (Fig. S7a).

72. Patellae I and II, lateral view, apical projection: 0 = absent (Fig. S7a); 1 = present (Fig. S7c).

73. Femora III and IV, coloration, marked color division: 0 = absent; 1 = present.

Opisthosoma

74. Dorsal view, median posterior projection: 0 = absent; 1 = present (Fig. S8h) (from Machado et al., 2017 – character 57).

75. Dorsal view, dorsolateral projection: 0 = absent; 1 = present (Fig. S8h) (from Machado et al., 2017 – character 59).

76. Dorsal view, ventrolateral projection: 0 = absent (Fig. S9c); 1 = present (Fig. S8h) (from Machado et al., 2017 – character 60).

77. Dorsal view, anterior border, curvature: 0 = convex (Fig. S9c); 1 = straight (Fig. S9b); 2 = concave (Fig. S9a) (from Machado et al., 2017 – character 62).

78. Dorsal surface, texture: 0 = fingerprint (Fig. S9g); 1 = cuspidate (Fig. S9d); 2 = granular (Fig. S9f); 3 = maze (Fig. S9e).

79. Dorsal surface, setae sockets, shape: 0 = conical (Fig. S9h); 1 = spherical (Fig. S9g).

80. Dorsal surface, setae, general shape: 0 = clavate (Fig. S9g); 1 = needle-shaped (Fig. S9h); 2 = foliaceous (same of carapace – Fig. S1c); 3 = baciliform; 4 = filamentous (Fig. S9h).

81. Dorsal surface, setae clusters: 0 = absent; 1 = present (Fig. S10a).

82. Dorsal surface, setae, texture: 0 = smooth (Fig. S9g); 1 = scaled; 2 = barbed (Fig. S10b).

Epigynum

83. Ventral view, median septum: 0 = absent; 1 = present (Figs 10c, 10d) (from Machado et al. (2017) – character 64).

84. Ventral view, median septum, type: 0 = complete (Fig. S10c); 1 = incomplete (Fig. S10d) (from Machado et al. (2017) – character 65).

85. Dorsal view, copulatory openings, entry direction: 0 = ascendant (Fig. S10e); 1 = descendent (Fig. S10f) (from Machado et al. (2017) – character 66).

86. Dorsal view, copulatory ducts, type: 0 = tubular (Fig. S10g); 1 = chamber-like (Fig. S10h)

87. Dorsal view, copulatory ducts, position: 0 = close to the copulatory openings (Fig. S10f); 1 = intermediated by a duct (Fig. S10h) (from Machado et al. (2017) – character 69).

88. Dorsal view, copulatory ducts, texture: 0 = sclerotized (Figs S10h); 1 = membranous (Fig. S11a).

89. Dorsal view, spermathecae, shape: 0 = elliptical (Fig. S10h); 1 = meandering cylinder (Fig. S10g).

90. Dorsal view, spermathecae, glandular-head: 0 = absent (Fig. S10h); 1 = present (Fig. S10g).

91. Ventral view, copulatory openings: 0 = exposed (Figs S10c, S10d); 1 = covered by the folds of the epigynal plate (Fig. S11c).

92. Ventral view, copulatory openings, shape: 0 = rounded (Fig. S11d); 1 = slit-shaped (Fig. S11e).

93. Ventral view, lateral teeth: 0 = absent; 1 = present (Fig. S11f).

Male palp

94. Ventral view, embolus, distal portion, tip, disposition: 0 = linear (Fig S11h); 1 = meandered (Fig. S11g).

95. Ventral view, tegulum, shape: 0 = disk-shaped (Figs S12a, S14c, S14e); 1 = oval-shaped (Figs S11g, S11h, S12c, S12d); 2 = pear-shaped (Fig. S12b) (adapted from Benjamin, 2011 – character 11).

96. Ventral view, tegulum, median apophysis: 0 = absent (Figs S12a, S12b); 1 = present (Figs S12c, S12d) (from Benjamin (2011) – character 16).

97. Ventral view, tibiae, prolateral macrosetae: 0 = absent (Fig. S12a); 1 = present (Fig. S12b).

98. Retrolateral view, patella, dorsal macrosetae: 0 = absent (Fig. S12f); 1 = present (Fig. S12e) (from Machado et al. (2017) – character 74).

99. Ventral view, tibiae, VTA: 0 = absent (Fig. S12b); 1 = present (Fig. S14f)

100. Ventral view, tibiae, RTA: 0 = absent (Fig. S14e); 1 = present (Figs S14a, S14g).

101. RTA, tip, curvature: 0 = ventrally curved (Fig. S12f); 1 = straight (Fig. S12g); 2 = dorsally curved (Fig. S13e); 3 = laterally curved (Fig. S11h).

102. Retrolateral view, RTA, cusps: 0 = absent (Figs S13a–S13e); 1 = present (Fig. S12h).

103. Retrolateral view, RTA, tip, shape: 0 = truncated (Fig. S13a); 1 = acute (Fig. S13h); 2 = rounded (Fig. S13b).

104. Retrolateral view, RTA, tip, texture: 0 = smooth (Fig. S13c); 1 = grooved (Figs S12h, S13a); 2 = nodose (Fig. S13b).

105. RTA, ventral branch: 0 = absent (Figs S11h, S12b, S12f, S13c); 1 = present (Figs S12e, S12g, S12h, S13a, S13b, S13d, S13e) (reinterpreted from Machado et al. (2017) – character 77).

The inclusion of more Stephanopinae genera in the data matrix allowed us to examine in detail a greater diversity of shapes, sizes and textures of certain structures such as the palpal apophyses. Thus, after exhaustive morphological comparisons, we realized that what Machado *et al*. (2017) considered as distal tibial apophysis (DTA), based solely on the position and direction of this structure in relation to the tegulum, is in fact the retrolateral tibial apophysis. The updated designation of what defines the RTA in the presence of other apophyses is based on the modified texture on the surface of its tip, which might be grooved or nodose. While this feature allows the

identification of homologous traits, we consider the DTA as absent in all taxa scored here, as it is seems to be the case for all crab-spiders. On the other hand, the RTA of stephanopines sampled in this study might present an accessory branch on its ventral portion. This branch can be truncated, acute, canoe-shaped or spoon-shaped. Therefore, what Machado *et al.* (2017) considered as the presence of DTA in *Epicadus*, is interpreted here as a clade of species with males having an RTA with a canoe-shaped ventral branch.

106. Retrolateral view, RTA, ventral branch, shape: 0 = truncated (Fig. S13a); 1 = acute (Fig. S12h); 2 = canoe-shaped (Fig. S13d); 3 = spoon-shaped (Fig. S13e).

107. Ventral view, embolus, shape: 0 = filiform (Figs S11g, S11h, S13h, S14a, S14c, S14e, S14g); 1 = laminar (Figs S13f, S13g, S14d, S14f) (from Machado et al. (2017) – character 84).

108. Ventral view, tegular ridge: 0 = absent (Figs S12b, S14c); 1 = present (Figs S13f, S14a, S14b, S14f) (from Machado et al. (2017) – character 80).

109. Ventral view, tegular ridge, position: 0 = median (Fig. S13f); 1 = apical (Figs S11g, S14g); 2 = retrolateral (Fig. S14b); 3 = peripheric (Fig. S14c).

110. Ventral view, tegulum, surface: 0 = smooth (Fig. S14c); 1 = scaled (Fig. S14d).

111. Ventral view, tibia, pair of filamentous setae: 0 = absent; 1 = present (Fig. S14g).

112. Ventral view, embolus, resting position: 0 = on cymbium (Figs S11h, S12b); 1 = on tegulum (Figs S13f–S13h); 2 = on tegular ridge (Figs S12a, S14c, S14g); 3 = on conductor (Figs S12c, S12d) (from Benjamin (2011) – character 20).

113. Ventral view, conductor: 0 = absent; 1 = present (Figs S12c, S12d) (from Machado et al. (2017) – character 81).

114. Ventral view, embolus length: 0 = half turn around the tegulum or less (Figs S11h, S12b, S13g, S14g; 1 = one turn around the tegulum or more (from Machado et al. (2017) – character 85).

115. Ventral view, pars pendulum: 0 = absent (Figs S13h, S14c, S14e); 1 = present (Figs S13g, S14d, S14g) (from Machado et al. (2017) – character 86). When present, it can be seen as an acessory membranous structure lying within a groove of the embolus,

116. Ventral view, cymbium, cymbial process: 0 = absent (Figs S12c, S12b, S12e, S13g, S14c, S14e); 1 = present (Figs S11g, S11h, S12f, S13a, S14a, S14g).

117. Prolateral view, cymbium, dorsal surface, brush: 0 = absent; 1 = present – a patch of arrow-shaped setae (Fig. S14h).

Appendix 3 — Pruned tree under equal weighting parsimony (EW).

```
┌─ Borboropactus_nyerere
├─ Borboropactus_cinerascens
├─ Geraesta_hirta
├─ Synalus_angustus
├─ Tmarus_elongatus
├─ Tmarus_polyandrus
├─ Phrynarachne_ceylonica
├─ Sidymella_rubrosignata
├─ Stephanopoides_simoni
├─ Stephanopoides_cognata
├─ Epidius_pallidus
├─ Hedana_ocellata
├─ Epicadinus_villosus
├─ Epicadinus_trispinosus
├─ Onocolus_intermedius
├─ Onocolus_infelix
├─ Rejanellus_mutchleri
├─ Rejanellus_pallescens
├─ Epicadus_granulatus
├─ Epicadus_tuberculatus
├─ Epicadus_caudatus
├─ Epicadus_trituberculatus
├─ Epicadus_taczanowskii
├─ Epicadus_dimidiaster
├─ Epicadus_camelinus
├─ Epicadus_rubripes
├─ Epicadus_heterogaster
├─ Epicadus_tigrinus
├─ Epicadus_pulcher
├─ Stephanopis_sp_1
├─ Stephanopis_championi
├─ Stephanopis_parahybana
├─ Stephanopis_renipalpis
├─ Stephanopis_macrostyla
├─ Stephanopis_quinquetuberculata
├─ Stephanopis_pentacantha
├─ Isala_punctata
├─ Stephanopis_similis
├─ Stephanopis_rufiventris
├─ Stephanopis_palliolata
├─ Stephanopis_longimana
├─ Stephanopis_cambridgei
├─ Stephanopis_spiralis
├─ Stephanopis_arenata
├─ Sidymella_sp_2
├─ Sidymella_angularis
├─ Sidymella_trapezia
├─ Sidymella_longipes
├─ Sidymella_bicuspidata
├─ Sidymella_sp_1
├─ Sidymella_hirsuta
├─ Sidymella_lobata
├─ Stephanopis_barbipes
├─ Coenypha_edwardsi
├─ Stephanopis_ditissima
├─ Stephanopis_nodosa
├─ Stephanopis_antennata
├─ Sidymella_furcillata
├─ Sidymella_longispina
├─ Sidymella_marmorata
├─ Sidymella_excavata
├─ Sidymella_lucida
├─ Sidymella_kolpogaster
├─ Stephanopis_squalida
├─ Stephanopis_angulata
├─ Stephanopis_fissifrons
├─ Stephanopis_lata
├─ Stephanopis_corticalis
├─ Stephanopis_bicornis
├─ Stephanopis_armata
├─ Stephanopis_monulfi
├─ Stephanopis_carcinoides
├─ Stephanopis_altifrons
├─ Stephanopis_nana
├─ Stephanopis_flagellata
└─ Stephanopis_nigra
```

Supplementary material data

Supplementary material data 1 — Data matrix.

https://drive.google.com/file/d/1K6Kpx29Z97sibW7rE9N80z1v6mFBlEgp/view?usp=sharing

Supplementary material data 2 — Parameters and search routine for implied weighting analyses.

https://drive.google.com/file/d/1nIHo9C2myj0xF8XVRNjBqLPg0yEunZxt/view?usp=sharing

Supplementary material data 3 — Command lines to calculate Branch supports (relative Bremer support and symmetric resampling).

https://drive.google.com/file/d/19r48HJbD-VCy2R9j-E-ztOH_dMePhSUX/view?usp=sharing
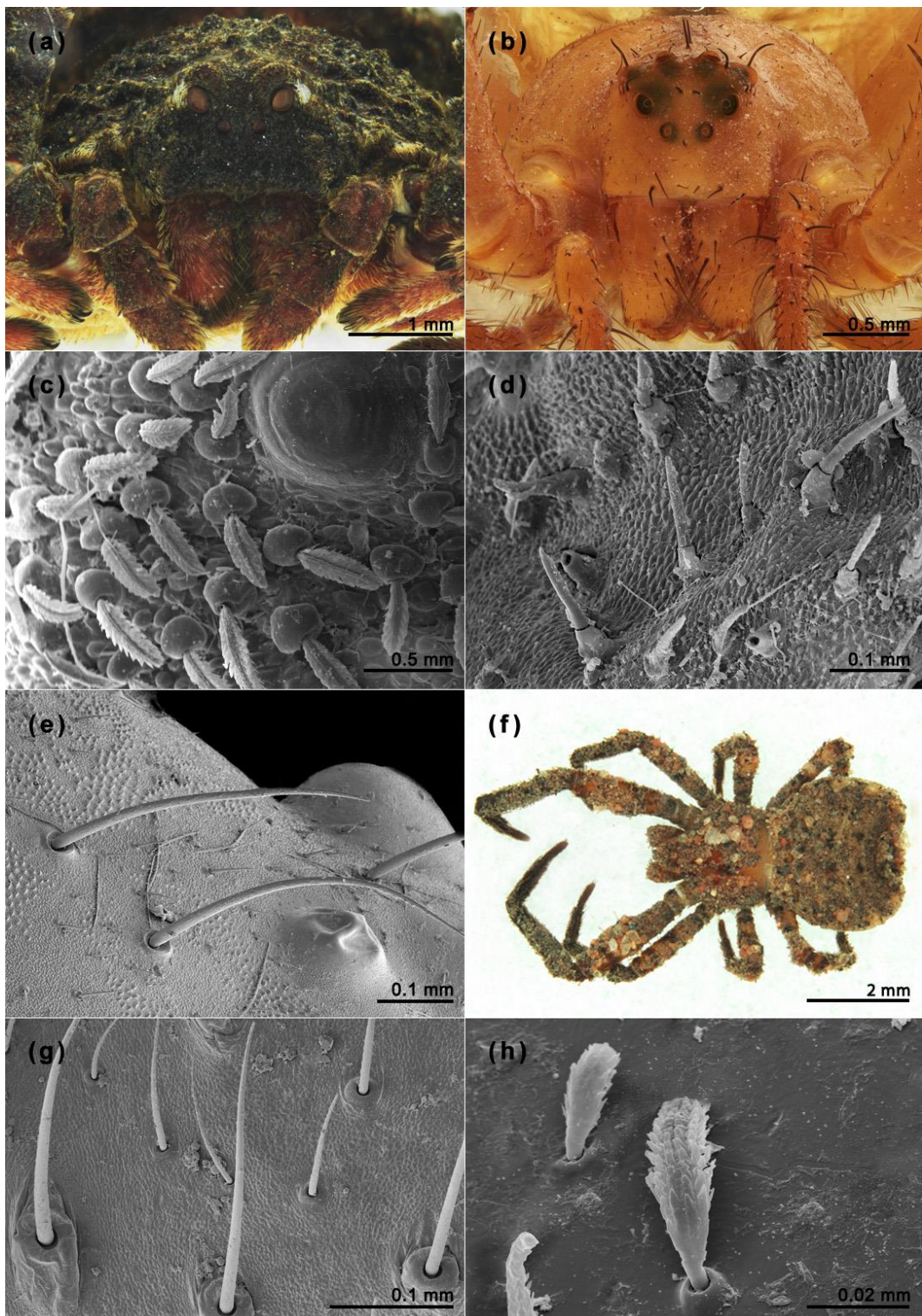
Figure S1. Characters relative to dorsal habitus and prosoma of specimens sampled in the present analysis: (a) *S. lata*, frontal view. (b) *S. excavata*, frontal view. (c) *S. pentacanha*, carapace. (d) *E. trispinosus*, carapace. (e) *T. polyandrus*, carapace. (f) *I. arenata* **comb. nov.**, dorsal habitus. (g) *E. granulatus*, sternum. (h) *B. nyerere*, sternum.
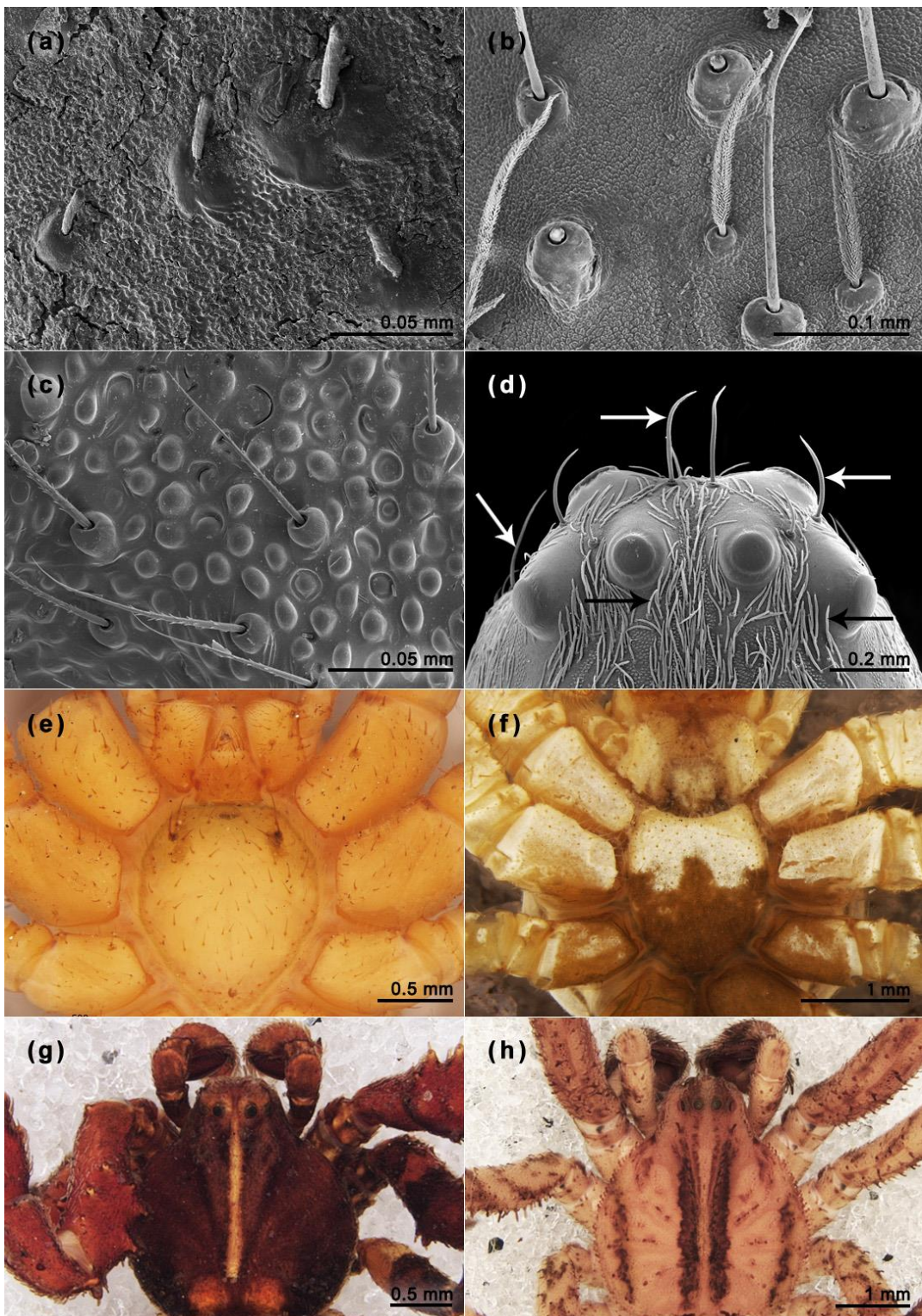
Figure S2. Characters relative to carapace and sternum of specimens sampled in the present analysis: (a) *S. bicuspidata*, sternum. (b) *E. caudatus*, sternum. (c) *O. intermedius*, sternum. (d) *G. hirta*, (white arrows indicate pointed setae; black arrows indicate filamentous setae). (e) *S. trapezia*, sternum. (f) *P. ceylonica*, sternum. (g) *S. macrostyla*, prosoma. (h) *I. cambridgei* **comb. nov.**, prosoma.
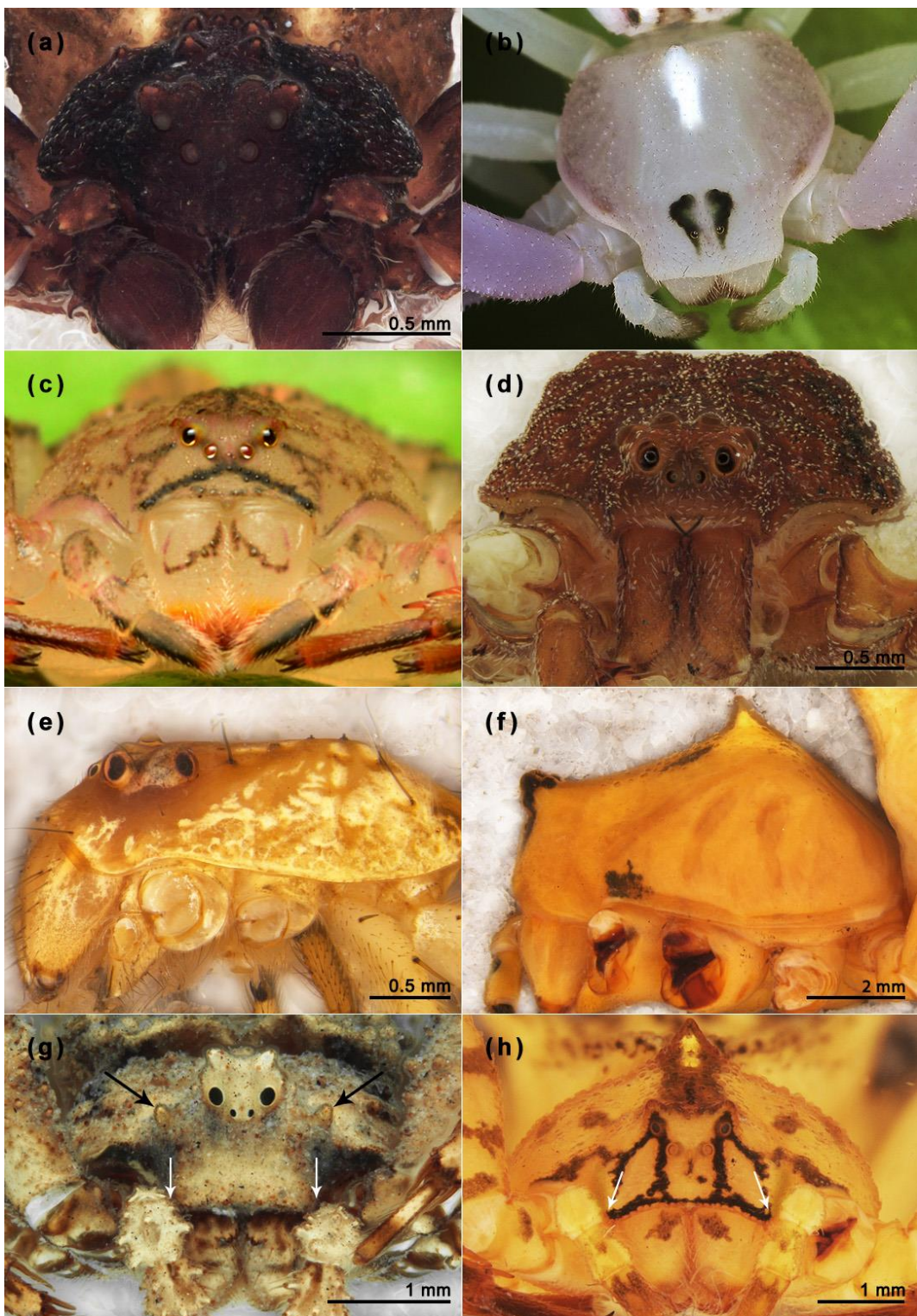
Figure S3. Characters relative to prosoma of specimens sampled in the present analysis: (a) *E. caudatus*, frontal view. (b) *E. heterogaster*, carapace. (c) *E. taczanowskii*, frontal view. (d) *S. bicuspidata*, (e) *T. elongatus*, lateral view. (f) *E. heterogaster*, lateral view. (g) *S. nana*, frontal view (black arrows indicate lateral cephalic tubercles; white arrows indicate the not projected lateral margin of the clypeus). (h) *E. rubripes*, frontal view (arrows indicate the lateral margins of the clypeus projected laterally).
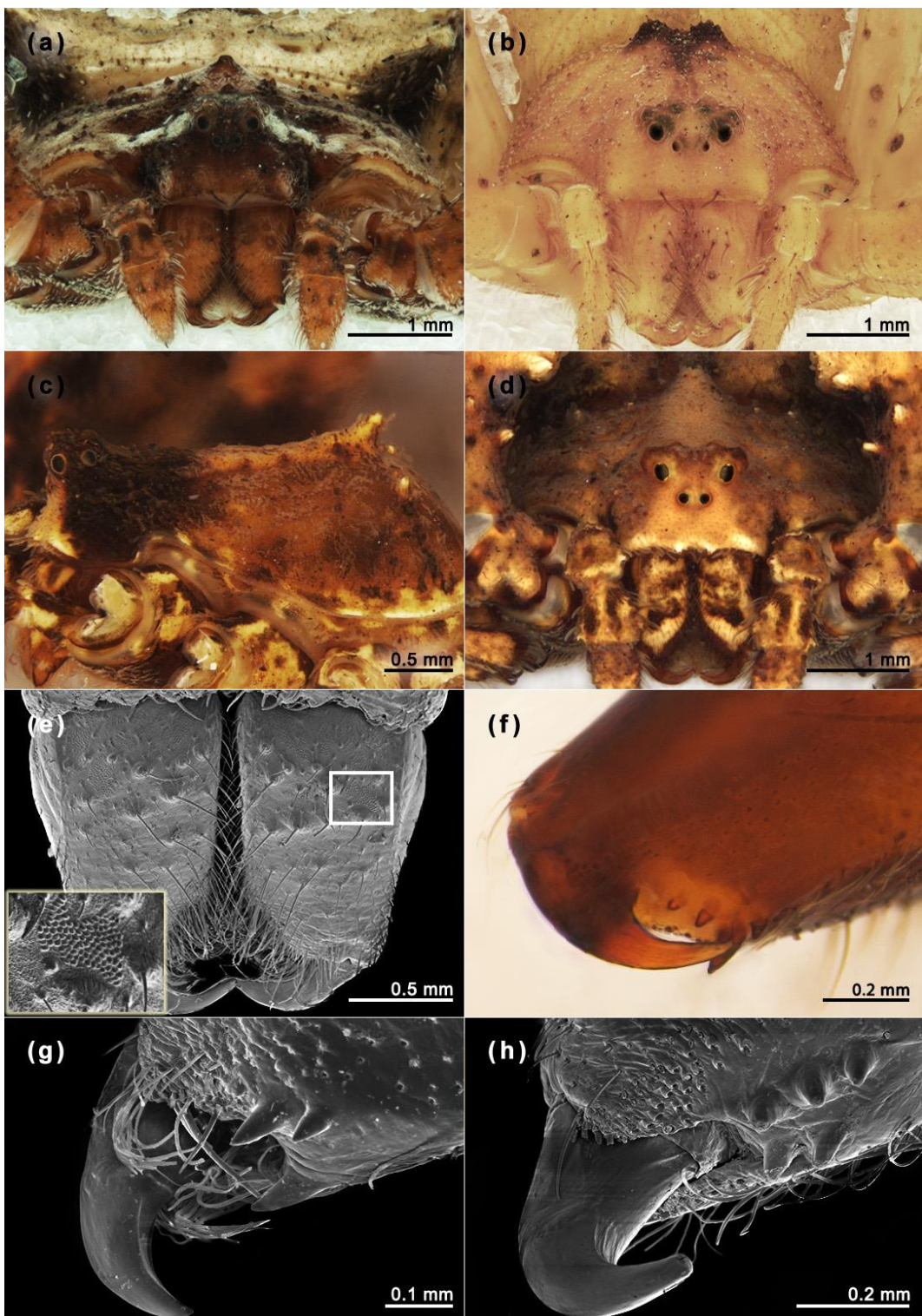
Figure S4. Characters relative to prosoma and mouth parts of specimens sampled in the present analysis: (a) *S. monulfi*, frontal view. (b) *Sidymella* sp. 2, frontal view. (c) *S. quinquetuberculata*, lateral view. (d) *S. pentacantha*, (e) *E. taczanowskii*, chelicerae (detail of papules). (f) *S. simoni*, chelicerae. (g) *P. ceylonica*, chelicerae. (h) *E. trituberculatus*, chelicerae.
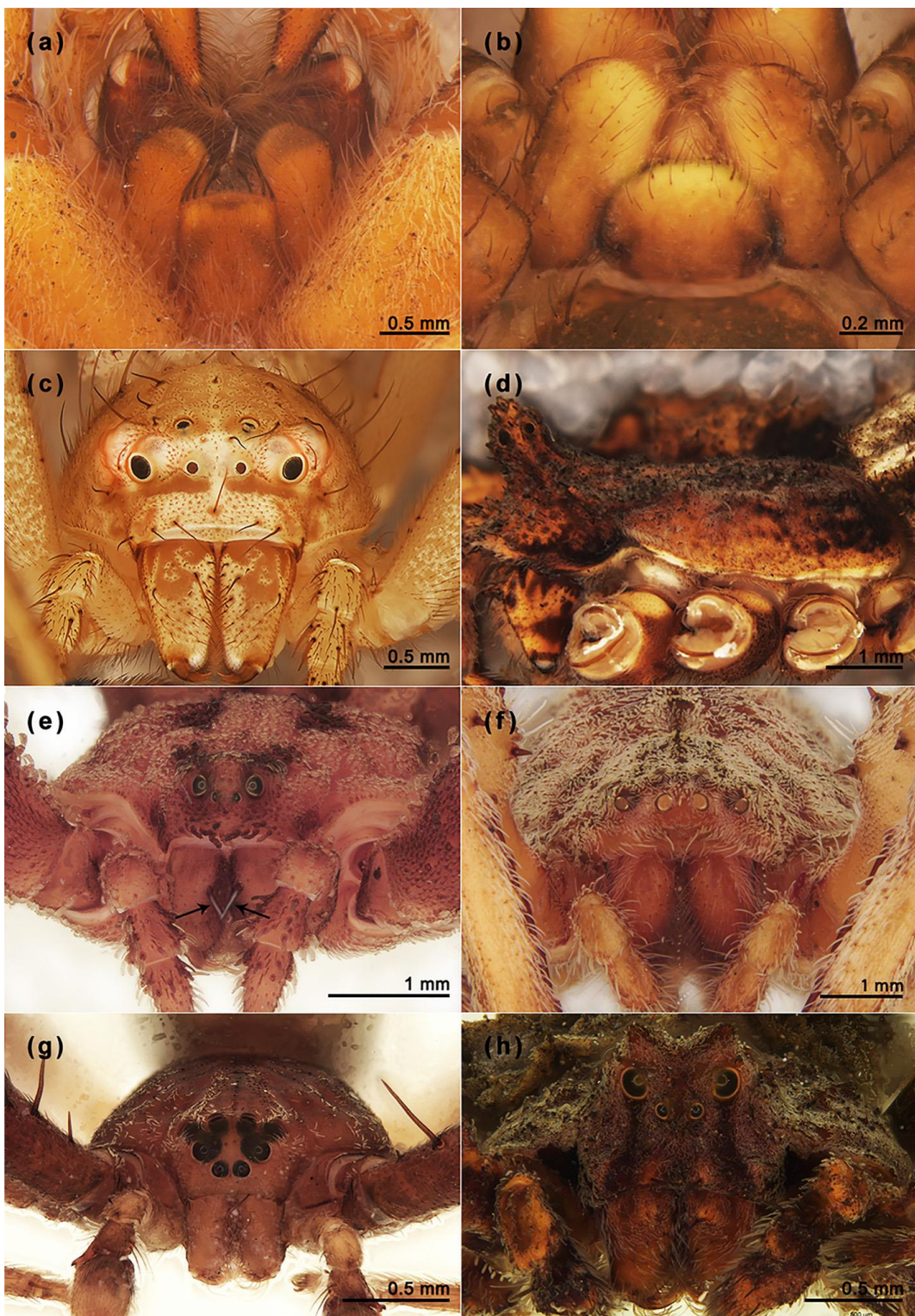
Figure S5. Characters relative to carapace and mouth parts of specimens sampled in the present analysis: (a) *B. cinerascens*, labium and endites. (b) *S. kolpogaster*, labium and endites. (c) *T. elongatus*, frontal view. (d) *S. altifrons*, lateral view. (e) *I. rufiventris* **comb. nov.**, frontal view (arrows indicate cheliceral macrosetae). (f) *B. cinerascens*, frontal view. (g) *S. barbipes*, frontal view. (h) *S. bicornis*, frontal view.

82
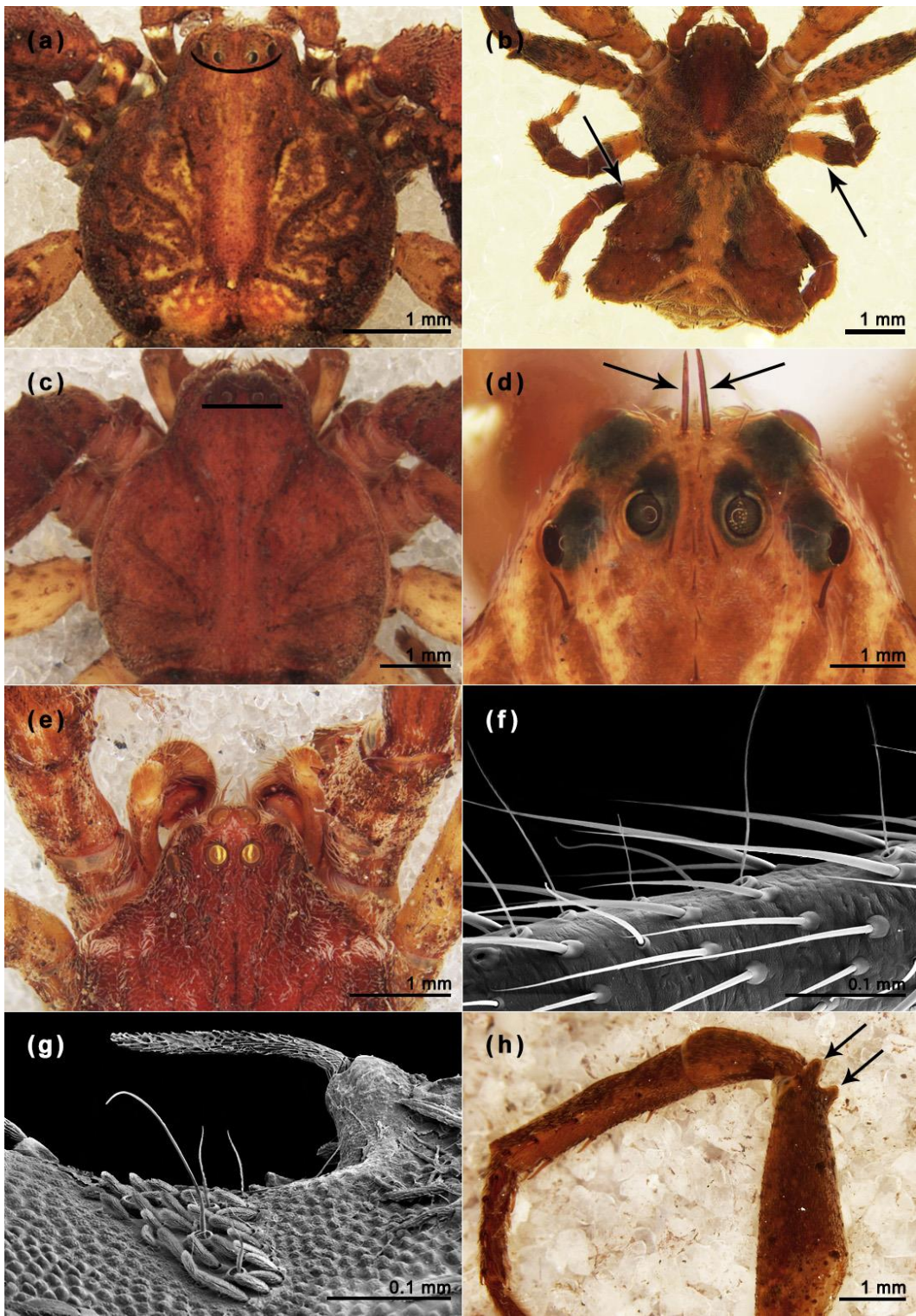
Figure S6. Characters relative to carapace and legs of specimens sampled in the present analysis: (a) *S. pentacantha*, prosoma (detail of the procurve posterior eye row). (b) *S. ditissma* (arrows indicate the marked color division on femora III and IV). (c) *S. fissifrons*, prosoma (detail of the straight posterior eye row). (d) *S. barbipes*, prosoma (arrows indicate MOQ macrosetae). (e) *B. cinerascens*, prosoma (canoe-shaped tapetum). (f) *T. elongatus*, tibiae I (trichobothria linearly distributed). (g) *S. pentacantha*, tibiae I (clustered trichobothria). (h) *C. edwardsi*, leg I (arrows indicate mesial and ectal apophysis on femur).
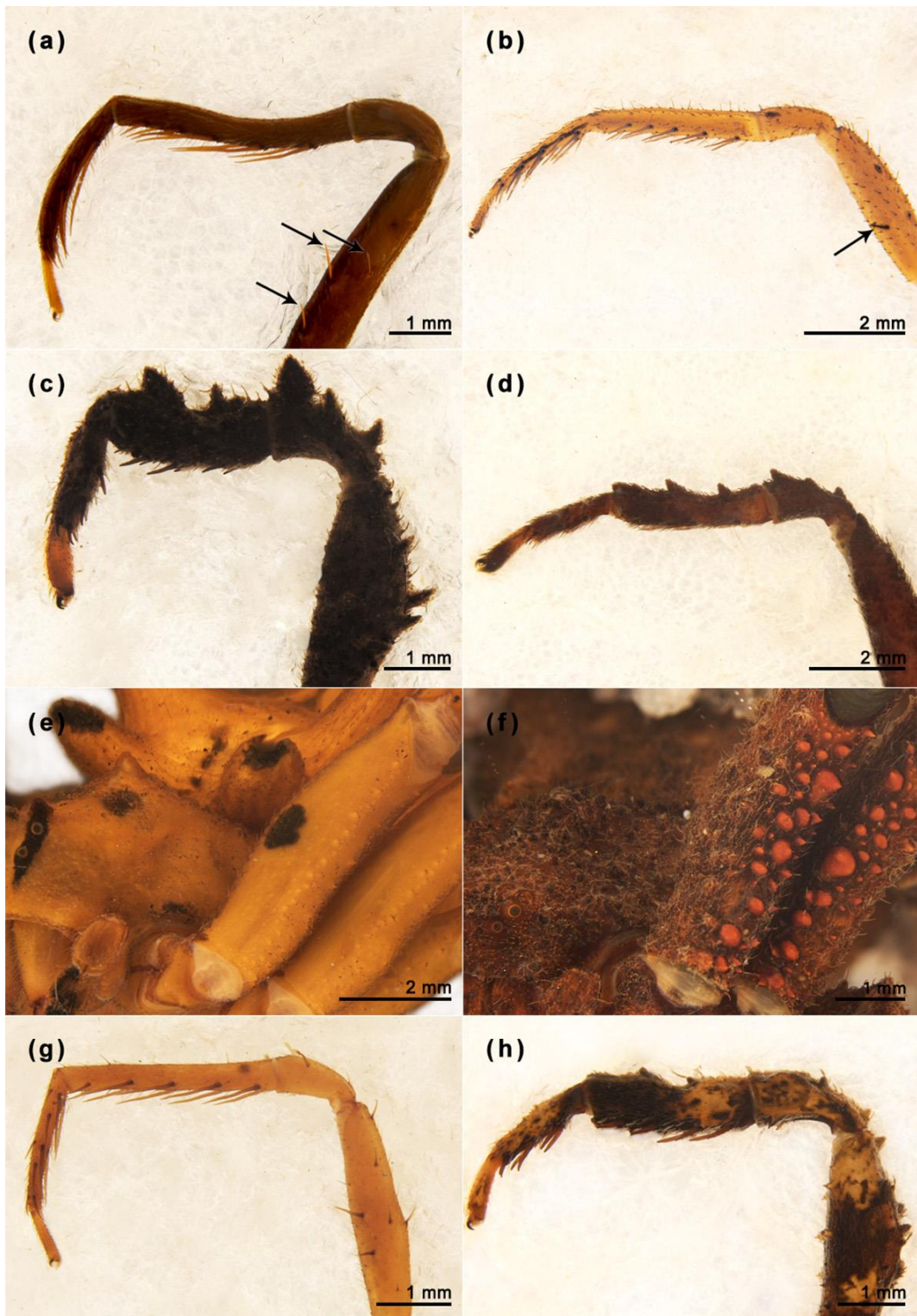
Figure S7. Characters relative to legs of specimens sampled in the present analysis: (a) *S. kolpogaster* (arrows indicate femoral setae). (b) *S. trapezia* (arrow indicates femoral setae). (c) *S. monulfi*, leg I. (d) *S. lata*, leg I. (e) *E. heterogaster*, femoral setiferous tubercles. (f) *E. caudatus*, femoral setiferous tubercles. (g) *G. hirta*, leg I. (h) *S. pentacantha*, leg I.
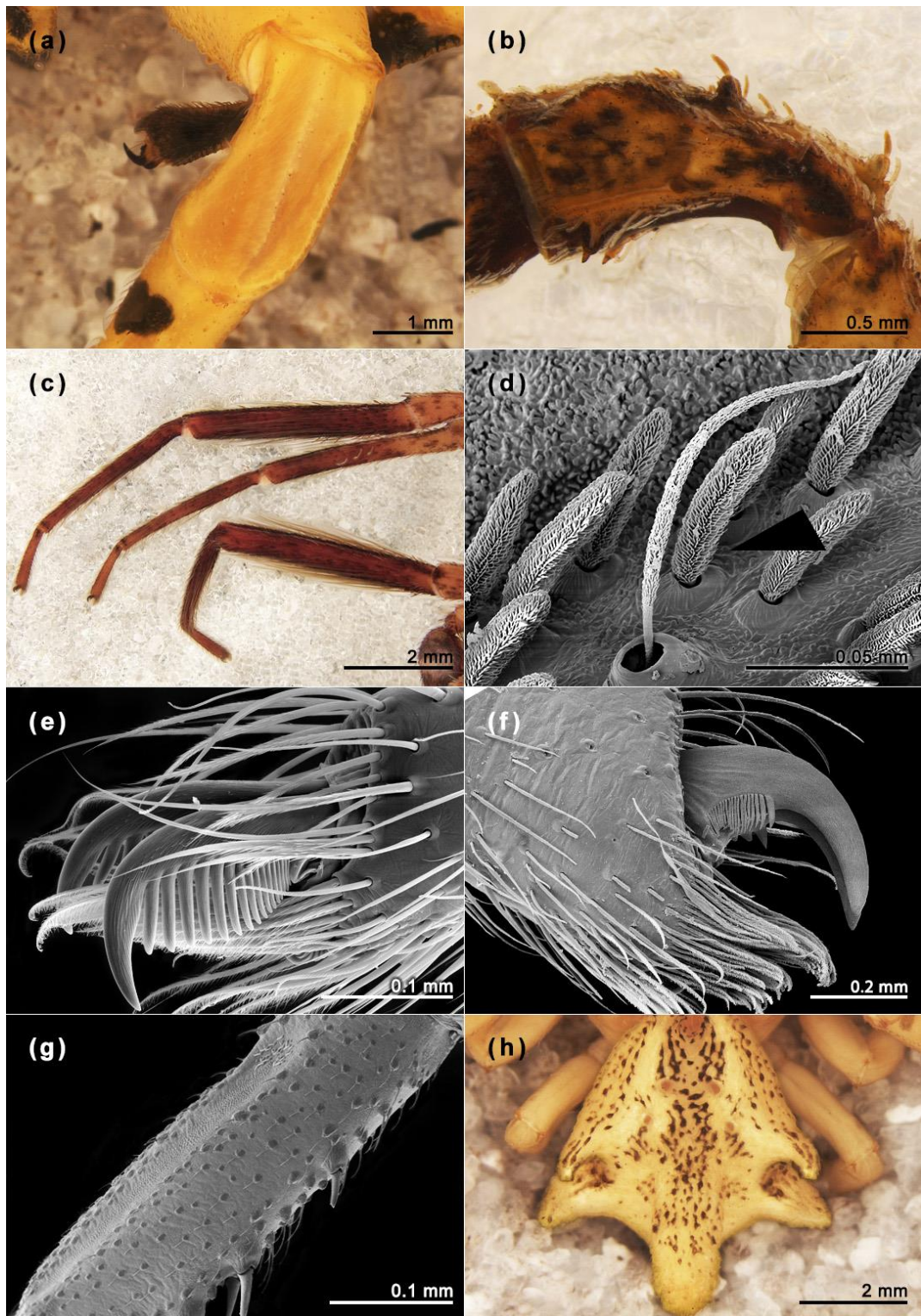
Figure S8. Characters relative to legs, claws and opisthosoma of specimens sampled in the present analysis: (a) *E. heterogaster*, patella I. (b) *S. pentacantha*, patella I. (c) *I. cambridgei* **comb. nov.**, male tibial brushes. (d) *E. caudatus*, trichobothrium and duster-shaped setae. (e) *T. elongatus*, tarsal claws of the right leg I (mesial view). (f) *E. taczanowskii*, tarsal claws of the right leg I (ectal view). (g) *E. heterogaster*, tibia I. (h) *E. trituberculatus*, opisthosoma.
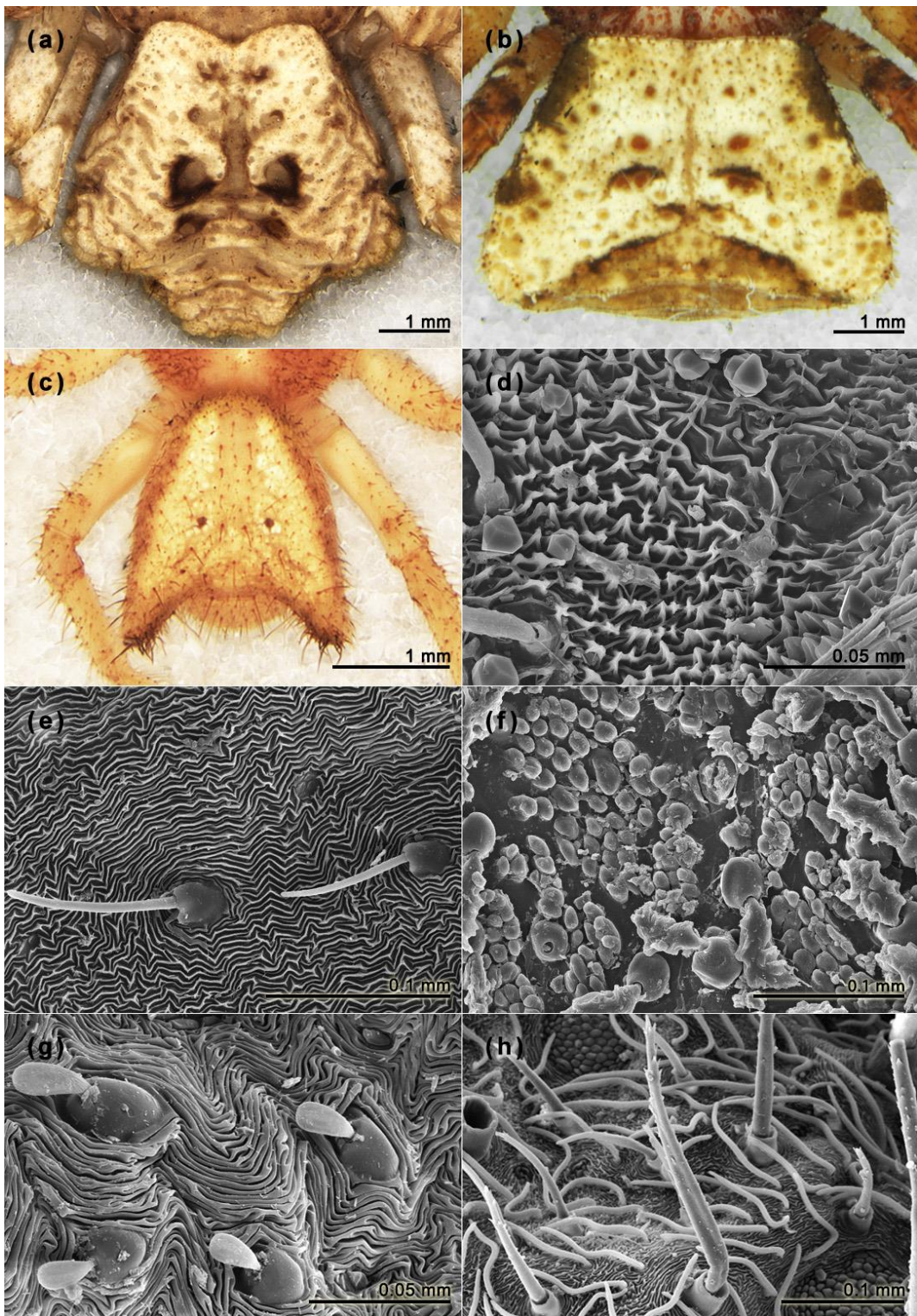
Figure S9. Characters relative to opisthosoma of specimens sampled in the present analysis: (a) *S. nana*. (b) *S. monulfi*. (c) *S. hirsuta*, (d) *S. altifrons*, cuspidate surface. (e) *T. elongatus*, mazed-surface. (f) *I. rufiventris*, granular surface. (g) *I. punctata*, fingerprint surface. (h) *S. hirsuta*, needle-shaped and filamentous setae.
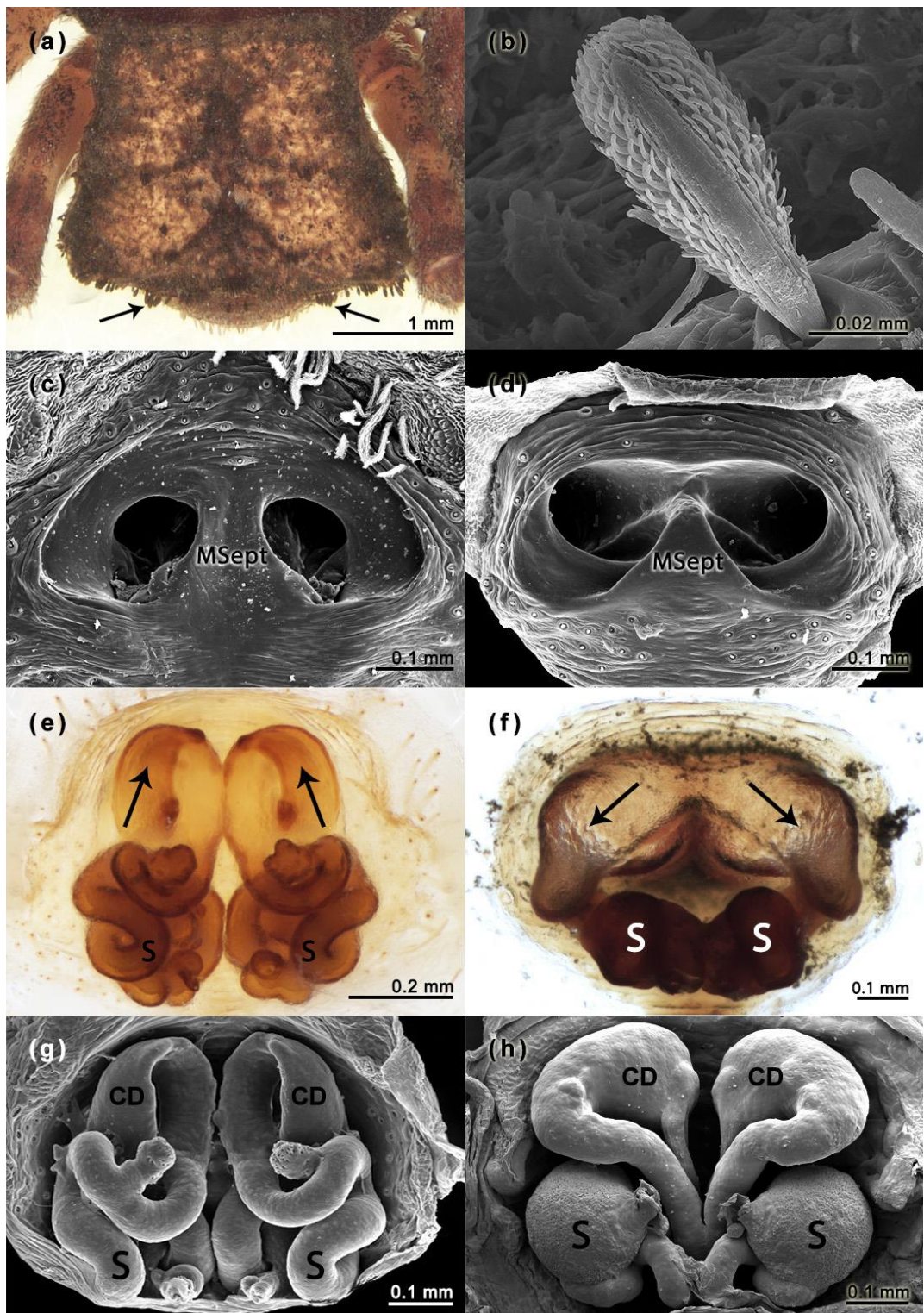
Figure S10. Characters relative to opisthosoma and female genitalia of specimens sampled in the present analysis: (a) *S. lata* (arrows indicate abdominal setae clusters). (b) *S. monulfi*, barbed setae. (c) *S. monulfi*, ventral view of the epigynal plate. (d) *S. antennata*, ventral view of the epigynal plate. (e) *S. hirsuta*, dorsal view of the epigynal plate (arrows indicate the direction of entry into the copulatory ducts). (f) *S. antennata*, dorsal view of the epigynal plate (arrows indicate the direction of entry into the copulatory ducts). (g) *Sidymella* sp.1, dorsal view of the epigynal plate. (h) *E. trituberculatus*, dorsal view of the epigynal plate.

87
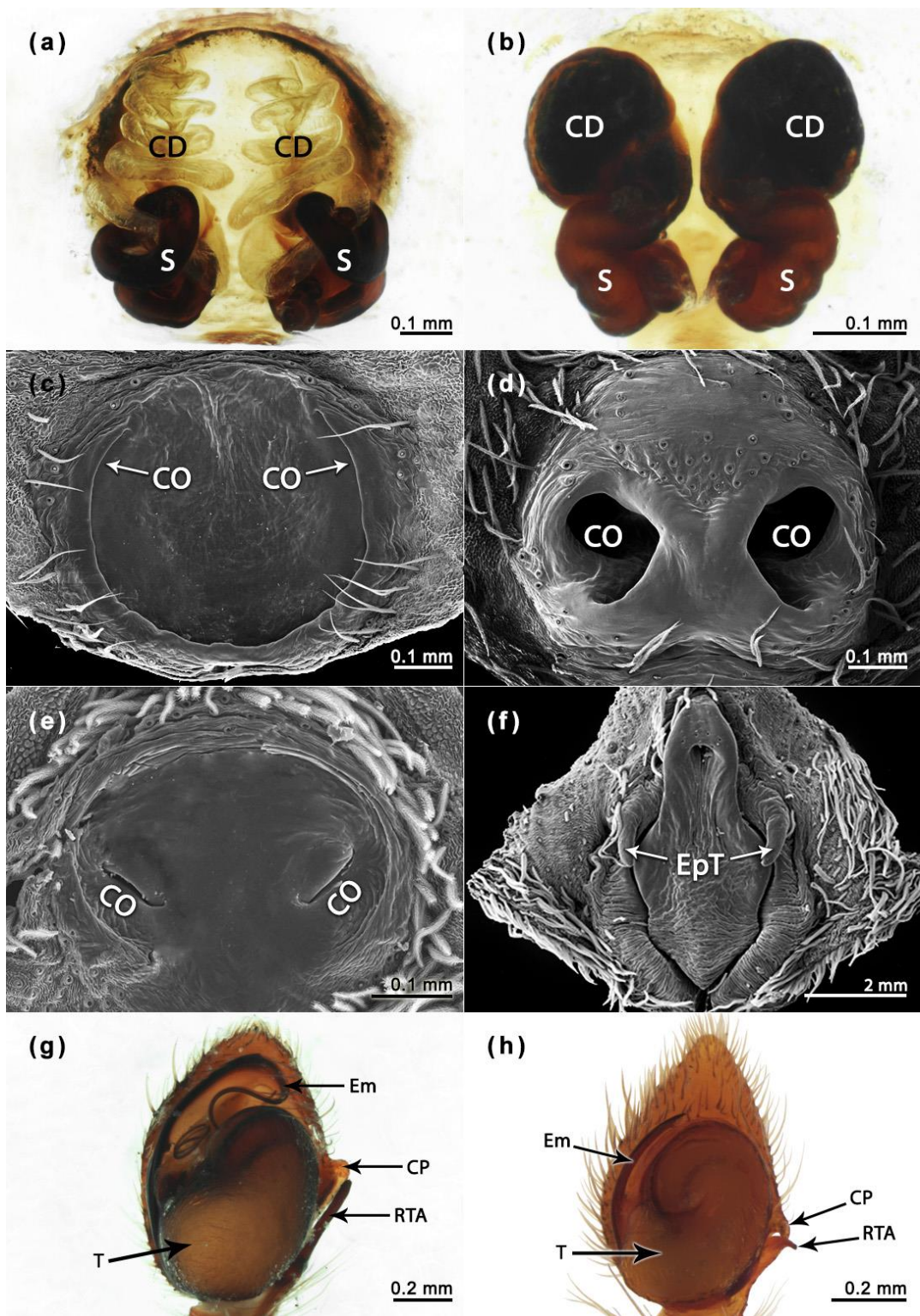
Figure S11. Characters relative to the female and male genitalia of specimens sampled in the present analysis: (a) *I. spiralis* **comb. nov.**, dorsal view of the epigynal plate. (b) *S. armata*, dorsal view of the epigynal plate. (c) *P. championi* **sp. rev.**, ventral view of the epigynal plate. (d) *S. nodosa*, ventral view of the epigynal plate. (e) *S. lata*, ventral view of the epigynal plate. (f) *B. cinerascens*, ventral view of the epigynal plate (arrows indicate the epigynal teeth). (g) *S. flagellata*, left palp. (h) *S. bicuspidata*, left palp.
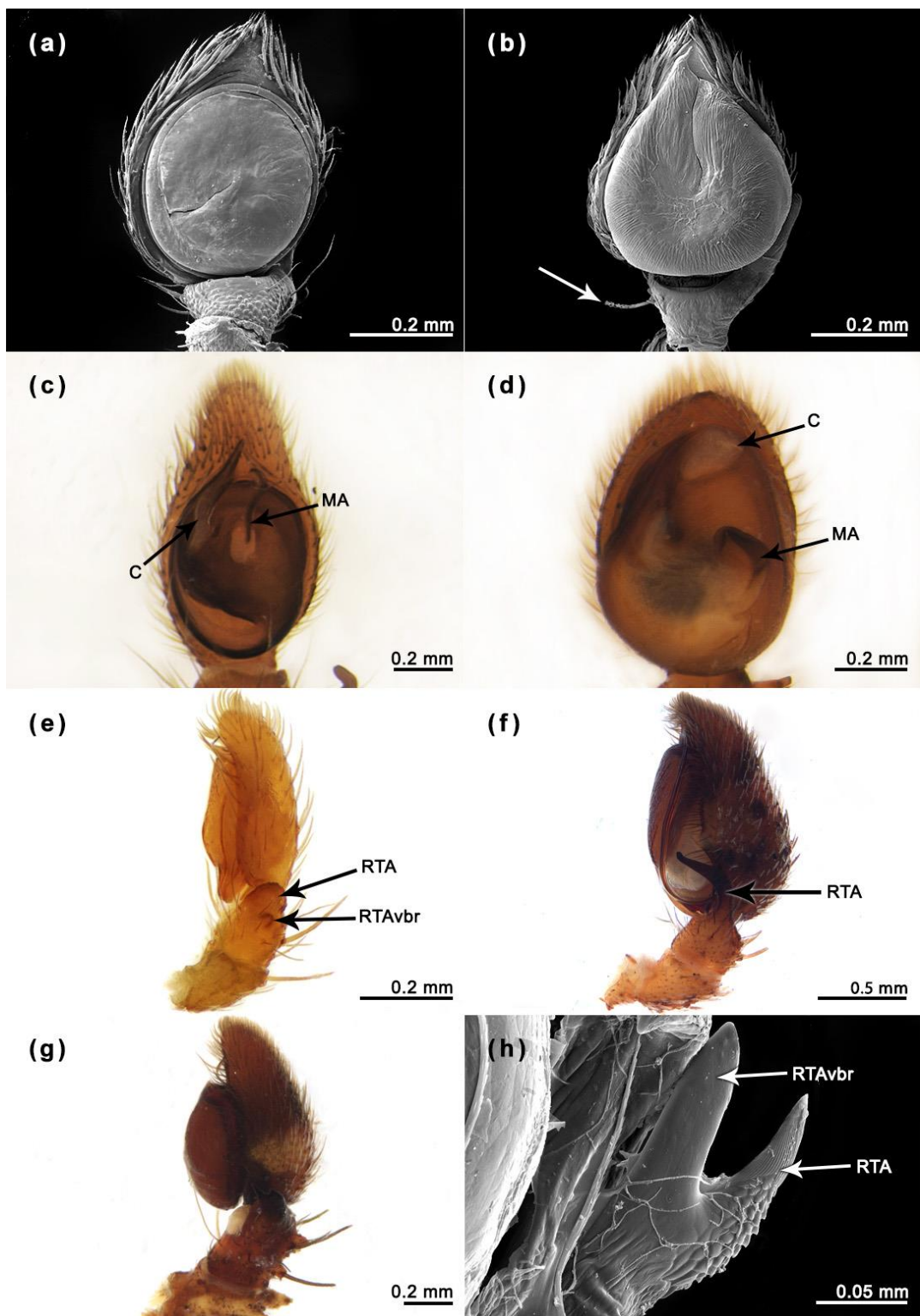
Figure S12. Characters relative to the male genitalia of specimens sampled in the present analysis: (a) *E. trituberculatus*, left palp. (b) *S. pentacantha*, left palp (arrow indicates the prolateral macrosetae). (c) *G. hirta*, left palp. (d) *S. lucida*, retrolateral view of left palp. (e) *B. nyerere*, left palp. (f) *I. cambridgei*, retrolateral view of left palp. (g) *S. nigra*, retrolateral view of left palp. (h) *S. altifrons*, detail of the RTA.
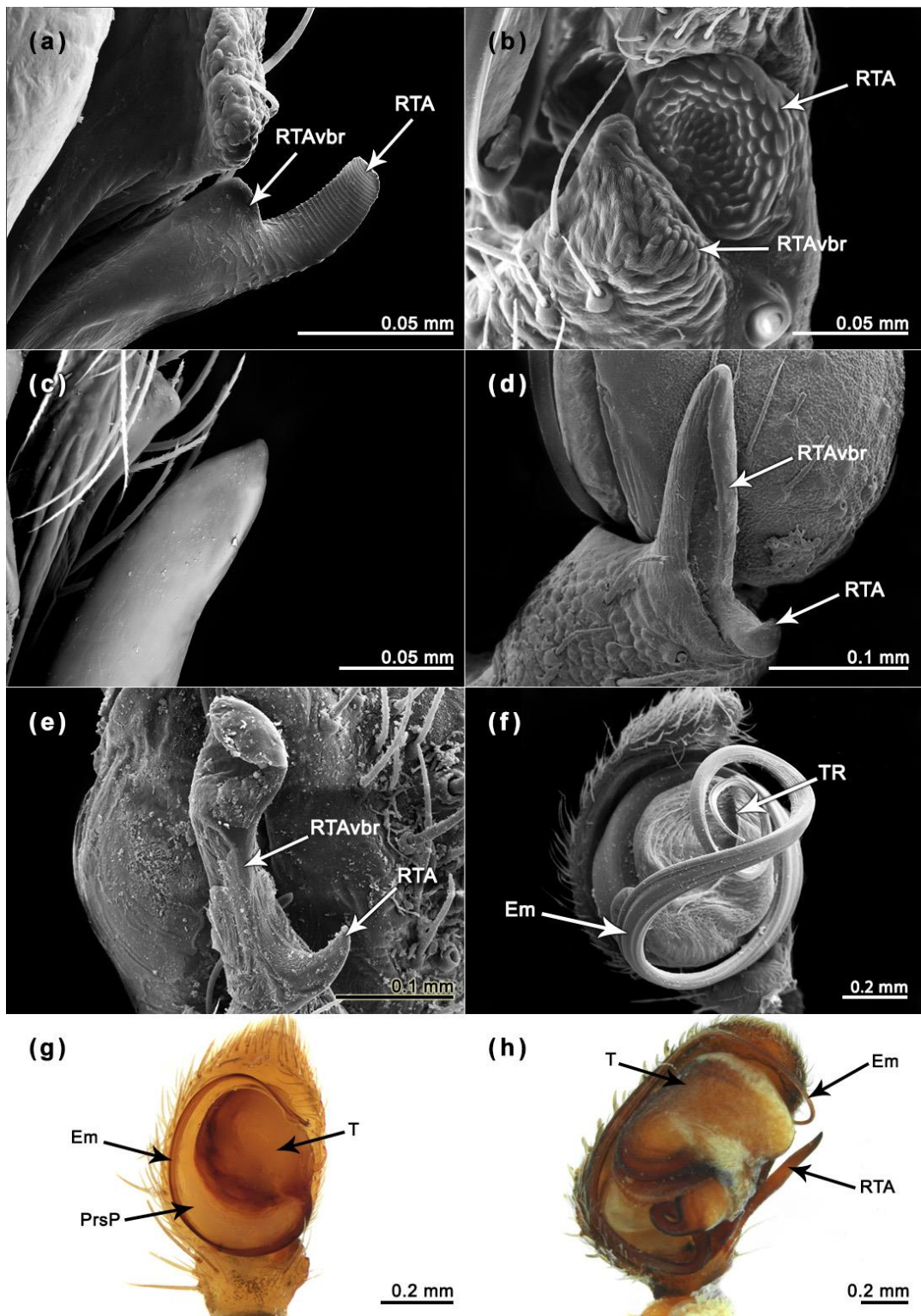
Figure S13. Characters relative to the male genitalia of specimens sampled in the present analysis: (a) *S. fissifrons*, grooved RTA. (b) *S. lucida*, nodose RTA. (c) *I. palliolata* **comb. nov.**, smooth RTA. (d) *E. taczanowskii*, canoe-shaped RTAbvr. (e) *S. hirsuta*, spoon-shaped RTAvbr. (f) *S. ditissima* **comb. nov.**, left palp. (g) *S. furcillata*, left palp. (h) *I. spiralis* **comb. nov.**, left palp.
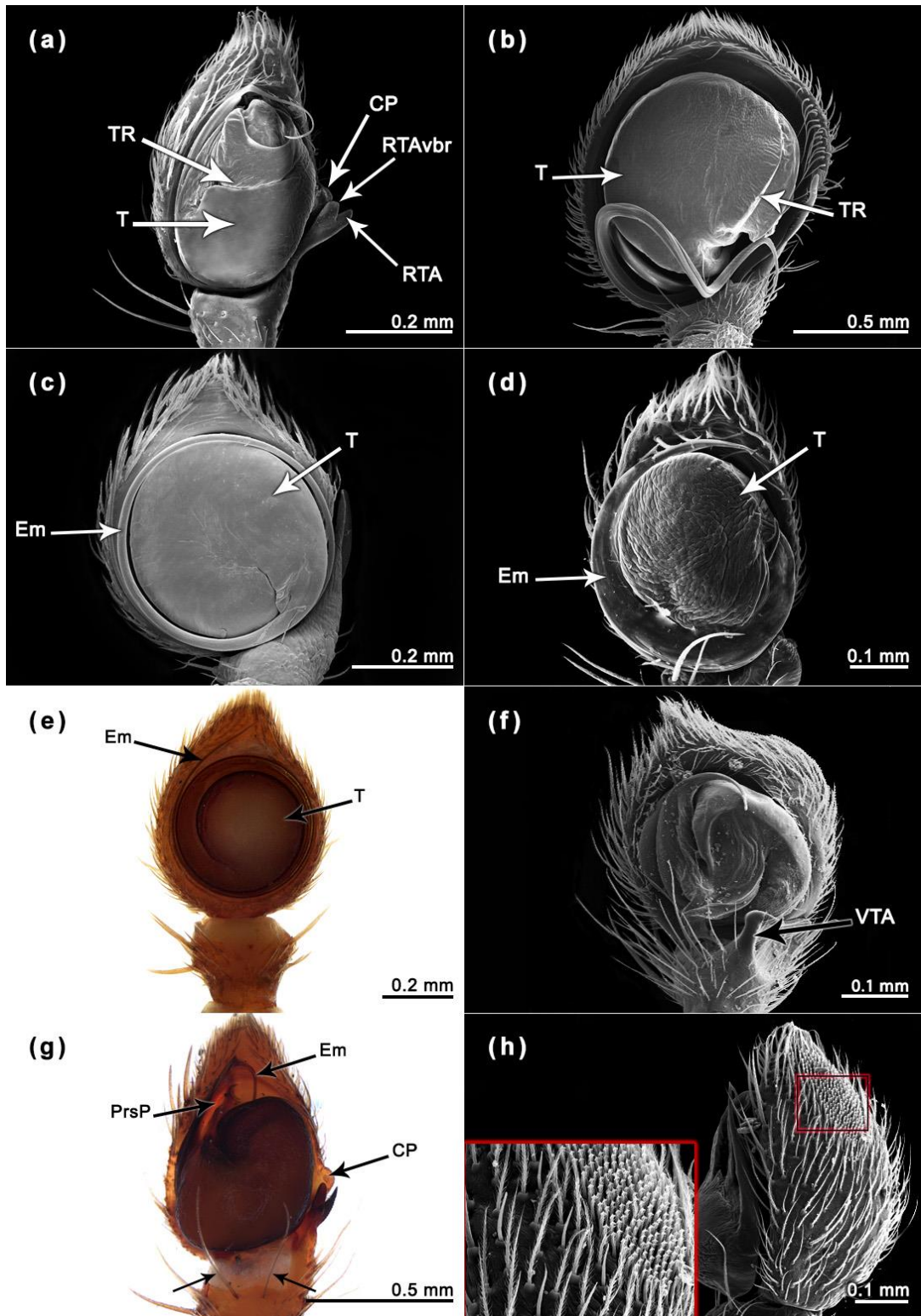
Figure S14. Characters relative to the male genitalia of specimens sampled in the present analysis: (a) *S. barbipes*, left palp. (b) *I. cambridgei*, left palp. (c) *O. intermedius*, left palp. (d) *S. longispina*, left palp. (e) *Paratobias* sp. 1, left palp. (f) *T. polyandrus*, left palp. (g) *S. altifrons*, left palp (lower arrows indicate the pair of ventral filamentous setae on tibiae). (h) *S. bicornis*, retrolateral view of left palp (detail of the cymbial setae brush).

Chapter 2: On bark-dweller crabs spiders: description of a new genus of Stephanopinae in the Neotropics (Araneae, Thomisidae)

On bark-dweller crabs spiders: description of a new genus of Stephanopinae in the Neotropics (Araneae, Thomisidae)

Miguel MACHADO [1,*], Rafaela VIECELLI [1], Catherine GUZATI [1], Cristian J. GRISMADO [2] & Renato A. TEIXEIRA [1]

[1] Laboratório de Aracnologia, Escola de Ciências, Pontifícia Universidade Católica do Rio Grande do Sul (PUCRS), Porto Alegre, Rio Grande do Sul, Brazil.

[2] División Aracnología, Museo Argentino de Ciencias Naturales "Bernardino Rivadavia", Buenos Aires, Argentina.

*Corresponding author: machadom.arachno@gmail.com

Abstract. Recent phylogenetic analysis have shown that the genus *Stephanopis* was comprised by several different lineages of bark-dweller crab spiders. The ones with South American distribution were recovered in a single clade by two synapomorphies (patellar macrosetae and pear-shaped tegulum), with high branch support and nodal stability. Although presenting remarkable morphological synapomorphies, this group had poorly resolved internal topology due to the conservative somatic features of its component species. Aiming to erect the status of the group to a generic level and clarify the distinctions between its component taxa, here we propose *Kryptochroma* **gen. nov.** to accommodate the species *K. renipalpis* **comb. nov.**, *K. parahybana* **comb. nov.** *K. pentacantha* **comb. nov.** *K. quinquetuberculata* **comb. nov.** *K. macrostyla* **comb. nov.** Four new species are described: *K. gigas* **sp. nov.**, *K. hilaris* **sp. nov.**, *K. quadrata* **sp. nov.** and *K. septata* **sp. nov.** Additional taxonomic acts are made, including synonymies, *species inquirenda* and *nomen dubium*, and new distribution records are provided.

Keywords. Taxonomy, Neotropical, new species, new records, *Stephanopis*.

Introduction

The morphological aspects and taxonomic boundaries of Neotropical stephanopines have been extensively studied during the past years (Machado *et al.* 2015; Silva-Moreira & Machado 2016; Machado *et al.* 2018; Machado *et al.* 2019a). Meanwhile, phylogenies based on morphological and molecular data were congruent in recovering some close related genera, corroborating classic propositions for the possible existence of tribes or even certain "groups" in this subfamily (Wheeler *et al.* 2017; Machado *et al.* 2017; Machado *et al.* 2019b).

In the taxonomic review of *Epicadus* Simon, 1895, Silva-Moreira & Machado (2016) highlighted that the morphological resemblances between this genus with *Epicadinus* Simon, 1895, *Onocolus* Simon, 1895 and *Rejanellus* Lise, 2005 could be a strong indication for a common ancestry of what the authors called '*Epicadus* group', despite the absence of a phylogenetic approach to test such hypothesis. One year later, Machado *et al.* (2017) stated that at least two features related to the male genitalia of species of the genera mentioned above could be interpreted as synapomorphies to recover the '*Epicadus* group', however, the placement of *Rejanellus* remained uncertain. Recently, the more inclusive approach on Australian stephanopines allowed Machado & Teixeira (Chapter 1) to widely score genital features of several representatives of this subfamily, helping not only to elucidate the relationships in *Stephanopis* O. Pickard-Cambridge, 1869 but also compile more evidences and improve the basis that point to the existence of the '*Epicadus* group', originally proposed by Silva-Moreira & Machado (2016).

Machado & Teixeira (Chapter 1) recovered a stable and well-supported clade gathering Neotropical species of *Stephanopis* that presents two synapomorphic characters (presence of ventral macrosetae on patellae I and II and male genitalia having a pear-shaped tegulum), calling it "*pentacantha* clade". The emergence of this clade as sister to *Rejanellus*, its remarkable morphology and coincident geographical distribution with the remaining genera of the '*Epicadus* group', were interpreted by Machado & Teixeira (Chapter 1) as clear evidences to justify the description of the clade as a new genus. The conservative morphology of the representatives of the "*pentacantha* clade" though, contributed to its poorly resolved internal topology. According to Machado & Teixeira (Chapter 1), species belonging to the "*pentacantha* clade" can only be distinguished from each other by details on their genitalia, as the curvature, size and shape of the RTA and embolus, or presence/absence of the median

septum on the epignal plate. Thus, hereinafter we propose the genus *Kryptochroma* **gen. nov.** to accommodate Stephanopis species hitherto attributed to the "*pentacantha* clade" (*sensu* Machado & Teixeira, Chapter 1). New distribution records are presented descriptions are updated, four new species are described and diagnostic features are represented in detail.

Material and methods

Repositories

The specimens examined are deposited in the following institutions (acronyms and curators in parentheses): Museu de Ciências e Tecnologia da Pontifícia Universidade Católica do Rio Grande do Sul, Porto Alegre, Brazil (MCTP, Renato A. Teixeira), Museum of the Zoological Institute of the Polish Academy of Sciences (MZPW, Jerzy Prószyński), Museu de Ciências Naturais da Fundação Zoo-Botânica do Rio Grande do Sul, Brazil (MCN, Ricardo Ott), Museu de Zoologia da Universidade de São Paulo, Brazil (MZSP, Ricardo Pinto-da-Rocha), Museu Nacional do Rio de Janeiro, Brazil (MNRJ, Adriano B. Kury), Museum of Comparative Zoology of Harvard, Cambridge, United States (MCZ, Gonzalo Giribet and Laura Liebensperger), Instituto Nacional de Pesquisas da Amazônia, Manaus, Brazil (INPA, L. R. França), The Field Museum, Chicago, United States (FMNH, Petra Sierwald), Museu Paraense Emílio Goeldi, Belém, Brazil (MPEG, Alexandre B. Bonaldo), Instituto Butantan, São Paulo, Brazil (IBSP, Antonio D. Brescovit), Museo Argentino de Ciencias Naturales "Bernardino Rivadavia", Buenos Aires, Argentina (MACN-Ar, Martín J. Ramírez), Museo de La Plata, La Plata, Argentina (MLP, Cristina Damborenea and Luis A. Pereira), Museum National d'Histoire Naturelle, Paris, France (MNHN, Christine Rollard), Museum für Naturkunde der Humboldt-Universität, Berlin, Germany (ZMHB, Jason Dunlop), Oxford University Museum of Natural History, Oxford, United Kingdom (OUMNH, Zoë M. Simmons), Staatliches Museum für Naturkunde Karlsruhe (SMNK, Hubert Höfer) and Universidade Federal de Minas Gerais, Belo Horizonte, Brazil (UFMG, Adalberto J. Santos).

Laboratory procedures and abbreviations

All measurements provided were taken in millimeters and the terminology used to name both somatic and copulatory structures follows Machado *et al.* (2018). The dissection procedure applied to study the female genitalia consisted in detach the epigynal plate from the spider body and submerge it in proteolytic enzyme (pancreatine solution). In order to accelerate the process of digestion of the soft tissues, the solution was putted in double boiler for a few minutes. Males had their left palpus removed and represented in ventral and retrolateral views. Photographs of the habitus, front and both male and female genitalia were taken on a Multipurpose Zoom Microscope Leica M205A with a digital camera. Scanning electron microscopy sessions were conducted at the Centro de Microscopia e Microanálises (CEMM) of the Pontifícia Universidade Católica do Rio Grande do Sul (PUCRS), using a microscope Philips XL 30.

The anatomical abbreviations used in this study are the following: AH, anterior hood; ALE, anterior lateral eyes; MOQ, median ocular quadrangle; AME, anterior median eyes; CD, copulatory duct; CO copulatory opening; FD, fertilization ducts; MS, median spire; PLE, posterior lateral eyes; PME, posterior median eyes; RTA, retrolateral tibial apophysis.

Results

Order Araneae Clerck, 1757

Family Thomisidae Sundevall, 1833

Stephanopinae O. Pickard-Cambridge, 1871

Kryptochroma Machado, 2020

Type species — *Kryptochroma pentacantha* (Mello-Leitão, 1929)

Diagnosis

The species of *Kryptochroma* **gen. nov.** resemble some of those of *Epicadus* (e.g., *E. caudatus* and *E. pustulosus*) due to their cryptic bark-dwelling habitus with predominant brown or reddish-brown body coloration and those of *Epicadinus*, particularly by their relative body size and opisthosomal projections. However, they can be easily recognized and distinguished from *Epicadus*, *Epicadinus* and others genera of Stephanopinae by the presence of a pair of ventral macrosetae on their anterior patellae (I and II) (Fig. 1D), sensorial pits (three to five trichobothria

surrounded by a small group of duster-shaped setae) on dorsal tibial depressions that are preceded by a strong plumose macrosetae and a pair of circular taints on the posterior slope of the prosoma (Fig. 1C). Differently from *Epicadinus*, *Kryptochroma* **gen. nov.** species have five opisthosomal projections (Figs 1E, 1F) instead of three and short leaf-shaped setae covering their entire body (Figs 1A, 1B) instead of long needle-shaped ones. Females present a flat epigynal plate (Figs 10C, 10E), short copulatory ducts and a single pair of oval spermathecae (Figs 10D, 10F). The male palp bears a pear-shaped tegulum with a short and fixed embolus (Figs 11C, 11E) and a single-tipped, stout and conical RTA (Figs 11D, 11F).

Description

Prosoma with granular surfaced due to the presence of spherical setae sockets (Fig. 1A,B); slightly longer than wide, peer-shaped and usually with organic particles associated. ALE almost two times bigger than AME, prosoma coloration presents a gradient of brown and dark-yellow shades (predominantly reddish brown in *Kryptochroma hilaris* **sp. nov.**), in some cases with a yellow longitudinal line between the MS and PME (Figs 3C, 5A, 7A, 9A). Anterior eye row very recurved, AME close to each other, and posterior eye row procurved (Fig. 11A, B). Clypeus with a central pair of serrated macrosetae (Fig. 1A). Sternum scutiform, slightly longer than wide in females and as long as wide in males, with brush-shaped setae. Anterior femora enlarged and bearing many conical setiferous tubercles; presence of a MS on carapace, and five opisthosomal projections (two smaller lateral pairs and one single and larger terminal projection). Mouthparts: chelicerae with five equal-sized teeth; three on the promarginal row and two on the retromarginal. Labium truncated, slightly wider than long. Endites truncated, longer than wide, with scarce promarginal scopula. Legs: legs I and II stouter and longer than legs III and IV, femora I and II present dorsal and dorsolateral stout macrosetae in conical sockets (tubercles) (Fig. 1E, F). Tibiae I and II with five pairs of ventral macrosetae while metatarsi I and II present three ventral and one distal pair (Figs 2D, 3A). Tarsal claws curved, pectinated, unequals in number of teeth; subungueal tufts scarce, with brush-shaped setae (Fig. 3B). Opisthosoma: present five short conical projections (one upper lateral pair, one lower lateral and a single median posterior termination), straight or slightly concave anterior border and rough surfaced, covered with leaf-shaped setae (Fig. 3C, D, E, F). Anal region projected back, elongated. Palpus: cymbium and tegulum pear-shaped, without

apophysis; RTA single tipped, conical (except in *Kryptochroma quadrata* **sp. nov.**) and presenting grooves at the apex (Figs 6D, 7D, 9D, 12D, 14D, 15D, 16D, 18D). The internal morphology of female genitalia is very conservative, presenting a single pair of kidney-shaped spermathecae without any accessory glands or coiled ducts (Figs 4D, 5D, 8D, 11D, 13D, 17D); in ventral view the copulatory openings are downgraded in relation to the rest of the epigynal plate, usually separated by a discrete septum, preceded by an "hood-like elevation" and located close to the edges of the posterior folds of the epigynal plate (Figs 5C, E, 11C, E).

Etymology

The name of the genus is a combination between the Greek words "Kryptos" and "Chroma", which mean "hidden" and "colour", respectively. The feminine name is a reference to the general colour pattern the spiders present, which is attributed to their cryptic behaviour.

Composition

Nine species distributed within the Neotropical Region: *Kryptochroma gigas* **sp. nov.**, *Kryptochroma hilaris* **sp. nov.**, *Kryptochroma septata* **sp. nov.**, *Kryptochroma quadrata* **sp. nov.**, *Kryptochroma quinquetuberculata* (Taczanowski, 1872) **comb. nov.**, *Kryptochroma macrostyla* (Mello-Leitão, 1929) **comb. nov.**, *Kryptochroma parahybana* (Mello-Leitão, 1929) **comb. nov.**, *Kryptochroma pentacantha* (Mello-Leitão, 1929) **comb. nov.** and *Kryptochroma renipalpis* (Mello-Leitão, 1929) **comb. nov.**

Distribution

Brazil (Amazonas, Bahia, Espírito Santo, Minas Gerais, Pará, Paraíba, Paraná, Pernambuco, Roraima, Rio de Janeiro, Rio Grande do Sul, Santa Catarina and São Paulo) and French Guiana (Cayenne, Maripasoula, Saint-Élie and Saül) (Figs 9, 18).
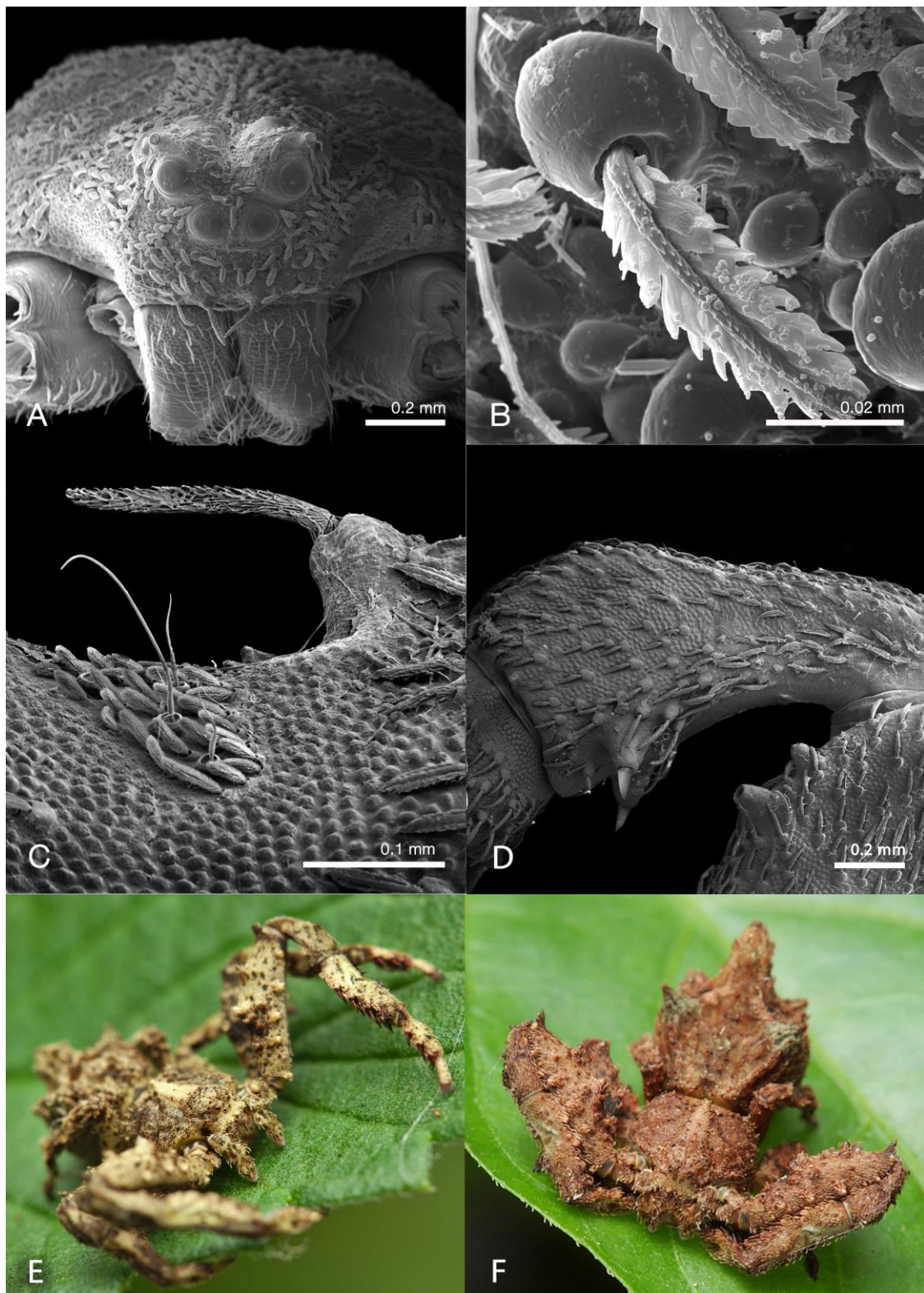
Fig. 1. Scanning electron microscopy of a male of *Kryptochroma pentacantha* (Mello-Leitão, 1929) (MCTP 7362): **(A)** frontal view of prosoma; **(B)** detail of a leaf-shaped setae and its spherical socket; **(C)** sensorial pit preceeded by a plumose macrosetae on tibia I; **(D)** pair of ventral macrosetae on patella I; **(E)** and **(F)** Register *in vivo* of females of *Kryptochroma* sp. (Photo credits: Thiago Carvalho).
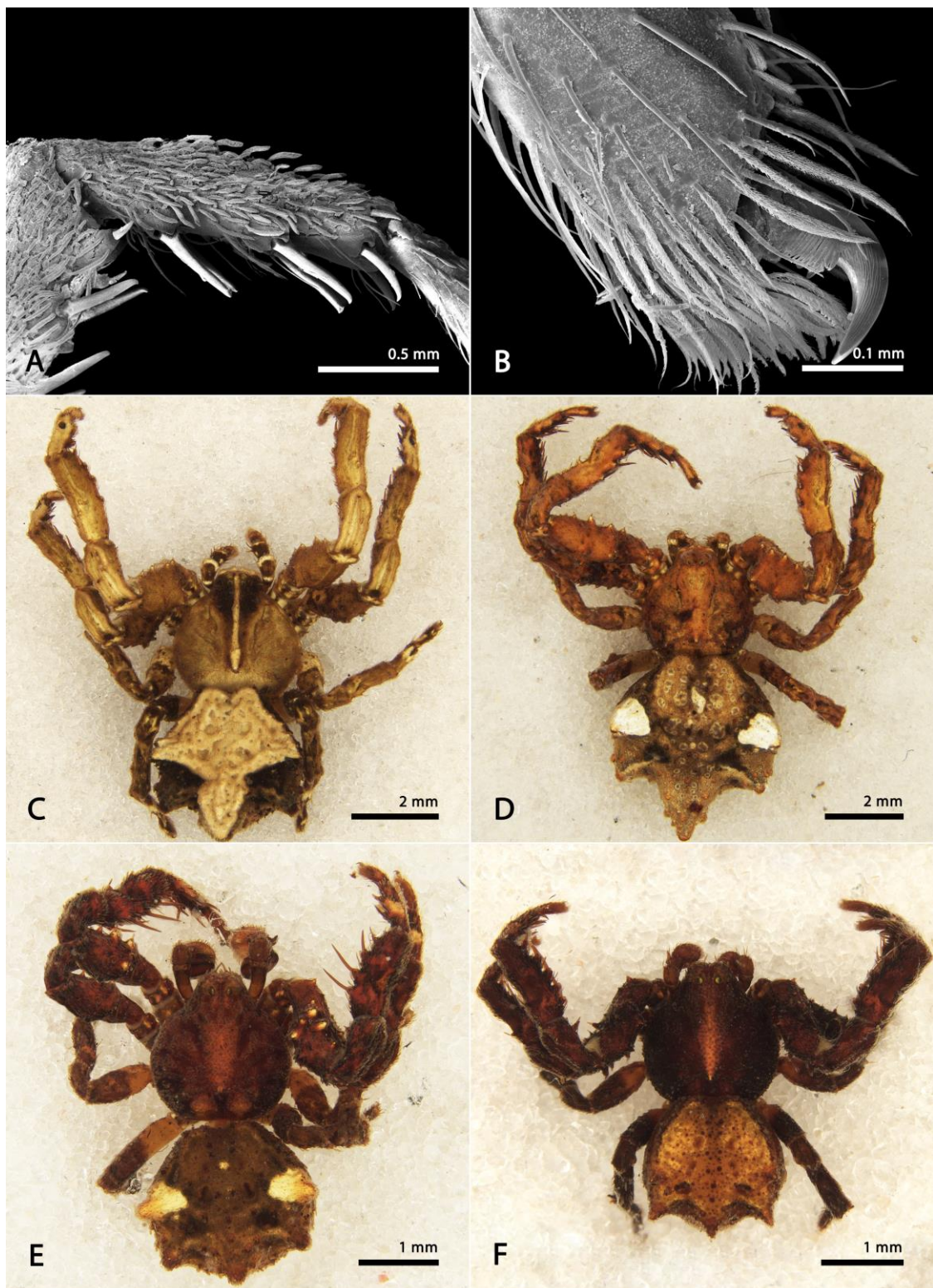
Fig. 2. Scanning electron microscopy of *Kryptochroma pentacantha* (Mello-Leitão, 1929) (MCTP 7362): **(A)** metatarsal ventral macrosetae on leg I; **(B)** detail of the ectal tarsal claw. **(C–F)** Color variations of *Kryptochroma* species: **(C, D)** females of *K. pentacantha*; (MCN 30853 and MCN 8079, respectively) **(E)** male of *K. pentacantha* (MCN 29059) **(F)** male of *K. quinquetuberculata* (IBSP 46738).

<div align="center">

Kryptochroma gigas Machado & Viecelli **sp. nov.**

Fig. 3

</div>

Diagnosis

The female of *Kryptochroma gigas* **sp. nov.** resembles those of *K. quadrata* **sp. nov.** and *K. pentacantha* (Mello-Leitão, 1929) **comb. nov.** by their large body size, which are significantly bigger than the other species here described. This species can be distinguished from the two other ones by the elevated and short opisthosoma and by the heart-shaped epigynal plate with a short and stout projection over a wide median septum, which divides the atrium in two individual longitudinal gutters ending in the copulatory openings (Fig. 3C, D, E, F).

Etymology

The epithet is a Latin feminine noun that means giant, refering to the bigger size of this species compared to other species of the genus.

Material examined

Holotype

BRAZIL • ♀; Estação Biológica da Mata do Sossego, Simonésia, Minais Gerais; 20°04′25″S 42°04′13″W; 28–30 Nov. 2010; M.T.T. Santos leg.; UFMG 4734.

Other material

Only the type material.

Description

Female (UFMG 4734) — Anterior eye row very recurved and posterior slightly procurved; prosoma dark-yellow with large lateral black taints, median region and posterior slope yellow, contoured by black lines (Fig. 3A, B). Femora I and II dorsally enlarged and with many setiferous tubercles, femora III and IV bicolor, half black, half yellow; chelicerae dark-yellow with black stains, endites and labium black, sternum black with a median yellow taint. Opisthosoma predominantly dark-yellow, black on the back of the abdominal projections and on the sides, rough surfaced and slightly concave on anterior border (Fig. 3A,B). Measurements: eyes diameters and eyes interdistances: AME 0.09, ALE 0.14, PME 0.12, PLE 0.12, AME-AME 0.08, AME-

ALE 0.12, PME-PME 0.24, PME-PLE 0.06, MOQ length 0.43, MOQ width 0.48; leg formula: 1-2-4-3: leg I – femur 4.66/ patella 2.59/ tibiae 3.10/ metatarsus 2.17/ tarsus 1.29/ total 13.81; II – 3.83/ 2.07/ 2.84/ 1.86/ 1.29/ 11.89; III – 2.07/ 1.29/ 1.86/ 1.19/ 0.82/ 7.23; IV – 2.59/ 1.19/ 1.86/ 1.29/ 0.82/ 7.75. Total body length 9.62; prosoma 4.40 length, 4.04 wide; opisthosoma length 4.62; clypeus 0.37 height; sternum 1.45 length, 1.20 width; endites 0.69 length, 0.40 width; labium 0.48 length, 0.53 width. — Male — unknown.
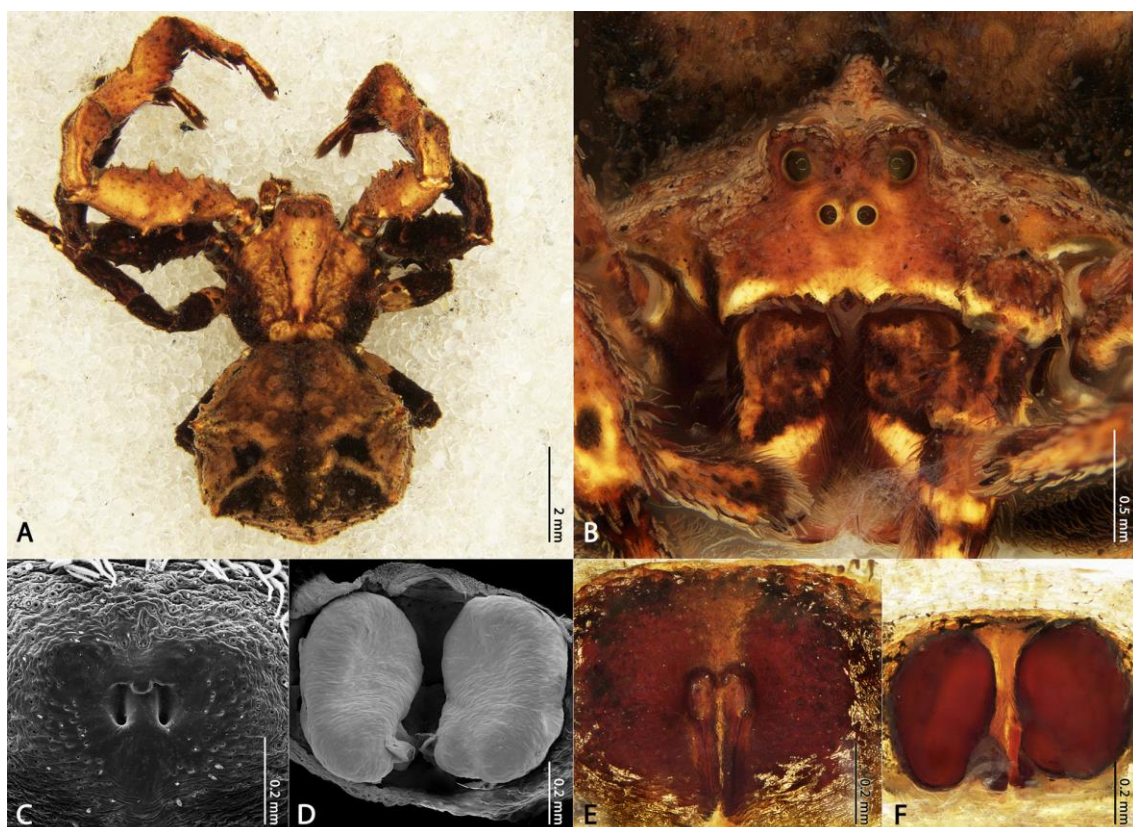

Fig. 3. Female of *Kryptochroma gigas* **sp. nov.**: **(A)** dorsal habitus; **(B)** front; **(C, E)** ventral view of the epigynal plate; **(D, F)** dorsal view of the spermathecae.

Distribution

Central Brazil (Minas Gerais) — Fig. 9.

Kryptochroma hilaris Machado & Teixeira **sp. nov.**

Figs 4, 5

Diagnosis

The males of *K. hilaris* **sp. nov.** present a body coloration that resemble those of *K. parahybana* (Mello-Leitão, 1929) **comb. nov.** However, they can be differentiated by the stouter, shorter and round embolus, which points retro-ventrally (Fig. 4C, E). The most striking differences between *K. hilaris* **sp. nov.** and other species of the genus are the discrete MS on prosoma (absent in males), and the number of ventral macrosetae on tibiae I and II: while other species have four pairs on each leg for both sexes, in *K. hilaris* **sp. nov.** the females bear six ventral macrosetae on tibiae I (Fig. 4A) while males present only five (Fig. 5A). Females can also be distinguished by the presence of two anterolateral and one median depression on the epigynal plate and by the copulatory openings located in a demilune-shaped concavity delimited by the posterior folds of the tegument (Fig. 4A, D, E, F).

Etymology

The specific name – a Latin adjective that means cheerful – is a reference to the shape of the posterior fold of the epigynal plate, which resembles a smiling face.

Material examined

Holotype

BRAZIL • ♀; Base de Operações Geólogo Pedro de Moura, Porto Urucu, Coari, Amazonas; 04°48′41″S 65°02′01″W; July 2006; S.C. Dias leg.; MPEG 13322.

Paratypes

BRAZIL • 1♂; same data as for holotype; September to November 2006; N.F. Lo Man Hung leg.; MCTP 42643 • 1♀; same data as for holotype; 13 July 2003; D. Guimarães leg.; MCTP 42642 • 1♀, same data as for holotype; September 2006; C.A.C. Santos Jr.; MPEG 13311.

Other Material

BRAZIL • 1♀; Tefé, Amazonas; 03°21'14" S, 64°42'39" W; Nov. 1919; H.S. Parrish leg.; MCZ • 1♂; Coari, Amazonas; 04°51'35" S, 65°06'17" W; Sep. 2006; C.A.C. Santos Jr. leg.; MPEG 13302 • 1♀; Coari, Amazonas; 04°53'45" S, 65°19'11" W; Oct. 2006; J.O. Dias leg.; MPEG 13307 • 1♀; Coari, Amazonas; 04°48'56" S,

65°01'53" W; Jul 2006; C.A.C. Santos Jr. leg.; MPEG 13318 • 1♂; Coari, Amazonas; 04°50'01" S, 65°03'53" W; Sep. 2006; D.F. Candiani leg.; MPEG 13354 • 1♀; Coari, Amazonas; 04°52'47" S, 65°20'09" W; Oct. 2006; N.F. Lo-Man-Hung leg.; MPEG 13363 • 1♀; Coari, Amazonas; 04°52'07" S, 65°15'53" W; 13 Jul. 2003; D. Guimarães leg.; MPEG 22795 • 1♂; Coari, Amazonas; 04°51'35" S, 65°06'17" W; Sep. 2006; S.C. Dias leg.; MPEG 13306 • 1♂; Coari, Amazonas; 04°52'36" S, 65°09'05" W; 14 Jul. 2003; J.O. Dias leg.; MPEG 22819 • 1♂; Coari, Amazonas; 04°51'54" S, 65°20'02" W; Oct. 2006; N.F. Lo-Man-Hung leg.; MPEG 13239 • 1♂; Coari, Amazonas; 04°51'54" S, 65°20'02" W; Oct. 2006; N.C. Bastos leg.; MPEG13243 • 1♀; Coari, Amazonas; 04°51'54" S, 65°20'02" W; Oct. 2006; N.F. Lo-Man-Hung leg.; MPEG 13245 • 1♂; Coari, Amazonas; 04°52'46" S, 65°09'50" W; Nov. 2006; N.F. Lo-Man-Hung leg.; MPEG 13247 • 1♂; Coari, Amazonas; 04°54'16" S, 65°19'37" W; Nov. 2006; C.A.C. Santos Jr. leg.; MPEG 13251 • 1♀; Coari, Amazonas; 04°48'47" S, 65°01'57" W; Jul. 2006; L.T. Miglio leg.; MPEG 13253 13245 • 1♂; Coari, Amazonas; 04°51'35"S, 65°06'17" W; Sep. 2006; N.F. Lo-Man-Hung leg.; MPEG 13263 • 1♂; same data as the previous vial; MPEG 13272 • 1♂; Coari, Amazonas; 04°48'47" S, 65°01'57" W; Jul. 2006; L.T. Miglio leg.; MPEG 13279 • 1♂; Coari, Amazonas; 04°52'25" S, 65°09'05" W; Oct. 2006; N.C. Bastos leg.; MPEG 13280 • 1♀; Coari, Amazonas; 04°50'30" S, 65°03'51" W; Sep. 2006; C.A.C. Santos Jr. leg.; MPEG 13289 • 1♂; Coari, Amazonas; 04°52'31" S, 65°10'27" W; Jul. 2006; L.T. Miglio leg.; MPEG 13290 • 1♀; Coari, Amazonas; 04°53'30" S, 65°20'07" W; Nov. 2006; N.F. Lo-Man-Hung leg.; MPEG 13298 • 04°48'45" S, 65°01'58" W04°48'41" S, 65°02'01" W; Jul. 2006; J.O. Dias leg.; MPEG 13299 • 1♂; Coari, Amazonas; 04°52'06" S, 65°15'52" W; Jul. 2006; L.T. Miglio leg.; MPEG 13304 • 1♀; Coari, Amazonas; 04°48'56" S, 65°01'53" W; Jul 2006; J.O. Dias leg.; MPEG 13317 • 1♀; Coari, Amazonas; 04°51'38" S, 65°20'04" W; Oct. 2006; N.F. Lo-Man-Hung leg.; MPEG 13321 • 1♀; Coari, Amazonas; 04°52'06" S, 65°15'52" W; Jul. 2006; C.A.C. Santos Jr. leg.; MPEG 13327 • 2♂; Coari, Amazonas; 04°48'45" S, 65°01'58" W; Jul. 2006; J.O. Dias leg.; MPEG 13329 • 1♀; Coari, Amazonas; 04°53'14" S, 65°13'37" W; Sep. 2006; J.O. Dias leg.; MPEG 13337 • 1♂, 1j; Coari, Amazonas; 04°51'54" S, 65°20'02" W; Oct. 2006; J.O. Dias leg.; MPEG 13342 • 1♂; Coari, Amazonas; 04°45'47" S, 65°02'41" W; Jul. 2006; C.A.C. Santos Jr. leg.; MPEG 13345 • 1♂; Coari, Amazonas; 04°50'32" S, 65°04'08" W; Sep. 2006; C.A.C. Santos Jr. leg.; MPEG 13348 • 1♂; Coari, Amazonas; 04°50'30" S, 65°03'51" W; Sep. 2006; J.O. Dias leg.; MPEG 13349 • 2♂; Coari,

Amazonas; 04°51'54" S, 65°20'02" W; Oct. 2006; N.F. Lo-Man-Hung leg.; MPEG 13352 • 1♂; Coari, Amazonas; 04°50'32" S, 65°04'08" W; Sep. 2006; N.F. Lo-Man-Hung leg.; MPEG 13359 • 1♂; Coari, Amazonas; 04°45'47" S, 65°02'41" W; Jul. 2006; L.T. Miglio leg.; MPEG 13362 • 1♂; Coari, Amazonas; 04°50'50" S, 65°05'03" W; Sep. 2006; C.A.C. Santos Jr. leg.; MPEG 13368 • 1♀; Coari, Amazonas; 04°52'36" S, 65°09'05" W; 13 Jul. 2003; J.O. Dias leg.; MPEG 22822 • 1♀; Coari, Amazonas; 04°51'17" S, 65°04'14" W; 17 Jul. 2003; A.B. Bonaldo leg.; MPEG 22830 • 1♂; same data as the previous vial; 19 Jul. 2002; A.B. Bonaldo leg.; MPEG 22835 • 2♀; same data as the previous vial; 21 Jul 2003; J.O. Dias leg.; MPEG 22840 • 1♂; same data as the previous vial; A.B. Bonaldo leg.; MPEG 22846.

Description

Female (MPEG 13322) — Anterior eye row strongly recurved, ALE slightly larger than AME, posterior eye row procurved with subequal eyes; prosoma knobby, light-brown with a thin longitudinal yellow line which widens anteriorly on clypeus (Fig. 4A). Anterior coxae and trochanters brown with dorsal yellow stains; other segments of legs I and II light-brown with darker taints randomly distributed; legs III entirely yellow, except by metatarsi and tarsi and legs IV with femora half yellow, half light-brown (Fig. 4A). Chelicerae and sternum light-brown with yellow stains, endites and labium truncated and totally light-brown. Opisthosoma rough surfaced with a large yellow taint covering the entire dorsal region, except the posterolateral abdominal projections. Measurements: eyes diameters and eyes interdistances: AME 0.06, ALE 0.09, PME 0.08, PLE 0.08, AME-AME 0.08, AME-ALE 0.08, PME-PME 0.14, PME-PLE 0.06, MOQ length 0.32, MOQ width 0.32; leg formula: 1-2-4-3: leg I – femur 2.95/ patella 1.55/ tibiae 2.33/ metatarsus 1.45/ tarsus 0.93/ total 9.21; II – 2.33/ 1.24/ 1.55/ 1.29/ 0.77/ 7.18; III – 1.55/ 0.77/ 1.24/ 0.72/ 0.51/ 4.79; IV – 2.07/ 0.77/ 1.29/ 0.88/ 0.67/ 5.68. Total body length 5.94; prosoma 2.84 length, 2.69 wide; opisthosoma length 3.10; clypeus 0.16 height; sternum 1.0 length, 0.88 width; endites 0.48 length, 0.29 width; labium 0.32 length, 0.38 width.
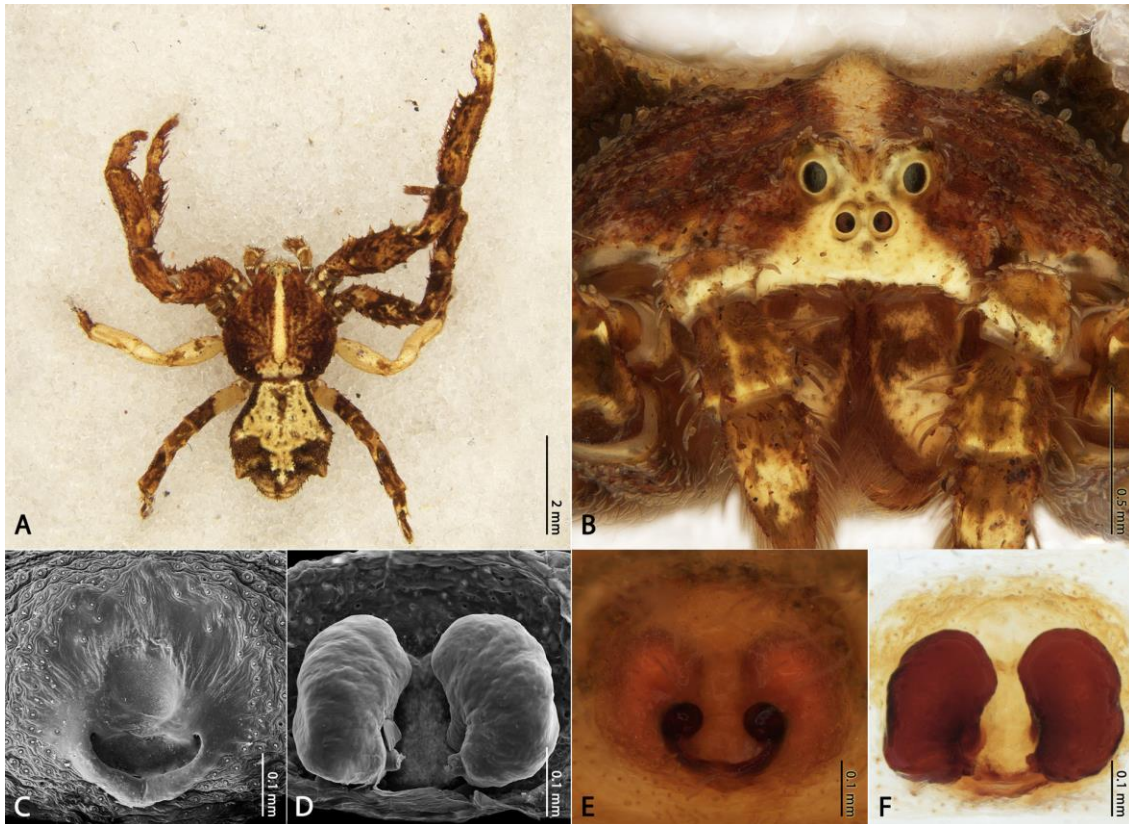
Fig. 4. Female of *Kryptochroma hilaris* **sp. nov.**: **(A)** dorsal habitus; **(B)** front; **(C, E)** ventral view of the epigynal plate; **(D, F)** dorsal view of the spermathecae.

Male (MPEG 13239) — Prosoma reddish brown with a median yellow stripe and dark posterior slope (Fig. 5A, B); vestigial MS and eye disposition as in females. Legs I and II predominantly light-brown with proximal yellow stains on tibiae and distal on metatarsi; posterior legs light-brown, except by the bicolor femora. Sternum scutiform, as long as wide, light-brown with a large yellow taint; labium and endites totally light-brown and truncated. Opisthosoma greyish brown with dark-yellow projections. Measurements: eyes diameters and eyes interdistances: AME 0.06, ALE 0.09, PME 0.06, PLE 0.06, AME-AME 0.06, AME-ALE 0.06, PME-PME 0.11, PME-PLE 0.04, MOQ length 0.24, MOQ width 0.25; leg formula: 1-2-4-3: leg I – femur 1.32/ patella 0.67/ tibiae 1.03/ metatarsus 0.72/ tarsus 0.45/ total 4.19; II – 0.96/ 0.53/ 0.77/ 0.56/ 0.40/ 3.22; III – 0.72/ 0.40/ 0.64/ 0.33/ 0.32/ 2.41; IV – 0.88/ 0.40/ 0.69/ 0.45/ 0.37/ 2.79. Total body length 3.06; prosoma 1.61 length, 1.43 wide; opisthosoma length 1.45; clypeus 0.16 height; sternum 0.72 length, 0.62 width; endites 0.32 length, 0.19 width; labium 0.16 length, 0.24 width.
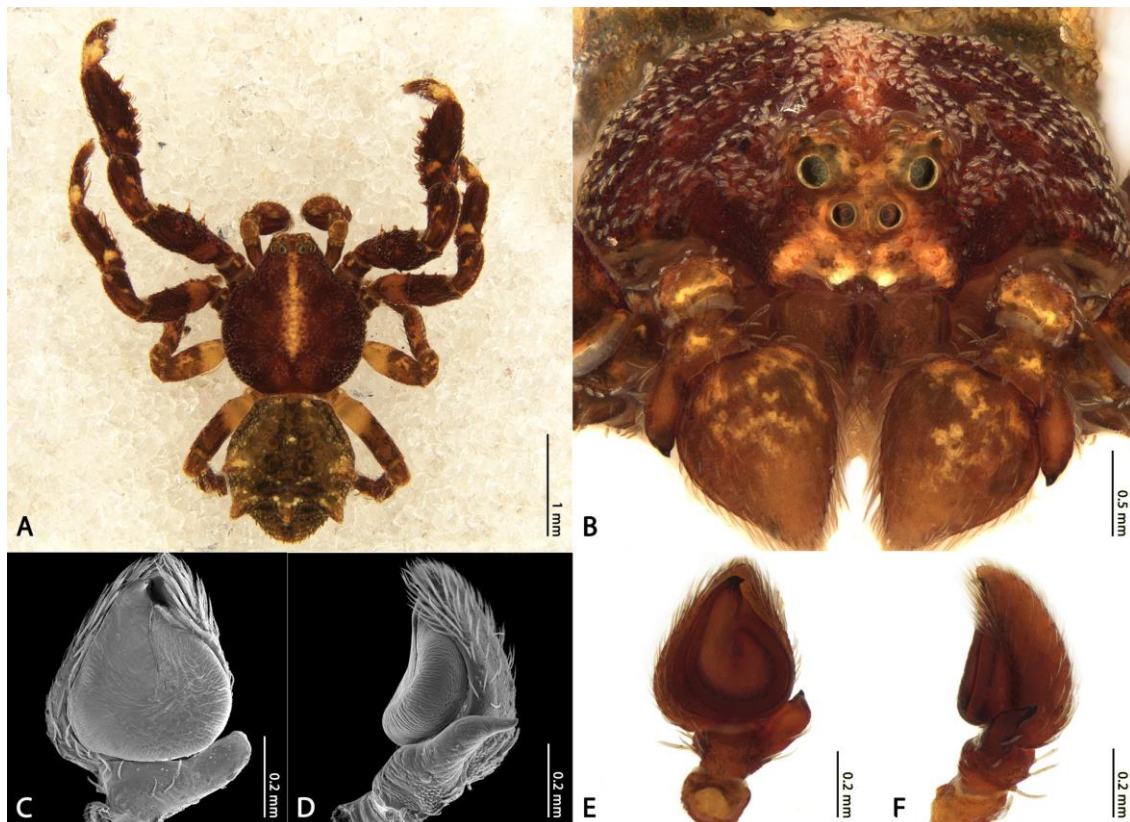
Fig. 5. Male of *Kryptochroma hilaris* **sp. nov.**: **(A)** dorsal habitus; **(B)** front; **(C, E)** ventral view of the left male palp; **(D, F)** retrolateral view of the left male palp.

Distribution

Brazil (Amazonas) – Fig. 9.

Kryptochroma macrostyla (Mello-Leitão, 1929) **comb. nov.**

Fig. 6

Stephanopis macrostyla Mello-Leitão, 1929: 61, fig. 145. **New combination.**

Diagnosis

The males of *K. macrostyla* resemble those of *K. pentacantha* by their relatively robust body and large size, when compared to other males of the genus, and shape of RTA, but can be easily distinguished by these and other congeneric species by their long, free and filiform embolous (Fig. 6C, E).

Material examined

Holotype

BRAZIL • ♂; Teresópolis, Rio de Janeiro, Rio de Janeiro; 22°25'1.06"S 42°58'32.17"W, MNHN 11467.

Other material

BRAZIL • 1♂, Nova Friburgo, Macaé de Cima, Rio de Janeiro; 22°22'11" S, 42°27'52" W; 30 Aug. 1996; R.S. Bérnils leg.; MZSP 15320 • 1♂, Estação Biológica de Boracéia, São Paulo; 23°37'51" S, 45°52'11" W; Jul. 2005; A.D. Brescovit leg.; IBSP 55197 • 1♂, Serra da Farinha Seca, Pinhais, Paraná; 25°23'45" S, 48°55'58" W; 15-20 Oct. 1995; lab staff leg.; MCTP 7665.

Description

Male (MZSP 15320) — Anterior eyes row strongly recurved, ALE slightly larger than AME (Fig. 6B); posterior eye row in a straight line with equal sized eyes. Prosoma predominantly dark-brown with a longitudinal yellow line which goes from the middle of PME to the edge of the MS (Fig. 6A); clypeus region and eyes tubercles lighter than the rest of the prosoma (Fig. 6B). Legs I and II reddish-brown, coxae I and II dark-brown with yellowish stains; legs III and IV dark-brown except by the femora which are yellow on its proximal region. Opisthosoma rough surfaced, predominantly yellow with dark-brown stains between the abdominal projections and on the sides; lateral projections orange and median dark-brown (Fig. 6A); RTA stout and conical (Fig. 6D, F). Measurements: eyes diameters and eyes interdistances: AME 0.06, ALE 0.11, PME 0.08, PLE 0.08, AME-AME 0.09, AME-ALE 0.11, PME-PME 0.17, PME-PLE 0.08, MOQ length 0.40, MOQ width 0.38; leg formula: 1-2-4-3: leg I – femur 2.43/ patella 1.04/ tibiae 1.61/ metatarsus 0.96/ tarsus 0.72/ total 6.76; II – 2.22/ 0.88/ 1.25/ 0.88/ 0.59/ 5.82; III – 1.12/ 0.64/ 1.01/ 0.56/ 0.48/ 3.81; IV – 1.29/ 0.61/ 0.96/ 0.64/ 0.53/ 4.03. Total body length 5.283; prosoma 2.59 length, 2.43 wide; opisthosoma length 2.69; clypeus 0.27 height; sternum 0.96 length, 0.88 width; endites 0.43 length, 0.24 width; labium 0.27 length, 0.32 width.

Female — unknown.
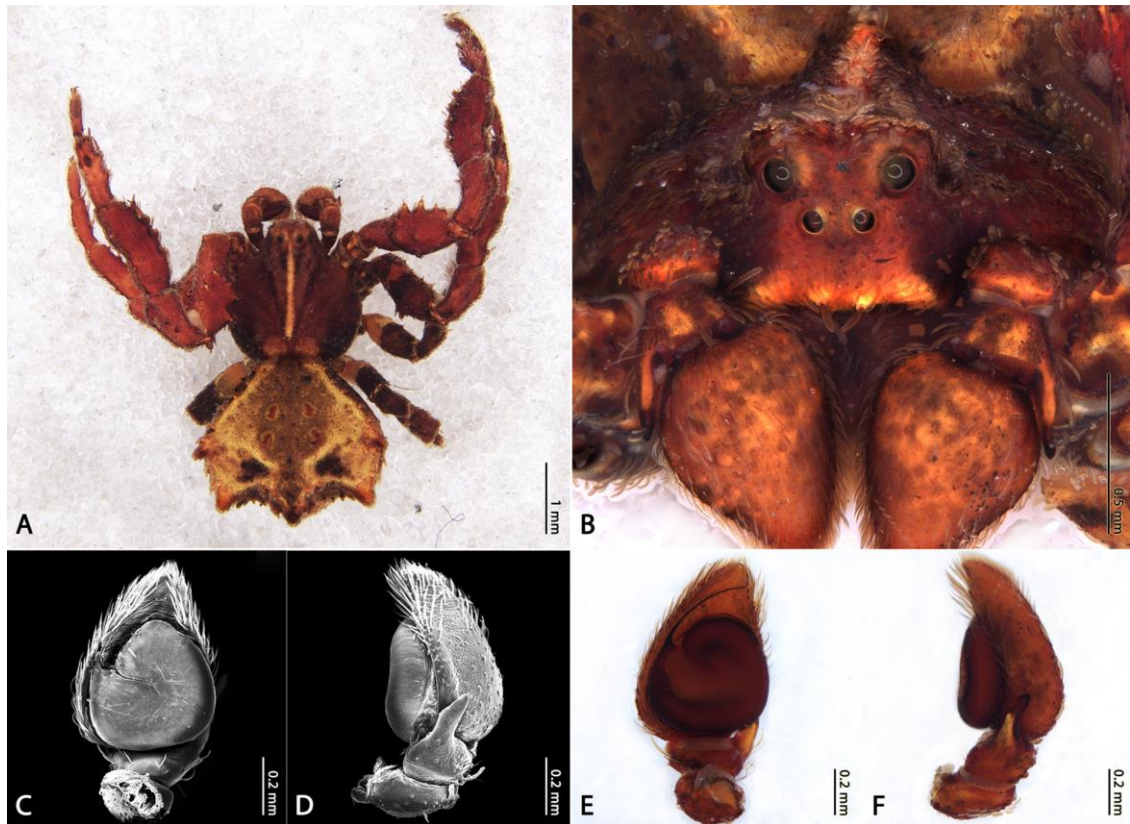
Fig. 6. Male of *Kryptochroma macrostyla* (Mello-Leitão, 1929): **(A)** dorsal habitus; **(B)** front; **(C, E)** ventral view of the left male palp; **(D, F)** retrolateral view of the left male palp.

Distribution

Brazil (Paraná, Rio de Janeiro and São Paulo) — Fig. 9.

Kryptochroma parahybana (Mello-Leitão, 1929) **comb. nov.**

Figs 7, 8

Stephanopis parahybana Mello-Leitão, 1929: 58, fig. 140. **New combination.**

Diagnosis. Females of *K. parahybana* resemble those of *K. hilaris* **sp. nov.** by the light median line on prosoma and withish clypeus (Fig. 7A), however, can be distinguished by the five pairs of ventral macrosetae on anterior tibiae instead of four, flatter prosoma with discrete medial spire (Fig. 7B), epigynal plate without median septum and with small and elliptical copulatory openings (Fig. 7C, E). Males may present a body coloration pattern similar to those of *K. hilaris* **sp. nov.**, however, can

108

be easily differentiated by the short abdominal projections (Fig. 8A, B), reduced RTA (Fig. 8D, F) with distal indentations and by the apical and sinuous embolus (Fig. 8C, E).

Examined material

Holotype
BRAZIL • ♂; Paraíba; 7°08'S" 34°52'W, MNHN 17824.

Syntypes
BRAZIL • 2♀; Salobro, Bahia; 11°41'10.56"S 41°46'5.10"W, MNHN 3973.

Other material
BRAZIL • 1♀, Reserva da Campina, Manaus, Amazonas; 2°36'19" S, 60°02'11" W; 18 Jul. 1973; L. Albuquerque leg.; INPA • 1♂, same data as the previous vial; 11 Jun. 1973; same collector; INPA • 1♂, same data as the previous vial; 11 Jun. 1973; INPA • 2♂, same data as the previous vial; 21 Mar. 1974; INPA • 1♀, same data as the previous vial; 18 Jun. 1973; INPA • 1♂, same data as the previous vial; 18 Jun. 1973; INPA • 1♂ and 3j, same data as the previous vial; 12 Jan. 1973; INPA • 2♂ and 1j, same data as the previous vial; 25 Apr. 1973; INPA • 1♂, Reserva Ducke, Manaus, Amazonas; 02°57'42" S, 59°55'40" W; 13 Nov. 1973; L. Albuquerque leg.; INPA • 1♀, same data as the previous vial; INPA • 1♂, same data as the previous vial; 16 Oct. 1973; INPA • 1♂, same data as the previous vial; 28 May 1973; INPA • 1♂, same data as the previous vial; 13 Aug. 1973; INPA • 2♂ and 1j, same data as the previous vial; 12 Mar. 1987; A.A. Lise leg.; INPA • 1♂ and 2j, same data as the previous vial; 04 Aug. 1987; INPA • 1♀, same data as the previous vial; 05 Aug. 1987; INPA • 1♂, same data as the previous vial; 12 Mar 1987; L. Aquino leg.; INPA • 1♀, Fazenda Esteio, Manaus, Amazonas; 02°22'60" S, 59°51'00" W; 30 Oct. 1985; B.C. Klein leg.; INPA 1208 • 1♂, PDBFF Dimona, Manaus, Amazonas; 02°25'00" S, 60°00'00" W; 20 Dec. 2001 – 20 Mar. 2002; F. Rego & A. Cardoso leg.; INPA 2772 • 1♂, same data as the previous vial; INPA 2773 • 1♂, same data as the previous vial; INPA 2774 • 1♂, same data as the previous vial; INPA 2775 • 1♂, same data as the previous vial; INPA 2776 • 1♀, Reserva da Campina, Manaus, Amazonas; 2°36'19" S, 60°02'11" W; 02 Sep. 1991; A.D. Brescovit leg.; MCN 21261 • 2♂, Reserva Duck, Manaus, Amazonas; 02°57'42" S, 59°55'40" W; 14-25 Aug. 1991; A.D. Brescovit leg.; MCTP 1080 • 2♂ and 1j, same data as the previous vial; 19-24 Feb. 1992; A.A. Lise leg.; MCTP 1693 •

1♂, same data as the previous vial; 04 Aug. 1987; MCTP 29942 • 1♂ and 3j, same data as the previous vial; 12 Mar. 1987; MCTP 29943 • 1♀, , same data as the previous vial; 28 May 1973; L. Albuquerque leg.; MCTP 29944 • 1♂, 1♀ and 1j, Reserva da Campina, Manaus, Amazonas; 2°36'19" S, 60°02'11" W; 25 Apr. 1973; L. Albuquerque leg.; MCTP 29946 • 1♂, 1♀ and 1j, same data as the previous vial; 12 Jan. 1973; MCTP 29947 • 1♀, same data as the previous vial; 14 May 1973; MCTP 29948 • 1♀, Br. 174. ZF 2. Km 34. LBA, Manaus, Amazonas; 02°40'34" S, 60°02'47" W; 15 Nov. 2005; S.M. Ketelhut leg.; MPEG 22723 • 1♂, Manaus, Amazonas; 2°35'54" S, 60°2'15" W; 17-19 Nov. 2013; B.T. Faleiro leg.; UFMG 14478 • 1♂, Reserva Ducke, Manaus, Amazonas; 02°57'42" S, 59°55'40" W; 14-25 Aug. 1991; A.D. Brescovit leg.; MACN-Ar 39669 • 1♂, same data as the previous vial; 12 Mar. 1987; A.A. Lise leg.; MACN-Ar 39672 • 1♂, Reserva Biológica do Trombetas, Oriximiná, Pará; 01°11'56" S, 56°41'49" W; 17 Dec. 1979; J. Grazia leg.; MCTP 4762 • 5♂, 1♀, Flora Caziuanã, Melgaço, Pará; 01°44'13" S, 51°25'32" W; 11 Aug. 1996; A.A. Lise leg.; MCTP 9514 • 8♂ and 1♀, same data as the previous vial; MCTP 9515 • 7♂ and 1♀, same data as the previous vial; MCTP 9516 • 4♂, Vale do Igarapé Mutum, Pará; 02°36'45" S, 56°11'38" W; 04 Aug. 2004; D.R. Santos-Souza leg.; MPEG 8767 • 2♂, Sítio Três Irmãos, Juruti, Pará; 02°27'51" S, 56°00'08" W; 04 Mar. 2006; S.C. Dias leg.; MPEG 9067 • 1♂, Estação Científica Ferreira Penna, Melgaço, Pará; 01°44'14" S, 51°27'19" W; 22 Nov. 2000; D.M. Takyia leg.; MPEG 37 • 1♂, same data as the previous vial; A.M. Barros leg.; MPEG 41 • 1♀, Sítio Barroso, Juruti, Pará; 02°27'41" S, 56°00'11" W; 14 Aug. 2006; D.F. Candiani leg.; MPEG 8391 • 2♂, Platô do Rio Juruti; Pará; 02°36'45" S, 56°11'38" W; 13 Aug. 2006; D.F. Candiani leg.; MPEG 8398 • 1♂, Sítio Barroso, Juruti, Pará; 02°27'41" S, 56°00'11" W; 14 Aug. 2006; N.F. Lo-Man-Hung leg.; MPEG 8415 • 1♂, same data as the previous vial; MPEG 8430 • 1♂, Vale do Igarapé Mutum; Pará; 02°36'45" S, 56°11'38" W; 06 Aug. 2004; D.R. Santos-Souza leg.; MPEG 8750 • 1♂, same data as the previous vial; 04 Aug. 2004; D.F. Candiani leg.; MPEG 8754 • 4♂, same data as the previous vial; 06 Aug. 2004; MPEG 8757 • 1♂, Sítio Barroso, Juruti, Pará; 02°27'41" S, 56°00'11" W; 13 Aug. 2004; D.R. Santos-Souza leg.; MPEG 8758 • 1♀, same data as the previous vial; MPEG 8762 • 1♀, Vale do Igarapé Mutum; Pará; 02°36'45" S, 56°11'38" W; 05 Aug. 2004; D.F. Candiani leg.; MPEG 8765 • 1♂, same data as the previous vial; MPEG 8766 • 1♂, Linha 168E, Platô Capiranga, Pará; 02°28'22" S, 56°12'29" W; 10 Mar. 2006; D.R. Santos-Souza leg.; MPEG 9062 • 3♂, same data as the previous vial;

S.C. Dias leg.; MPEG 9064 • 2♂ and 2j, same data as the previous vial; 07 Mar. 2006; MPEG 9066 • 2♂, same data as the previous vial; 10 Mar. 2006; MPEG 9069 • 1♂ and 1j, Sítio Três Irmãos, Juruti, Pará; 02°27'51" S, 56°00'08" W; 04 Mar. 2006; D.R. Santos-Souza leg.; MPEG 9065 • 1♂, Sítio Barroso, Juruti, Pará; 02°27'41" S, 56°00'11" W; 11 Feb. 2007; J.A.P. Barreiros leg.; MPEG 14941 • 1♀, same data as the previous vial; 08 Feb. 2007; N.F. Lo-Man-Hung leg.; MPEG 14944 • 1♂, Vale do Igarapé Mutum, Pará; 02°36'45" S, 56°11'38" W; 07 Feb 2007; J.A.P. Barreiros leg.; MPEG 14942 • 1♂, same data as the previous vial; 12 Feb. 2007; MPEG 14953 • 1♂, Sítio Três Irmãos, Juruti, Pará; 02°27'51" S, 56°00'08" W; 11 Feb. 2007; J.A.P. Barreiros leg.; MPEG 14951 • 1♀, Melgaço, Pará; 01°44'13" S, 51°25'32" W; 10 Jun. 2006; E.J. Sales leg.; MPEG 30335 • 2♂ and 1♀, same data as the previous vial; J.A.P. Barreiros leg.; MPEG 30336 • 1♀, same data as the previous vial; 27 May 2006; E.J. Sales leg.; MPEG 30337 • 1♀, same data as the previous vial; 31 May 2006; B.B. Santos leg.; MPEG 30338 • 1♀, same data as the previous vial; 05 Jun 2006; B.C. Araújo leg.; MPEG 30339 • 1♂ and 1♀, same data as the previous vial; 26 May 2006; E.J. Sales leg.; MPEG 30340 • 1♀, same data as the previous vial; 27 May 2006; J.A.P. Barreiros leg.; MPEG 30341 • 3♂, same data as the previous vial; 05 Jun. 2006; B.C. Araújo leg.; MPEG 30342 • 4♂, same data as the previous vial; 01 Jun. 2006; B.B. Santos leg.; MPEG 30343 • 1♂, same data as the previous vial; 26 May 2006; E.J. Sales leg.; MPEG 30344 • 6♂, same data as the previous vial; 01 Jun. 2006; J.A.P. Barreiros leg.; MPEG 30345 • 1♂, same data as the previous vial; 27 May 2006; MPEG 30346 • 2♂, same data as the previous vial; 05 Jun. 2006; B.C. Araújo leg.; MPEG 30347 • 1♂, Sítio Três Irmãos, Juruti, Pará; 02°27'51" S, 56°00'08" W; 04 Mar. 2006; S.C. Dias leg.; MPEG 9068; • 1♂, Flona Caxiuanã, Melgaço, Pará; 01°44'13" S, 51°25'32" W; 11 Aug. 1996; A.A. Lise leg.; MACN-Ar 39670 • 1♂, same data as the previous vial; MACN-Ar 39671 • 1♂, Fazenda Dínamo, Ilha de Maracá, Roraima; 03°24'00" N, 61°42'00" W; 20 Aug. 1987; A.A. Lise leg.; MCTP 29949. FRENCH GUIANA • 1♂, Trinité Reserve, Sant-Élie; 04°35'00" N, 53°18'00" W; 07 Oct. 2010; V. Vedel leg.; MCTP 31973; • 1♂, same data as the previous vial; 09 Sep. 2010; MCTP 31992 • 1♂, Saül; 3°37′22″ N, 53°12′30″ W; 2015; V. Vedel leg.; MCTP 41965 • 1♂, same data as the previous vial; MCTP 41966 • 1♂, same data as the previous vial; MCTP 41967 • 1♂, same data as the previous vial; MCTP 41968 • 1♂, same data as the previous vial; MCTP 41969 • 1♂, same data as the previous

vial; MCTP 41970 • 1♂, same data as the previous vial; MCTP 41971 • 1♂, Les Gros Arbres, Saül; 03°37'29" N, 53°12'28" W; 31 Mar. 2011; D. Comus leg.; MCTP 31965.

Description

Female (MPEG 30339) — anterior eye row strongly recurved, posterior eye row slightly procurve and ocular mounds discrete (Fig. 7A, B). Prosoma predominantly reddish-brown with black pigmentation increasing on the sides and on cephalic area; posterior slope scar whitish-yellow and surrounded by a pair of setae emerging from cylindrical sockets (Fig. 7A, B). Chelicerae yellow with dark-brown taints, sternum slightly longer than wide, brown with a median yellow taint; endites and labium truncated, brown. Legs I and II present femora and tibiae predominantly black, with some yellow regions, while posterior legs are lighter, predominantly light-yellow with few light-brown spots (Fig. 7A). Opisthosoma predominantly brown with yellow pigmentation on the edge of the abdominal projections; spermathecae rounded, slightly narrowed posteriorly (Fig. 7D, F). Measurements: eyes diameters and eyes interdistances: AME 0.06, ALE 0.13, PME 0.09, PLE 0.09, AME-AME 0.09, AME-ALE 0.11, PME-PME 0.22, PME-PLE 0.04, MOQ length 0.38, MOQ width 0.43; leg formula: 1-2-4-3: leg I – femur 3.62/ patella 2.17/ tibiae 2.84/ metatarsus 1.76/ tarsus 1.03/ total 11.42; II – 2.95/ 1.65/ 2.12/ 1.34/ 0.93/ 8.99; III – 1.76/ 1.03/ 1.60/ 0.77/ 0.56/ 5.72; IV – 1.96/ 1.03/ 1.55/ 1.03/ 0.72/ 6.29. Total body length 7.24; prosoma 3.62 length, 3.36 wide; opisthosoma length 3.62; clypeus height 0.24; sternum 1.20 length, 1.04 width; endites 0.61 length, 0.33 width; labium 0.40 length, 0.45 width.
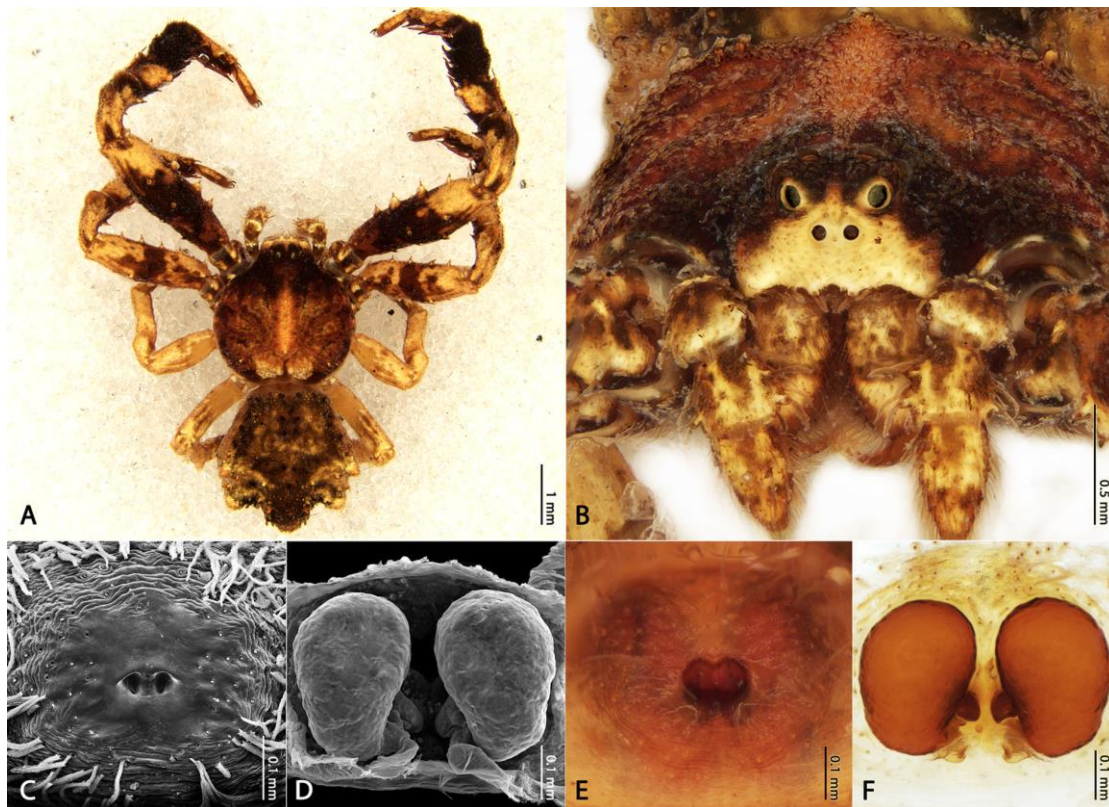
Fig. 7. Female of *Kryptochroma parahybana* (Mello-Leitão, 1929): **(A)** dorsal habitus; **(B)** front; **(C, E)** ventral view of the epigynal plate; **(D, F)** dorsal view of the spermathecae.

Male (MPEG.ARA 09069) — Anterior eye row strongly recurved, posterior slightly procurved; prosoma predominantly brownish-red with median thoracic region and clypeus light-yellow (Fig. 8A, B). Legs also brownish-red with yellowish taints on anterior tarsi (I and II) and on the proximal half of the posterior femora (III and IV). Labium, endites and chelicerae brown. Opisthosoma predominantly yellow with a whitish line-like macula connecting the five reddish spiniform projections (Fig. 8A). Measurements: eyes diameters and eyes interdistances: AME 0.08, ALE 0.12, PME 0.10, PLE 0.10, AME-AME 0.06, AME-ALE 0.06, PME-PME 0.16, PME-PLE 0.06, MOQ length 0.44, MOQ width 0.30; leg formula: 1-2-4-3: leg I – femur 1.60/ patella 0.90/ tibiae 1.10/ metatarsus 0.90/ tarsus 0.50/ total 5; II – 1.40/ 0.76/ 1/ 0.70/ 0.44/ 4.30; III – 0.90/ 0.50/ 0.80/ 0.50/ 0.40/ 3.10; IV – 1.10/ 0.50/ 0.80/ 0.56/ 0.40/ 3.36. Total body length 4.03; prosoma 2 length, 1.76 wide; opisthosoma length 2.03; clypeus height 0.20; sternum 0.90 length, 0.84 width; endites 0.48 length, 0.24 width; labium 0.26 length, 0.26 width.
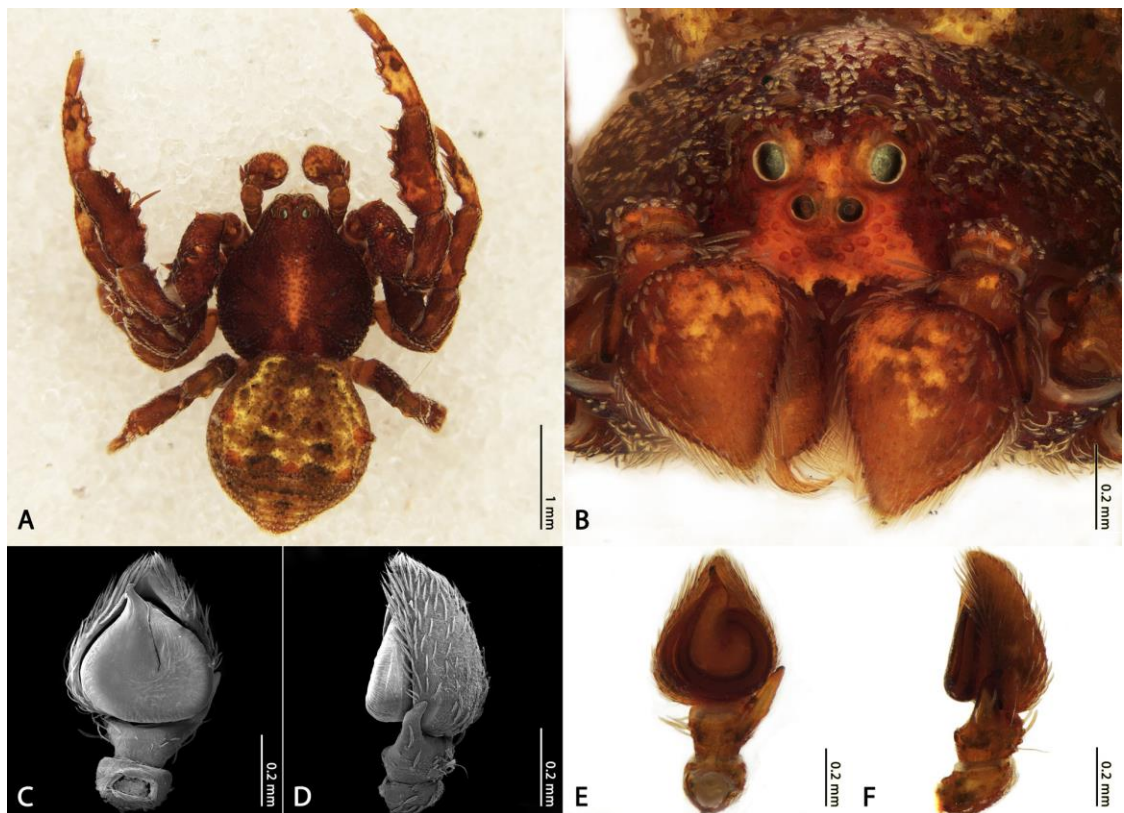
Fig. 8. Male of *Kryptochroma parahybana* (Mello-Leitão, 1929): **(A)** dorsal habitus; **(B)** front; **(C, E)** ventral view of the left male palp; **(D, F)** retrolateral view of the left male palp.

Distribution

Brazil (Amazonas, Bahia, Pará, Roraima) and French Guiana (Maripasoula, Saint-Élie and Saül) — Fig. 9.
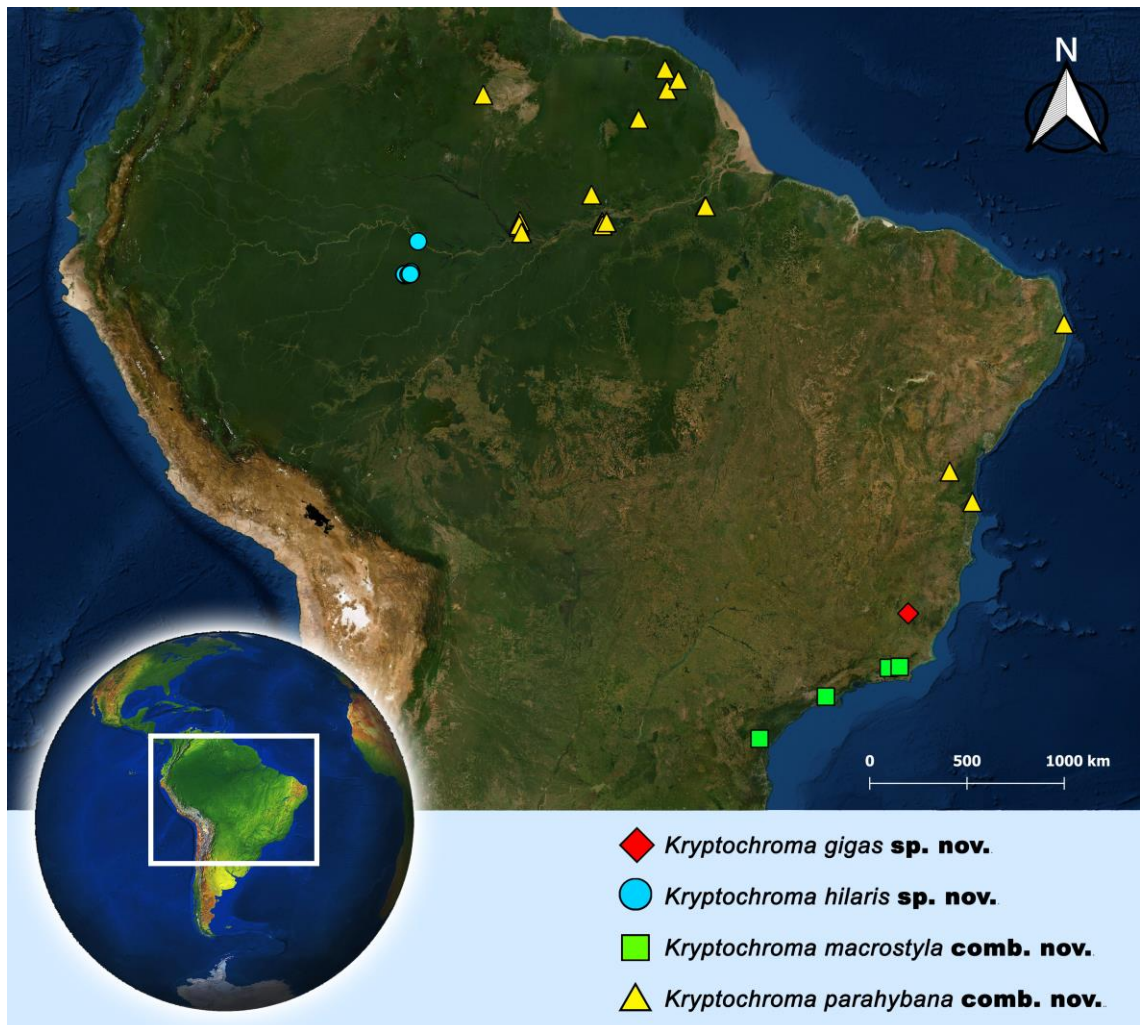
Fig. 9. Distribution records of *Kryptochroma* **gen. nov.**

Kryptochroma pentacantha (Mello-Leitão, 1929) **comb. nov.**

Figs 10, 11

Stephanopis pentacantha Mello-Leitão, 1929: 59. **New combination.**

Diagnosis. The males of *K. pentacantha* resemble those of *K. quadrata* **sp. nov.** by the wide tegulum and sinuous embolus (Fig. 11C, E), however, can be distinguished by their stout and conical RTA (Fig. 11D, F) and larger body size, since they are the largest males of genus, being the sexual size dimorphism in this species, less pronounced. Females can be recognized by the external genitalia bearing a median septum and a pair of long longitudinal depressions leading to the copulatory openings (Fig. 10C, E). The most common body color pattern for both males and females

115

present a diagnostic median white spot on the dorsum of the opisthosoma (Figs 10A, 11A).

Material examined

Lectotype (designated here)

BRAZIL • ♂; Caraça, Minas Gerais; MNHN 8227.

Paralectotypes (designated here)

BRAZIL • 2♀, 3♂; same data as for lectotype; MNHN 8203.

Other material

BRAZIL • 1♂, Fazenda Esteio, Manaus, Amazonas; 02°22'60"S, 59°51'00"W; 16 Dec. 1988; M.V.B. Garcia leg.; SMNK • 1♂, Morro dos Seis Lagos, São Gabriel da Cachoeira, Amazonas; 0°16'57"N, 66°40'44"W; 01 Oct. 1990; A.A. Lise leg.; MCTP 1195 • 1♀, Reserva Florestal Vale do Rio Doce, São Mateus, Espírito Santo; 19°09'05"S, 40°04'15"W; 19-25 Jul. 1997; A.D. Brescovit et al. leg.; IBSP 12719 • 3♂, same data as the previous vial; IBSP 24354 • 1♂, Estação Biológica Santa Lucia, Santa Tereza, Espírito Santo; 19°57'54"S, 40°32'25"W; May 2007; T. Souza et al. leg.; IBSP 160118 • 1♂, same data as the previous vial; IBSP 160128 • 1♂, 1♀, Linhares, Espírito Santo; 19°23'27"S, 40°04'19"W; Aug. 1997; A. Santos leg.; MCTP 10366 • 1♂, Estação Biológica de Santa Lúcia, Santa Teresa, Espírito Santo; 19°57'43"S, 40°31'56"W; 07 Sep. 1999; R.L.C. Baptista leg.; MNRJ 13922 • 1♂, same locality of the previous vial; 07 Jul. 2013; P.H. Martins & M.T.T. Santos leg.; UFMG 14048 • 1♂, Domingos Martins, Espírito Santo; 20°25'57"S, 41°01'12"W; 12 Jul. 2013; P.H. Martins & M.T.T. Santos leg.; UFMG 16338 • 2♂, 1j, Ilha da Queimada Grande, Itanhaém, São Paulo; 24°29'16"S, 46°40'27"W; 04-05 Dec. 1995; A.D. Brescovit & R. Bertani leg.; IBSP 10097 • 1♂, Vale do Ribeira, São Paulo; 24°32'15"S, 48°41'52"W; 26 Jun. 2005; D. Batesti leg.; IBSP 55502 • 1♂, Parque Ilha dos Eucaliptos, Guarapiranga, São Paulo; 23°44'02"S, 46°44'00"W; 06-12 Nov. 1999; R.P. Indicatti leg.; IBSP 132306 • 1♂, Vale do Ribeira, São Paulo; 24°39'42"S, 47°30'16"W; Jun. 2002; E.H. Wienkoski leg.; MNRJ 11511 • 1♂, Cananeia, São Paulo; 25°00'53"S, 47°55'36"W; Oct. 2001; E.H. Wienkoski leg.; MNRJ 11515 • 1♂, Pariquera-Açu, São Paulo; 24°42'54"S, 47°52'33"W; Dec. 2001; E.H. Wienkoski leg.; MNRJ 11534 • 1♂, Morro do Fau, Micaratu, São Paulo; 24°16'51"S, 47°27'36"W; 19 Dec. 1998; R. Pinto-da-Rocha, R.S. Bérnils & E. Howaldt leg.; MZSP 16980 • 1♀, Estação Ecológica de Juréia-Itatins, Peruíbe, São Paulo; 24°23'13"S, 47°01'03"W; 21-26 Apr. 2012; G.H.F.

Azevedo & J.P.P. Pena-Barbosa leg.; UFMG 13029 • 1♂, Serra da Graciosa, Morretes, Paraná; 25°22'31"S, 48°52'09"W; 09-20 Jan. 1995; A.A. Lise et al. leg.; MACN-Ar 39674 • 1♂, 4j, Serra da Graciosa, Morretes, Paraná; 25°22'31"S, 48°52'09"W; 09-20 Jan. 1995; lab staff leg.; MCTP 7166 • 1♂, 2j, same locality and date of the previous vial; A.A. Lise leg.; MCTP 7362 • 1♂, Antonina, Paraná; 25°25'44"S, 48°42'43"W; 01 Dec. 1986; Profaupar leg.; MCTP 19453 • 1♂, Jundiaí do Sul, Paraná; 23°26'13"S, 50°14'52"W; 01 Sep. 1986; Profaupar leg.; MCTP 19646 • 1♂, 2j, Reserva Biológica Marinha do Arvoredo, Santa Catarina; 27°17'45"S, 48°21'25"W; 06 Oct. 1995; A.A. Lise leg.; MCTP 7447 • 1♂, Reserva Biológica Marinha do Arvoredo, Santa Catarina; 27°17'45"S, 48°21'25"W; 03 May 1996; A.A. Lise leg.; MCTP 9703 • 1♂, Centro de Estudos e Pesquisas Ambientais Vila da Glória, São Francisco do Sul, Santa Catarina; 26°13'13"S, 48°41'19"W; 12-15 Dec. 2011; I.L.F. Magalhães leg.; UFMG 10317 • 1♂, Reserva Biológica Marina do Arvoredo, Santa Catarina; 27°17'45"S, 48°21'25"W; 05 Oct. 1995; A.A. Lise et al. leg.; MACN-Ar 39675 • 1♂, same locality and collectors of the previous vial; 14 Oct. 1994; MACN-Ar 39676 • 1♂, Reserva Biológica Marinha do Arvoredo, Santa Catarina; 27°17'45"S, 48°21'25"W; 13-14 Oct. 1994; A.A. Lise leg.; MCTP 5119 • 1♂, 1♀, 1j, Rancho Queimado, Santa Catarina; 27°40'22"S, 49°01'19"W; 08-12 Oct. 1994; A.B. Bonaldo & L.A. Moura leg.; MCTP 5960 • 1♂, same locality of the previous vial; 09-13 Oct. 1995; A.A. Lise leg.; MCTP 6982 • 3♂, 2♀, 10j, Montenegro, Rio Grande do Sul; 29°41'20"S, 51°27'39"W; 03 Nov. 1977; A.A. Lise leg.; MCN 8075 • 2♂, 3♀, 4j, Canela, Rio Grande do Sul; 29°21' 56"S, 50°48' 56"W; 02 Dec. 1976; A.A. Lise leg.; MCN 8079 • 1♀, Fazenda Três Cachoeiras, São Francisco de Paula, Rio Grande do Sul; 29°27'15"S, 50°33'36"W; 16 Dec. 1999; A. Franceschini leg.; MCN 32046 • 1♀, 17j, Montenegro, Rio Grande do Sul; 29°41'20"S, 51°27'39"W; 15 Dec. 1977; A.A. Lise leg.; MCN 7509 • 1♀, 4j, same locality and collector as the previous vial; 29 Sep. 1977; MCN 8080 • 1♂, 4j, Estação Experimental da Fepagro, Maquiné, Rio Grande do Sul; 29°39'41"S, 50°12'47"W; 06-08 Mar. 1998; L. Moura leg.; MCN 29059 • 3♂, 1♀, 10j, Barragem dos Bugres, São Francisco de Paula, Rio Grande do Sul; 29°20'34"S, 50°41'46"W; 01-04 Feb. 1999; L. Moura leg.; MCN 30853 • 1♀, Barragem de Itaúba, Estrela Velha, Rio Grande do Sul; 29°15'36"S, 53°14'14"W; 17-21 Jan. 2000; A. Franceschini leg.; MCN 32130 • 1♀, same locality of the previous vial; 07 Mar. 2001; R. Ott leg.; MCN 33697 • 1♂, São Francisco de Paula; 29°26'52"S, 50°35'02"W; 21-24 Mar. 1996; A.A. Lise leg.; MCTP 9855 • 1♀, Santa Maria, Rio Grande do Sul; 29°41'02"S,

53°48'25"W; 17 Jan. 1995; L. Indrusiak leg.; MCTP 10257 • 1♂, São Francisco de Paula, Rio Grande do Sul; 29°26'52"S, 50°35'02"W; 09-12 Jan. 1997; A.A. Lise leg.; MCTP 10742 • 1♂, Potreiro Velho, Pró-Mata, São Francisco de Paula, Rio Grande do Sul; 29°28'51"S, 50°10'28"W; 05-08 Dec. 1996; A.A. Lise leg.; MCTP 13988 • 1♀, same locality and collector of the previous vial; 23-25 Jul. 1996; MCTP 13992 • 1♂, same locality of the previous vial; Dec. 2001; L.A. Bertoncello & A.A. Lise leg.; MCTP 19427 • 1♂, same locality and collectors of the previous vial; Sep. 2001; MCTP 25750 • 1♂, same locality and collectors of the previous vial; Oct. 2001; MCTP 25761 • 1♂, same locality and collectors of the previous vial; Jul. 2001; MCTP 25762 • 1♀, same locality and collector of the previous vial; Jan 2002; MCTP 19429 • 1♂, same locality and collector of the previous vial; Nov. 2001; MCTP 19430 • 1♀, same locality and collector of the previous vial; Feb. 2002; MCTP 19435 • 1♀, same locality and collector of the previous vial; Dec. 2001; MCTP 19437 • 1♀, Barra do Ouro, Maquiné, Rio Grande do Sul; 29°32'18"S, 50°14'48"W; 23 Mar. 2011; R.A. Teixeira leg.; MCTP 35069 • 1♂, same locality and collector of the previous vial; 05 Jun. 2011; MCTP 35109 • 1♀, same locality and collector of the previous vial; 04 May 2011; MCTP 39906 • 1♂, Floresta Nacional de São Francisco de Paula, Rio Grande do Sul; 29°25'24"S, 50°23'13.0"W; 19 Dec. 2010; R.A. Teixeira leg.; MCTP 39903 • 1♀, same locality and collector of the previous vial; 23 Jan. 2011; MCTP 39904 • 1♀, Viamão, Rio Grande do Sul; 30°04'25"S, 51°06'27"W; 23 Sep. 1994; A.A. Lise leg.; MACN-Ar 39673 • 1♂, Sapiranga, Rio Grande do Sul; 29°37'59"S, 51°00'00"W; 14 Nov. 2005; E.L.C. da Silva leg.; MCTP 19755 • 1♀, 1j, Barra do Ouro, Maquiné, Rio Grande do Sul; 29°32'18"S, 50°14'48"W; 03 Dec. 2010; R.A. Teixeira leg.; MCTP 31532 • 1♀, Cidade dos Meninos, Santa Maria, Rio Grande do Sul; 29°40'31"S, 53°43'10"W; 15 Jan. 1998; L. Indrusiak & M. Monteiro leg.; MCTP 38671 • 1♂, Barra do Ouro, Maquiné, Rio Grande do Sul; 29°32'18"S, 50°14'48"W; 05 Jun. 2011; R.A. Teixeira leg.; MCTP 39905 • 1♂, Santa Maria, Rio Grande do Sul; 29°41'02"S, 53°48'25"W; 15 Dec. 2004; L. Indrusiak leg.; MCTP 40017 • 1♂, same locality and collector of the previous vial; 27 Aug. 2003; MCTP 40019 • 1♂, Estação Fitotécnica de Viamão, Viamão, Rio Grande do Sul; 30°02'11"S, 51°01'18"W; 06 May 1994; A.A. Lise leg.; MCTP 4678 • 1♂, 1♀, Viamão, Rio Grande do Sul; 30°04'25"S, 51°06'27"W; 23 Sep. 1994; A.A. Lise leg.; MCTP 8407 • 1♂, Pró-Mata, Potreiro Velho, São Francisco de Paula, Rio Grande do Sul; 29°28'51"S, 50°10'28"W; Jul.

2001; L.A. Bertoncello & A.A. Lise leg.; MCTP 19434 • 1♂, same locality and collectors of the previous vial; Oct. 2001; MCTP 19436.

Description

Female (MCTP 38671) — Anterior eye row strongly recurved and posterior slightly procurve, prosoma predominantly dark-brown with yellowish stains on sides; thoracic region with a pronounced median spire (Fig. 10A, B). Legs dark-brown with dispersed lighter stains; femora I and II dorsally enlarged, suffused with dorsolateral and ventral conical sockets with a conical macrosetae in each one; tibiae I and II with four pairs of ventral macrosetae (Fig. 10A). Clypeus lighter than the rest of prosoma, with a marginal yellowish triangle-shaped mark; chelicerae brown with yellowish stains (Fig. 10B), sternum scutiform, slightly longer than wide, dark-brown with a yellow median macula, endites and labium truncated and totally dark-brown. Opisthosoma dark-brown, rough surfaced, with concave anterior border and a remarkable white taint between the anterior muscular sigilla; the median posterior opisthosomal projection presents acuminate orange tubercles at the tip, with many leaf-shaped setae (Fig. 10B). Measurements: eyes diameters and eyes interdistances: AME 0.09, ALE 0.14, PME 0.09, PLE 0.09, AME-AME 0.09, AME-ALE 0.12, PME-PME 0.24, PME-PLE 0.08, MOQ length 0.45, MOQ width 0.40; leg formula: 1-2-4-3: leg I – femur 3.83/ patella 2.07/ tibiae 2.59/ metatarsus 1.81/ tarsus 1.29/ total 11.59; II – 3.78/ 1.96/ 2.38/ 1.76/ 1.29/ 11.17; III – 1.96/ 1.29/ 1.70/ 1.03/ 0.77/ 6.75; IV – 2.48/ 1.29/ 1.81/ 1.34/ 0.82/ 7.74. Total body length 9.81; prosoma 4.14 length, 3.83 wide; opisthosoma length 4.87; clypeus 0.28 height; sternum 1.41 length, 1.12 width; endites 0.74 length, 0.38 width; labium 0.41 length, 0.51 width.

Fig. 10. Female of *Kryptochroma pentacantha* (Mello-Leitão, 1929): **(A)** dorsal habitus; **(B)** front; **(C, E)** ventral view of the epigynal plate; **(D, F)** dorsal view of the spermathecae.

Male (MCTP 25762): eyes disposition and prosoma coloration pattern as in female, except by the posterior slope scars, which are yellow (Fig. 11A). Metatarsi of all legs with a distal yellow stain and posterior femora noticeably bicolor, half yellow, half dark-brown; other leg characteristics as in females (Fig. 11A). Front lighter than the rest of prosoma due to a yellowish triangular mark that extends from the clypeus until the ALE (Fig. 11B). Sternum scutiform, as long as wide, dark-brown with a yellow taint; labium and endites totally dark-brown and truncated. Opisthosoma as in female, except by the shorter median posterior opisthosomal projection and the lack of agglomerated orange tubercles. Measurements: eyes diameters and eyes interdistances: AME 0.08, ALE 0.11, PME 0.08, PLE 0.08, AME-AME 0.06, AME-ALE 0.06, PME-PME 0.16, PME-PLE 0.06, MOQ length 0.32, MOQ width 0.35; leg formula: 1-2-4-3: leg I – femur 1.61/ patella 0.88/ tibiae 1.24/ metatarsus 0.91/ tarsus 0.56/ total 5.20; II – 1.38/ 0.72/ 0.88/ 0.75/ 0.51/ 4.24; III – 0.88/ 0.48/ 0.72/ 0.48/ 0.35/ 2.91; IV – 1.12/ 0.48/ 0.72/ 0.56/ 0.40/ 3.28. Total body length 5.17; prosoma 2.43 length, 2.33 wide;

opisthosoma length 2.74; clypeus 0.29 height; sternum 0.87 length, 0.80 width; endites 0.04 length, 0.24 width; labium 0.25 length, 0.32 width.
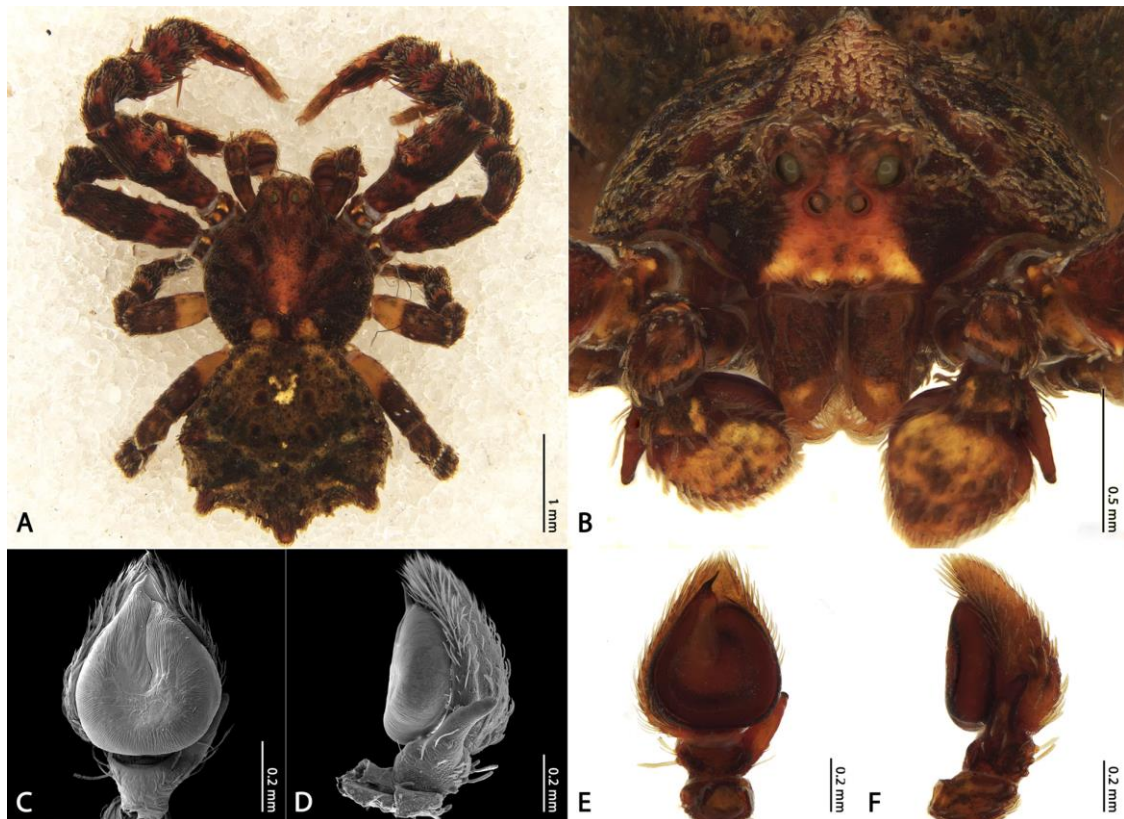

Fig. 11. Male of *Kryptochroma pentacantha* (Mello-Leitão, 1929): **(A)** dorsal habitus; **(B)** front; **(C, E)** ventral view of the left male palp; **(D, F)** retrolateral view of the left male palp.

Remarks

Females may present a longitudinal yellow line on prosoma and the opisthosoma entirely yellowish on dorsum (Fig. 2C). In some cases, males and females may bear a pair of white spots on the upper lateral opisthosomal projections (Fig. 2D, E).

Distribution

Brazil (Amazonas, Espiríto Santo, São Paulo, Paraná, Santa Catarina and Rio Grande do Sul) — Fig. 18.

Kryptochroma quadrata Machado & Viecelli **sp. nov.**

Figs 12, 13

Diagnosis. Males of *K. quadrata* **sp. nov.** resemble those of *K. pentacantha* by the sinuous and apical embolus (Fig. 13C, E), however, it can be distinguished from those and other males of the genus by the rounded tegulum, which also presents a retrolateral reentrance, and by the squared-tipped RTA with remarkable grooved surface (Fig. 13D, F). The female presents an anterior longitudinal ruckle connected to a shallow and convex hood structure on the epigynal plate, with no median outgrowth, gutters or septum separating the copulatory openings (Fig. 12C, E).

Etymology

The epithet – a Latin feminine adjective that means squared – is a direct reference to the shape of the RTA tip, which ends abruptly.

Material examined

Holotype

BRAZIL • ♂; Base de Operações Geólogo Pedro de Moura, Porto Urucu, Coari, Amazonas; 4°53′42.5″S 65°11′18.2″W; 28 Sep. 2006; C.A.C. Santos Jr. leg.; UFMG 22673.

Paratypes

BRAZIL • ♀; Base de Operações Geólogo Pedro de Moura, Coari, Amazonas; 4°53′42.5″S 65°11′18.2″W; 28 Sep. 2006; C.A.C. Santos Jr. leg.; MPEG 22669 • ♀; Base de Operações Geólogo Pedro de Moura, Porto Urucu, Coari, Amazonas 04°50′01″S 65°03′53″W; 28 Sep. 2006; D. Guimarães leg.; UFMG 22673 • ♀, Base de Operações Geólogo Pedro de Moura, Coari, Amazonas; Sep. 2006; D. Candiani leg.; MPEG 13297.

Other material

Only the type material.

Description

Female (MPEG 13297) — Anterior eye row strongly recurved and posterior procurve, ocular mounds discrete, not as elevated as in other species, prosoma predominantly yellow, black on the sides, MS well developed (Fig. 12A, B). Legs

122

coloration as in *K. gigas* **sp. nov.** Chelicerae yellow with two pairs of dark stains, sternum slightly longer than wide, brown with a large yellow stain, endites and labium truncated and totally brown. Opisthosoma with concave anterior border, predominantly yellow, dark-brown on sides and on the back of the abdominal projections (Fig. 12A). Spermathecae rounded and smooth surfaced (Fig. 12D, F). Measurements: eyes diameters and eyes interdistances: AME 0.06, ALE 0.11, PME 0.08, PLE 0.08, AME-AME 0.12, AME-ALE 0.16, PME-PME 0.27, PME-PLE 0.09, MOQ length 0.48, MOQ width 0.51; leg formula: 1-2-4-3: leg I – femur 5.18/ patella 2.59/ tibiae 3.47/ metatarsus 2.07/ tarsus 1.39/ total 14.70; II – 4.14/ 2.33/ 2.84/ 1.81/ 1.29/ 9.57; III – 2.33/ 1.29/ 2.07/ 1.03/ 0.88/ 7.60; IV – 2.90/ 1.29/ 1.91/ 1.24/ 0.93/ 8.27. Total body length 7.25; prosoma 3.50 length, 3.37 wide; opisthosoma length 3.75; clypeus 0.32 height; sternum 1.53 length, 1.29 width; endites 0.80 length, 0.40 width; labium 0.56 length, 0.58 width.
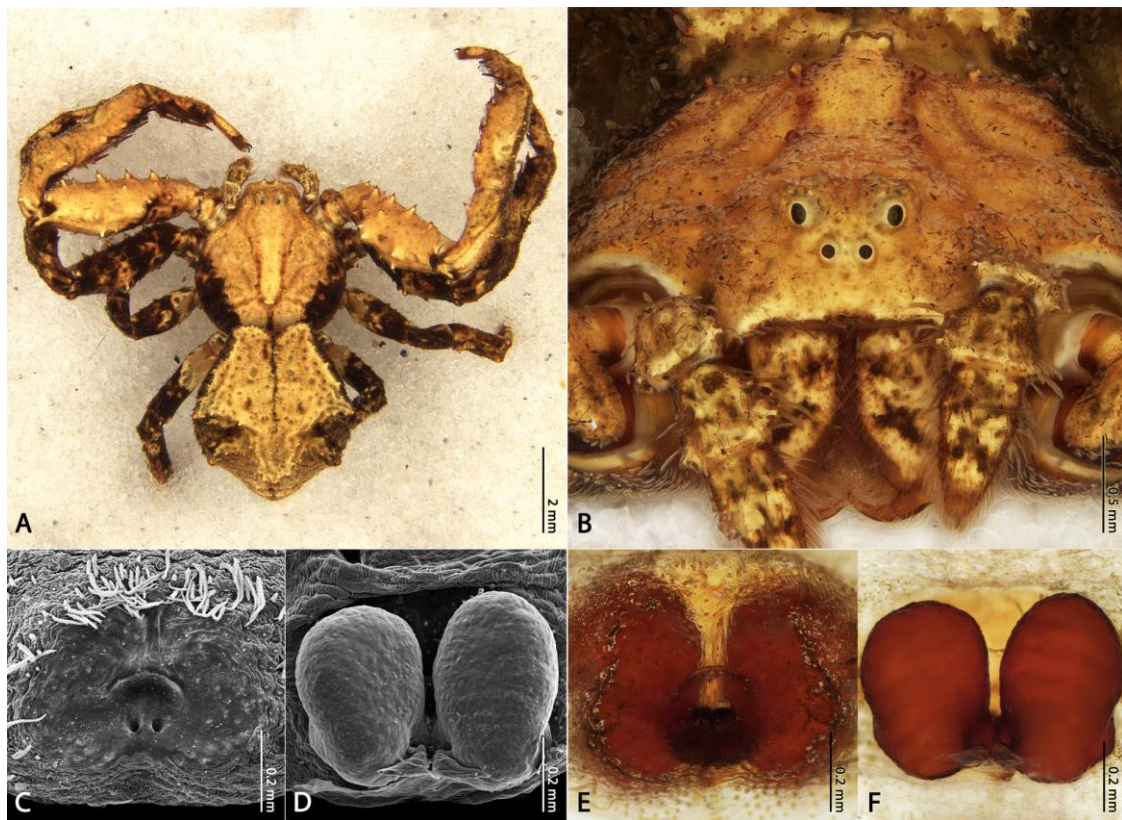

Fig. 12. Female of *Kryptochroma quadrata* **sp. nov.**: **(A)** dorsal habitus; **(B)** front; **(C, E)** ventral view of the epigynal plate; **(D, F)** dorsal view of the spermathecae.

Male (MPEG 22673) — Anterior eye row very recurved, posterior procurved, ALE with almost two times the size of AME; prosoma knobby, predominantly light

brown with its median region, clypeus and posterior slope scars yellowish; medial spire absent (Fig. 13A, B). Anterior legs light-brown with some darker taints while legs III and IV are lighter, with extensive whitish areas; anterior femora enlarged, with dorsolateral setiferous tubercles randomly distributed and ventral region dark-brown; tibiae I and II with four pairs of ventral macrosetae and anterior metatarsi with three pairs (Fig. 13A). Sternum scutiform, light-brown with a median white stain. Opisthosoma pale yellow with small white punctuations and posterior black spots; straight anterior border and five short spiniform projections. Measurements: eyes diameters and eyes interdistances: AME 0.06, ALE 0.08, PME 0.06, PLE 0.06, AME-AME 0.06, AME-ALE 0.08, PME-PME 0.16, PME-PLE 0.06, MOQ length 0.29, MOQ width 0.32; leg formula: 1-2-4-3: leg I – femur 2.23/ patella 1.24/ tibiae 1.33/ metatarsus 0.88/ tarsus 0.56/ total 6.24; II – 1.45/ 0.72/ 1.04/ 0.72/ 0.50/ 4.43; III – 0.87/ 0.48/ 0.80/ 0.45/ 0.37/ 2.97; IV – 1.12/ 0.48/ 0.80/ 0.56/ 0.40/ 3.36. Total body length 4.61; prosoma 2.28 length, 2.18 width; opisthosoma length 2.33; clypeus 0.24 height; sternum 0.83 length, 0.72 width; endites 0.40 length, 0.24 width; labium 0.20 length, 0.32 width.

**Distribution.** Brazil (Amazonas) — Fig. 18.
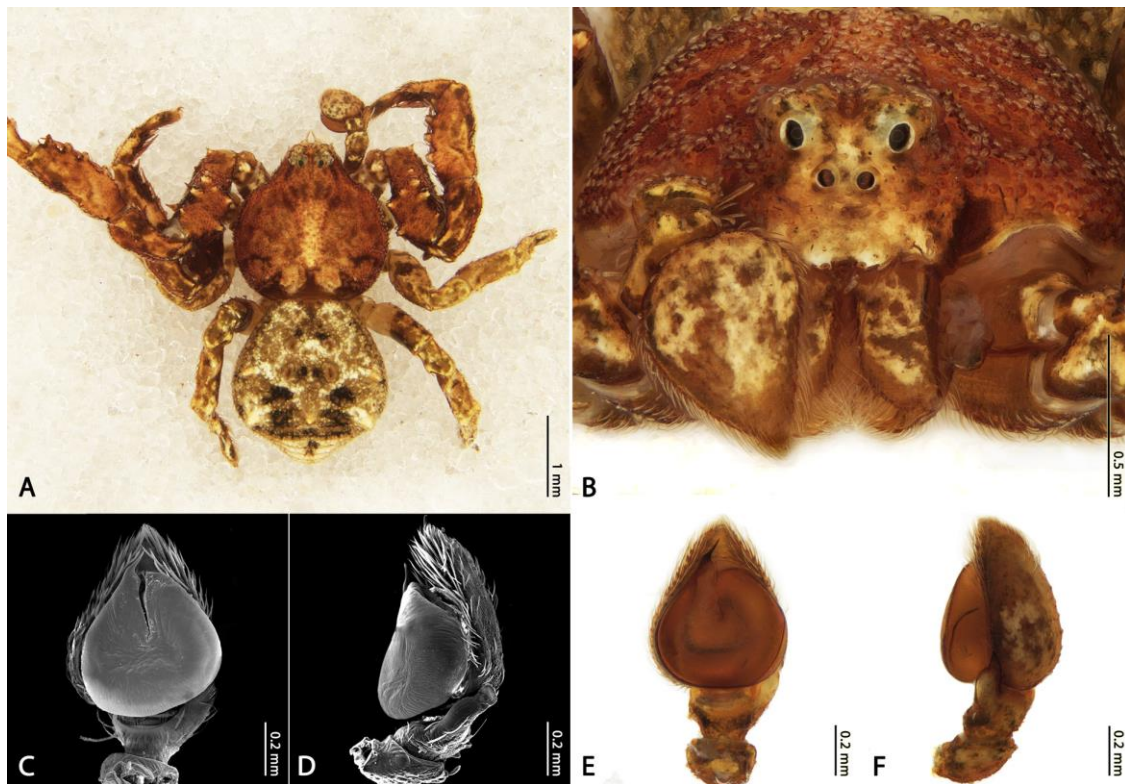
Fig. 13. Male of *Kryptochroma quadrata* **sp. nov.**: **(A)** dorsal habitus; **(B)** front; **(C, E)** ventral view of the left male palp; **(D, F)** retrolateral view of the left male palp.

Kryptochroma quinquetuberculata (Taczanowski, 1872) **comb. nov.**

Fig. 14

Thomisus quinquetuberculatus Taczanowski, 1872: 100.

Stephanopis quinquetuberculata Keyserling, 1880: 171, fig. 94.

Tobias quinquetuberculatus Simon, 1895: 1053.

Stephanopis quinquetuberculata Mello-Leitão, 1929: 62; Machado, Teixeira & Lise, 2017: 454, f. S4D, S5B, S7E, S10C, S11D, S13E, S14D. **New combination.**

Diagnosis

Males of *K. quinquetuberculata* (Taczanowski, 1872) **comb. nov.** resemble those of *K. pentacantha* by their stout opisthosomal projections and by the presence of a dorsal white macula on the opisthosoma (Fig. 14A). However, they can be recognized by their more "water drop-shaped" tegulum with straight and tip-narrowed embolous instead of a curved termination observed in its closest correlated species (Fig. 14D, E). Moreover, *K. quinquetuberculata* bears a remarkable RTA which is

large at the basis, sharpen abruptly at the tip, curved and sinuous, pointing towards to the dorsum of the cymbium (Fig. 14D, F).

Material examined

Genotype

COLOMBIA • ♂; (MNHN 3479).

Other Material

FRENCH GUIANA • 1♂; Massif du Mitaraka, Maripasoula; 02°17'26"N, 54°31'18"W; 2015; Vedel leg.; MCTP 42644 • 1♂; Mont Itoupe, Sommet Tabulaire, Maripasoula; 03°32'13"N, 53°34'25"W; 13 Nov. 2014; Vedel & Lalague leg.; MCTP 42645. BRAZIL • 1♂, 1j; Horto Dois Irmãos, Recife; 8°00'35"S, 34°56'51"W; 13 Sep. 1999; M. Peres leg.; IBSP 38639 • 1♂; Reserva Biológica de Una, Una, Bahia; 15°10'42"S, 39°06'13"W; 15-28 Nov. 2000; A.D. Brescovit leg.; IBSP 46738 • 1♂; same locality and collector of the previous vial; IBSP 46712 • 1♂; same locality and collector of the previous vial; IBSP 46714 • 1♂; same locality and collector of the previous vial; IBSP 46724 • 1♂; same locality and collector of the previous vial; IBSP 46726 • 1♂; same locality and collector of the previous vial; IBSP 46740 • 1♂; Reserva Zoobotânica CEPLAC, Bahia; 14°46'22"S, 39°13'13"W; 08 Dec. 2010; G.H.F. Azevedo & A.J. Santos leg.; UFMG 9484.

Description

Male (IBSP 46712) — Anterior eye row strongly recurved, posterior slightly procurved; prosoma predominantly dark-brown with discrete MS; clypeus lighter than the rest of prosoma with light spots at its lateral margins (Fig. 14B). Anterior legs (I and II) dark-brown and posterior femora (III and IV) presenting their proximal half yellow; labium, endites and chelicerae dark-brown. Opisthosoma predominantly brown with a dorsal white macula at its median region and a light transversal line connecting the anterolateral projections (Fig. 14A). Measurements: eyes diameters and eyes interdistances: AME 0.06, ALE 0.11, PME 0.09, PLE 0.09, AME-AME 0.06, AME-ALE 0.08, PME-PME 0.16, PME-PLE 0.04, MOQ length 0.32, MOQ width 0.35; leg formula: 1-2-4-3: leg I – femur 1.61/ patella 0.88/ tibiae 1.19/ metatarsus 0.88/ tarsus 0.56/ total 5.12; II – 1.45/ 0.72/ 0.96/ 0.72/ 0.48/ 4.33; III – 0.88/ 0.48/ 0.72/ 0.48/ 0.37/ 2.93; IV – 1.01/ 0.48/ 0.80/ 0.48/ 0.40/ 3.17. Total body length 4.39;

prosoma 2.12 length, 2.07 wide; opisthosoma length 2.22; clypeus 0.24 height; sternum 0.85 length, 0.72 width; endites 0.32 length, 0.25 width; labium 0.16 length, 0.29 width.

Female — unknown.
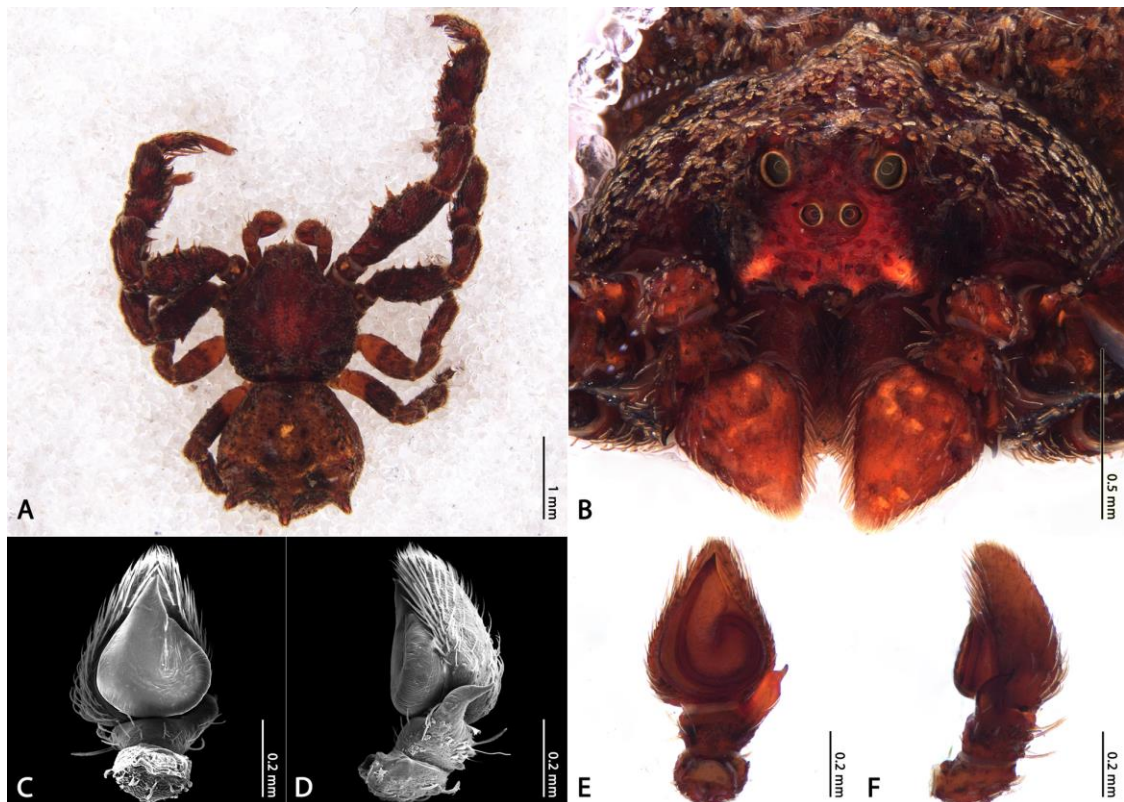
Fig. 14. Male of *Kryptochroma quinquetuberculata* (Taczanowski, 1872): **(A)** dorsal habitus; **(B)** front; **(C, E)** ventral view of the left male palp; **(D, F)** retrolateral view of the left male palp.

Remarks

According to Keyserking (1880), the description of the species in his work was based on the holotype originally proposed by Taczanowski (1872), from Cayenne (French Guiana). Although this specimen has been posteriorly lost, Keyserling (1880) designated a genotype (MNHN 3479) from a near locality of the original one. We consider the genotype as the closest evidence and certainly as being co-specific of the holotype. The species can be easily recognized by the illustrations provided by Keyserling (1880), where this author highlighted the diagnostic features of the male palpus: sinuous RTA and the tip-narrowed tegulum.

The specimen illustrated in the phylogenetic analysis by Machado *et al.* (2017) as *S. quinquetuberculata* is in fact a *K. pentacantha*, ergo represents a misidentification.

Males may present opisthosoma predominantly dark-yellow and a faded yellowish dorsal stain going from the MS almost until the PME (Fig. 2F).

Distribution

Brazil (Bahia and Pernambuco) and French Guiana (Cayenne and Maripasoula) — Fig. 18.

Kryptochroma renipalpis (Mello-Leitão, 1929) **comb. nov.**

Fig. 15

Stephanopis renipalpis Mello-Leitão, 1929: 60, fig. 143-144.

Diagnosis

Males of *K. renipalpis* (Mello-Leitão, 1929) **comb. nov.** are similar to those of *K. quinquetuberculata* (Taczanowski, 1872) **comb. nov.** due to their well-developed MS, light clypeus and white macula on dorsum (Fig. 15A, B). However, can be distinguished from this and other co-generic species by the medially positioned spermatic duct (Fig. 15C, E) and extreme curvature of the RTA, which is thinner than in the other species and smooth at the tip (Fig. 15D, F).

Material examined

  Holotype

BRAZIL • ♂; Rio de Janeiro; MNHN 6945

  Other material

BRAZIL • 1♂; Enseada das Palmas, Ilha Grande, Angra dos Reis, Rio de Janeiro; 23°08'30"S, 44°08'26"W; 02-12 Fev. 1997; M. Ramírez leg.; MCTP 42730.

Description

Male (MCTP 42655) — Anterior row eye strongly recurved and posterior slightly procurved (Fig. 16A, B); prosoma predominantly reddish-brown with clypeus whitish (Fig. 15B); sternum slightly longer than wide, entirely reddish-brown; labium truncated and totally dark-brown; chelicerae reddish-brown with distal lighter spots. Anterior legs (I and II) mostly reddish-brown, with yellowish spots on the proximal portion of metatarsi and tarsi; posterior legs (III and IV) with bicolor femora; opisthosoma rough surfaced, dark-yellow with red spiniform projections (Fig. 15A). Measurements: eyes diameters and eyes interdistances: AME 0.06, ALE 0.09, PME 0.08, PLE 0.08, AME-AME 0.08, AME-ALE 0.06, PME-PME 0.12, PME-PLE 0.04,MOQ length 0.27, MOQ width 0.37; leg formula: 1-2-4-3:leg I – femur 1.91/ patella 21.03/ tibiae 1.29/ metatarsus 1.03/ tarsus 0.67/ total 5.93; II – 1.29/ 0.67/ 0.88/ 0.70/ 0.48/ 4.02; III – 0.85/ 0.45/ 0.64/ 0.41/ 0.32/ 2.67; IV – 0.91/ 0.40/ 0.72/ 0.51/ 0.37/ 2.91. Total body length 4.24; prosoma 2.07 length, 1.96 wide; opisthosoma length 2.17; clypeus 0.19 height; sternum 0.74 length, 0.67 width; endites 0.38 length, 0.29 width; labium 0.22 length, 0.29 width.

Female — unknown.

Remarks

Mello-Leitão (1929) designated a "cotype" (MNHN 17335) of *S. renipalpis* from Pernambuco, however, the specimen was not found.

Distribution

Brazil (Rio de Janeiro) — Fig. 18.
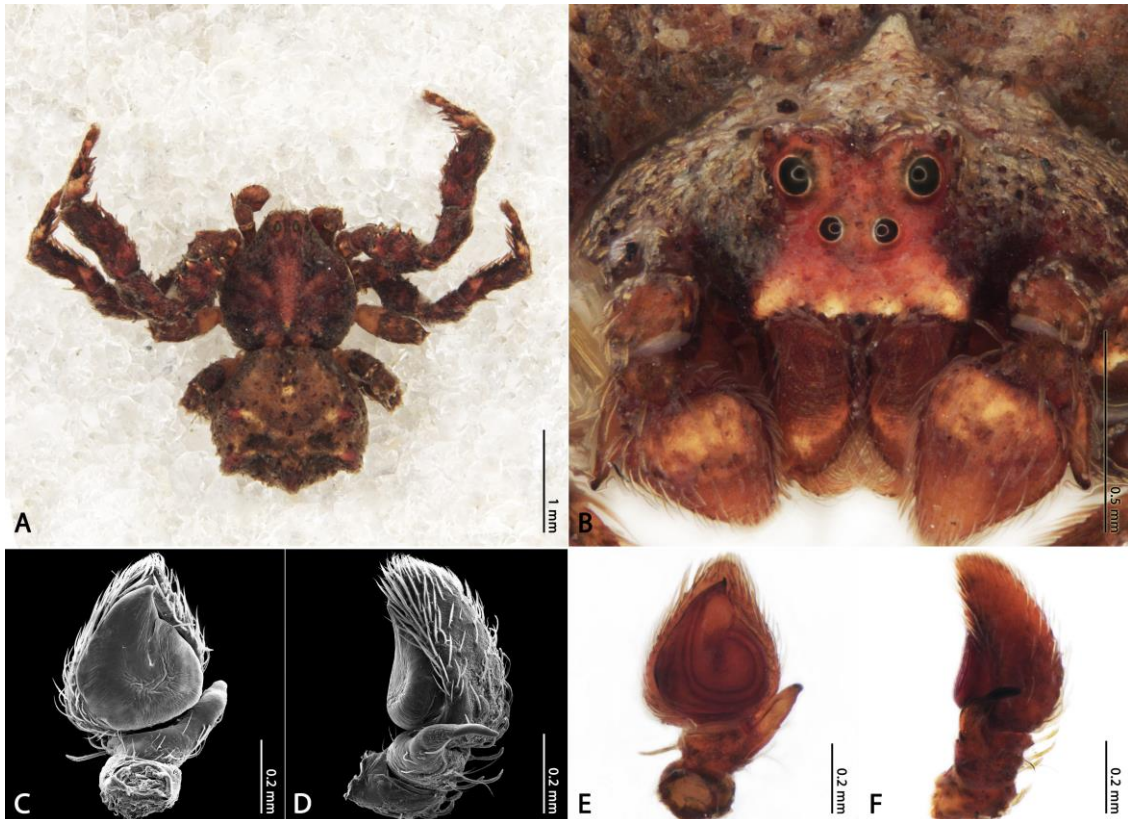
Fig. 15. Male of *Kryptochroma renipalpis* (Mello-Leitão, 1929): **(A)** dorsal habitus; **(B)** front; **(C, E)** ventral view of the left male palp; **(D, F)** retrolateral view of the left male palp.

Kryptochroma septata Machado & Teixeira **sp. nov.**

Figs 16, 17

Diagnosis

The females of *K. septata* **sp. nov.** are similar to those of *K. pentacantha* (Mello-Leitão, 1929) **comb. nov.** by their general body shape, prominent thoracic spire and well-developed median opisthosomal projection, however, females of *K. septata* **sp. nov.** can be recognized by the large median septum on the epigynal plate and by the deep excavations where the elliptical copulatory openings are located (Fig. 16C, E). Males are similar to those of *S. quadrata* **sp. nov.** by the more rounded tegulum and to *K. pentacantha* by the stout and conical RTA, however, can be distinguished from these two species by its shorter, thicker and more curved embolous (Fig. 17C, E). Differently from *K. pentacantha*, in males of *K. septata* **sp. nov.** the RTA presents a terminal curvature that makes this apophysis points vertically rather to the backwards of the cymbium (Fig. 17D, F).

Etymology

The name is a reference to the remarkable median septum on the epigynal plate of females.

Material examined

Holotype

BRAZIL • ♀; Parque Nacional do Caparaó, Vale Verde, Minas Gerais; 20°25′5.9″S 41°50′48.7″W; 24–30 Nov. 2014; B.T. Faleiro leg.; UFMG 18269.

Paratype

BRAZIL • ♂; same data as for holotype; UFMG 22431

Other material

Only the type material.

Description

Female (UFMG 18296) — Anterior row eye strongly recurved and posterior slightly procurved (Fig. 16B); ALE slightly larger than AME; prosoma predominantly dark-yellow with cephalic region dark-brown; clypeus yellow; sternum slightly longer than wide, dark-brown with a central yellow stain; labium truncated and totally dark-brown; chelicerae and anterior legs (I and II) dark-yellow with dark taints randomly distributed; posterior legs (III and IV) predominantly yellow; opisthosoma rough surfaced, predominantly dark-yellow, with dark-brown stains bypassing the upper-lateral opisthosomal projections and the median posterior one; a central white macula can be observed on the dorsum (Fig. 16A); spermathecae smooth surfaced and kidney-shaped (Fig. 16D, F). Measurements: eyes diameters and eyes interdistances: AME 0.10, ALE 0.16, PME 0.14, PLE 0.14, AME-AME 0.12, AME-ALE 0.14, PME-PME 0.22, PME-PLE 0.07, MOQ length 0.12, MOQ width 0.20; leg formula: 1-2-4-3: leg I – femur 4/ patella 2.15/ tibiae 2.75/ metatarsus 1.75/ tarsus 1.15/ total 11.80; II – 3.25/ 1.80/ 2.25/ 1.50/ 1.15/ 9.95; III – 1.75/ 1/ 1.50/ 0.90/ 0.90/ 6.05; IV – 2.25/ 0.75/ 1.75/ 1/ 0.80/ 6.55. Total body length 7.80; prosoma 3.65 length, 3.75 wide; opisthosoma length 4.15; clypeus 0.40 height; sternum 1.70 length, 1.50 width; endites 0.90 length, 0.46 width; labium 0.48 length, 0.74 width.
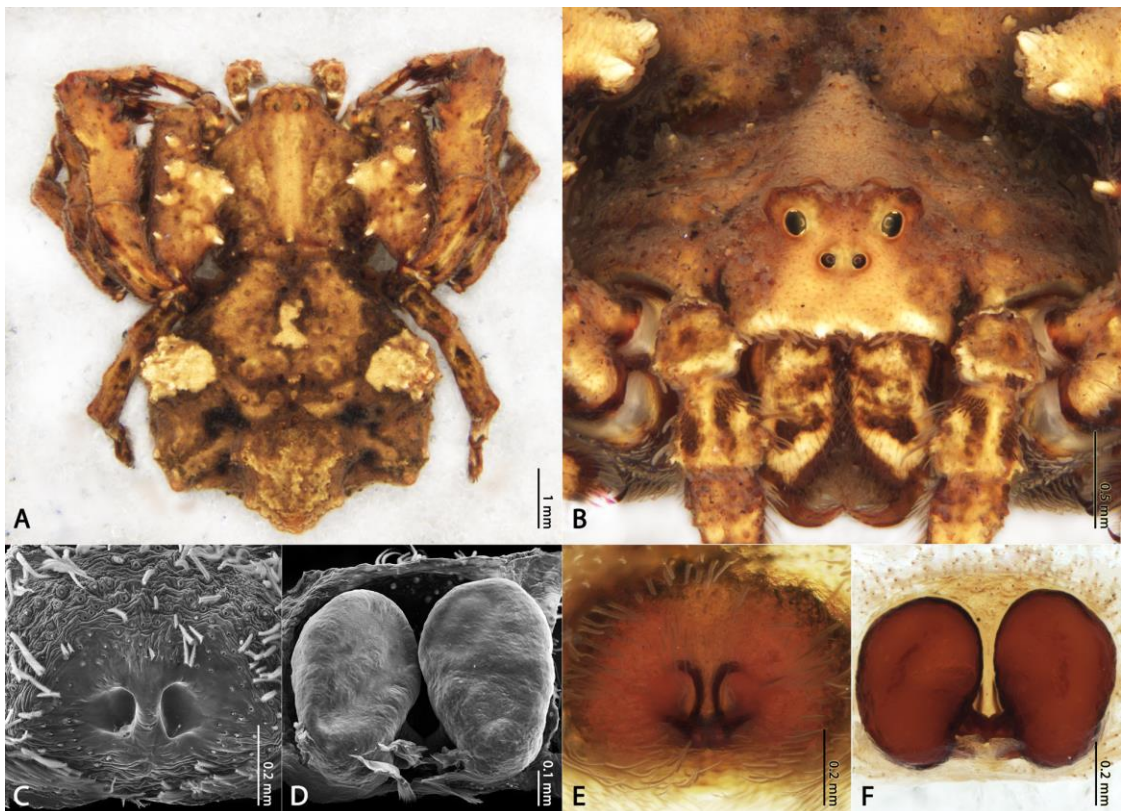
Fig. 16. Female of *Kryptochroma septata* **sp. nov.**: **(A)** dorsal habitus; **(B)** front; **(C, E)** ventral view of the epigynal plate; **(D, F)** dorsal view of the spermathecae.

Male (UFMG 22431) — Prosoma reddish-brown with lighter median area and clypeus (Fig. 17A, B). Anterior legs (I and II) reddish-brown with macrosetae sockets yellowish-white; posterior femora (III and IV) bicolor, yellow on their proximal half and reddish-brown on its distal part. Opisthosoma predominantly brown with black punctuations; opisthosomal projections are reddish and bear white maculae on its basis; a dorsal white guanine spot can be also observed on the median region of the dorsum (Fig. 17A). Measurements: eyes diameters and eyes interdistances: AME 0.07, ALE 0.09, PME 0.07, PLE 0.07, AME-AME 0.09, AME-ALE 0.09, PME-PME 0.16, PME-PLE 0.07, MOQ length 0.28, MOQ width 0.23; leg formula: 1-2-4-3: leg I – femur 1.71/ patella 0.92/ tibiae 1.35/ metatarsus 1.02/ tarsus 0.57/ total 5.57; II – 1.33/ 0.83/ 1.04/ 0.80/ 0.59/ 4.59; III – 0.88/ 0.57/ 0.78/ 0.54/ 0.38/ 3.15; IV – 1.09/ 0.57/ 0.85/ 0.64/ 0.42/ 3.57. Total body length 4.16; prosoma 1.97 length, 1.85 wide; opisthosoma length 2.19; clypeus 0.23 height; sternum 0.88 length, 0.88width; endites 0.40 length, 0.21 width; labium 0.21 length, 0.30 width.
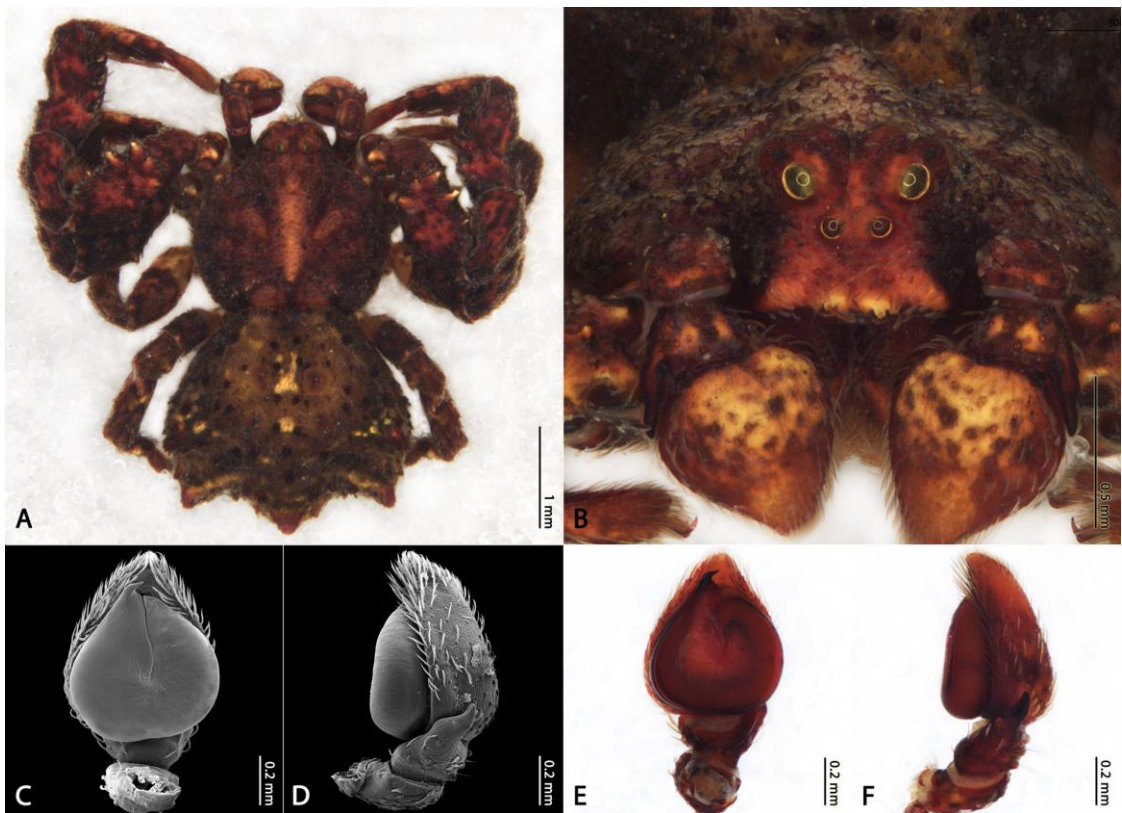
Fig. 17. Male of *Kryptochroma septata* **sp. nov.**: **(A)** dorsal habitus; **(B)** front; **(C, E)** ventral view of the left male palp; **(D, F)** retrolateral view of the left male palp.

Distribution

Brazil (Espírito Santo and Minas Gerais) — Fig. 18.
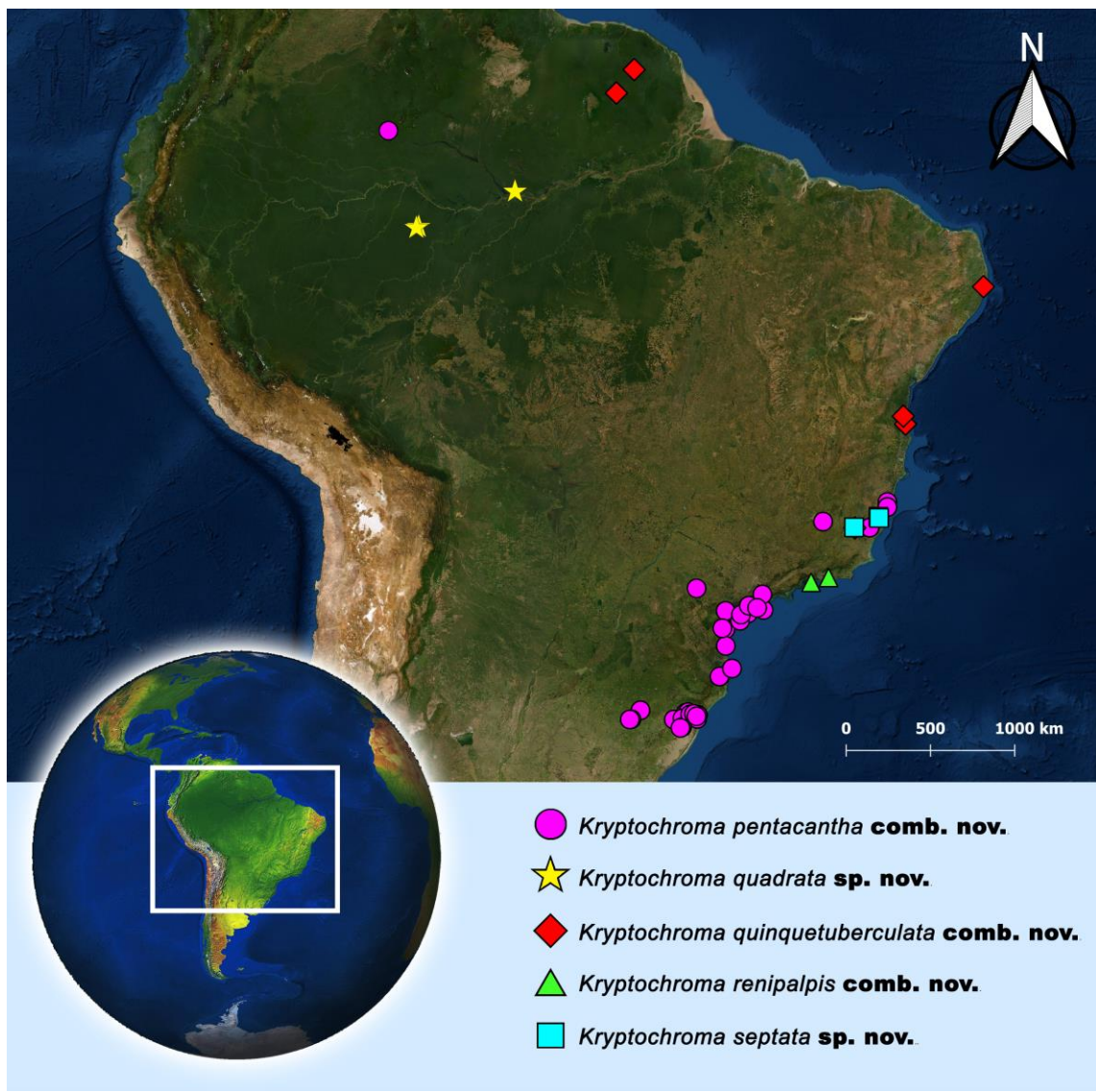
Fig. 18. Distribution records of *Kryptochroma* **gen. nov.**

Misplaced species

Stephanopis aheneus Soares & Soares, 1946: p. 57, Figs 5, 6 (male holotype from Rio São José, Colatina, Espírito Santo, Brazil, Soares, B.A.M. leg.,15 September 1942, deposited in MZSP 666, examined).

This species is proposed here as junior synonymy of the *Epicadus tuberculatus* (Petrunkevitch, 1910) based on the shape of the tegulum, RTA and the presence of tubercles on the thoracic portion of the prosoma (Fig. S4) – complete synonymic list in Prado *et al*. (2018).

Stephanopis borgmeyeri Mello-Leitão, 1929: p. 54, fig. 40 (female immature holotype from Petrópolis, Rio de Janeiro, Brazil, deposited in MNRJ 917, examined).

Proposed as *nomen dubium* once the immature specimen does not allow a reliable identification.

Stephanopis furcillata Keyserling, 1880: p. 179, plate 4, fig. 98 (female holotype from Brazil, deposited in ZMHB 2406, examined).

We propose *Stephanopis furcillata* as senior synonym of *Sidymella multispinulosa* (Mello-Leitão, 1944), based on the distinct opisthosoma presenting a long pair of projections with a terminal tubercle at their tips (Fig. S5C, D).

Stephanopis quimiliensis Mello-Leitão, 1942: p. 408, Figs 33, 34 (male holotype from Quimilí, Santiago del Estero, Argentina, Birabén, M. leg., deposited in MLP 15455, examined).

This species lacks the typical cheliceral teeth that is still considered as a diagnostic feature for Stephanopinae. Instead, its elongated labium and peglike-setae on endites allow us to undoubtedly consider this spider as an Aphantochilinae (Teixeira *et al.* 2014). We propose the transference of *S. quimiliensis* to *Ulocymus* based on the presence of stout and conical projections on the dorsum of the prosoma (Teixeira *et al.* 2014) and shape of the copulatory structures (Fig. S6).

Stephanopis salobrensis Mello-Leitão, 1929: p. 57, Figs 137–139 (in part – male syntype, collected from Salobro, Bahia, Brazil, deposited in MNHN 3973, examined).

The syntypic series of *S. salobrensis* is constituted by four individuals of three different species: the male specimen (Fig. S7A, B) is conspecific to those described by Machado et al. (2015) as *Epicadus caudatus*, whose is synonymized here to *Epicadus stelloides* (Walckenaer, 1837) **comb. nov.** On the other hand, there are two different female species in this same series. Two females are clearly conspecific to those *K. parahybana* (represented here) (Fig. S7C, D), however, the other one is a subadult female, what made imposible to safely assign its identity. Therefore, we consider the male of *Stephanopis salobrensis* as a junior synonymy of the *E. stelloides* **comb. nov.**, two females as junior synonym of *K. parahybana* **comb. nov.** and, given that the other female is subadult, propose the name as *nomen dubium*.

Stephanopis stelloides (Walckenaer, 1837): *Thomisus stelloides* Walckenaer, 1837: p. 514 (female holotype from "Ilê Tortue", Tortuga, Haiti, deposited in MNHN, probably lost). *Stephanopis stelloides*: Keyserling, 1880: p. 173 (female "cotype" collected from "Tortosa" by Meneville, G., not located).

Despite the holotype described by Walckenaer (1837) is presumably lost, and the 'conspecific' and sympatric specimen used by Keyserling (1880) to describe *S. stelloides* had not been found, the original descriptions and illustrations allowed us to identify this species as the same as *Epicadus caudatus*. Thus, we propose a new combination of *Stephanopis stelloides* to *Epicadus* and their senior synonymy to *E. caudatus*. (Fig. S8).

Stephanopis trilobata Mello-Leitão, 1929: p. 56, fig. 136 (female holotype by original designation, collected in Goiás, Brazil, deposited in MNHN 21629, examined; female cotype, collected in Goiás, Brazil, deposited in MNHN 21628, examined).

This species is recognized here as a junior synonymy of *Epicadus stelloides* (Walckenaer, 1837) **comb. nov.** (Fig. S9) based on the remarkable shape of the epigynal plate of this species (large median septum and elliptical copulatory openings) and opisthosoma bearing three projections, being the tips of the lateral pair curved anteriorly (see Machado *et al*. 2015 — Figs 1, 2).

References

Keyserling E. 1880. *Die Spinnen Amerikas, I. Laterigradae*. Bauer & Raspe (E. Küster), Nürnberg. https://doi.org/10.5962/bhl. title.64832

Machado M., Teixeira R.A., Lise A.A. 2015. Taxonomic notes on the crab spider genus *Tobias* Simon, 1895 (Araneae, Thomisidae, Stephanopinae). *Zootaxa* 4034: 565–576. http://dx.doi.org/10.11646/zootaxa.4034.3.8

Machado M., Teixeira R.A., Lise A.A. 2017. Cladistic analysis supports the monophyly of the Neotropical crab spider genus *Epicadus* and its senior synonymy over *Tobias* (Araneae: Thomisidae). *Invertebrate Systematics* 31: 442–455. https://doi.org/10.1071/IS16074

Machado M., Teixeira R.A., Lise A.A. 2018. There and back again: More on the taxonomy of the crab spider genus *Epicadus* (Thomisidae: Stephanopinae). *Zootaxa* 4382: 501–530. https://doi.org/10.11646/zootaxa.4382.3.4

Machado M., Guzati C., Viecelli R., Molina-Gómez D., Teixeira R.A. 2019a. A taxonomic review of the crab spider genus *Sidymella* (Araneae, Thomisidae) in the Neotropics. *Zoosystematics and Evolution* 95: 319–344.
https://doi.org/10.3897/zse.95.34958

Machado M., Teixeira R.A., Milledge G.A. 2019b. On the Australian bark crab spiders genus *Stephanopis*: Taxonomic review and description of seven new species (Araneae: Thomisidae: Stephanopinae). *Records of the Australian Museum* 71: 217–276. https://doi.org/10.3853/j.2201-4349.71.2019.1698

Mello-Leitão C.F. 1929. *Aphantochilidas e Thomisidas do Brasil*. Archivos do Museu Nacional, Rio de Janeiro.

Prado A.W., Baptista R.L.C., Machado M. 2018. Taxonomic review of *Epicadinus* Simon, 1895 (Araneae: Thomisidae). *Zootaxa* 4459: 201–234. http://dx.doi.org/10.11646/zootaxa.4459.2.1

Simon, E. 1895. *Histoire naturelle des araignées*. Librairie Encyclopédique de Roret, Paris.

Silva-Moreira T., Machado M. 2016. Taxonomic revision of the crab spider genus *Epicadus* Simon, 1895 (Arachnida: Araneae: Thomisidae) with notes on related genera of Stephanopinae Simon, 1895. *Zootaxa* 4147: 281–310. http://dx.doi.org/10.11646/zootaxa.4147.3.4

Taczanowski L. 1872. '*Les Aranéides de la Guyane Française*, *Vol. 9*'. Horae Societatis Entomologicae Rossicae, Saint Petersburg.

Wheeler W.C., Coddington J.A., Crowley L.M., Dimitrov D., Goloboff P.A., Griswold C.E., Hormiga G., Prendini L., Ramírez M.J., Sierwald P., Almeida-Silva L., Álvarez-Padilla F., Arnedo M.A., Benavides Silva L.R., Benjamin S.P., Bond J.E., Grismado C.J., Hasan E., Hedin M., Izquierdo M.A., Labarque F.M., Ledford J., Lopardo L., Maddison W.P., Miller J.A., Piacentini L.N., Platnick N.I., Polotow D., Silva-Dávila D., Scharff N., Szuts T., Ubick D., Vink C.J., Wood H.M., Zhang J. 2017. The spider tree of life: phylogeny of Araneae based on target-gene analyses from an extensive taxon sampling. *Cladistics* 33: 574–616. https://doi.org/10.1111/cla.12182

Chapter 3: Taxonomic review of the Andean flat crab spiders genus *Coenypha* Simon, 1895 (Thomisidae: Stephanopinae)

Taxonomic review of the Andean flat crab spiders genus *Coenypha* Simon, 1895 (Thomisidae: Stephanopinae)

MIGUEL MACHADO[1]* & RENATO AUGUSTO TEIXEIRA [1]

[1]Laboratório de Aracnologia, Faculdade de Biociências, Pontifícia Universidade Católica do Rio Grande do Sul (PUCRS), Porto Alegre, RS, BRAZIL. E-mail: machadom.arachno@gmail.com; renato.teixeira@pucrs.br.

Abstract

Our recent cladistic analysis corroborates and extends preliminary results in recovering a well-supported clade composed by all "Andean *Stephanopis*" species with *Coenypha* nested within, based on a series of shared somatic and genital features. In the present work we propose the transference of *S. nodosa* (senior synonym of *S. verrucosa* and *S. hystrix*), *S. ditissima* (senior synonym of *S. spissa* and *S. maulliniana*) and *S. antennata* to *Coenypha*. The type species *C. edwardsi* is considered senior synonym of *C. lucasi*, *C. fuliginosa* and *C. fasciata* and two new species are described: *C. doritos* **sp. nov.** and *C. foliacea* **sp. nov.** The taxonomic review presented hereinafter also provides updated diagnoses, descriptions and new distributions records. *Stephanopis exigua* (Nicolet, 1849) is considered *nomen dubium* and *Stephanopis verrucosa* is combined to *Ozyptila* (Simon, 1864).

Key Words: New species, revision, taxonomy, morphology.

139

Introduction

The subfamily Stephanopinae Simon, 1895 gathers distinctive crab spiders that despite being extensively studied in the past few years (Silva-Moreira & Machado, 2016; Machado et al. 2017; Machado et al. 2018; Prado et al. 2018; Machado et al. 2019a; Machado et al. 2019b), comprise a challenging and widely heterogeneous group that has been weakly supported or recovered as paraphyletic in recent phylogenies (Benjamin *et al*., 2008; Benjamin, 2011; Ramírez, 2014; Wheeler *et al*., 2017). According to Benjamin (2011), the lack of revisions and the considerable number of species yet to be described, could be the main reasons for the instability and weak support for this group.

Blurred taxonomic boundaries were observed between two Neotropical Stephanopinae genera by Machado et al. (2017), who pointed similarities regarding the copulatory structures and somatic features of the hitherto *Stephanopis* species from the Andean Region and *Coenypha*. The proximity between these genera were corroborated by a more inclusive morphological dataset provided by Machado & Teixeira (Chapter 1), who discussed such resemblances highlighting the stability and support of the recovered clade, allied to the coincident geographical distribution of it component species, to justify the combination of all "Andean *Stephanopis*" to *Coenypha*. The genus *Coenypha*, originally formed by four endemic species from Chile (World Spider Catalog, 2020), is a genus of Stephanopinae characterized by spiders with flattened prosoma (wider than long), anterior eyes disposed in a strongly recurved row, anterior pairs of legs (I and II) long, with dilated femora, opisthosoma wider than long, bearing small posterior projections and a truncate anterior border. Despite their remarkable morphology, the genus remains known by its poorly detailed original description and lack of clear diagnostic characters and illustrations, making difficult its undoubtful

recognition. In this paper we provide a taxonomic review of the genus, presenting new distribution records, updated diagnoses and the description of two new species.

Material and methods

The abbreviations related to the eye diameter, interdistances and median ocular quadrangle, as the name of the structures of body and genitalia of the specimens, follows Machado *et al.* (2019). Male palps are presented in retrolateral and ventral view, while epygina were detached and submerged in proteolytic enzyme for three to five in order to eliminate soft tissues, and then, photographed and subjected to scanning electronical microscopy. Photographs were taken by a Multipurpose Zoom Microscope Leica M205A at the Museu de Ciências e Tecnologia of Pontifícia Universidade Católica do Rio Grande do Sul (PUCRS) and all measurements are presented in millimeters.

The examined material are deposited in American Museum of Natural History, New York (AMNH, L. Prendini), Muséum National D' Histoire Naturelle, Paris (MNHN, C. Rollard), California Academy of Sciences, San Fransico (CAS, L. Esposito), Field Museum of Natural History, Chicago (FMHN, P. Sierwald), Museo Argentino de Ciencias Naturales, Buenos Aires (MACN, M. Ramirez), Museum of Comparative Zoology, Cambridge (MCZ, L. Liebensperger), Museo de Historia Natural de Chile, Santiago (MNNC, M. Elgueta) and Instituto Butantan (IBSP, A.D. Brescovit).

Taxonomy

Thomisidae Sundevall, 1833

Stephanopinae O. Pickard-Cambridge, 1871

Coenypha **Simon, 1895**

Thomisus Nicolet, 1849: 391, pl. 3, fig. 7; 392, pl. 3, figs 8, 11.

Stephanopis Keyserling, 1880: 187, pl 4, fig 103.

Coenypha Simon, 1895: 1051; 1053, fig. 1090; Mello-Leitão, 1926: 322, fig. 43.

Type species. *Coenypha edwardsi* (Nicolet, 1849)

Diagnosis. See Machado et al. (Chapter 1)

Description. Medium sized spiders with marked sexual size dimorphism (total length 3.75–4.44 in males, 6.55 – 8.60 in females) and cryptic coloration, varying from yellow to dark-brown. Prosoma wider than long, presenting rough texture, many hyaline setae and sparse clavated ones. Opisthosoma trapezoidal, wider than long with anterior border varying from straight to deeply excavated. Tibia I bears four pairs of ventral macrosetae while tibiae II present only three pairs equally distant; posterior legs (III and IV) very reduced, with dense tarsal scopula. Epigynum with membranous and coiled copulatory ducts; spermatheca subdivided in smaller chambers; male palp with discoid tegulum, pointed RTA and RTAvbr short, truncated or acute; embolus long, flattened, ribbon-shaped and presenting hyaline pars pendulum.

Composition. Six valid species: *Coenypha edwardsi* (Nicolet, 1894), *Coenypha antennata* (Tullgren, 1902) **comb. nov.**, *Coenypha ditissima* (Nicolet, 1894) **comb. nov.**, *Coenypha doritos* **sp. nov.**, *Coenypha foliacea* **sp. nov.** and *Coenypha nodosa* (Nicolet, 1894) **comb. nov.**

Coenypha edwardsi (**Nicolet, 1849) comb. nov.**

Figs 1—3

Thomisus edwardsii Nicolet, 1849: 392, pl. 3, figs. 8, 11.

Stephanopis edwardsi Keyserling, 1880: 187, pl 4, fig 103.

Coenypha edwardsi Simon, 1895: 1053, fig 1090 (Holotype female from Punta Arenas, Chile, deposited in MNHN 3406, examined)

Coenypha lucasi Simon, 1895: 1051 (Syntypes: 2 females from Valdivia, Chile, deposited in MNHN 3392, examined). **New Synonymy.**

Coenypha fuliginosa Simon, 1895: 1051 (Syntypes: 1 male and 8 juveniles from Chile, deposited in MNHN 6967, examined). **New Synonymy.**

Coenypha fasciata Mello-Leitão, 1926: 322, Fig. 43 (Holotype female from Valdivia, Chile, deposited in MNHN 18242). **New Synonymy.**

Type material: Holotype: female, Punta Arenas [53°9'49.80"S, 70°55'1.45"W, Magalhães, Chile], (MNHN 3406, examined).

Other material examined. CHILE: *Aconcagua***:** 1f#, La Ligua, 32°27'9.72"S, 71°13'31.45"W, 27 September 1980 (AMNH). *Coquimbo***:** 1m#, Ovalle, 30°36'15.66"S, 71°11'49.19"W, 01 December 1950, Ross & Michelbacher (CAS 9072303). *Valparaiso***:** 1j, Viña del Mar, 32°59'40.93"S, 71°32'33.68"W, 04 December 1982, M. Pino (MNNC 862); 1f#, Granizo, 32°58'58.96"S, 71°10'45.12"W, October 1982, M. Pino (MNNC 632); 1m#, same locality and collector of the previous vial, 18 December 1983 (MNNC 919); 1f#, Quintero, 33°2'49.45"S, 71°35'23.18"W, 12 December 1980, L. Peña (AMNH). *Santiago***:**1j, Cajón del Rio Maipo, 33°47'53.86"S, 70°51'52.50"W,

November 1984, G. Arriagada (MNNC 892); 1f#, Pudahuel (Parque Laguna Carén), 33°25'51.39"S, 70°50'24.79"W, same collector and date of the previous vial (MNNC 881); 1f# and 2j, Quilicura, 33°21'27.63"S, 70°43'45.38"W, May 1979, L. Peña (AMNH); 1m# and 2j, Cerro Manquehue, 33°21'3.00"S, 70°34'56.01"W, August 1979, L. Peña (AMNH); 1f#, Cordoba Coast, 33°26'56.00"S, 70°40'9.35"W, 15-20 February 1979, L. Peña (AMNH); 6m#, 2f# and 7j, Cuesta La Dormida, 33°31'16.74"S, 70°47'42.40"W, 13-18 November 1982, L. Peña (AMNH); 1f# and 1j, Pirque, 33°41'14.91"S, 70°35'18.17"W, 30 November 1982 (AMNH). *Talca*: 1m#, Maule, 35°25'23.68"S, 71°38'54.53"W, 22 December 1950, Ross & Michelbacher (CAS 9046659). *Bio-Bío*: 1f#, Ñuble (40 Km from Coihueco), 36°37'45.12"S, 71°49'57.81"W, 15 February 2005, M. Ramírez & F. Labarque (MACN 27638); 1m#, Concepción (Palo Grande), 36°48'46.51"S, 73° 1'4.14"W, 29 December 1996, T. Cekalovic (AMNH); 2j, Concepción (Camino Chome Ramuntcho), 36°49'8.18"S, 73° 3'1.15"W, 08 November 1996, T. Cekalovic (AMNH); 1m#, Ñuble (Recinto), 36°41'59.98"S, 71°53'38.73"W, 01-03 October 1983, L. Peña (AMNH); 1m#, Concepción (Periquillo), 36°55'53.72"S, 73° 0'33.94"W, 16 March 1997, T. Cekalovic (AMNH); 1m#, Concepción (Estero Nonquen), 36°49'14.35"S, 73° 0'55.31"W, 11 November 1996, T. Cekalovic (AMNH); 1m#, 1#f and 4j, Concepción (Lomas Colorada), 36°50'54.14"S, 73°7'59.64"W, 24 November 1996, T. Cekalovic (AMNH). *Araucanía*: 1j, Malleco, 38°9'48.82"S, 72°31'13.74"W, February 1965, Fritz (MACN-Ar 18678); 4f#, same locality of the previous vial, November 1979, L. Peña (AMNH); 1f#, Angol, 37°48'21.87"S, 72°42'13.70"W, 1950, S. Bullock (CAS 9046660); 1f#, same locality of the previous vial, 29 January 1951, Ross & Michelbacher (CAS 9072302); 2j, Cautín (Chacamo), 38°34'56.21"S, 73° 3'11.75"W, 17-23 February 1981, L. Peña (AMNH). *Los Rios*: 2j, Valdivia, 39°49'2.59"S, 73°14'33.12"W, no collection

date (MNNC 18242); 1f#, Valdivia, 39°49'2.65"S, 73°14'33.07"W, 12 October 1976, E. Krahmer (ex. MCZ 133392); 2m#, 2f# and 1j, same locality and collector of the previous vial, 1983 (MNNC 802); 1#, 2f# and 1j, same locality and collector of the previous vial, 1984 (MNNC 840); 1f#, same locality and collector of the previous vial, 12 October 1976 (MCZ 133392); 1m# and 6j, same locality of the previous vial, 15 January 1951, Ross & Michelbacher (CAS 9072304); 1j, same locality of the previous vial, 10 January 1989, M. Ramírez (MACN 18680); 1m# and 1j, Enco River Region, 39°54'39.75"S, 72° 8'53.29"W, 3 March 1955, L. Peña (MACN-Ar 9539). *Los Lagos*: 1m# and 2j, Lepihue, 39°50'38.25"S, 73°13'53.43"W, 21 January 1951, Ross & Michelbacher (CAS 9072300); 1m# and 1j, Osorno (Salto Pilmaiquén), 40°38'50.88"S, 72°39'26.90"W, 27 January 1951, Ross & Michelbacher (CAS 9072301); 3j, Osorno (Puyehue), 40°43'43.88"S, 72°18'43.16"W, 13-17 December 1998, M. Ramírez, L. Compagnucci, C. Grismado & L. Lopardo (MACN-Ar 18676); 1j, Llanquihue, 41°2'44.04"S, 72°55'22.32"W, 12 November 1994, R. Leschen & C. Carlton (AMNH); 4m#, Petrohue, 41°8'27.52"S, 72°24'28.23"W, 29 March 1968, L. Peña (MCZ 133669); 1j, same locality of the previous vial, 26 February 1972, Bondon (MACN-Ar 18679); 1f#, , same locality of the previous vial, 29 March 1968, L. Peña (MCZ 133408); 1m# and 4j, Puerto Montt, 41°28'8.10"S, 72°56'28.09"W, 24-29 January 1983, G. Arriagada (MNNC 728); 3j, same locality and collector of the previous vial, 30 January to 15 Feburary 1983 (MNNC 717); 1f#, same locality, date and collector of the previous vial (MNNC 710); 1m#, Isla Chiloé (Butalcura), 42°13'59.88"S, 73°44'60.00"W, 21 February 1997, T. Cekalovic (AMNH); 1f#, Isla Chiloé (Dalcahue), 42°22'29.25"S, 73°39'6.35"W, 01 February 1981, L. Peña (AMNH); 2m#, Chiloé Province, 42°22'39.47"S, 73°39'6.78"W, 01-04 April 1968, L. Peña (MCZ 133665); 1m#, same locality and collector of the previous vial, February 1967 (MCZ 133409); 1j, Cole Cole,

42°25'22.39"S, 74° 4'58.62"W, 08-11 February 1991, M. Ramírez (MACN-Ar 18681); 1j, Chepu, 42°31'24.34"S, 73°52'47.36"W, 30 January 1981, L. Peña (AMNH); 1j, Isla Quinchao, 42°32'4.24"S, 73°25'16.10"W, 19 February 1997, T. Cekalovic (AMNH); 1f#, Isla Chiloé, 42°37'25.31"S, 73°55'35.34"W, 19 February 1996, T. Cekalovic (AMNH); 1m# and 3j, same locality of the previous vial, 01 February 1981, L. Peña (AMNH); 4j, same locality of the previous vial, 22 February 1997, T. Cekalovic (AMNH); 1f#, Huequetrumao, 42°37'26.29"S, 73°55'35.66"W, 27 December 1981, L. Peña (AMNH); 1m#, Isla Lemuy (Puerto Haro), 42°38'19.00"S, 73°38'32.36"W, 20 February 1996, T. Cekalovic (AMNH); 1f#, Santo Antonio de Chadmo, 42°55'5.71"S, 73°39'41.42"W, 08 February 2001, T. Cekalovic (FMNH 61793); 1f#, Puerto Carmen, 43°7'49.25"S, 73°45'21.85"W, 15-19 March 1981, L. Peña (AMNH); 4j, Gicao, 43°9'0.20"S, 73°41'57.38"W, February 1981, L. Peña (AMNH)

Diagnosis. Females of *C. edwardsi* resemble those of *C. fasciata* by the flattened and wide opisthosoma (posteriorly enlarged) and by the anterior femora robust, bearing a pair of apical projections (Fig. 1A). However, they can be distinguished by their wider thoracic area, lower clypeus (Fig. 1B), epigynal plate with oblique slits leading to the copulatory openings, and a flattened median septum (Fig. 1C). The copulatory ducts present two twists before getting to the spermatechae, which present an apical porous gland (Fig. 1D). Males of *C. edwardsi* can be easily recognized by the shape of their opisthosoma (with eight tiny posterior projections) (Fig. 2A), well-developed apical tegular ridge (Fig. 2C) and by the short and acute RTAvbr (Fig. 2D).

Description. *Female* (**MNNC 840**)**:** Anterior eye row recurved and posterior row straight; ALE almost twice as large as the AME (Figs 1A, 1B). Prosoma granulated, with many setiferous tubercles and hyaline setae; light brown, cephalic area and center of the thoracic portion dark brown (Fig. 1B). Clypeus bears a pair of central macrosetae

on its margin. Sternum brown, scutiform and slightly wider than long. Femora I brown, robust and presenting few setiferous tubercles on its dorsal and prolateral surface; anterior patellae, tibiae and metatarsi (I and II) predominantly brown, dark brown on their dorsal surface; posterior legs entirely brown. Opisthosoma light brown with a horizontal darker line; anterior border slightly concave and posteriorly beveled (Fig. 1B). Epigynal plate with copulatory openings preceded by obliquely convergent slits and divided by a wide and flattened and median septum (Fig. 1C); copulatory ducts corrugated, membranous and coiled (two twists); spermatechae formed by two kidney-shape chambers — the primary ones bear a porous glandular head (Fig. 1D). Measurements: eyes diameters and eyes interdistances: AME 0.09, ALE 0.15, PME 0.12, PLE 0.12, AME-AME 0.18, AME-ALE 0.12, PME-PME 0.24, PME-PLE 0.14. MOQ length 0.44, MOQ posterior width 0.26, MOQ anterior width 0.20; leg formula: 1243: leg I—femur 5.60/ patella 2.35/ tibia 3.90/ metatarsus 2.25/ tarsus 1.50/ total 15.60; II—3.20/ 1.50/ 2.20/ 1.25/ 1.10/ 9.25; III—1.25/ 0.95/ 0.90/ 0.60/ 0.55/ 4.25; IV—1.55/ 0.95/ 1.10/ 0.60/ 0.55/ 4.75; total length 8.60, prosoma length 3.60, width 3.90, opisthosoma length 5.00, clypeus height 0.30, sternum length 1.46, width 1.59, endites length 0.82, width 0.46, labium length 0.52, width 0.70.
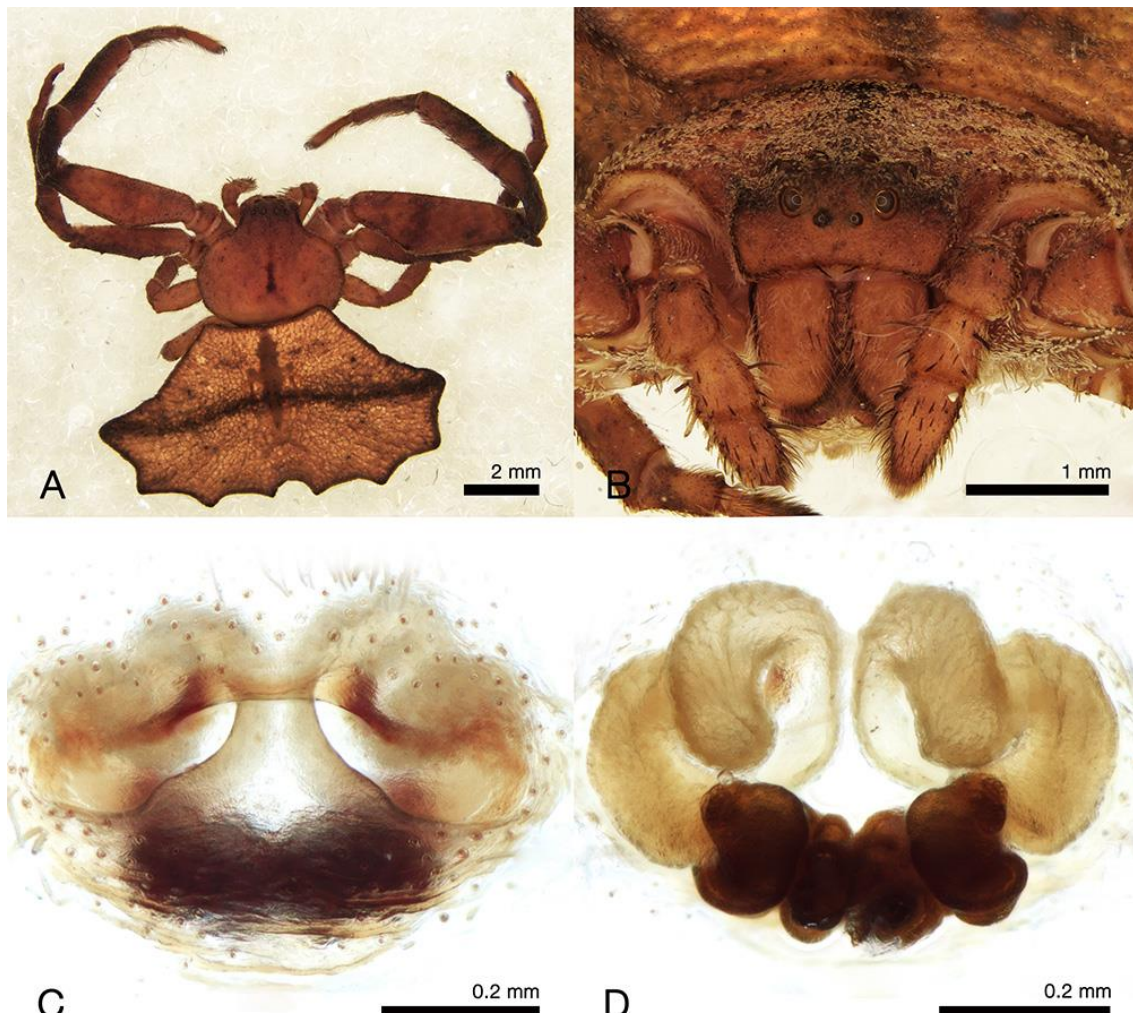
Figure 1. *Coenypha edwardsi* (Nicolet, 1849), female (MNNC 840). A) dorsal habitus; B) frontal habitus; C) ventral view of epigynal plate; D) dorsal view of epigynal plate.

Male **(CAS 9046659):** Anterior eye row recurve and posterior slightly recurve (Figs 2A, 2B). Prosoma and other eyes characteristics as in female. Sternum brown, scutiform and slightly wider than long. Legs I, II and IV predominantly brown, with randomly darker spots; legs III entirely yellow with few brown stains. Opisthosoma as in female. Palp present oval cymbium, tegulum with an apical tegular ridge and no apophyses (Fig. 2C); palpal tibiae bears three prolateral macrosetae, a short and conical RTAvbr and an acute RTA (Fig. 2D). Measurements: eyes diameters and eyes interdistances: AME 0.06, ALE 0.12, PME 0.10, PLE 0.09, AME-AME 0.12, AME-

148

ALE 0.08, PME-PME 0.16, PME-PLE 0.12. MOQ length 0.34, MOQ posterior width 0.24, MOQ anterior width 0.16; leg formula: 1234: leg I—femur 3.05/ patella 1.15/ tibia 2.25/ metatarsus 1.30/ tarsus 0.80/ total 8.55; II—1.48/ 0.64/ 1.12/ 0.70/ 0.58/ 4.52; III—0.76/ 0.48/ 0.62/ 0.39/ 0.36/ 2.61; IV—0.88/ 0.46/ 0.58/ 0.28/ 0.36/ 2.56; total length 4.44, prosoma length 1.94, width 2.00, opisthosoma length 2.50, clypeus height 0.22, sternum length 0.80, width 0.94, endites length 0.46, width 0.24, labium length 0.26, width 0.38.

Distribution. CHILE: Aconcagua, Coquimbo, Valparaíso, Santiago, Talca, Bío-Bío, Araucanía, Los Ríos and Los Lagos (Fig. 15).

Note. Females of *C. edwardsi* present a wide range of body coloration, varying from the most common morphotype, which was described above, to specimens entirely dark-brown with a longitudinal black line on prosoma (Fig. 3C), or brown on prosoma and legs with opisthosoma light-brown (Fig. 3E), to even spiders with reddish-brown prosoma and legs and yellowish-brown opisthosoma (presenting several black spots randomly distributed all over the body) (Fig. 3D). The females also present a variation on the shape of the opisthosma. There is at least four types of abdominal forms, according to the shape of the posterior edge of the opisthosoma: beveled (with eight projections) (Fig. 1A), rounded (Fig. 3E), bilobed (Fig. 3D) or misshapen (3C). On the other hand, although the males may present different body colorations, the shape of the opisthosoma seems to be more conservative (Figs 3A, 3B).

Figure 2. *Coenypha edwardsi* (Nicolet, 1849), male (CAS 9046659). A) dorsal habitus;

B) frontal habitus; C) ventral view of the left palp; D) retrolateral view of the left palp.

Figure 3. *Coenypha edwardsi* (Nicolet, 1849), variations; males (A and B) and females (C—F). Photo credit: Fernando Escobar Barraza (F).

Coenypha antennata (Tullgren, 1902) comb. nov.

Figs 4—5

Stephanopis antennata Tullgren, 1902: 52, pl. 5, Fig. 4. **New combination.**

Type material: Holotype: female from Aysén, Chile (deposited in the NHRS, not located; presumably lost).

Neotype: 1 female, La Junta [43°58'20.78"S, 72°24'12.63"W, Aysén, Chile], (MNNC).

Other material examined. CHILE: *Bío-Bío***:** 1j, Concepcíon (Estero Nonguén), 36°49'12.49"S, 73°2'39.80"W, 05 October 1996, T. Cekalovic (MNNC); 1f#, Concepción (Periquillo), 36°49'12.49"S, 73°2'39.80"W, 16 March 1997, T. Cekalovic (MNNC). *Araucanía***:** 1f#, Malleco (Monumento Natural Contulmo), 38°0'51.64"S, 73°10'48.24"W, 19-21 December 1998, M. Ramírez, L. Coapagnucci, C. Grismado & L. Lopardo (MNNC). *Los Ríos***:** 3j, Valdivia (Huachocopihue), 39°50'2.23"S, 73°14'17.32"W, 07 March 1965, H. Levi (MCZ). *Los Lagos***:** 1m# and 1f#, Osorno (Termas de Puyehue), 40°43'16.58"S, 72°19'3.85"W, 19-25 December 1982, A. Newton & M. Thayer (MNNC); 1f#, Osorno (Aguas Calientes), 40°43'43.88"S, 72°18'43.17"W, 13-17 December 1998, M. Ramírez, L. Coapagnucci, C. Grismado & L. Lopardo (MNNC); 1f#, same locality, collector and date of the previous vial (MACN-Ar 10423); 1f#, Llanquihue (Puerto Montt), 41°28'8.10"S, 72°56'28.09"W, February 1983, G. Arriagada (MNNC 715); 1f#, same locality and collector of the previous vial, 24-29 January 1983 (MNNC 725); 1f#, Llanquihue, 41°34'60.00"S, 72°40'60.00"W, 23 November 1993, N. Platnick & M. Ramírez (MNNC); 1f#, same locality of the previous vial, April 1989, L. Peña (MNNC); 1f#, Chamisa, 41°15'38.27"S, 73°0'28.23"W, 13 December 1981; 1m#, Isla Grande de Chiloé (Huequetrumao), 42°27'22.52"S,

73°52'47.36"W, 27 December 1981, L. Peña (MNNC); 1f#, Isla Grande de Chiloé (Puente La Caldera), 42°37'26.28"S, 73°55'35.66"W, 18 February 1997, T. Cekalovic (MNNC); 1m#, Isla Grande de Chiloé (Lago Huillinco), 42°41'45.02"S, 73°55'52.42"W, 12-22 December 2002, M. Thayer & A. Newton (MNNC 2857855); 1f# and 1j, Isla Quinchao, 42°28'9.00"S, 73°30'53.00"W, 19 February 1997, T. Cekalovic (MNNC).

Diagnosis. Females of *C. antennata* are similar to those of *C. nodosa* due to the presence of a single pair of posterior projections on the opisthosoma (Fig. 4A), anal region well-developed and a strong spiniform macrosetae on the mesial surface of femora I, nevertheless, they can be distinguished by their narrow and longer cephalic portion and by the epigynum that looks like a "diving mask", having a short and incomplete septum between the copulatory openings (Fig. 4C). Males of *C. antennata* are distinguished from those of *C. nodosa* by their stronger legs (Fig. 5A), palp with wider tegulum, rounded cymbium (Fig. 5C) and RTAvbr close to the tip of the RTA, curving towards the axis of this latter (Fig. 5D). Both males and females present a diagnostic feature that gives name to the species: a pair of long macrosetae in the middle of the MOQ area that makes look that these spiders have antennas (Fig. 4B).

Description. *Female* (**MNNC**): Anterior eye row recurved and posterior row slightly procurved; ALE have twice the size of the AME (Figs 4A, 4B). Prosoma and anterior legs (I and II) predominantly orangish-brown with few darker spots (or stripes, in the case of the carapace); legs III and IV brown, except for the tarsi and the proximal region of the femora, that are lighter (Fig. 4A). Opisthosoma yellowish with a median brown taint on the dorsum, splitting posteriorly and covering the abdominal projections (Fig. 4A). Copulatory ducts wide, short and sclerotized; spermathecae walnut-shaped with porous gland (Fig. 4D). Measurements: eyes diameters and eyes interdistances: AME 0.08, ALE 0.17, PME 0.17, PLE 0.17, AME-AME 0.13, AME-ALE 0.11, PME-

PME 0.15, PME-PLE 0.13. MOQ length 0.44, MOQ posterior width 0.49, MOQ anterior width 0.28; leg formula: 1243: leg I—femur 2.63/ patella 1.25/ tibia 1.99/ metatarsus 1.63/ tarsus 0.79/ total 8.29; II—2.12/ 1.13/ 1.63/ 1.44/ 0.66/ 6.98; III—1.38/ 0.76/ 1.08/ 0.83/ 0.59/ 4.64; IV—1.78/ 0.77/ 1.31/ 1.05/ 0.61/ 5.52. Prosoma length 2.76, width 2.39, opisthosoma length 3.55, total body length 6.31; clypeus height 0.29, sternum length 1.24, width 1.17, endites length 0.65, width 0.32, labium length 0.34, width 0.48.

Male (**FMNH 2857855**): Eye arrangement as in the female. Prosoma dark-brown, anterior legs (I and II) brown and posterior ones (III and IV) brown with darker spots on tibiae and on the distal portion of femora (Figs 5A, 5B). Opisthosoma greyish-brown on the median portion of the dorsum, from its anterior margin until the spinnerets, and yellow on the sides. Palp has many tibial setae; embolus rests behind the tegulum and it is short when compared to those of the males of other congeneric species (Fig. 5C). Measurements: eyes diameters and eyes interdistances: AME 0.09, ALE 0.19, PME 0.17, PLE 0.17, AME-AME 0.14, AME-ALE 0.13, PME-PME 0.19, PME-PLE 0.12. MOQ length 0.48, MOQ posterior width 0.56, MOQ anterior width 0.34; leg formula: 1243: leg I—femur 2.72/ patella 1.25/ tibia 2.19/ metatarsus 1.87/ tarsus 1.05/ total 9.08; II—2.32/ 1.09/ 1.78/ 1.55/ 0.82/ 7.56; III—1.52/ 0.74/ 1.14/ 0.94/ 0.65/ 4.99; IV—1.97/ 0.88/ 1.34/ 1.04/ 0.75/ 5.98. Prosoma length 2.71, width 2.51, opisthosoma length 2.82, total body length 5.53; clypeus height 0.35, sternum length 1.16, width 1.14, endites length 0.67, width 0.34, labium length 0.35, width 0.50.

Distribution. CHILE: Bío-Bío, Araucanía, Los Rios, Los Lagos and Aysén (Fig. 14).

Note. According to Tullgren (1902), the type material was originally deposited in the "Entom. Dep. of the Royal Museum" in Stockholm. After check the online database

and get in contact with the staff of the Swedish Museum of Natural History, such material was not found, so it was considered lost. Notwithstanding, the remarkable somatic characters and specially the unique shape of the female epigynal plate, which was represented by Tullgren (1902), allowed the recognition of the species. Aiming to secure the identity and taxonomic status of the species, we elected a female specimen from the same type locality as the Neotype for *C. antennata*.
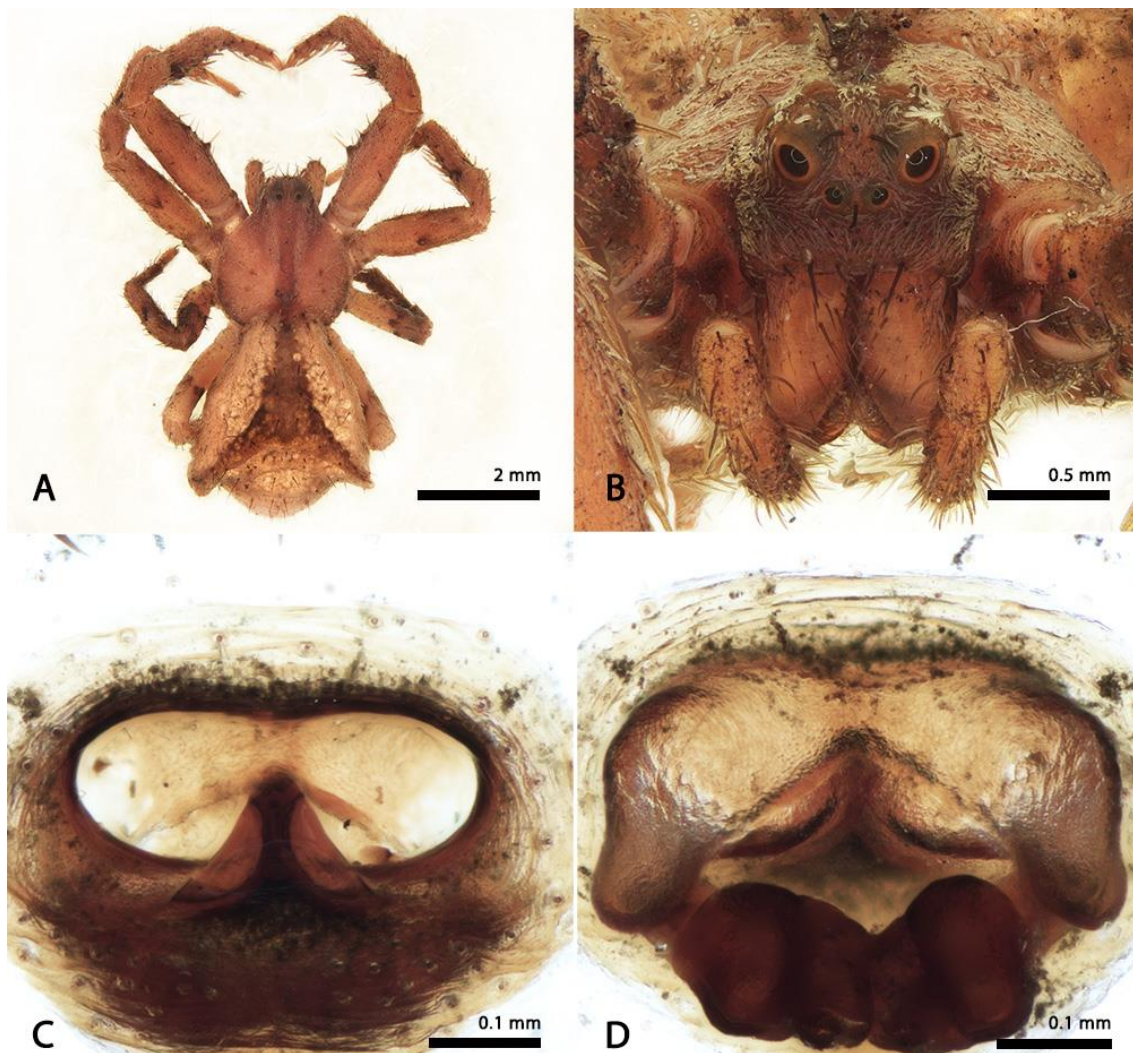

Figure 4. *Coenypha antennata* (Tullgren, 1902), female (MNNC). A) dorsal habitus; B) frontal habitus; C) ventral view of epigynal plate; D) dorsal view of epigynal plate.
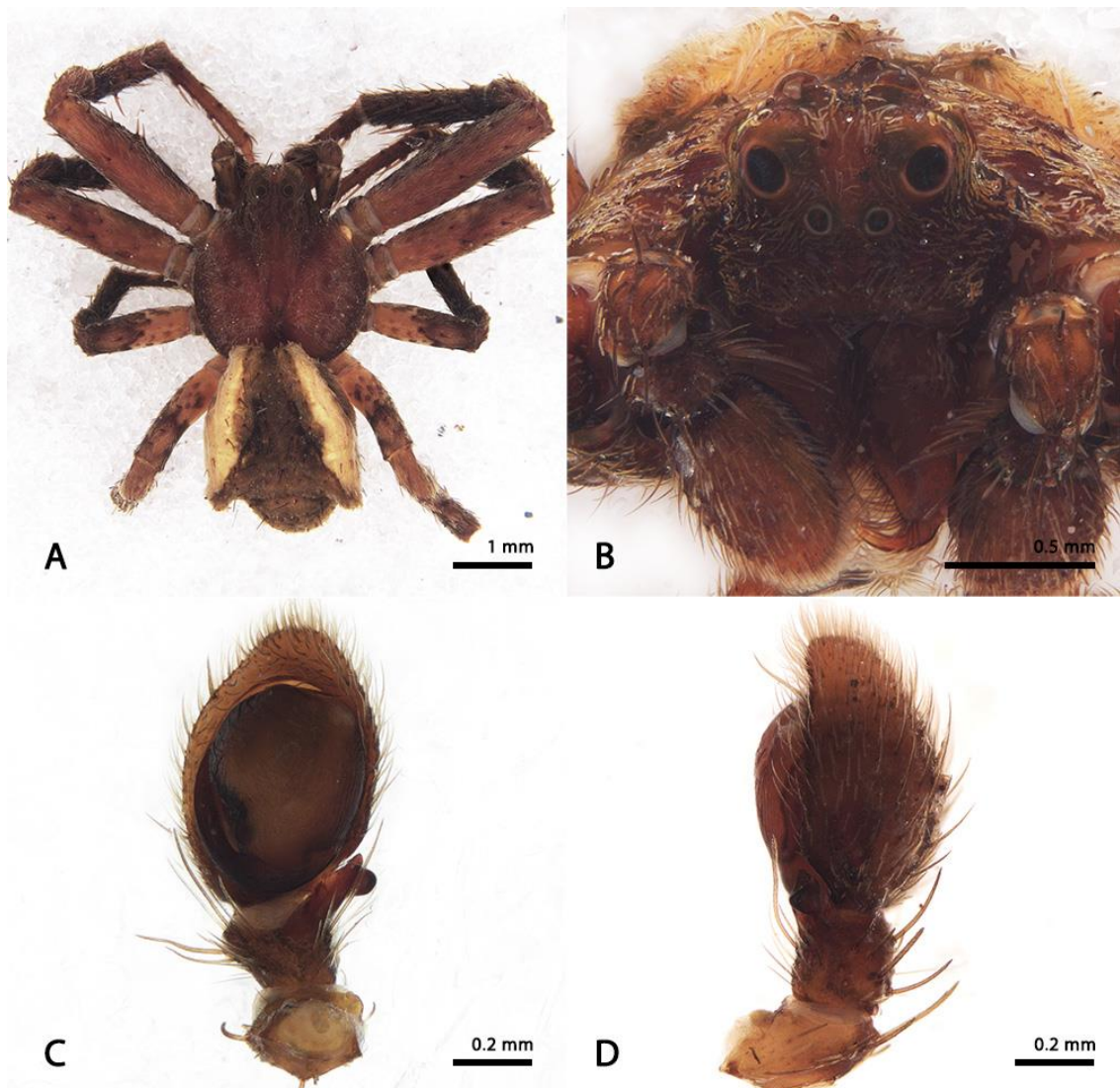
Figure 5. *Coenypha antennata* (Tullgren, 1902), male (FMNH 2857855). A) dorsal habitus; B) frontal habitus; C) ventral view of the left palp; D) retrolateral view of the left palp.

Coenypha ditissima (Nicolet, 1849) comb. nov.

Figs 6, 7

Thomisus ditissimus Nicolet, 1849: 394, pl. 3, Fig. 9.

Stephanopis ditissima Keyserling, 1880: 175, pl. 3, Fig. 96; Simon, 1887: E8, pl. 2, Fig. 1; Mello-Leitão, 1951: 332, Fig. 7; Ramírez, 2014: 223, Figs 151E-F, 172E; Machado et al. 2017: 454, Fig. S12C. **New combination.**

Stephanopis spissa Simon, 1895: 1054 (Holotype female from Chile, deposited in MNHN 4178, examined). **New Synonymy.**

Stephanopis maulliniana Mello-Leitão, 1951: 334 (Holotype female from Maullín, Llanquihue, Chile, deposited in MNRJ, examined) **New Synonymy.**

Type material: Holotype: female from Chile, (MNHN 4176, examined).

Other material examined. ARGENTINA: *Neuquén***:** 1j, Hua-hum, 38°58'19.37"S, 68°4'16.41"W, 17 January 1985, Maury-Toth (MACN-Ar 18677); 1m# and 1f#, Neuquén (Lanín), 40°6'19.00"S, 71°40'11.00"W, January 1985, M. Ramírez (MACN-Ar 18651); 1j, Neuquén (Lago Lacar), 40°10'37.79"S, 71°29'38.80"W, January 1954, N. Kormilev (MACN-Ar 4164); 1j, Neuquén (Parque Nacional Nahuel Huapi), 40°53'27.87"S, 71°34'34.11"W, 30 January 1985, M. Ramírez (MACN-Ar 18663); 1m#, Nahuel Huapi, 40°55'36.13"S, 71°29'34.65"W, 1945, D. Hiebermann (MACN-Ar 18669); 1f#, Nahuel Huapi (Puerto Blest), 41°1'59.98"S, 71°49'0.05"W, 07-20 January 2000, L. Lopardo & A. Quaglino (MACN-Ar 18650); 2j, Neuquén (Bariloche), 41°8'44.93"S, 71°17'56.85"W, February 1954, M.E. Galliano (MACN-Ar 5404). *Chubut***:** 1j, Parque Nacional Los Alerces, 42°58'26.85"S, 71°38'37.90"W, February 1985, M. Ramírez (MACN-Ar 18657). *Tierra del Fuego***:** 1f#, Isla de los Estados, 54°47'59.46"S, 64°25'36.47"W, April 1935, J.B. Daguerre-Cancelles (MACN-Ar

18652); 2f# and 7j, Ushuaia, 54°48'19.44"S, 68°19'27.14"W, 16 February 1949, B. Aguirre (MACN-Ar 2796); 1f#, same locality of the previous vial, 23 January 1960, A. Bachmann (MACN-Ar 18658); 1f#, same locality of the previous vial, 04 December 2012, M. Ramírez, C. Grismado, A. Ojaguren & E.M. Soto (MACN 29783); 1j, same locality of the previous vial, February 1963, Maury (MACN-Ar 18666). **CHILE:** *Coquimbo***:** 3j, Choapa, 31°48'14.70"S, 71°0'8.03"W, 13 November 1987, Maurj (MACN-Ar 18668). *Valparaíso***:** 1f# and 2j, Zapallar, 32°33'13.70"S, 71°27'29.29"W, 27 November, Ross & Michelbacher (CAS 9071265); 2m# and 2j, same locality, date and collectors of the previous vial (CAS 9071264); 2j, Quintero, 32°46'20.32"S, 71°31'59.88"W, 12 December 1980, L. Peña (AMNH); 1f#, Caracoles, 32°47'30.18"S, 70° 3'38.57"W, August 1943, Rosa (CAS 9072308); 1f#, Quillota (Parque Nacional La Campana), 32°57'40.40"S, 71° 3'34.00"W, 18 February 2005, M. Ramírez & F. Labarque (MACN-Ar 10848); 6j, El Melón, 33° 3'55.11"S, 71°35'25.08"W, 03 November 1981, L. Peña (AMNH); 1j, Tunquén, 33°16'25.45"S, 71°38'49.10"W, 14 October 1982, M. Pino (MNNC 630). *Santiago***:** 6f# and 4j, Quilicura, 33°21'27.63"S, 70°43'45.38"W, May 1979, L. Peña (AMNH); 1f#, Las Condes, 33°23'56.33"S, 70°33'26.32"W, January 1983, no collector (MNNC 739); 5f# and 3j, Cordoba Coast, 33°26'56.00"S, 70°40'9.35"W, 15-20 February 1979, L. Peña (AMNH); 1f#, Malleco, 33°30'37.01"S, 70°40'16.68"W, November 1979, L. Peña (AMNH); 15j, Cuesta La Dormida, 33°31'16.74"S, 70°47'42.40"W, 13-18 November 1982, L. Peña (AMNH); 2f#, 15j, El Canelo, 33°34'34.36"S, 70°27'0.00"W, 1980, L. Peña (AMNH); 1f#, Guayacán, 33°35'60.00"S, 70°22'0.12"W, January 1984, P. Goloboff (MACN-Ar 18704); 1f#, Pirque, 33°40'45.64"S, 70°34'59.19"W, 05 October 1982, L. Peña (AMNH); 1f# and 1j, Rio Maipo Región, 33°42'6.78"S, 70°20'8.44"W, November 1984, G. Arriagada (MNNC 892); 3f#, Melipilla (La Viluma), 33°46'54.04"S, 71°4'44.55"W,

14 May 1980, L. Peña (AMNH). *Maule*: 1m#, Talca (Provincia de Linares), 35°50'47.07"S, 71°35'58.61"W, 11-20 November 1964, L. Peña (MCZ). ***Bío-Bío***: 1m#, Ñuble (Las Trancas), 36°37'9.12"S, 72° 4'55.24"W, 17 February 1983, L. Peña (AMNH); 1f#, Ñuble (Fundo Los Robles), 36°42'16.20"S, 71°36'9.60"W, 15 February 2005, M. Ramírez & F. Labarque (MACN-Ar 10847); 1f#, Concepción (Chome), 36°42'52.73"S, 73° 8'21.39"W, 07 December 1995, T. Cekalovic (AMNH); 1f# and 1j, 50 Km east of San Carlos, 36°43'21.27"S, 71°45'44.09"W, 26 December 1950, Ross & Michelbacher (CAS 9072307); 1j, Concepción (Bosque Ramuntcho), 36°45'10.41"S, 73°11'8.79"W, 14-16 October 1961, A.F. Archer (AMNH); 1f#, Concepción (Hualpén), 36°47'12.03"S, 73°6'35.83"W, 11 January 1989, M. Ramírez (MACN-Ar 18655); 2m#, Concepción (Periquillo), 36°49'12.49"S, 73°2'39.80"W, 21 December 1996, T. Cekalovic (AMNH); 1f# and 1m#, same locality and collector of the previous vial, 16 March 1997 (AMNH); 1f#, same locality and collector of the previous vial, 20 January 1996 (AMNH); 1f#, same locality and collector of the previous vial, 22 March 1997 (AMNH); 4m# and 2j, same locality and collector of the previous vial, 29 December 1996 (AMNH) 2j, Camino Chome Ramuntcho, 36°49'8.18"S, 73°3'1.15"W, 08 November 1996, T. Cekalovic (AMNH); 1f#, Ñuble (Las Comadres), 36°53'14.22"S, 71°34'12.75"W, 05-09 February 1983, L. Peña (AMNH); 1j, El Manzano, 36°54'58.31"S, 72°54'49.50"W, 23 December 1996, T. Cekalovic (AMNH); 1f#, El Abanico, 37°20'27.52"S, 71°31'57.53"W, 30 December 1950, Ross & Michelbacher (CAS 9072309); 1m# and 1j, Ancon, 37°48'21.86"S, 72°42'13.70"W, 28 November 1950, E. Zapudo (CAS 9071267). *Araucanía*: 1f#, Parque Nacional Nahuelbuta, 37°49'24.60"S, 72°58'57.00"W, 07-25 December 2002, M. Thayer & A. Newton (FMNH 2857856); 2j, Parquenco, 38°9'48.82"S, 72°31'13.74"W, 06 January 1951, Ross & Michelbacher (CAS 9071271); 11j, Malalcahuello, 38°28'19.37"S, 71°36'21.67"W,

13-31 December 1982, A. Newton & M. Thayer (AMNH); 9m#, 9f# and 6j, Cautín (Chacamo), 38°34'56.21"S, 73°3'11.75"W, 17-23 February 1981, L. Peña (AMNH); 1m#, Cautín (Temuco), 38°44'9.25"S, 72°35'25.35"W, January 1989, M. Ramírez (MACN-Ar 18656); 1f#, Villarica, 39°16'55.24"S, 72°13'50.81"W, 03 March 1965, H. Levi (MCZ 133890); 2m#, 1f# and 1j, same locality, date and collector of the previous vial (MCZ 133891); 1f#, Northeast of Villarica, 39°16'55.25"S, 72°13'50.81"W, 16-31 December 1964, L. Peña (MCZ). *Los Ríos*: 2m# and 3f#, Valdivia (Sender Los Tapuales as Renoval Canelos), 39°49'10.51"S, 73°14'42.76"W, 09 January 2002, T. Cekalovic (FMNH 71617); 4m# and 3j, Las Lajas, 39°49'10.51"S, 73°14'42.76"W, 09-13 January 1990, L. Peña (AMNH); 1f# and 1j, Valdivia, 39°49'6.53"S, 73°14'37.94"W, 13 January 1951, Ross & Michelbacher (CAS 9071266); 4f# and 11j, same locality of the previous vial, December 1982, E. Krahmer (MNNC 695); 1m#, 3f# and 3j, same locality and collector of the previous vial, 1984 (MNNC 841); 1m#, 11f# and 1j, same locality and collector of the previous vial, 1983 (MNNC 804); 1m# and 1f#, Corral, 39°53'18.87"S, 73°25'53.76"W, 16 January 1989, C. Grismado (MACN-Ar 18654). *Los Lagos*: 1f#, Osorno (Pucatrihue), 40°32'6.87"S, 73°42'31.82"W, February 1967, L. Peña (MCZ 133410); 1f#, same locality and collector of the previous vial, 25-31 January 1978 (AMNH); 3m#, 1f# and 9j, Osorno (Puyehue), 40°34'34.28"S, 73°6'53.81"W, 24 January 1951, Ross & Michelbacher (CAS 9072306); 3m#, 3f# and 4j, same locality and collector of the previous vial, 25 January 1951 (CAS 9071270); 2f# and 2j, Osorno (La Picada), 40°34'48.75"S, 73°10'34.90"W, 15-20 January 1980, L. Peña (AMNH); 1m# and 1f#, Osorno (Petrohue), 40°34'52.18"S, 73°9'19.58"W, 13 January 1980 L. Peña (AMNH); 1m#, 2f# and 2j, Osorno (Salto Pilmaiquén), 40°39'11.36"S, 72°39'36.24"W, 26 January 1951, Ross & Michelbacher (CAS 9071268); 1j, Osorno (Anticura), 40°39'12.71"S, 72°15'44.90"W, November 1982, no collector (MNNC 709);

6j, Aguas Calientes (Parque Nacional Puyehue), 40°43'16.56"S, 72°19'3.87"W, 19-26 December 1982, A. Newton & M. Thayer (AMNH); 4j, Aguas Calientes (Parque Nacional Puyehue), 40°43'43.88"S, 72°18'43.16"W, 13-17 December 1998, M. Ramírez, L. C. Grismado & L. Lopardo (MACN-Ar 18662); 1f#, Aguas Calientes (Parque Nacional Puyehue), 40°43'43.88"S, 72°18'43.17"W, 02-05 January 1982, L. Peña (AMNH); 1f#, Llanquihue (Entre Lagos), 40°58'36.61"S, 72°52'55.06"W, 20 January 1969, L. Peña (MCZ 133667); 1f#, Llanquihue (Ensenada), 41°12'25.50"S, 72°32'19.60"W, 18 March 1965, H. Levi (MCZ 133893); 1m#, Llanquihue (Correntoso), 41°15'38.27"S, 73°0'28.23"W, January 1969 L. Peña (MCZ); 1m#, 1f# and 3j, Puerto Varas, 41°19'0.12"S, 72°58'59.88"W, 16 January 1951, Ross & Michelbacher (CAS 9072305); 1m#, Llanquihue (Chamisa), 41°21'38.30"S, 72°31'13.74"W, 13 December 1968, L. Peña (MCZ 133413); 2m#, 3f# and 6j, Llanquihue (Los Muermos), 41°23'57.87"S, 73°27'53.96"W, 19 January 1951, E.I. Schlinger & E.S. Ross (CAS 9071269); 4m#, 4f# and 5j, same locality and date of the previous vial, Ross & Michelbacher (CAS 9071272); 1m#, 9f# and 5j, same locality date and collectors of the previous vial (CAS 9071273); 3m# and 1j, Llanquihue (Correntoso), 41°25'13.82"S, 72°40'11.31"W, December 1968, L. Peña (MCZ 133407); 1m# and 2j, same locality ad collector of the previous vial, 20-25 January 1980 (AMNH); 1m#, Llanquihue (Puerto Montt), 41°28'8.10"S, 72°56'28.09"W, February 1983, G. Arriagada (MNNC 715); 1m#, Llanquihue (X Región), 41°34'59.99"S, 72°40'60.00"W, 13-15 January 1990, L. Peña (AMNH); 1m#, Lepihué, 41°35'17.85"S, 73°33'52.64"W, 21 January 1951, Ross & Michelbacher (CAS 9071263); 1m# and 1f#, Isla Grande de Chiloé (Guabún), 41°49'34.75"S, 74° 1'57.21"W, 13-15 January 1980, L. Peña (AMNH); 1f#, Isla Grande do Chiloé (Puente Rio Pudeto), 41°52'40.12"S, 73°50'9.60"W, 17 February 1996, T. Cekalovic (AMNH); 1f#, Isla Grande de Chiloé

(Duhatao), 41°58'50.74"S, 74° 2'25.97"W, 16-21 January 1981, L. Peña (AMNH); 1m#, Puntra, 42°7'7.39"S, 73°48'39.88"W, 21-23 December 1981, L. Peña (AMNH); 1m#, Isla Grande de Chiloé (Butalcura), 42°13'59.88"S, 73°44'60.00"W, 21 February 1997, T. Cekalovic (AMNH); 14m#, 15f# and 10j, Isla Grande de Chiloé (Dalcahue), 42°22'29.25"S, 73°39'6.35"W, 01 February 1981, L. Peña (AMNH); 2f#, Isla Grande de Chiloé (Dalcahue), 42°22'39.47"S, 73°39'6.78"W, same collector of the previous vial, 01-04 April 1941 (MCZ 133412); 1f#, Isla Grande de Chiloé (Cole Cole), 42°25'22.39"S, 74°4'58.62"W, 08-11 February 1991, M. Ramírez (MACN-Ar 18648); 2f# and 3j, Isla Grande de Chiloé (Gicao), 42°27'22.52"S, 73°52'47.37"W, February 1981, L. Peña (AMNH); 1f# and 1j, Isla Grande de Chiloé (Cerros de Cucao), 42°28'60.00"S, 74°3'46.00"W, 01 March 1981, L. Peña (AMNH); 2f#, Isla Quinchao (Hullar Alto), 42°28'9.00"S, 73°30'53.00"W, 15 January 2002, T. Cekalovic (FMNH 71620); 4m#, 3f# and 1j, same locality and collector of the previous vial, 19 February 1997 (AMNH); 2f#, same locality and collector of the previous vial, 16 February 1996 (AMNH); 2m#, Isla Grande de Chiloé (Chepu), 42°31'24.34"S, 73°52'47.36"W, 30 January 1981, L. Peña (AMNH); 1f# and 1j, Isla Grande de Chiloé (Puente La Caldera), 42°37'26.28"S, 73°55'35.66"W, 18 February 1997, T. Cekalovic (AMNH); 2f#, same locality and collector of the previous vial, 15 February 1996 (AMNH); 1m# and 1f#, Isla Grande de Chiloé, 42°37'26.29"S, 73°55'35.66"W, 04 February 2001, T. Cekalovic (FMNH 71619); 1f#, same locality and collector of the previous vial, 10 January 2002 (FMNH 71630); 11f#, same locality and collector of the previous vial, 19 February 1996 (AMNH); 1m# and 2f#, same locality and collector of the previous vial, 14 February 1996 (AMNH); 2m# and 4f#, same locality and collector of the previous vial, 17 February 1997 (AMNH); 1f#, same locality and collector of the previous vial, 19 February 1997 (AMNH); 1m# and 1f#, same locality and collector of the previous vial,

22 February 1997 (AMNH); 2f#, same locality of the previous vial, 15-19 March 1981, L. Peña (AMNH); 1f# and 2j, same locality of the previous vial, 22 February 1997, T. Cekalovic (AMNH); 1m#, Isla Grande de Chiloé (Piruquihue), 42°37'26.29"S, 73°55'35.65"W, 10 February 1993, T. Cekalovic (AMNH); 1f#, Isla Grande de Chiloé (Cucao), 42°37'59.88"S, 74°7'0.12"W, 01 February 1991, M. Ramírez (MACN-Ar 18649); 1f# and 1j, Isla Lemuy (Puerto Haro), 42°37'9.00"S, 73°38'57.00"W, 20 February 1996, T. Cekalovic (AMNH); 1f#, Isla Grande de Chiloé (Puente Trainel), 42°40'30.57"S, 73°47'57.64"W, 18 February 1997, T. Cekalovic (AMNH); 3m# and 3j, Isla Grande de Chiloé (Terao), 42°42'40.07"S, 73°39'16.15"W, 18-21 February 1990, L. Peña (AMNH); 4f#, Isla Grande de Chiloé (San Antonio de Chadmo), 42°54'15.73"S, 73°38'17.02"W, 08 February 2001, T. Cekalovic (FMNH 61793); 2j, Palena (Chaitén), 42°54'41.51"S, 72°42'56.30"W, 04 December 1981, N. Platnick & R.T. Schuh (AMNH). *Aysén*: 2f#, 46°23'54.41"S, 72° 0'1.76"W, 17 February 1991, M. Ramírez (MACN-Ar 18647); 2f# and 10j, Aisén del General Carlos Ibanez del Campo, 46°24'43.55"S, 72°14'33.98"W, 27 January 1990, L. Peña (AMNH); 1f#, Parque Nacional Los Glaciares, 50°19'50.00"S, 73°14'3.00"W, 17 January 1972, E. Hernandez (MACN-Ar 18665); 2f#, Magallanes (Puerto Natales, Torres del Paine), 51°43'40.76"S, 72°30'5.84"W, 12 December 2009, L. Almeida, H. Wood & C. Griswold (IBSP 155000).

Diagnosis. Females of *C. ditissima* resemble those of *C. foliacea* **sp. nov.** by the short prosoma covered by hyaline setae (Fig. 6B) and opisthosoma posteriorly enlarged, bearing two pairs of projections disposed laterally (Fig. 6A). However, *C. ditissima* can be recognized by the presence of stouter femoral apophysis on legs I and II, epigynal plate with thin median septum and copulatory ducts longer than in *C. foliacea* **sp. nov.** (Figs 6C, 6D). Males can be distinguished by the presence of a guanine white-spot on

the thoracic portion of prosoma (Fig. 7A) and by the palp presenting a long ribbon-shaped embolus that rests coiled on the tegular ridge instead of encircling the tegulum (Fig. 7C).

Description. *Female* (AMNH): Anterior eye row recurved and posterior row slightly procurved; ALE have almost twice the diameter of the AME (Figs 6A, 6B). Prosoma reddish-brown on the cephalic portion and yellowish-brown on the thoracic area, being entirely covered by needle-shaped and filamentous setae (Figs 6A, 6B). Legs I and II predominantly yellowish-brown, with darker patellae; legs III and IV predominantly reddish-brown with metatarsi, tarsi and the proximal portion of the femora lighter. Opisthosoma with an accentuated concavity on the anterior margin, yellowish-brown on the dorsum and median-posterior area; reddish-brown on the sides and projections (Fig. 6A). Copulatory openings are long and narrowed (Fig. 6C), leading to long and membranous copulatory ducts; spermathecae black, walnut-shaped and sclerotized (Fig. 6D). Measurements: eyes diameters and eyes interdistances: AME 0.09, ALE 0.15, PME 0.15, PLE 0.17, AME-AME 0.19, AME-ALE 0.09, PME-PME 0.17, PME-PLE 0.15. MOQ length 0.41, MOQ posterior width 0.51, MOQ anterior width 0.38; leg formula: 1243: leg I—femur 2.52/ patella 1.23/ tibia 1.69/ metatarsus 1.56/ tarsus 0.93/ total 7.93; II—2.28/ 1.06/ 1.47/ 1.29/ 0.80/ 6.90; III—1.28/ 0.81/ 0.79/ 0.63/ 0.52/ 4.03; IV—1.72/ 0.80/ 1.11/ 0.75/ 0.55/ 4.93. Prosoma length 2.50, width 2.62, opisthosoma length 3.56, total body length 6.06; clypeus height 0.35, sternum length 1.27, width 1.14, endites length 0.68, width 0.34, labium length 0.39, width 0.46.

Male (FMNH 71619): Eye arrangement as in the female. Prosoma reddish-brown, lighter in the median portion and presenting a triangular guanine spot on the thoracic area (Fig. 7A). Anterior legs (I and II) light-brown and posterior (III and IV) predominantly yellow, darker on patellae. Palp have a well-developed cymbium with a

retrolateral reentrance that helps to accommodate the embolus (Fig. 7D). Tegulum discoid, rough surfaced (Fig. 7C); RTA short and acute. Measurements: eyes diameters and eyes interdistances: AME 0.08, ALE 0.12, PME 0.13, PLE 0.11, AME-AME 0.14, AME-ALE 0.09, PME-PME 0.16, PME-PLE 0.15. MOQ length 0.32, MOQ posterior width 0.41, MOQ anterior width 0.30; leg formula: 1243: leg I—femur 2.36/ patella 0.94/ tibia 1.86/ metatarsus 1.64/ tarsus 1.01/ total 7.81; II—1.96/ 0.80/ 1.40/ 1.27/ 0.78/ 6.21; III—1.02/ 0.57/ 0.70/ 0.55/ 0.46/ 3.30; IV—1.28/ 0.56/ 0.90/ 0.74/ 0.49/ 3.97. Prosoma length 2.07, width 1.90, opisthosoma length 2.02, total body length 4.09; clypeus height 0.30, sternum length 0.89, width 0.95, endites length 0.51, width 0.27, labium length 0.30, width 0.37.

Distribution. ARGENTINA: Neuquén, Chubut and Terra del Fuego; CHILE: Coquimbo, Valparaiso, Santiago, Maule, Bío-Bío, Araucanía, Los Rios, Los Lagos and Aysén (Fig. 14).
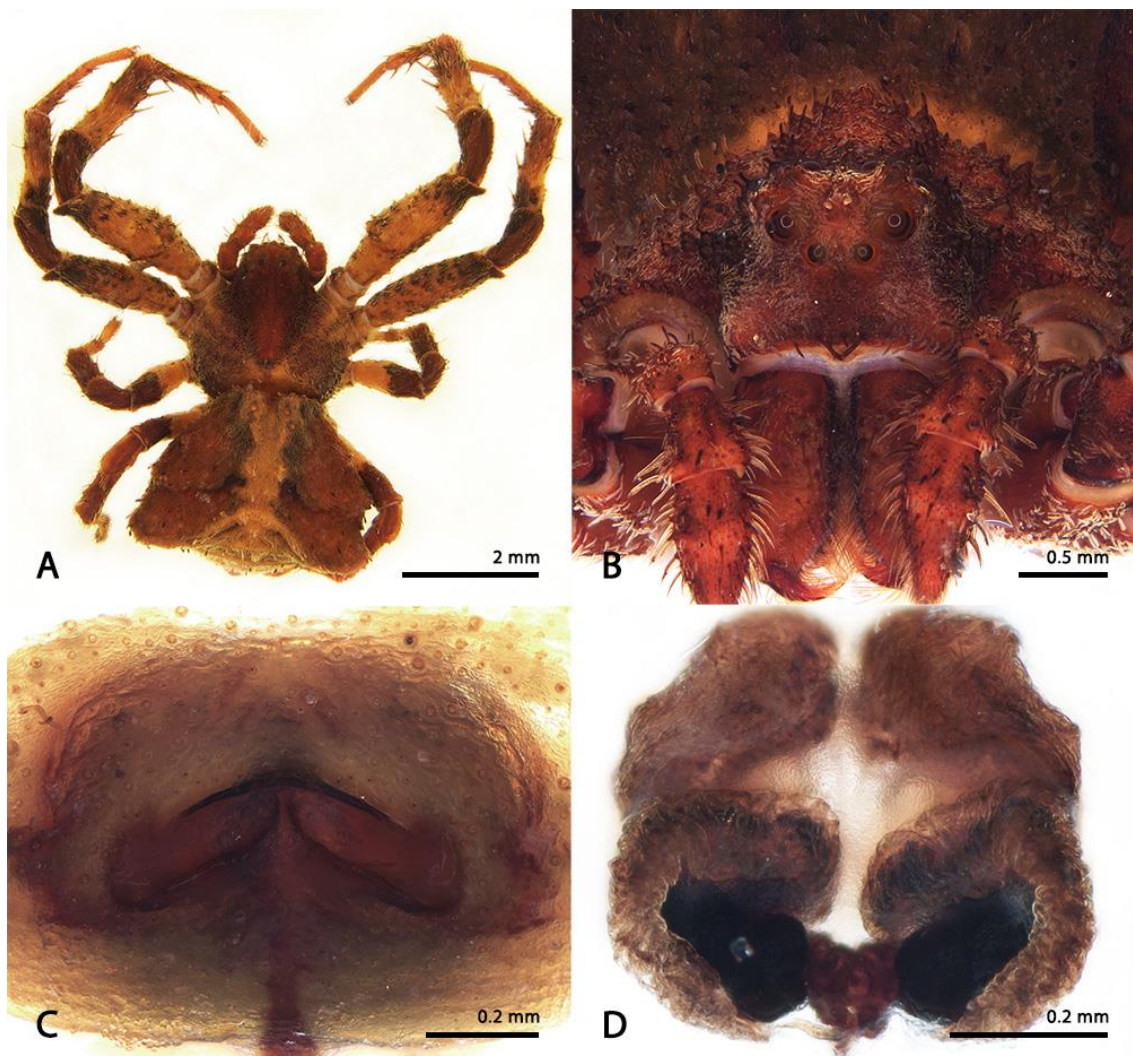
Figure 6. *Coenypha ditissima* (Nicolet, 1849), female (AMNH). A) dorsal habitus; B) frontal habitus; C) ventral view of epigynal plate; D) dorsal view of epigynal plate.
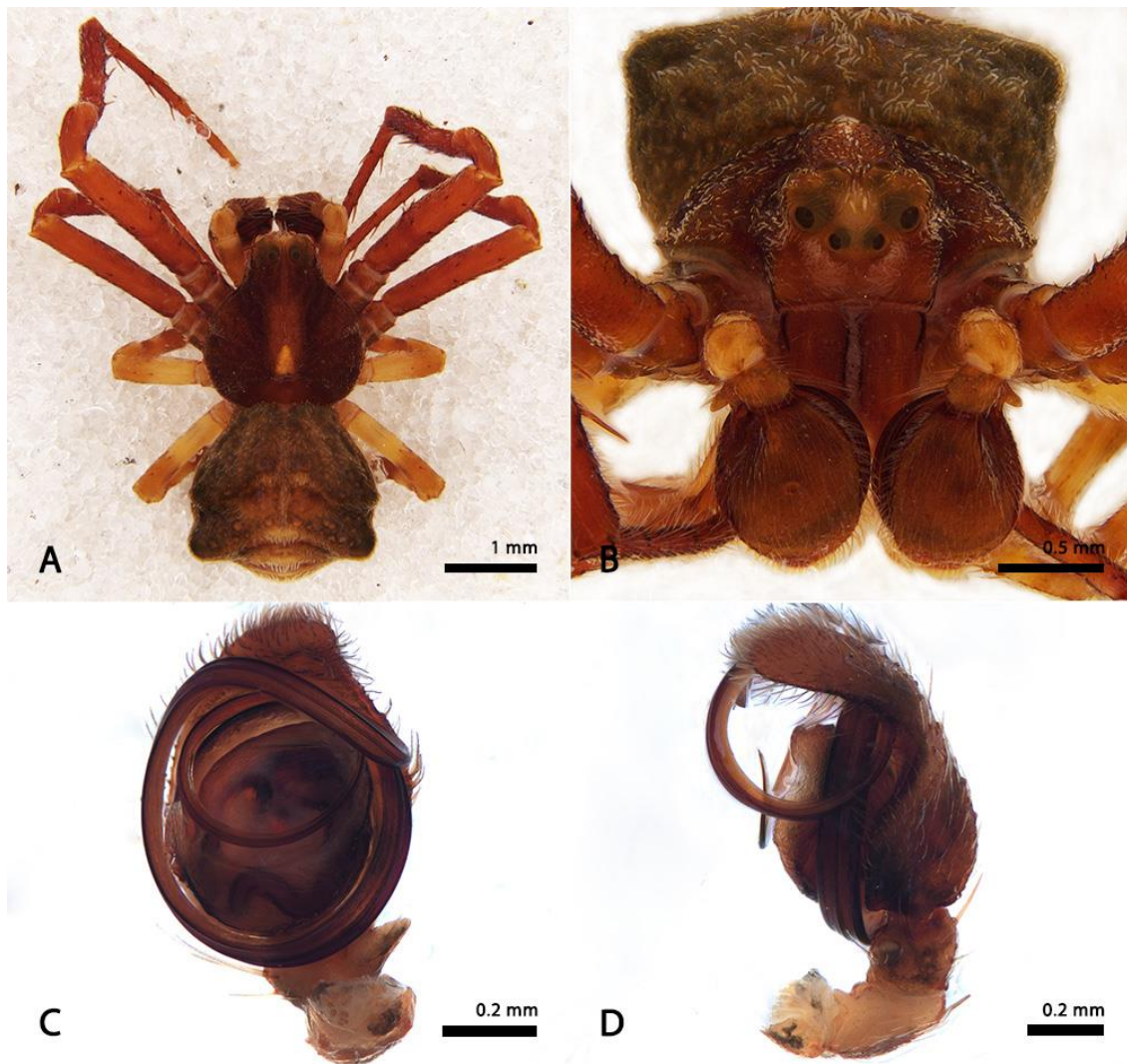
Figure 7. *Coenypha ditissima* (Nicolet, 1849), male (FMNH 71619). A) dorsal habitus; B) frontal habitus; C) ventral view of the left palp; D) retrolateral view of the left palp.

Coenypha doritos **sp. nov.**

Figs 8, 9

Type material: Holotype: 1 female, Pukará de Quitor [22°53'29.00"S, 68°12'43.70"W, San Pedro de Atacama, Antofagasta, Chile], 15 December 1965, Giai leg. (MACN-Ar 18675).

Paratype: 1 male, Parque Nacional La Campana [32°57'15.69"S, 71°4'38.13"W, Quillota, Valparaiso, Chile], 29 December 2002, Thayer, Newton & Solodovnikov leg.

(FMNH 2857851); 1 male, Cuesta La Dormida [33°31'16.74"S, 70°47'42.40"W, Santiago, Chile], 13 November 1982, L. Peña leg. (AMNH).

Other material examined. Only the type material.

Etymology. The specific name is given after the brand Doritos® due to the shape of the female opisthosoma, which resembles a tortilla-chip.

Diagnosis. Females of *C. doritos* **sp. nov.** differ from those of *C. edwardsi* by the yellowish body coloration, higher clypeus, prosoma as long as wide and opisthosoma with only two pairs of posterior-lateral projections (Figs 8A, 8B). They can also be distinguished by the epigynal plate with a thin median septum and slits arranged horizontally (Fig. 8C), and by the triple twisted copulatory ducts (Fig. 8D). Males can be recognized by their long ventral setae on the anterior tibiae and metatarsi (I and II), anal region pronounced (Fig. 9A), and by the RTAvbr truncated and bearing a terminal concavity (Fig. 9D).

Description. *Female* (**MACN-Ar 18675**): Anterior eye row recurved and posterior row slightly procurve; ALE almost twice as large as the AME (Figs 8A, 8B). Prosoma totally orange, with few clavate setae on conical sockets; sternum orange, scutiform and wide as long. Legs are predominantly orange with few sparse dark punctuations. Opisthosoma yellow with small black spots symmetrically arranged; anterior border straight and posterior with a median concavity and two posterior lateral projections (Fig. 8A). Copulatory ducts membranous, spermatechae subdivided in two chambers and with no accessory glands (Fig. 8D). Measurements: eyes diameters and eyes interdistances: AME 0.08, ALE 0.14, PME 0.14, PLE 0.14, AME-AME 0.14, AME-ALE 0.10, PME-PME 0.22, PME-PLE 0.14. MOQ length 0.44, MOQ posterior width 0.32, MOQ anterior width 0.24; leg formula: 1243: leg I—femur 4.20/ patella

1.78/ tibia 2.75/ metatarsus 1.68/ tarsus 1.00/ total 11.41; II—3.40/ 1.45/ 2.20/ 1.22/ 0.80/ 4.75; III—1.42/ 0.90/ 1.02/ 0.56/ 0.54/ 4.44; IV—1.74/ 0.92/ 1.22/ 0.62/ 0.54/ 5.04; total length 7.54, prosoma length 3.09, width 3.10, opisthosoma length 4.45, clypeus height 0.38, sternum length 1.36, width 1.33, endites length 0.72, width 0.34, labium length 0.46, width 0.52.
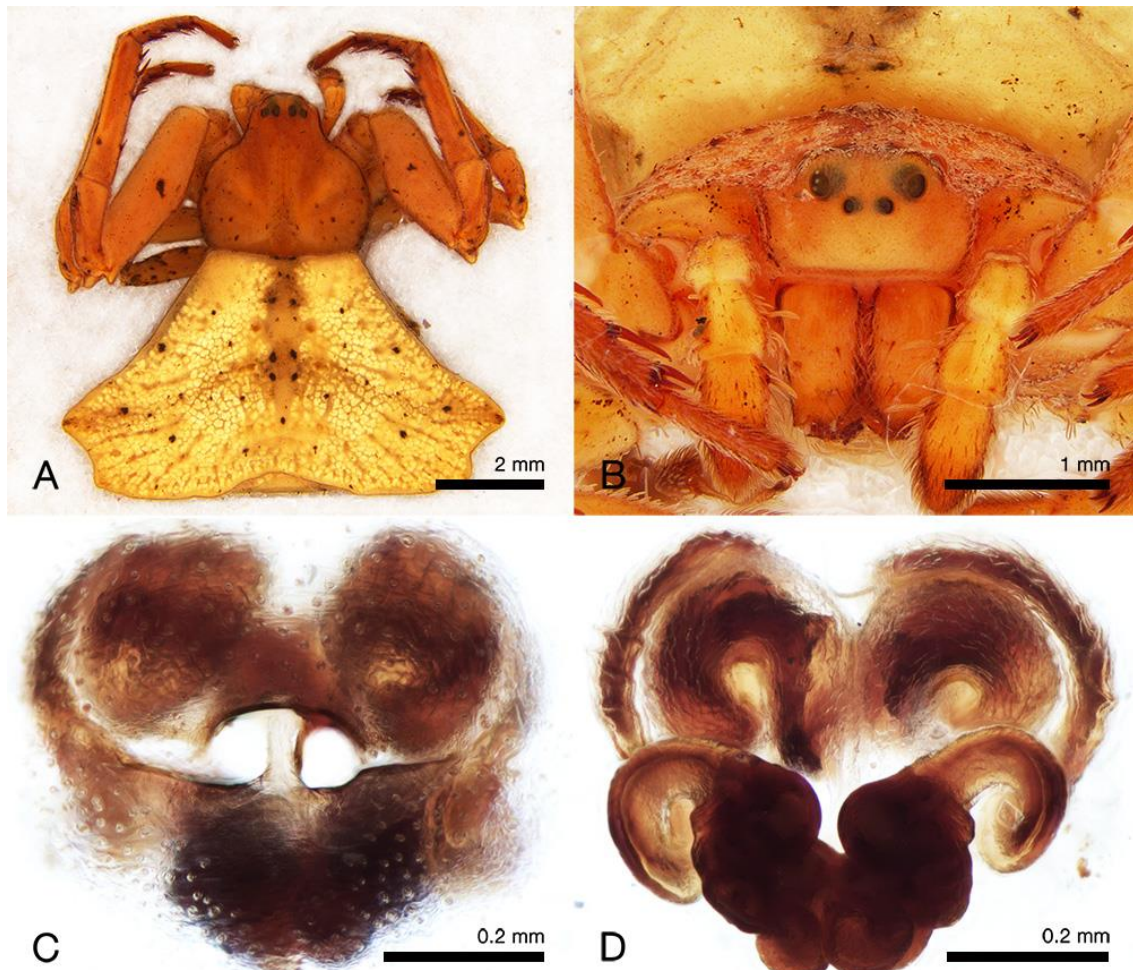

Figure 8. *Coenypha doritos* **sp. nov.**, female (MACN-Ar 18675). A) dorsal habitus; B) frontal habitus; C) ventral view of epigynal plate; D) dorsal view of epigynal plate.

Male (**FMNH-ISN 2857851**): Anterior eye row recurve and posterior slightly procurve (Figs 9A, 9B). Prosoma brown with darker stains randomly distributed, sternum brown, scutiform and slightly wider than long. Legs present the same coloration pattern of the prosoma, except by the femora IV, which are yellow up to half

of their proximal portion (Fig. 9A). Opisthosoma totally yellow with many dark clavate setae and differing from those of the female by having and additional round lobe right after the posterior abdominal projections (Fig. 9A). Palp bears a discoid tegulum (Fig. 9C), a sinuous, grooved and pointed RTA and a truncated RTAvbr with bulged tip (Fig. 9D). Measurements: eyes diameters and eyes interdistances: AME 0.08, ALE 0.18, PME 0.12, PLE 0.06, AME-AME 0.10, AME-ALE 0.06, PME-PME 0.18, PME-PLE 0.12. MOQ length 0.40, MOQ posterior width 0.24, MOQ anterior width 0.20; leg formula: 1234: leg I—femur 3.04/ patella 1.20/ tibia 2.44/ metatarsus 1.46/ tarsus 0.84/ total 8.98; II—2.00/ 0.81/ 1.44/ 1.00/ 0.44/ 5.69; III—0.88/ 0.56/ 0.62/ 0.42/ 0.40/ 2.88; IV—1.16/ 0.60/ 0.81/ 0.50/ 0.44/ 3,51; total length 4.58, prosoma length 2.15, width 2.00, opisthosoma length 2.43, clypeus height 0.22, sternum length 0.90, width 0.98, endites length 0.50, width 0.28, labium length 0.26, width 0.40.

Distribution. CHILE: Antofagasta, Valparaiso and Santiago (Fig. 14).

Figure 9. *Coenypha doritos* **sp. nov.**, male (FMNH 2857851). A) dorsal habitus; B) frontal habitus; C) ventral view of the left palp; D) retrolateral view of the left palp.

Coenypha foliacea **sp. nov.**
Figs 10, 11

Type material: Holotype: 1 female, Cautín [38°56'56.12"S, 72°19'52.01"W, Araucanía, Chile], (MACN-Ar 18708).

Paratypes: 1 male, Monumento Natural Contulmo [38°0'51.55"S, 73°10'48.24"W, Purén, Malleco, Aracucanía, Chile], (MACN-Ar 18705); 1 female, Cerro Ñielol [38°43'27.08"S, 72°35'18.33"W, Temuco, Cautín, Araucanía], (MACN-Ar 18706).

Other material examined. Only the type material.

Etymology. The specific name derives from the latin word *foliacea*, that means "leaf-shaped", referring to the shape of the opisthosoma of this species that, combined to the cryptic coloration of the individuals, resembles a dry leaf.

Diagnosis. The females of *C. foliacea* **sp. nov.** resemble those of *C. ditissima* by their relative body-size and shape of opisthosoma, however, they can be easily recognized by their enlarged femora I (which it is more similar to what is observed in *C. edwardsi*) bearing a pair of sockets each, accommodating two hyaline and plumose macrosetae (Fig. 10A). The prosoma of *C. foliacea* **sp. nov.** also differ from those of *C. ditissima* by its more flattened profile, while the epigynum has a wider septum, copulatory openings with narrower entrances, shorter copulatory ducts and bigger spermathecae (Figs 10C, 10D). Males are recognized by the presence of a prolateral macrosetae on cymbium (Fig. 11C), which also has a retrolateral reentrance to accommodate the embolus (Fig. 11D), like in *C. ditissima*. However, in *C. foliacea* **sp. nov.** the embolus is shorter, resting in this region instead of on a median tegular ridge.

Description. *Female* **(MACN-Ar 18706):** Anterior eye row recurved and posterior row slightly procurved; MOQ area covered by many whitish setae (Figs 10A, 10B). Prosoma light brown on the sides and darker on the median thoracic area and cephalic region (Fig. 10A). Anterior legs (I and II) predominantly light-brown and posterior ones dark-brown from the distal portion of femora until the tarsi; proximal portion of femora yellowish (Fig. 10A). Opisthosoma brown, flattened, with rounded anterior margin and two pairs of posterior projections. Epigynal plate with wide posterior folds converging in the middle to form an intromittent median septum (Fig. 10C); copulatory ducts hyaline, membranous and frilled, leading to a pair of

172

spermathecae with porous distributed on its anterior surface, not acuminated on a specific region or forming a glandular head (Fig. 10D). Measurements: eyes diameters and eyes interdistances: AME 0.07, ALE 0.12, PME 0.13, PLE 0.14, AME-AME 0.09, AME-ALE 0.05, PME-PME 0.10, PME-PLE 0.08. MOQ length 0.30, MOQ posterior width 0.33, MOQ anterior width 0.20; leg formula: 1243: leg I—femur 2.81/ patella 0.93/ tibia 1.45/ metatarsus 1.18/ tarsus 0.67/ total 7.04; II—2.64/ 0.74/ 1.14/ 0.95/ 0.65/ 6.12; III—1.06/ 0.62/ 0.71/ 0.53/ 0.50/ 3.42; IV—1.41/ 0.63/ 0.98/ 0.78/ 0.57/ 4.37. Prosoma length 2.11, width 2.08, opisthosoma length 2.63, total body length 4.74; clypeus height 0.25, sternum length 0.92, width 0.98, endites length 0.50, width 0.27, labium length 0.23, width 0.42.

Male (MACN-Ar 18705): Eye disposition and eye row arrangements as in the female. Prosoma and opisthosoma entirely dark-brown, anterior legs (I and II) brown, with tibiae slighty curved; leg III entirely yellow and leg IV yellow only on the proximal half of the femora, being the other leg segments dark-brown (Fig. 11A). Opisthosoma similar to that of females, however, with a small and acute lateral projection on each side (Fig. 11A). Palp has a cymbium with projected apical portion and oval tegulum (Fig. 11C); RTA is thin and acute, while the RTAvbr is conical and as long as the RTA (Fig. 11D). Measurements: eyes diameters and eyes interdistances: AME 0.10, ALE 0.18, PME 0.15, PLE 0.19, AME-AME 0.13, AME-ALE 0.11, PME-PME 0.18, PME-PLE 0.13. MOQ length 0.41, MOQ posterior width 0.51, MOQ anterior width 0.33; leg formula: 1243: leg I—femur 3.15/ patella 1.27/ tibia 2.36/ metatarsus 1.77/ tarsus 0.91/ total 9.46; II—2.63/ 1.09/ 2.00/ 1.40/ 0.84/ 7.96; III—1.69/ 0.99/ 1.10/ 0.90/ 0.78/ 5.46; IV—2.01/ 0.90/ 1.33/ 0.96/ 0.74/ 5.94. Prosoma length 3.35, width 3.15, opisthosoma length 3.37, total body length 6.72; clypeus height 0.29,

sternum length 1.33, width 1.30, endites length 0.78, width 0.40, labium length 0.44, width 0.57.

**Distribution.** CHILE: Araucanía (Fig. 15).
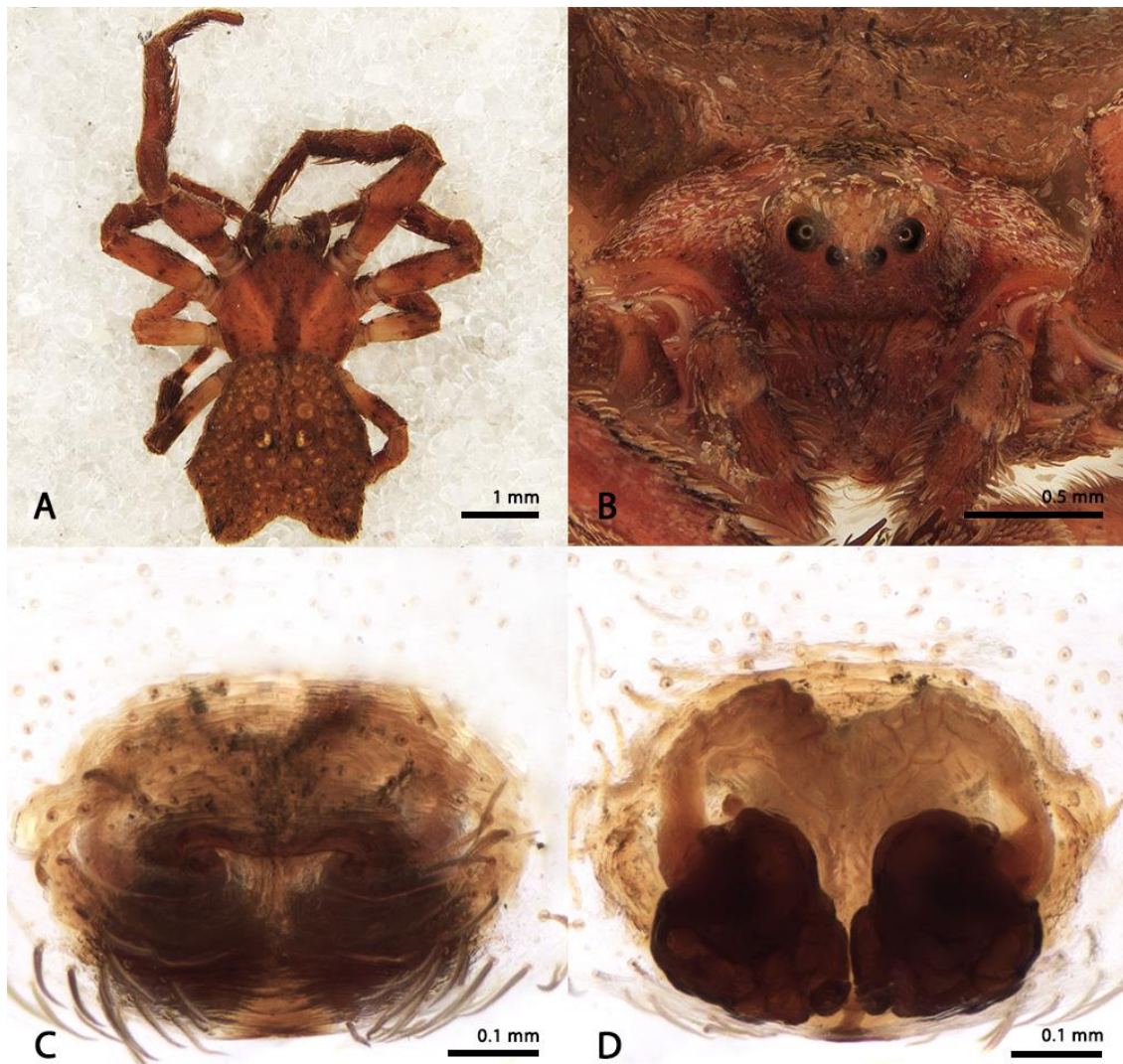
Figure 10. *Coenypha foliacea* **sp. nov.**, female (MACN-Ar 18706). A) dorsal habitus; B) frontal habitus; C) ventral view of epigynal plate; D) dorsal view of epigynal plate.
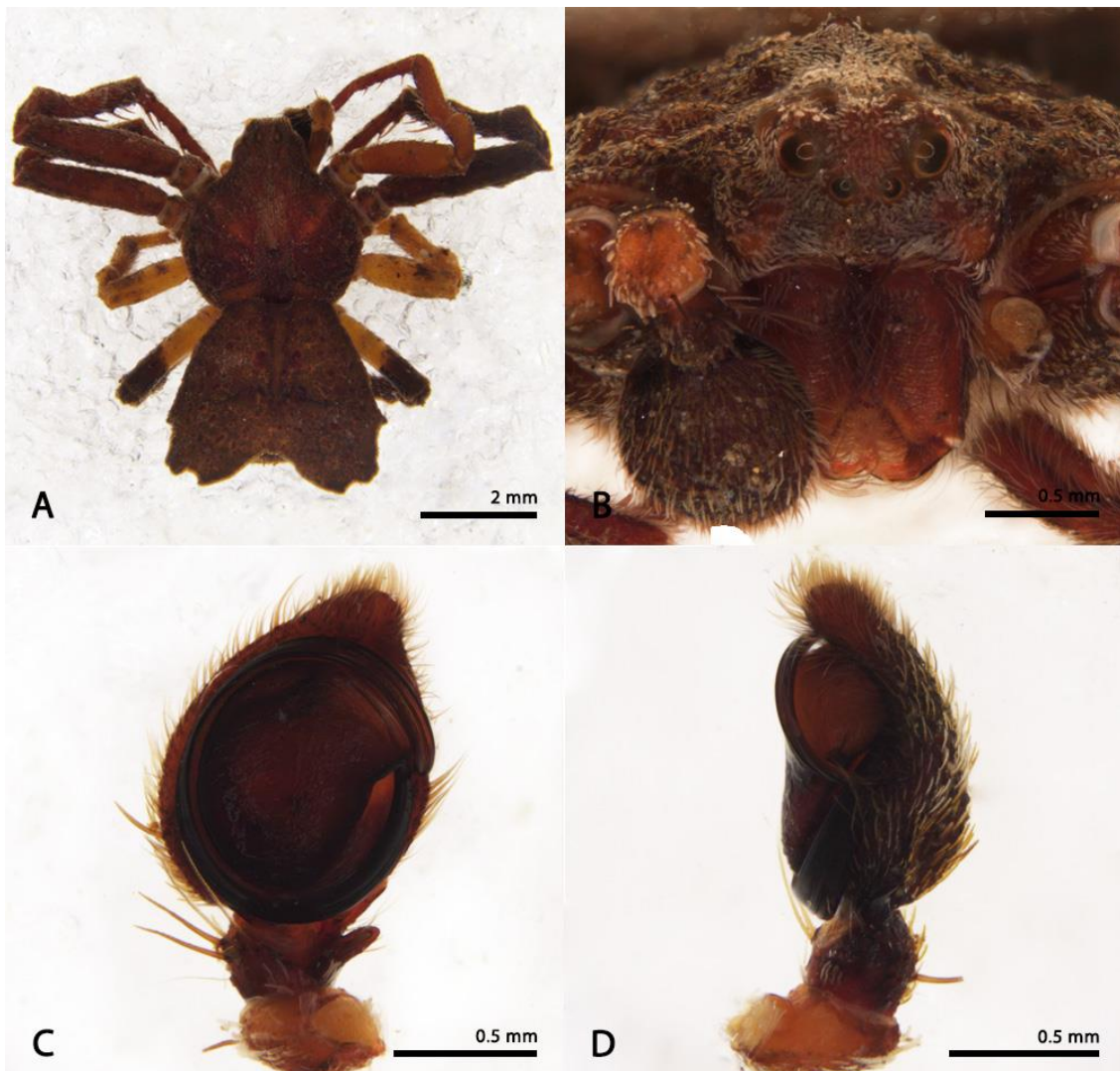
Figure 11. *Coenypha foliacea* **sp. nov.**, male (MACN-Ar 18705). A) dorsal habitus; B) frontal habitus; C) ventral view of the left palp; D) retrolateral view of the left palp.

Coenypha nodosa (Nicolet, 1849) comb. nov.

Figs 12, 13

Thomisus nodosus Nicolet, 1849: 397.

Stephanopis nodosa Simon, 1895: 1054.

Thomisus verrucosus Nicolet, 1849: 398 (Syntypes: 2 females from Valdivia, Chile, deposited in MNHN 4174, examined).

Stephanopis verrucosa (Nicolet): Simon, 1895: 1054. **New Synonymy.**

Stephanopis hystrix Mello-Leitão, 1951: 333, Fig. 8 (Holotype female from Maullín, Llanquihue, Chile, deposited in MNRJ, examined). **New Synonymy.**

Type material: Holotype: female from Valdivida, Chile, (MNHN 4194, examined).

Other material examined. CHILE: *Bío-Bío***:** 1j, Ñuble, 36°42'16.20"S, 71°36'9.60"W, 15 February 2005, M. Ramírez & F. Labarque (MACN-Ar 10865); 2f#, Concepción (Chome), 36°42'52.73"S, 73°8'21.39"W, 07 December 1995, T. Cekalovic (AMNH); 1m#, Concepción (Hualpén), 36°47'12.03"S, 73°6'35.83"W, 11 January 1989, M. Ramírez (MACN-Ar 18703); 1f#, same locality, collector and date of the previous vial (MACN-Ar 18702); 1f#, Concepción, 36°49'12.49"S, 73°2'39.80"W, 14 January 1977, T. Cekalovic (MCZ 133404); 1f# and 1j, Concepción (Estero Nonguén), 36°49'41.25"S, 73°0'19.52"W, 02 November 1996, T. Cekalovic (AMNH); 1f#, Escuadrón, 36°58'55.02"S, 73°9'12.86"W, 15 November 1996, T. Cekalovic (AMNH). *Araucanía***:** 7j, Malleco (Monumento Natural Contulmo), 38°0'51.55"S, 73°10'48.24"W, 19-21 December 1998, M. Ramírez, L. Coapagnucci, C. Grismado & L. Lopardo (MACN-Ar 18709). *Los Ríos***:** 4f# and 8j, Valdivia, 39°49'6.53"S, 73°14'37.94"W, 1984, E. Krahmer (MNNC); 1m# and 1f#, same locality and collector of the previous vial, December 1982 (MNNC 841); 1f# and 2j, same locality and collector of the previous vial, 1983 (MNNC 800); 1j, Valdivia (Huachocopihue), 39°50'2.23"S, 73°14'17.32"W, 07 March 1965, H. Levi (MCZ 133400). *Los Lagos***:** 1f# and 1j, Osorno (Pocatrihue), 40°32'6.87"S, 73°42'31.82"W, March 1968, L. Peña (MCZ 133406); 1f# and 4j, Osorno (20 Km East of Puyehue), 40°34'34.28"S, 73°6'53.81"W, 25 January 1951, Ross & Michelbacher (CAS 9071270); 3j, Osorno (Termas de

Puyehue), 40°40'0.00"S, 71°13'60.00"W, 30 November 1994, R. Leschen & C. Carlton (AMNH); 2j, Osorno (Parque Nacional Puyehue), 40°43'16.56"S, 72°19'3.87"W, 19-26 December 1982, A. Newton & M. Thayer (AMNH); 7j, Osorno (Aguas Calientes), 40°43'43.88"S, 72°18'43.16"W, 13-17 December 1998, M. Ramírez, L. Coapagnucci, C. Grismado & L. Lopardo (MACN-Ar 18662); 4j, Llanquihue (Los Muermos), 41°23'57.87"S, 73°27'53.97"W, 19 January 1951, Ross & Michelbacher (CAS 9071273); 1j, Isla Grande de Chiloé (Cole Cole), 42°25'22.39"S, 74°4'58.62"W, 08-11 February 1991, M. Ramírez (MACN-Ar 18648); 2f# and 2j, Isla Grande de Chiloé, 42°37'26.29"S, 73°55'35.66"W, 22 February 1997, T. Cekalovic (AMNH); 1j, Palena (Chaitén), 42°54'41.51"S, 72°42'56.30"W, 04 December 1981, N. Platnick and R.T. Schuh (AMNH).

Diagnosis. The resemblance of *C. nodosa* with *C. antennata* is based on the shape of the opisthosoma, with a posterior pair of projections and anal region well-developed (Fig. 12A), but different of its close related species, the females of *C. nodosa* do not have the long pair of macrosetae between the ALE (Fig. 12B); their prosoma is as wide as long, with cephalic portion short, while the epignyal plate presents a stout and complete median septum that separate the copulatory openings completely (Fig. 12C). Males can be distinguished by their long and thin legs with many needle-shaped setae (Fig. 13A) and sinuous cymbium, narrowing at the tip and forming an acute distal portion (Fig. 13C).

Description. *Female* **(MCZ 133404):** Anterior eye row strongly recurved and posterior row slightly procurved; ALE have twice the diameter of the AME (Figs 12A, 12B). Prosoma brown with a median longitudinal darker stain; All legs are predominantly brownish-yellow with dark-brown spots randomly distributed, except by the tibiae and metatarsi I and II, which are almost entirely dark-brown (Fig. 12A).

Opisthosoma brownish-yellow with darker spots on the median portion of the dorsum and on the sides of the anal region (Fig. 12A). Epigynal plate in ventral view resembles a "dog snout" (Fig. 12C); copulatory ducts are long, coiled and hyaline, leading to a pair of spermathecae with nodose exterior surface (Fig. 12D). Measurements: eyes diameters and eyes interdistances: AME 0.10, ALE 0.20, PME 0.20, PLE 0.22, AME-AME 0.18, AME-ALE 0.14, PME-PME 0.24, PME-PLE 0.16. MOQ length 0.58, MOQ posterior width 0.65, MOQ anterior width 0.40; leg formula: 1243: leg I—femur 3.78/ patella 1.76/ tibia 3.01/ metatarsus 2.17/ tarsus 1.14/ total 11.86; II—3.32/ 1.50/ 2.42/ 2.19/ 0.95/ 10.38; III—1.98/ 1.00/ 1.54/ 1.39/ 0.80/ 6.71; IV—2.57/ 1.10/ 1.88/ 1.66/ 0.83/ 8.04. Prosoma length 3.53, width 3.23, opisthosoma length 3.84, total body length 7.37; clypeus height 0.43, sternum length 1.55, width 1.43, endites length 0.88, width 0.44, labium length 0.53, width 0.63.

Male (MNNC 691): Eye arrangement and disposition as in the female; prosoma entirely brown and legs predominantly dark-yellow, with few darker spots randomly distributed (Figs 13A, 13B). Opisthosoma greyish-brown with a median darker taint on the median area of the dorsum (Fig. 13A). Palpi have a short and obtuse RTA and a densely sclerotized squared RTAvbr (Fig. 13D); tegulum reduces, oval-shaped and embolus with well-developed pars pendulum (Fig. 13C). Measurements: eyes diameters and eyes interdistances: AME 0.10, ALE 0.21, PME 0.18, PLE 0.19, AME-AME 0.14, AME-ALE 0.11, PME-PME 0.19, PME-PLE 0.11. MOQ length 0.49, MOQ posterior width 0.45, MOQ anterior width 0.31; leg formula: 1243: leg I—femur 3.81/ patella 1.43/ tibia 3.53/ metatarsus 3.43/ tarsus 1.46/ total 13.66; II—3.38/ 1.25/ 2.90/ 2.71/ 1.35/ 11.59; III—1.76/ 0.80/ 1.49/ 1.28/ 0.81/ 6.14; IV—2.25/ 0.90/ 1.73/ 1.49/ 0.82/ 7.19. Prosoma length 2.61, width 2.41, opisthosoma length 2.73, total body length 5.34;

clypeus height 0.27, sternum length 1.20, width 1.15, endites length 0.68, width 0.35, labium length 0.33, width 0.51.

Distribution. CHILE: Bío-Bío, Araucanía, Los Rios and Los Lagos (Fig. 15).
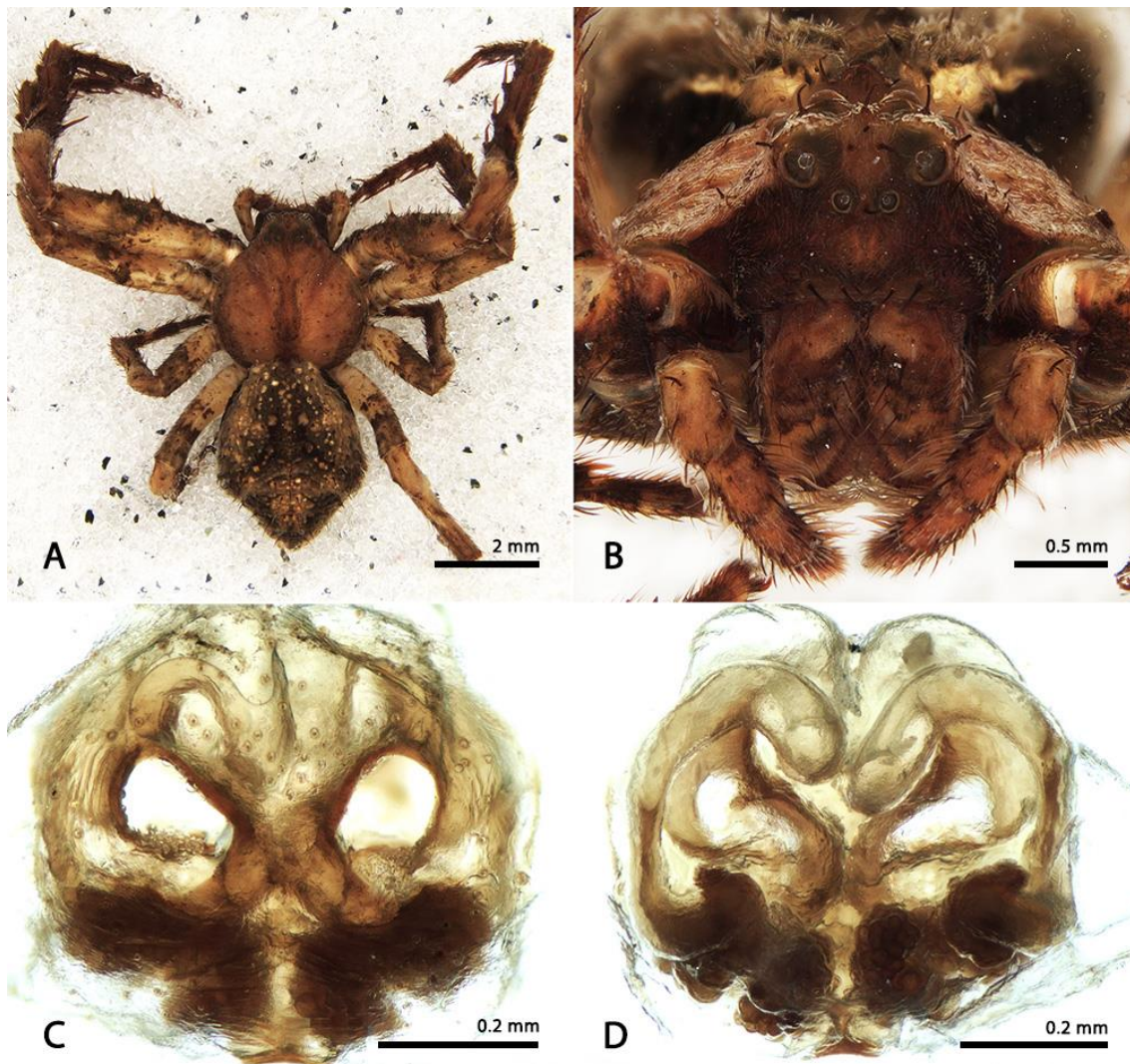

Figure 12. *Coenypha nodosa* (Nicolet, 1849), female (MCZ 133404). A) dorsal habitus; B) frontal habitus; C) ventral view of epigynal plate; D) dorsal view of epigynal plate.
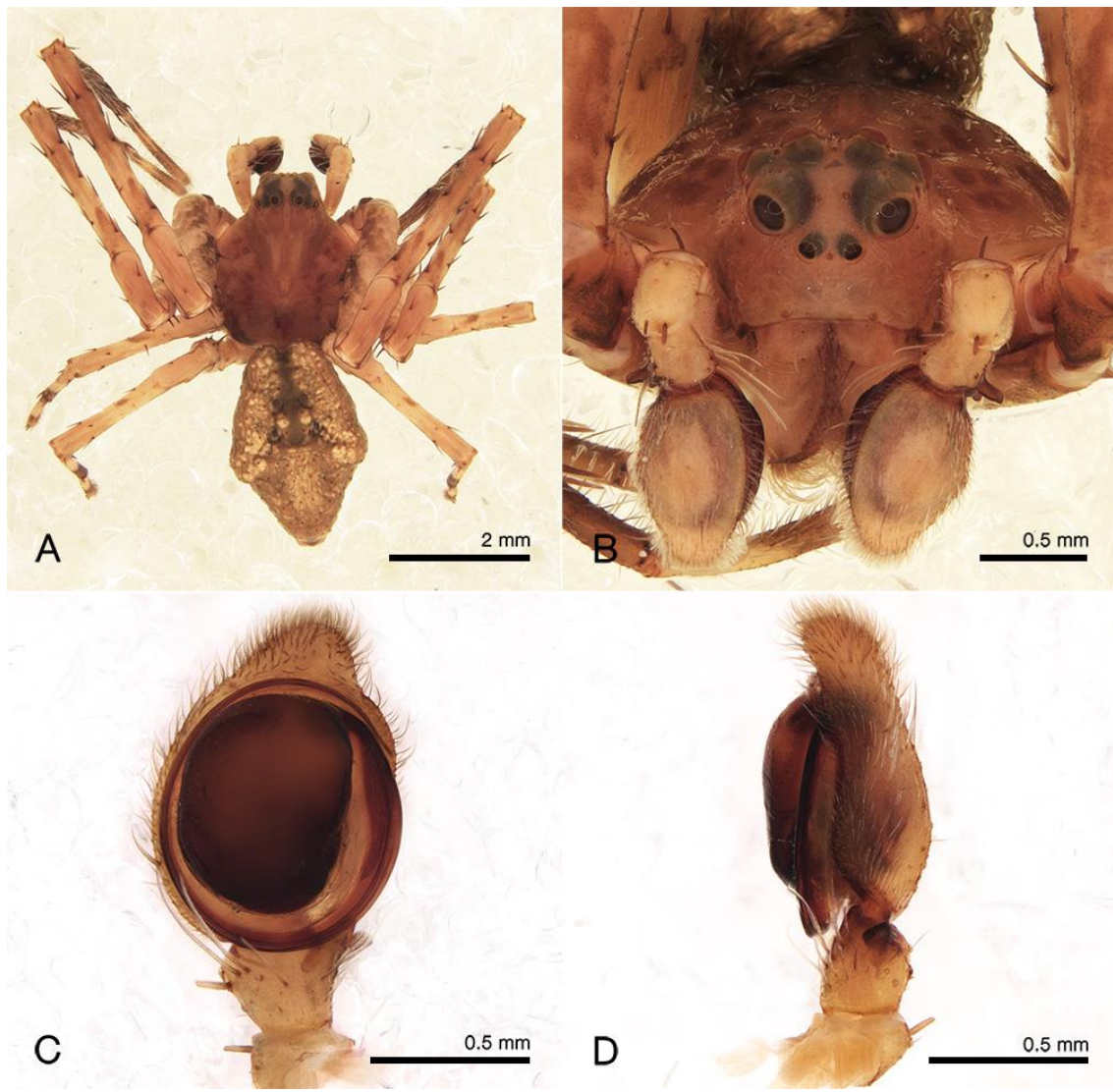
Figure 13. *Coenypha nodosa* (Nicolet, 1849), male (MNNC 691). A) dorsal habitus; B) frontal habitus; C) ventral view of the left palp; D) retrolateral view of the left palp.

Note. In the same vial where the syntype females of *S. verrucosa* where found, there were also two males. However, these two co-specific specimens do not belong to *Coenypha*. The careful examination of somatic and genital features of the individuals allowed us to identify them as species belonging to a genus of the subfamily Thomisinae. The ocular arrangement with the MOQ area wider on its anterior portion, legs I and II short and robust, and tibiae I and II bearing two pairs of ventral macrosetae, match with the most updated diagnosis of *Ozyptila* Simon, 1864, provided

by Almquist (2006). The palpal tibiae with three apophyses, presence of VTA and tegular apophysis, as well as the prosoma with a whitish dorsal median band and the opisthosoma narrowed anteriorly and wide on its posterior portion are also similar to those of males of *Ozyptila*,

Figure 14. Distribution records of *Coenypha antennata*, *Coenypha ditissima* and *Coenypha doritos* **sp. nov.**

Figure 15. Distribution records of *Coenypha edwardsi*, *Coenypha foliacea* **sp. nov.**, and

Coenypha nodosa.

References

Almquist, S. (2006) Swedish Araneae, part 2- Families Dictynidae to Salticidae. *Insect Systematics & Evolution*, 63, 285–601.

Benjamin, S. P., Dimitrov, D., Gillespie, R. G. & Hormiga, G. (2008) Family ties: molecular phylogeny of crab spiders (Araneae: Thomisidae). *Cladistics*, 24, 708–722. https://doi.org/10.1111/j.1096-0031.2008.00202.x

Benjamin, S. P. (2011) Phylogenetics and comparative morphology of crab spiders (Araneae: Thomisidae). *Zootaxa*, 3080, 1–108. https://doi.org/10.11646/zootaxa.3080.1.1

Machado, M., Teixeira, R. A. & Lise, A. A. (2017) Cladistic analysis supports the monophyly of the Neotropical crab spider genus *Epicadus* and its senior synonymy over *Tobias* (Araneae: Thomisidae). *Invertebrate Systematics*, 31, 442–455. https://doi.org/10.1071/IS16074

Machado, M., Teixeira, R. A. & Lise, A. A. (2018) There and back again: More on the taxonomy of the crab spider genus *Epicadus* (Thomisidae: Stephanopinae). *Zootaxa*, 4382, 501–530. https://doi.org/10.11646/zootaxa.4382.3.4

Machado, M., Guzati, C., Viecelli, R., Molina-Gómez, D. & Teixeira R. A. (2019a) A taxonomic review of the crab spider genus *Sidymella* (Araneae, Thomisidae) in the Neotropics. *Zoosystematics and Evolution*, 95, 319–344.

https://doi.org/10.3897/zse.95.34958

Machado, M., Teixeira, R. A. & Milledge, G. A. (2019b) On the Australian bark crab spiders genus *Stephanopis*: Taxonomic review and description of seven new species (Araneae: Thomisidae: Stephanopinae). *Records of the Australian Museum*, 71, 217–276.

https://doi.org/10.3853/j.2201-4349.71.2019.1698

Nicolet, A. C. (1849) Aracnidos. In: Gay, C. (ed.) Historia física y política de Chile. Zoología 3, 319-543, pl. 1-5.

https://doi.org/10.5962/bhl.title.16172

Prado, A. W., Baptista, R. L. & Machado, M. (2018) Taxonomic Review of *Epicadinus* Simon, 1895 (Araneae: Thomisidae). *Zootaxa*, 4459, 201–234. https://doi.org/10.11646/zootaxa.4459.2.1

Ramírez, M. J. (2014) The morphology and phylogeny of dionychan spiders (Araneae: Araneomorphae). *Bulletin of the American Museum of Natural History*, 390, 1–374.

Silva-Moreira, T. & Machado, M. (2016) Taxonomic revision of the crab spider genus *Epicadus* Simon, 1895 (Arachnida: Araneae: Thomisidae) with notes on related genera of Stephanopinae Simon, 1895. *Zootaxa*, 4147 (3), 281–310. https://doi.org/10.11646/zootaxa.4147.3.4

Tullgren, A. (1902) Spiders collected in the Aysén Valley by Mr P. Dusén. *Bihang till Kungliga Svenska Vetenskaps-Akademiens Handlingar*, 28(4), 1–77.

Wheeler, W. C., Coddington, J. A., Crowley, L. M., Dimitrov, D., Goloboff, P. A., Griswold, C. E., Hormiga, G., Prendini, L., Ramírez, M. J., Sierwald, P., Almeida-Silva, L., Alvarez-Padilla, F., Arnedo, M. A., Benavides Silva, L. R., Benjamin, S. P., Bond, J. E., Grismado, C. J., Hasan, E., Hedin, M., Izquierdo, M. A., Labarque, F. M., Ledford, J., Lopardo, L., Maddison, W. P., Miller, J. A., Piacentini, L. N., Platnick, N. I., Polotow, D., Silva-Dávila, D., Scharff, N., Szuts, T., Ubick, D., Vink, C. J., Wood, H. M. & Zhang, J. (2017) The spider tree of life: phylogeny of Araneae based on target-gene analyses from an extensive taxon sampling. *Cladistics*, 33, 574–616. https://doi.org/10.1111/cla.12182

World Spider Catalog (2020) World Spider Catalog, Natural History Museum Bern, Bern. Available from: http://wsc.nmbe.ch (accessed 8 Nov. 2020) [version 21.0]

Chapter 4: A taxonomic review of the crab spider genus Sidymella (Araneae: Thomisidae) in the Neotropics

MUSEUM FÜR NATURKUNDE BERLIN

A taxonomic review of the crab spider genus *Sidymella* (Araneae, Thomisidae) in the Neotropics

Miguel Machado[1], Catherine Guzati[1], Rafaela Viecelli[1], Diana Molina-Gómez[1], Renato Augusto Teixeira[1]

1 *Laboratório de Aracnologia, Faculdade de Biociências, Pontifícia Universidade Católica do Rio Grande do Sul (PUCRS), Avenida Ipiranga 6681, Porto Alegre, RS, Brazil*

http://zoobank.org/1AC7C423-2E9A-42B0-AD01-902985656BE6

Corresponding author: *Miguel Machado* (machadom.arachno@gmail)

Abstract

Four Neotropical species of *Sidymella* Strand, 1942, *S. furcillata* Keyserling, 1880, *S. longispina* (Mello-Leitão, 1943), *S. lucida* (Keyserling, 1880), and *S. kolpogaster* (Lise, 1973) are redescribed from both sexes. The holotype of *S. nigripes* (Mello-Leitão, 1947) is lost and this taxon is considered a *species inquierenda*. *Sidymella obscura* (Mello-Leitão, 1929), *S. parallela* (Mello-Leitão, 1929), and *S. spinifera* (Mello-Leitão, 1929) are all *nomina dubia*. Two new species are described: *Sidymella excavata* **sp. nov.** (males and females) and *S. marmorata* **sp. nov.** (female).

Key Words

Introduction

Crab spiders (Araneae, Thomisidae) are distributed worldwide but the highest diversity is found in tropical regions (WSC 2019). The group has been studied in many recent phylogenetic works, but its relationships are still being discussed (Benjamin et al. 2008; Benjamin 2011; Ramírez 2014; Wheeler et al. 2017) and broader relationships among basal thomisids such as the subfamily Stephanopinae remain weakly supported and unstable (Ramírez 2014). The presence of cheliceral teeth, which was previously considered as a synapomorphy for this group (Ono 1988), was recovered as a plesiomorphy by Benjamin (2011), and this subfamily remains as the most controversial and the least studied group in Thomisidae; it has many genera in need of revision and a considerable number of species yet to be described (Benjamin 2011). Based on the work of Mello-Leitão (1929), subsequent efforts were made to update the taxonomy of some Neotropical stephanopines (Lise 1973, 1981; Bonaldo and

Lise 2001; Machado et al. 2015, 2017; Silva-Moreira and Machado 2016; Prado et al. 2018). However, many genera are still known only from the original descriptions and poor diagnoses, and the accurate identification of many species is practically impossible.

The genus *Sidymella* Strand, 1942 is a prime example of such difficulties. The genus has a disjunct Gondwanan distribution, with 11 described species occuring in Australia and New Zealand whilst 10 are found in the Neotropics (WSC 2019). *Sidymella* is currently defined by a convex prosoma, both anterior and posterior eye rows recurved, anterior tibiae and metatarsi (I and II) with stout and spiniform macrosetae, and opisthosoma posteriorly bifurcated (Strand 1942; Mello-Leitão 1929; Lise 1973). Although the Neotropical *Sidymella* have been revised by Lise (1973), this author focused on somatic characters to describe and diagnose the species, neglecting both external and internal structures of female genitalia and the position, shape, and size of palpal apophyses of males. Therefore, the present paper provides a taxonomic review of the Neo-

Link de acesso ao artigo completo:

https://drive.google.com/file/d/1lJ8zaIKt3M5wN0fdZNuZ-ugkGydVzAd0/view?usp=sharing

On the Australian Bark Crab Spider Genus *Stephanopis*: Taxonomic Review and Description of Seven New Species (Araneae: Thomisidae: Stephanopinae)

MIGUEL MACHADO*[1], RENATO AUGUSTO TEIXEIRA[1], AND GRAHAM A. MILLEDGE[2]

[1] Laboratório de Aracnologia—Escola de Ciências
Pontifícia Universidade Católica do Rio Grande do Sul (PUCRS), Porto Alegre, Brazil

[2] Australian Museum Research Institute,
Australian Museum, 1 William Street, Sydney NSW 2010, Australia

ABSTRACT. Here we present a revision of the Australian species of *Stephanopis*. The type species *S. altifrons* is redescribed and *S. aspera*, *S. depressa*, *S. monticola*, *S. elongata* and *S. scabra* are considered its junior synonyms. Males of *S. altifrons*, *S. angulata*, *S. nigra*, *S. armata*, *S. fissifrons* and *S. longimana* are described for the first time. We propose neotypes for *S. nigra* and *S. barbipes* and describe the female of the latter. Nine species are considered *species inquirendae*, *S. thomisoides* as *nomen dubium* and *S. cheesmanae* is transferred to *Phrynarachne*. Seven new species are described, new distribution records are provided and comments are made about the validity of the genus and its relationship with *Sidymella* species and other Stephanopinae genera from the Australian region.

Introduction

The family Thomisidae is composed of diurnal ambush-hunter species commonly known as "crab spiders", due to the way they move and the size, proportion and disposition of their legs (Dippenaar-Schoeman & Jocqué, 1997). The thomisids comprise the seventh largest family of spiders with 2163 species described in 170 genera (World Spider Catalog, 2019). Among the currently accepted groups in Thomisidae, the subfamily Stephanopinae has been the focus of many recent revisions (Benjamin, 2013; Benjamin, 2015; Machado *et al.*, 2015; Benjamin, 2016; Silva-Moreira & Machado, 2016; Machado *et al.* 2017; Machado *et al.*, 2018; Prado *et al.*, 2018). However, most of its component genera are still little known and poorly diagnosed, resulting in a lack of resolution and the consistent recovery of a polyphyletic phylogeny (Benjamin *et al.*, 2008; Benjamin, 2011; Wheeler *et al.*, 2017). Despite these recent efforts to better describe the morphology and understand the phylogenetic relationships of the group, the genus *Stephanopis*, which gives name to the subfamily, remains in need of a taxonomic review and analyses to test its monophyly.

The genus *Stephanopis* O. Pickard-Cambridge, 1869 was erected for five newly described species, including *S. altifrons*, from Australia. It was characterized by the high cephalic region with unequally sized anterior eyes (ALE larger than AME) disposed in a strongly recurved row, opisthosoma ending in several spiniform projections and dorsoventrally depressed habitus (Pickard-Cambridge, 1869; Simon, 1895). According to Pickard-Cambridge (1869) himself, the single specimen used for the description of *S. altifrons* was dry-pinned and therefore could not be properly examined. It was not possible to determine if the specimen was adult. Moreover, this author states his own sketch of the spider as "hasty". This may explain why the somatic characters were inadequately described, genitalic features were not mentioned at all, and the illustrations were not detailed enough making the species unidentifiable.

Link de acesso ao artigo completo:

https://drive.google.com/file/d/14uTTdB4fnaDOzJDZ-E1AEbYD_cZdoCaW/view?usp=sharing

Correspondence

On Neotropical crab spiders: description of a new species of *Onocolus* (Araneae: Thomisidae)

RENATO AUGUSTO TEIXEIRA[1,2] & MIGUEL MACHADO[1]

[1]*Laboratório de Aracnologia, Escola de Ciências, Pontifícia Universidade Católica do Rio Grande do Sul (PUCRS), Porto Alegre, RS, Brazil.*
[2]*Corresponding author. E-mail: renato.teixeira@pucrs.br*

The systematics and taxonomy of Neotropical stephanopines have been extensively studied over the last years (Machado *et al.* 2015; Silva-Moreira & Machado 2016; Machado *et al.* 2017, 2018; Prado *et al.* 2018). According to Machado *et al.* (2017), the genera *Epicadus* Simon, *Epicadinus* Simon and *Onocolus* Simon form a clade of taxa with characteristic structure of the male genitalia, consisting of a long and filiform embolus, discoid tegulum and the canoe-shaped RTA fused at the basis with an acute and curved DTA. However, the better diagnostic characters are remarkable somatic features and the structure of the female genitalia. While *Epicadus* present large species with three or five stout opisthosomal projections, elevated thoracic portion, sometimes presenting a median spire (Machado *et al.* 2018), *Epicadinus* is composed of smaller spiders with just three pointed opisthosomal projections and the teguement covered by elongated needle-shaped setae, which give these spiders a spiny appearance (Prado *et al.* 2018). The species of *Onocolus*, on the other hand, can be recognized by the dorsoventrally compressed prosoma, pentagonal opisthosoma, female genitalia with coiled or S-shaped copulatory ducts and predominant green body coloration. The genus *Onocolus* has been revised by Lise (1981). Here, we describe *O. ankeri* **sp. nov.**, a species from the Amazon Forest that is remarkable by its size and color (Fig. 1).

The examined specimens are deposited in the Museu Paraense Emílio Goeldi, Belém (MPEG, A. B. Bonaldo), Instituto Butantan, São Paulo (IBSP, A. D. Brescovit) and Instituto de Ciencias Naturales de la Universidad Nacional de Colombia, Bogotá (ICN, A. E. Flórez). All measurements were taken in millimeters and the terminology and dissection procedures follows Machado *et al.* (2018). Photos of the preserved specimen were taken on a Multipurpose Zoom Microscope Leica M205A with a digital camera.

Onocolus ankeri sp. nov. (Fig. 1A–F)

[zoobank: urn:lsid:zoobank.org:act:126D850C-80CB-452A-A5A2-AA4D7304E657]
Type material: Holotype: BRAZIL: *Pará:* Melgaço, Castanhal do Jacaré, 1°44'13.5"S, 51°25'32.8"W, 1 female, 15 April 1997, J.A.P. Barreiros (MPEG 35307).

Paratypes: BRAZIL: *Roraima:* Alto Alegre, Aldeia Budu, 3°12'09"N, 63°23'30"W, 1 female, 20 July to 05 August 2009, C. Kirsh (IBSP 151198). **COLOMBIA:** *Caquetá:* Solano (Parque Nacional Chiribiquete), 0°44'44,80"N, 72°44'17"W, 1 female, 25 June 2000, F. Quevedo (ICN-AR 8979).

Etymology. The epithet is an homage to Dr. Arthur Anker, who kindly provided us with photos of a live specimen. The name was chosen through a popular survey proposed by the Museu de Ciências e Tecnologia da Pontifícia Universidade Católica do Rio Grande do Sul (MCTP—PUCRS) to promote science popularization.

Diagnosis. Females of *O. ankeri* **sp. nov.** show the characteristic green body coloration as other females of the genus (Figs 1A–B, live specimens) and resemble those of *O. simoni* Mello-Leitão in the shape and disposition of the copulatory ducts, with wide anterior curves forming a pair of primary spermathecae (Fig. 1F). However, the new species is distinct from all its congeners by presenting an accentuated curvature on its anterior tibiae (I and II) and three robust pairs of lateral projections on the opisthosoma (Figs 1A, 1C). Also, *O. ankeri* **sp. nov.** presents diagnostic setiferous tubercles on the median area of the prosoma, which are black pigmented and remarkably contrasting with the green background of the teguement (Figs 1A, 1C, 1D).

Description (Holotype). Anterior eye row recurved, posterior eye row slightly procurved; prosoma whitish-green with darker green spots radially disposed on the prosomal ridges (Figs 1A–D). Legs with same coloration as prosoma; anterior femora robust, with median black spot on the mesial surface (well developed on femora I and smaller on femora

II); metatarsi and patellae II suffused with many dark spots (Figs 1A, 1C). Opisthosoma with three pairs of dorsal sigillae (the median pair largest and most noticeable); three pairs of opisthosomal projections disposed laterally, the anterior and median pairs of equivalent size and the posterior pair more robust and longer (Figs 1A, 1C). Epigynal plate wide and flattened, with copulatory openings oriented anteriorly; copulatory ducts long and hyaline on their first portion (before reaching the secondary spermathecae S2), getting gradually sclerotized along their trajectory towards the primary spermathecae S1 (Figs 1E, 1F). Measurements: eyes diameters and eyes interdistances: AME 0.12, ALE 0.16, PME 0.15, PLE 0.11, AME-AME 0.18, AME-ALE 0.08, PME-PME 0.34, PME-PLE 0.15, MOQ length 0.53, MOQ width 0.62; leg formula: 2-1-3-4: leg I—femur 5.74/ patella 2.66/ tibiae 3.56/ metatarsus 3.22/ tarsus 1.71/ total 16.89; II—5.44/ 2.61/ 4.02/ 3.21/ 1.73/ 17.01; III—2.34/ 1.33/ 1.88/ 1.36/ 0.57/ 7.48; Iv—2.06/ 1.30/ 2.24/ 1.28/ 0.58/ 7.46. Total body length 8.85; prosoma 5.05 length, 5.32 wide; opisthosoma length 3.75 (including the projections); clypeus 0.25 height; sternum 2.16 length, 1.95 width; endites 1.20 length, 0.51 width; labium 0.79 length, 0.85 width.

Distribution. Amazon rainforest: Brazil (States of Roraima and Amazonas) and Colombia (Caquetá) (Fig. 2).
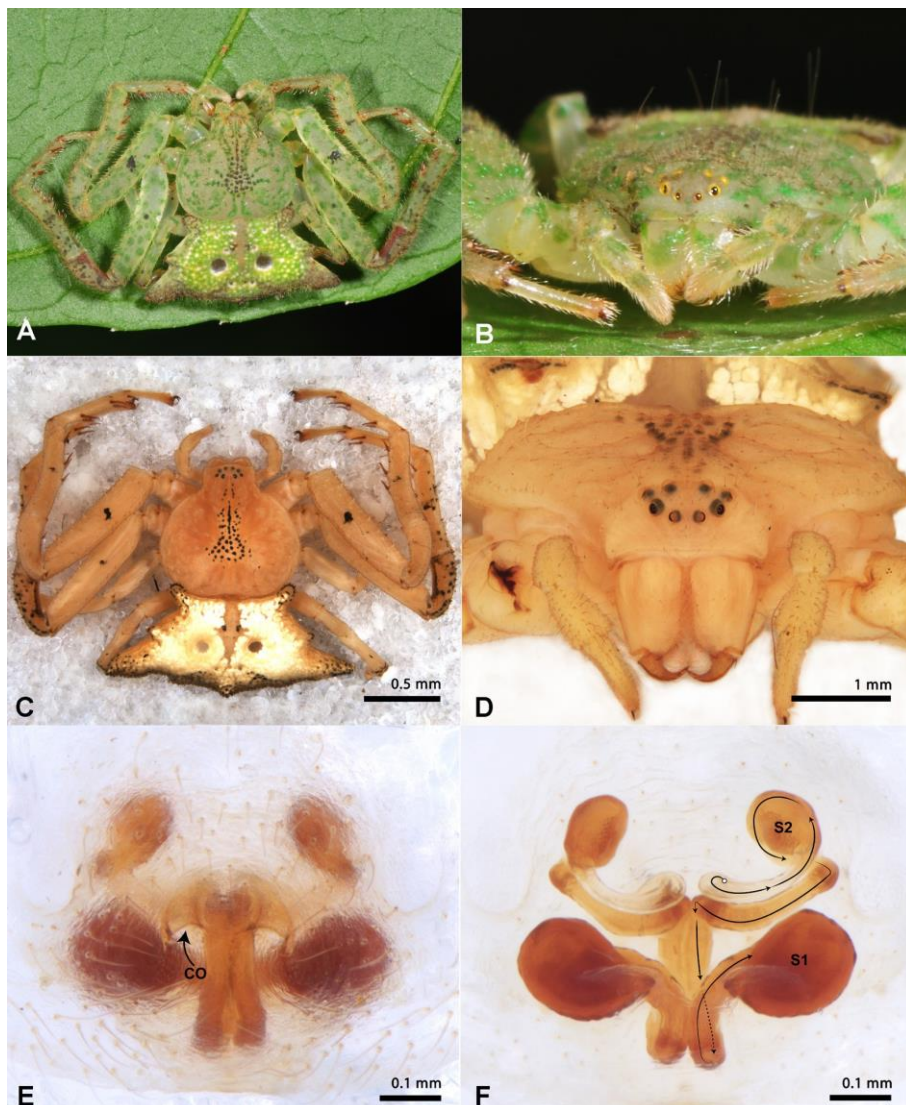

FIGURE 1. *Onocolus ankeri* **sp. nov.** A–B Live specimens photographed by Arthur Anker at the surroundings of Mamori Lake, near Manaus, Brazil (A habitus dorsal, B prosoma frontal); C–D preserved specimens from MPEG 35307 (C habitus dorsal, D prosoma frontal); E–F epigynum from IBSP 151198 (E epigynum ventral, F vulva dorsal). Arrows indicate the course of the copulatory ducts system. Abbreviations: CO—copulatory openings; S1—primary spermathecae; S2—secondary spermathecae.
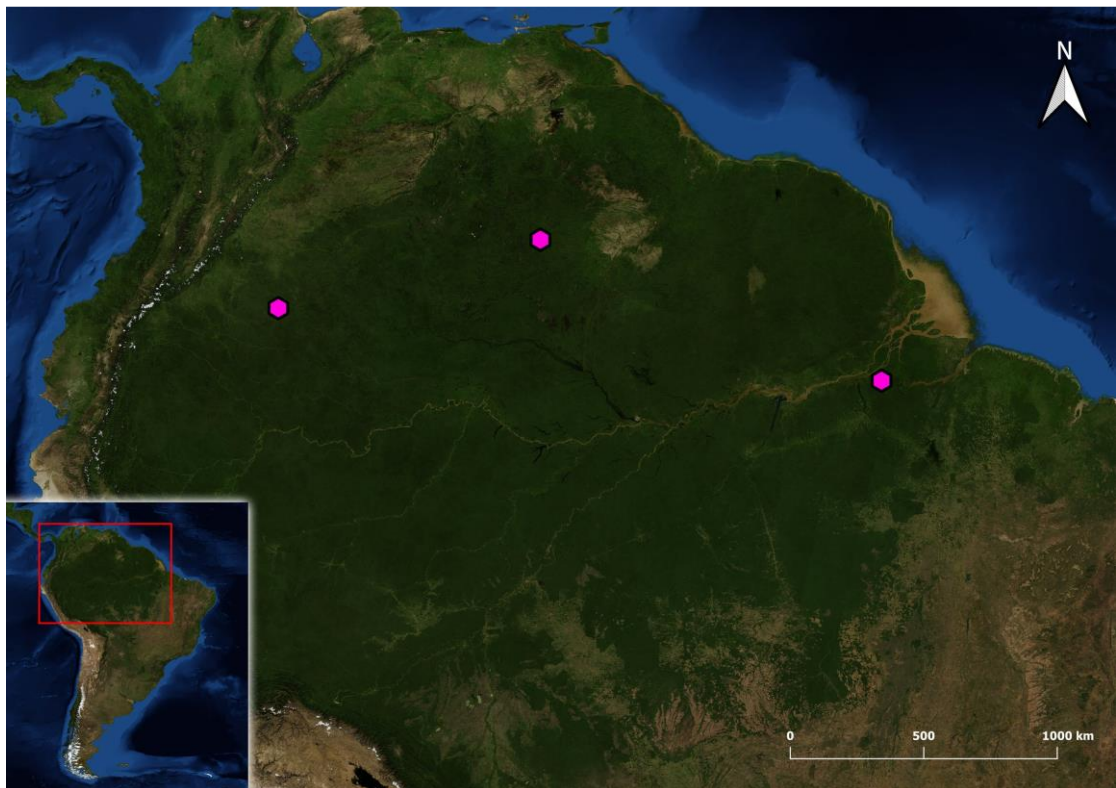
FIGURE 2. Distribution records of *Onocolus ankeri* **sp. nov.**

References

Lise, A.A. (1981) Tomisídeos Neotropicais v: Revisão do gênero *Onocolus* Simon, 1895 (Araneae, Thomisidae, Stephanopinae) [Neotropical thomisids v: revision of the genus *Onocolus*]. *Iheringia, Série Zoologia,* 57, 3–97.

Machado, M., Teixeira, R. A. & Lise, A. A. (2015). Taxonomic notes on the crab spider genus *Tobias* Simon, 1895 (Araneae, Thomisidae, Stephanopinae). *Zootaxa*, 4034 (3), 565–576.
https://doi.org/10.11646/zootaxa.4034.3.8

Machado, M., Teixeira, R.A. & Lise, A.A. (2017) Cladistic analysis supports the monophyly of the Neotropical crab spider genus *Epicadus* and its senior synonymy over *Tobias* (Araneae: Thomisidae). *Invertebrate Systematics,* 31, 442–455.
https://doi.org/10.1071/IS16074

Machado, M., Teixeira, R.A. & Lise, A.A. (2018) There and back again: More on the taxonomy of the crab spider genus *Epicadus* (Thomisidae: Stephanopinae). *Zootaxa,* 4382 (3), 501–530.
https://doi.org/10.11646/zootaxa.4382.3.4

Prado, A.W.; Baptista, R.L.C. & Machado, M. (2018) Taxonomic review of *Epicadinus* Simon, 1895 (Araneae: Thomisidae). *Zootaxa,* 4459 (2), 201–234.
https://doi.org/10.11646/zootaxa.4459.2.1

Silva-Moreira, T. & Machado, M. (2016) Taxonomic revision of the crab spider genus *Epicadus* Simon, 1895 (Arachnida: Araneae: Thomisidae) with notes on related genera of Stephanopinae Simon, 1895. *Zootaxa,* 4147 (3), 281–310.
https://doi.org/10.11646/zootaxa.4147.3.4